Technical Report

TR-10-46

# Fuel and canister process report for the safety assessment SR-Site

Svensk Kärnbränslehantering AB

December 2010

**Svensk Kärnbränslehantering AB**
Swedish Nuclear Fuel
and Waste Management Co

Box 250, SE-101 24 Stockholm
Phone +46 8 459 84 00

ISSN 1404-0344
SKB TR-10-46

# Fuel and canister process report for the safety assessment SR-Site

Svensk Kärnbränslehantering AB

December 2010

# Preface

This document compiles information on processes in the fuel and in the canister relevant for long-term safety of a KBS-3 repository. It supports the safety assessment SR-Site that will support the licence application for a final repository in Sweden.

Lars Werme, SKB, and later Christina Lilja, SKB, have edited the report.

The following persons have had the main responsibilities for specific subject areas: Lars Werme (canister and part of fuel processes), Kastriot Spahiu (part of fuel processes), Christina Lilja (canister processes) and Patrik Sellin (part of fuel processes). The specific parts of their contributions are listed in Section 1.3 in the report.

The report has been reviewed by David Shoesmith, University of Western Ontario (all parts except mechanical processes in the canister) and Rolf Sandström, Royal Institute of Technology (mechanical processes in the canister).

Stockholm, December 2010

*Allan Hedin*
Project leader SR-Site

# Contents

# 1 Introduction

## 1.1 Role of this process report in the SR-Site assessment

### 1.1.1 Overall methodology

This report documents fuel and canister processes identified as relevant to the long-term safety of a KBS-3 repository. It forms an important part of the reporting of the safety assessment SR-Site. The detailed assessment methodology, including the role of the process reports in the assessment, is described in the SR-Site Main report /SKB 2011/. The following excerpts describe the methodology and clarify the role of this process report in the assessment.

The repository system broadly defined as the deposited spent nuclear fuel, the engineered barriers surrounding it, the host rock, and the biosphere in the proximity of the repository will evolve over time. Future states of the system will depend on:

- the initial state of the system,
- a number of radiation related, thermal, hydraulic, mechanical, chemical and biological processes acting within the repository system over time, and
- external influences acting on the system.

A methodology in eleven steps has been developed for SR-Site as summarised in Figure 1-1 and described below.

1. Identification of factors to consider (FEP processing).

   This step consists of identifying all the factors that need to be included in the analysis. Experience from earlier safety assessments and KBS-3 specific and international databases of relevant features, events and processes (FEPs) influencing long-term safety are utilised. An SKB FEP database is developed in which the great majority of FEPs are classified as being either initial state FEPs, internal processes or external FEPs. Remaining FEPs are either related to assessment methodology in general or deemed irrelevant for the KBS-3 concept. Based on the results of the FEP processing, an SR-Site FEP catalogue, containing FEPs to be handled in SR-Site, has been established. This step is documented in the SR-Site FEP report /SKB 2010a/.

2. Description of the initial state.

   The initial state of the system is described based on the design specifications of the KBS-3 repository, a descriptive model of the repository site and a site-specific layout of the repository. The initial state of the fuel and the engineered components is that immediately after deposition, as described in the respective SR-Site Production line report /SKB 2010b, c, d, e, f, g/. The initial state of the geosphere and the biosphere is that of the natural system prior to excavation, as described in the site descriptive model /SKB 2008/. The repository layout adapted to the Forsmark site is provided in underground design report /SKB 2009a/.

3. Description of external conditions.

   Factors related to external conditions are handled in the categories “climate related issues”, “large-scale geological processes and effects” and “future human actions”. The handling of climate related issues is described in the SR-Site Climate report /SKB 2010h/, whereas the few external, large-scale geosphere processes are addressed in the Geosphere process report /SKB 2010i/. The treatment of future human actions in SR-Site is described in the SR-Site FHA report /SKB 2010j/.

4. Compilation of process reports.

   The identification of relevant processes is based on earlier assessments and FEP screening. All identified processes within the system boundary relevant to the long-term evolution of the system are described in dedicated Process reports, i.e. this report and process reports for the buffer, backfill and closure /SKB 2010k/ and the geosphere /SKB 2010i/. Also short-term geosphere processes/alterations due to repository excavation are included. For each process, its general characteristics, the time frame in which it is important, the other processes to which it is coupled, and how the process is handled in the safety assessment, are documented.


***Figure 1-1.*** *An outline of the eleven main steps of the SR-Site safety assessment. The boxes at the top above the dashed line are inputs to the assessment.*

5. Definition of safety functions, function indicators and function indicator criteria.

   This step consists of an account of the safety functions of the system and of how they can be evaluated by means of a set of function indicators that are, in principle, measurable or calculable properties of the system. Criteria for the safety function indicators are provided. The Process reports are important references for this step. A FEP chart is developed, showing how FEPs are related to the function indicators.

6. Compilation of input data.

   Data to be used in the quantification of repository evolution and in dose calculations are selected. The process of selection and the data adopted are reported in a dedicated data report /SKB 2010l/. Also, a template for discussion of input data uncertainties has been developed and applied.

7. Definition and analysis of reference evolution.

   A reference evolution, providing a description of a plausible evolution of the repository system, is defined and analysed. The isolation potential of the system over time is analysed, yielding a description of the general system evolution and an evaluation of the safety function indicators. Each process is handled in accordance with the plans outlined in the process reports. Radiological consequences of potential canister failures are not analysed in this step.

8. Selection of scenarios.

   A set of scenarios for the assessment is selected. A comprehensive main scenario is defined in accordance with SSM's regulations SSMFS 2008:21. The main scenario is closely related to the reference evolution analysed in step 7. The selection of additional scenarios is focused on the safety functions of the repository, and the safety function indicators defined in step 4 form an important basis for the selection. For each safety function, an assessment is made as to whether any reasonable situation where it is not maintained can be identified. If this is the case, the corresponding scenario is included in the risk evaluation for the repository, with the overall risk determined by a summation over such scenarios. The set of selected scenarios also includes scenarios explicitly mentioned in applicable regulations; e.g., human intrusion scenarios, and scenarios and variants to explore design issues and the roles of various components in the repository.

9. Analysis of scenarios.

   The main scenario is analysed essentially by referring to the reference evolution in step 7, complemented by consequence calculations for potential canister failures in the reference evolution yielding a calculated risk contribution from the main scenario. The additional scenarios are analysed by focusing on the factors potentially leading to situations in which the safety function in question is not maintained. In most cases, these analyses are carried out by comparison with the evolution for the main scenario, meaning that they only encompass aspects of repository evolution for which the scenario in question differs from the main one. If the scenario leads to canister failures, consequence calculations are carried out. If the likelihood of the scenario is non-negligible, a risk contribution is also calculated.

10. Additional analyses.

    In this step, a number of additional analyses, required to complete the safety assessment, are carried out. These comprise e.g. sensitivity analyses of the outcome of the scenario analyses, analyses required to demonstrate optimisation and use of best available technique, analyses of design options alternative to the reference design, analyses supporting risk discussion for the initial 1,000 years and an account of supporting arguments based on natural analogues.

11. Conclusions.

    This step includes integration of the results from the various scenario analyses, development of conclusions regarding safety in relation to acceptance criteria and feedback concerning design, continued site investigations, and the R&D programme.

This fuel and canister process report is one of the process reports required to complete step 4. The purpose of the process reports is to document the scientific knowledge of the processes to a level required for their adequate treatment in the safety assessment. The documentation is not exhaustive from a scientific point of view, since such a treatment is neither necessary for the purposes of the safety assessment nor possible within the scope of an assessment. However, it must be sufficiently detailed to facilitate, by arguments founded on scientific understanding, the treatment of each process in the safety assessment. The purpose is to determine how to handle each process in the safety assessment at an appropriate degree of detail, and to demonstrate how uncertainties are taken care of, given the suggested handling. The handlings established in this report are used in the analysis of the reference evolution, step 7, and in the analyses of scenarios, step 9.

### 1.1.2 Identification of processes

The process documentation in this SR-Site version of the process report is an update of the descriptions in the SR-Can version of the Process report /SKB 2006a/. The SR-Can version of the report, in turn, builds on the process documentation in the SR 97 version of the process report /SKB 1999/ and the FEP processing carried out in SR-Can. The complementary FEP processing carried out in SR-Site (step 1 above) did not identify any need to modify the list of relevant processes that were included in the SR-Can version of the process report /SKB 2006a/, see the SR-Site FEP report /SKB 2010a/ for details. However, experience from SR-Can point out the need to address additional mechanisms related to fuel alteration. Therefore, the process chemical alteration of the fuel has been added in this SR-Site version, as compared to the SR-Can version of the report. A complete list of processes described in the SR-Site process reports can be found in the abovementioned FEP report.

### 1.1.3 Relation to specific sites

SKB has undertaken site characterisation at two different locations, Forsmark and Laxemar-Simpevarp, as candidate sites for a final repository for spent nuclear fuel. The SR-Site assessment builds on site-specific data and site-descriptive models of the selected Forsmark site /SKB 2008/, but site-specific data and site-descriptive models of the Laxemar site /SKB 2009b/ are also used in evaluations to support the site selection /SKB 2010m/. Therefore, the process descriptions are of a sufficiently general nature to be applicable to both these sites. The result of the quantitative evaluations of the processes in the different scenarios analysed in SR-Site will, in many cases, be dependent on site-specific data. These data are not given here, but in dedicated model studies. In addition, the most essential data for the safety assessment are thoroughly evaluated in the SR-Site data report /SKB 2010l/, step 6 above.

### 1.1.4 Intended audience for this report

This report is written by, and for, experts in the relevant scientific fields. It should though be possible for a generalist in the area of long-term safety assessments of geologic nuclear waste repositories to comprehend the contents of the report. The report is an important part of the documentation of the SR-Site project and an essential reference within the project, providing a scientifically motivated plan for the handling of fuel and canister processes. It is, furthermore, foreseen that the report will be essential for reviewers scrutinising the handling of fuel and canister issues in the SR-Site assessment.

## 1.2 Structure for process descriptions

All identified processes are documented using a template, where, in essence, all of the headings are the same as those used in the SR-Can version of the report. These are described below.

#### *Overview/general description*

Under this heading, a general description of the knowledge regarding the process is given. For most processes, a basis for this is the content of the SR-Can version of the fuel and canister process report /SKB 2006a/, but reviewed and updated as necessary.

#### *Dependencies between process and fuel and canister variables*

For each system component, in this case the fuel and canister systems, a set of physical variables that defines the state of the system is specified. For each process, a table is presented under this heading with documentation of how the process is influenced by the specified set of physical variables and how the process influences the variables. In addition, the handling of each influence in SR-Site is indicated in the table.

#### *Boundary conditions*

The boundary conditions for each process are discussed. These refer to the boundaries of the fuel and canister systems, respectively. The processes for which boundary conditions need to be described are, in general, related to transport of material or energy across the boundaries.

#### *Model studies/experimental studies*

Model and experimental studies of the process are summarised. This documentation constitutes the major source of information for many of the processes.

#### *Natural analogues/observations in nature*

If relevant, natural analogues and/or observations in nature that contribute to the present understanding of the process are documented under this heading.

#### *Time perspective*

The timescale or timescales on which the process occurs are documented, if such timescales can be defined.

#### *Handling in the safety assessment SR-Site*

Under this heading, the handling in the safety assessment SR-Site is described. Typically, the process is either

- neglected on the basis of the information under the previous headings, or
- included by means of modelling.

The following aspects need to be covered, although no prescribed format for the documentation is given:

*Boundary conditions:* The handling of boundary conditions is discussed, especially any spatial and temporally varying chemical and hydraulic conditions.

*Influences and couplings to other processes:* The handling of the documented influences will be discussed, as will couplings to other processes within the system component.

As a result of the information under this subheading, a mapping of all processes to method of treatment and, in relevant cases, applicable models will be produced for all processes.

#### *Handling of uncertainties in SR-Site*

Given the adopted handling in the safety assessment SR-Site, the handling of different types of uncertainties associated with the process is summarised.

*Uncertainties in mechanistic understanding:* The uncertainty in the general understanding of the process is discussed based on the available documentation and with the aim of addressing whether the basic scientific mechanisms governing the process are understood to the level necessary for the suggested handling.

*Model simplification uncertainties:* In most cases, the quantitative representation of a process will contain simplifications. These may be a significant source of uncertainty in the description of the system evolution. These uncertainties are discussed and approaches to addressing them are identified including alternative models or alternative approaches to simplification of a particular conceptual model.

*Input data and data uncertainties:* The set of input data necessary to quantify the process for the suggested handling is documented. The further treatment of important input data and input data uncertainties is described in a separate report, the SR-Site data report /SKB 2010l/, to which reference is made when relevant.

#### *Adequacy of the references supporting the handling in SR-Site*

Under this heading, statements are provided concerning the adequacy of the references in a quality assurance perspective. These statements are restricted to the references supporting the selected handling and are, together with the arguments and justifications for the selected handling provided in the preceding subsections, evaluated in the factual review of the process report.

#### *References*

A list of references used in the process documentation is given at the end of the report.

## 1.3 Participating experts

The experts involved in assembling the basic information on the processes are listed in Table 1-1. All these experts are included in the SR-Site list of experts as required by the SR-Site QA plan, see further the SR-Site Main report /SKB 2011/.

**Table 1-1. Experts responsible for the process documentations.**

| Fuel processes | Expert author, affiliation |
|---|---|
| Radioactive decay | Lars Werme, SKB |
| Radiation attenuation/heat generation | Lars Werme, SKB |
| Induced fission (criticality) | Lars Werme, SKB |
| Heat transport | Lars Werme, SKB |
| Water transport in the canister cavity, boiling/condensation | Lars Werme, SKB |
| Mechanical cladding failure | Lars Werme, SKB |
| Structural evolution of the fuel matrix | Lars Werme, SKB |
| Advection and diffusion | Lars Werme, SKB |
| Residual gas radiolysis/acid formation | Lars Werme, SKB |
| Water radiolysis | Kastriot Spahiu, SKB |
| Metal corrosion | Lars Werme/Kastriot Spahiu, SKB |
| Fuel dissolution | Kastriot Spahiu, SKB |
| Dissolution of the gap inventory | Kastriot Spahiu, SKB |
| Speciation of radionuclides, colloid formation | Kastriot Spahiu, SKB |
| Helium production | Lars Werme, SKB |
| Chemical alteration of the fuel matrix | Lars Werme, SKB |
| Radionuclide transport | Patrik Sellin, SKB |
| **Canister processes** | |
| Radiation attenuation/heat generation | Lars Werme, SKB |
| Heat transport | Lars Werme/Christina Lilja, SKB |
| Deformation of the cast iron insert | Lars Werme, SKB |
| Deformation of the copper canister from external pressure | Lars Werme, SKB |
| Thermal expansion (both cast iron insert and copper canister) | Lars Werme, SKB |
| Deformation from internal corrosion products | Lars Werme, SKB |
| Radiation effects | Lars Werme, SKB |
| Corrosion of the cast iron insert | Lars Werme, SKB |
| Galvanic corrosion | Lars Werme, SKB |
| Stress corrosion cracking of the cast iron insert | Lars Werme, SKB |
| Corrosion of the copper canister | Lars Werme/Christina Lilja, SKB |
| Stress corrosion cracking of the copper canister | Lars Werme, SKB |
| Earth currents – stray current corrosion | Christina Lilja, SKB/<br>Claes Taxén, Swerea KIMAB/<br>Martin Löfgren, Niressa |
| Deposition of salts on the canister surface | Lars Werme, SKB |
| Radionuclide transport | Patrik Sellin, SKB |

## 1.4 Initial state of the fuel in SR-Site

The following is an overview description of the initial state of the fuel, i.e. its state at the time of deposition. Additional information is given in the Spent fuel report /SKB 2010b/.

### 1.4.1 General

This repository sub-system comprises the spent fuel and the cavity in the canister. The total quantity of spent fuel obtained from the Swedish nuclear reactors will depend on operating time, energy output and fuel burnup. The existing reactors in Sweden are light water reactors of both boiling water (BWR) and pressurized water (PWR) types. The fuel quantities presented here are based on SKB's reference scenario. In this scenario the reactors in Ringhals (1 BWR + 3 PWR) and Forsmark (3 BWR) are assumed to have an operating time of 50 years and the operating time of the reactors in Oskarshamn (3 BWR) is set to 60 years. The maximum enrichment is set to 5% and the burnup is limited to 60 MWd/kgU for the PWR and BWR uranium oxide (UOX) fuel and 50 MWd/kgHM for the BWR mixed uranium-plutonium oxide (MOX) fuel. In the reference scenario, the last reactor will be taken out of operation in 2045 /SKB 2010b/.

### 1.4.2 Fuel types

Several types of fuel will be emplaced in the repository. The major portion of the fuel to be deposited is UOX fuel from PWR and BWR reactors. There will also be small amounts of BWR MOX fuel, spent heavy water reactor fuel from the decommissioned Ågesta reactor, German MOX assemblies (from an exchange project involving reprocessing waste) as well as fuel residues from Studsvik. The total amount of spent fuel and the total number of fuel elements are given in Table 1-2.

Fuel burnups are expected to vary from about 15 MWd/kgU up to 60 MWd/kgU /SKB 2010b/. The burnup distribution in the interim storage facility for spent nuclear fuel, Clab, in December 2007 is given in Figure 1-2 and Figure 1-3 together with the burnup distribution for future fuel assumed in the reference scenario (from the Spent fuel report /SKB 2010b/.

Differences between different fuel types are important for criticality assessments.

To allow for these quantities, the safety assessment assumes a total of 6,000 canisters corresponding to 12,000 tonnes of fuel.

**Table 1-2. Amount of spent fuel and number of fuel elements (from Spent fuel report /SKB 2010b/).**

| Fuel type | Number in interim storage (31 December 2007) | Total number for the reference scenario | Total initial weight for the reference scenario (tonnes of U or HM) |
|---|---|---|---|
| BWR assemblies | 21,194 | 47,498[1] | 8,312 |
| PWR assemblies | 2,552 | 6,016 | 2,791 |
| Fuel assemblies from Ågesta | 222 (1 unirradiated) | 222 (1 unirradiated) | 20 |
| Fuel residues in protection boxes from Studsvik | 19 | approximately 25 | 3 |
| Swap MOX assemblies (BWR) | 184 | 184 | 14.1 |
| Swap MOX assemblies (PWR) | 33 | 33 | 8.4 |

[1] Including 83 BWR MOX assemblies from Oskarshamn.

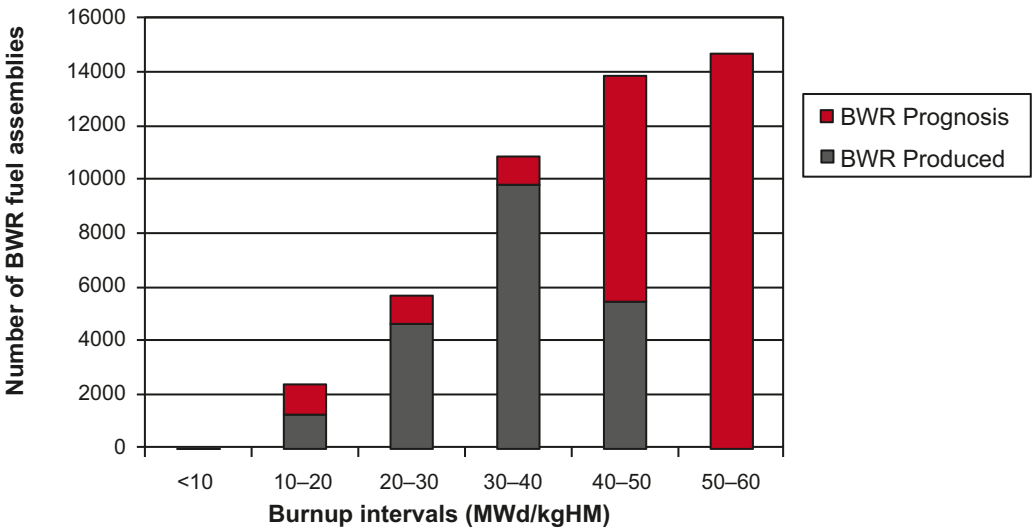


***Figure 1-2.*** *Burnup distribution of spent BWR fuel assemblies stored in Clab 31 December 2007 (grey) and prognosis of the burnup distribution for the assemblies resulting from the future operations of the nuclear power plants as assumed for the reference scenario (Figure 2-1 in /SKB 2010b/).*

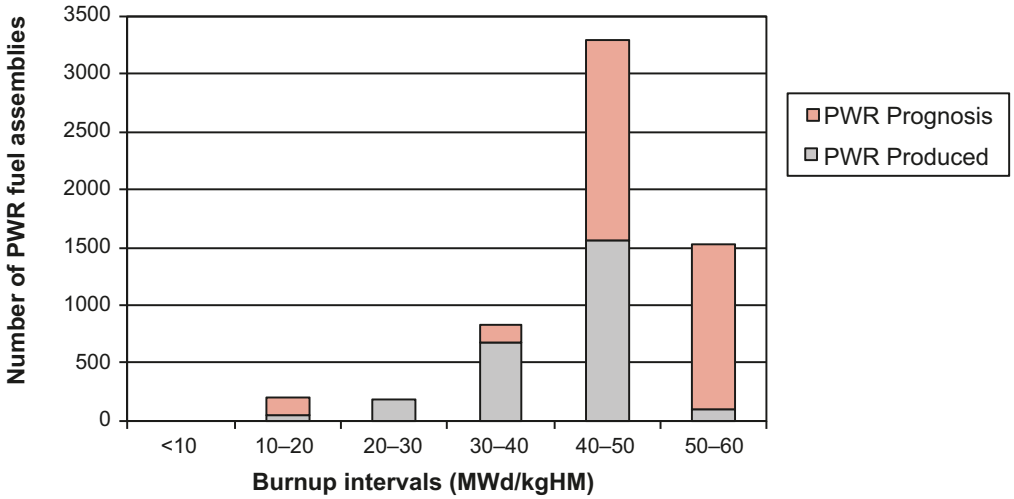


***Figure 1-3.*** *Burnup distribution of spent PWR fuel assemblies stored in Clab 31 December 2007 (grey) and prognosis of the burnup distribution for the assemblies resulting from the future operations of the nuclear power plants as assumed for the reference scenario (Figure 2-1 in /SKB 2010b/).*

### 1.4.3 Structure of the fuel assemblies

Nuclear fuel, here exemplified by Svea 96 BWR fuel, consists of cylindrical pellets of uranium dioxide. The pellets are 11 mm high and have a diameter of 8 mm. They are stacked in approximately 4-metre-long cladding tubes of Zircaloy, a durable zirconium alloy. The tubes are sealed with welds and bundled together into fuel assemblies. Each assembly contains 96 cladding tubes. The fuel assembly also contains components made of the nickel alloys Inconel and Incoloy, and of stainless steel. Pellets in a cladding tube and a fuel assembly are shown in Figure 1-4.

Aspects of importance in the safety assessment, for example the geometrical arrangements and dimensions of the fuel cladding tubes are, as a rule, handled sufficiently pessimistically in analyses of radionuclide release and transport that differences between different fuel types are irrelevant.

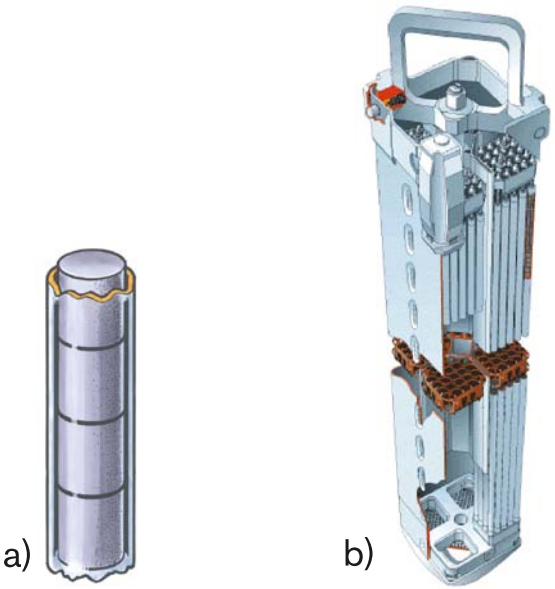


***Figure 1-4.*** *a) Cylindrical fuel pellets in cladding tubes of Zircaloy. The pellets have a diameter of approximately one centimetre. b) Fuel assembly of type Svea 96. The assembly consists of 96 fuel tubes and has a height of approximately 4 metres.*

### 1.4.4 Description of fuel structure and radionuclide distribution in the structure

#### *Fuel*

The nuclear fuel consists of very nearly stoichiometric uranium dioxide in the form of cylindrical pellets. The size of the pellets varies between different fuel types, but is on the order of 1 cm in diameter and 1 cm in length. The grain size is normally in the range of a few μm to about ten μm. The uranium in the present fuel has been enriched in the isotope U-235 from the naturally occurring concentration of 0.7% up to 3.6% in BWR fuel (4.2% in gadolinium-bearing fuel) and 4.2% in PWR fuel. In the future, the enrichment will be increased to 5%.

The fuel typically develops a power of 15 to 25 kW per metre of fuel rod during operation, which corresponds to a centre temperature in the fuel pellet of 800 to 1,200°C. After use in the reactor, the fuel contains 2–6% fission products, depending on the burnup, and approximately 1% higher actinides formed by neutron capture and radioactive decay. The average burnup for Swedish nuclear fuel is currently (December 2007) 34 MWd/kgU for BWR fuel and 41 MWd/kgU for PWR fuel. Since the beginning of 1970, the burnup of nuclear fuel has gradually increased from approximately 23 MWd/kgU to about 53 MWd/kgU. The calculated future average burnup of spent fuel to be deposited in the repository is 40.4 MWd/kgU for BWR fuel and 44.8 MWd/kgU for PWR fuel.

The majority of the fission products and the higher actinides are present in solid solution within the uranium dioxide matrix. Besides the chemical alteration of the uranium dioxide this entails, the fuel has also been altered physically during operation in the reactor.

#### *Enrichment of radionuclides on the pellet surface*

In the case of fuel that has been irradiated at a relatively low temperature, the radial variation in grain size and porosity is small, with moderate grain growth in the centre of the pellet. An exception to this rule is the sharp increase in porosity in the pellet rim. To a depth of a few μm on the rim of the pellet, the porosity is several times higher than inside the fuel. This rim zone also deviates in microstructure from the rest of the pellet in that the original grains have been subdivided into many smaller grains. The reason for this lies in local variations in the fission rate across the diameter of the fuel.

Self-shielding in the fuel leads to a radial variation in the frequency of U-235 fissions, but more importantly, increased formation and fission of plutonium isotopes, in the rim of the fuel pellet. The result is increased burnup and alpha activity at the periphery of the fuel pellets. The increased burnup is also accompanied by a higher content of fission products. For an average burnup of about 40 MWd/kg U, this surface layer can have a burnup up to twice the average, as well as more than four times the average alpha activity /Forsyth 1995/.

#### *Radionuclides in the fuel-clad gap*

During irradiation in the reactor, a fraction of the radionuclide inventory will have segregated either to the gap between the fuel and the cladding or to the grain boundaries in the fuel. Of these radionuclides, the behaviour of the fission gases is best known. A number of studies of fission gas releases have been published over the years. The behaviour of other potentially segregated radionuclides is far less well known. This is of concern because these radionuclides will be released more rapidly than the radionuclides that are embedded in the fuel's $UO_2$ matrix. The fraction of the radionuclides that is incompatible with the $UO_2$ matrix, and thus present in the fuel/cladding gap, is generally considered to be comparable to the fission gas release to the fuel/cladding gap as measured in gas release testing of fuel rods /Johnson and Tait 1997, Johnson and McGinnes 2002, Werme et al. 2004, Johnson et al. 2004, Ferry et al. 2008/. Considering this correlation, and since there are far more data available on fission gas release than on the release from the matrix of other radionuclides, it can be of interest to discuss the fission gas release even though the fission gases are of little concern for a long-term safety assessment. Fission gas release is more strongly correlated to the linear heat rating than to the burnup of the fuel /Kamimura 1992/. Up to about 2000, the operating conditions were such that the linear heat rating was kept relatively low and the fission gas release minimised. Up to a burnup of about 40 MWd/kgU, the fission gas releases are typically less than one percent (see e.g.

/Werme et al. 2004, Johnson et al. 2004/). In SR-Can /SKB 2006b/, the fuel was assumed to have a burnup of 38 MWd/kgU. At that time, about 75% of the Swedish fuel inventory had a burnup of less than 40 MWd/kgU and the number of fuel elements with an average burnup exceeding 50 MWd/kgU was very small. As of June 2005, only 45 fuel elements had a burnup exceeding 50 MWd/kgU. For the interval 40 to 50 MWd/kgU, the fission gas release is generally below 1.5% for PWR, while for BWR it can go as high as 5% with an average in the range of 2.5%. Very little experimental data are available for fission gas release from BWR fuel with higher burnup than 50 MWd/kgU /Matsson et al. 2007/. For PWR fuel, the measured fission gas release for fuel in the burnup interval 50 to 60 MWd/kgU appears to be a few percent, pessimistically up to 5% /Werme et al. 2004, Johnson et al. 2004/.

The Swedish reactors have been, or are in the process of being, uprated. As a consequence, the linear heat rating is increased and higher fission gas release is to be expected. Having only limited data for a burnup of 60 MWd/kgU, fission gas release was calculated for typical equilibrium cores for Swedish BWR /Oldberg 2009/ and PWR reactors /Nordström 2009/.

There are relatively few systematic studies of the release of segregated radionuclides other than fission gases in fuel. Only one very comprehensive study has been published /Stroes-Gascoyne 1996/. In that publication, the rapid releases of $^{137}$Cs, $^{90}$Sr, $^{99}$Tc, $^{129}$I and $^{14}$C from CANDU fuel were reported. For light water reactor (LWR) fuel, there are far less data available (see e.g. /Forsyth and Werme 1992, Gray et al. 1992, Gray 1999, Johnson et al. 2004, 2005, Roudil et al. 2007/).

Based on these studies, it is generally assumed that the fission gas release and the rapid release of other segregated radionuclides are correlated. This seems to be a reasonable assumption for LWR fuel with gas releases in the range of a few percent /Johnson and McGinnes 2002/

For some radionuclides, a one-to-one relationship seems to be a reasonable assumption, while for others the relationship seems to be more complex /Werme et al. 2004, Johnson et al. 2004/.

#### *Radionuclide segregation to grain boundaries*

In addition to the release of gaseous fission products, other elements that are incompatible with the structure of the uranium dioxide are also segregated to form separate phases. Light water reactor fuel contains inclusions of metal alloys of Mo-Tc-Ru-Rh-Pd (4d metals), known as ε-phases. In normal fuel, these particles can be up to micrometres in size and observable by optical microscopy /Forsyth 1995/. The fraction of 4d metals, which Forsyth was able to determine by optical microscopy (particles larger than 0.5 μm), corresponded to only 1% of their calculated total inventory in the fuel. By electron microscopy, it has been possible to determine that ε-phases also occur in the size range 1 to 100 nm /Thomas and Guenther 1989/. When fuel is dissolved in nitric acid, the 4d metals form an insoluble residue. By analysing these residues, Forsyth concluded that at least 80% of the residues consisted of ε-particles. The particle size distribution depends on the temperature at which the fuel has been operated and can, therefore, vary between fuel samples.

Besides these known segregations, the possibility that other fission products have segregated to the grain boundaries in the uranium dioxide has been discussed. For CANDU fuel, which is irradiated with higher linear power density (20–55 kW/m) than light water reactor fuel, it has been established by photoelectron spectroscopy that Cs, Rb, Te and Ba are present in the grain boundaries, often with high surface enrichments /Hocking et al. 1994/. /Gray et al. 1992/ determined the grain boundary inventory of Cs in light water reactor fuel to be less than 1%. The values of gap and grain boundary inventories for Tc and Sr were near their detection limits at less than 0.2% of their total inventory. An Auger spectroscopy study on fuels with moderate burnup and low fission gas release showed no detectable amounts of Cs, Sr and Tc /Thomas et al. 1992/. On a PWR fuel with extremely high fission gas release (18%; equivalent fuel was also included in the study by /Gray et al. 1992/), ε-phases were found with high surface concentrations of Cs, Te and Pd /Thomas et al. 1992/. This observation was interpreted as indicating that Cs and other fission products are mainly associated with the ε-phases and, thereby only indirectly with the grain boundaries that contain them. The implication of the lack of detectable quantities of Cs, Sr and Tc in other grain boundary locations /Thomas et al. 1992/, is that the grain boundary inventory of these fission products is small.

The question of Sr segregation and the differences between Sr and U release from spent fuel in leaching experiments at Studsvik has been discussed extensively. /Werme and Forsyth 1988/ offer the hypothesis that most of the strontium released comes from selective leaching of cracks and grain boundaries. Attempts have been made to determine grain boundary inventories by microprobe analysis in a fuel with a burnup of 37 MWd/kg U (linear power density < 20 kW/m) that had been subjected to controlled power ramping to 43 kW/m in the Studsvik R2 reactor /Forsyth et al. 1988/. The rod had an appreciable release of Kr and Xe, as well as redistribution of Cs to the fuel-clad gap during the power increase. Sharp concentration gradients within the individual grains could be observed for Xe and Cs, but not for Nd. In the case of Sr, the concentrations were far too close to the detection limit to yield reliable data. Subsequently, a fuel with a burnup of 44–48 MWd/kgU (linear power density < 15 kW/m), was subjected to a similar power ramping to a peak of 43 kW/m /Forsyth et al. 1994/. In a corrosion experiment a significant increase, compared to the reference samples, in the release of Cs and Rb was observed, and some increase for Ba and Tc as well as possibly also for Mo. No significant redistribution of Sr was found.

Available data thus suggest that, in contrast to CANDU fuel, light water reactor fuel irradiated with moderate power densities has, at most, a few tenths of a percent of the inventory of radionuclides in the grain boundaries.

## 1.5 Definition of fuel variables

The spent fuel is described by the variables in Table 1-3, which together characterise the spent fuel in a suitable manner for the safety assessment. The description applies not only to the spent fuel itself, but also to the cavities in the canister.

The fuel and the cavity in the canister are characterised with respect to radiation by the intensity of $\alpha$, $\beta$, $\gamma$ and neutron radiation and thermally by the temperature. Hydraulically, it is necessary to characterise the cavity only if the copper canister should be damaged and water should enter. The cavity is then characterised by water flows and water pressures as well as by gas flows and gas pressures, which are jointly termed hydro-variables. Mechanically, the fuel is characterised by stresses in the materials, and chemically by the material composition of the fuel matrix and metal parts, as well as by the radionuclide inventory. The gas composition and, if water enters the canister, the water composition are also relevant for the description.

**Table 1-3. Variables for fuel/cavity in the canister.**

| Variable | Definition |
|---|---|
| Radiation intensity | Intensity of alpha, beta, gamma and neutron radiation as a function of time and space in the fuel assembly. |
| Temperature | Temperature as a function of time and space in the fuel assembly. |
| Hydro-variables (pressure and flow) | Flows, volumes and pressures of water and gas as a function of time and space in the cavities in the fuel and canister. |
| Fuel geometry | Geometric dimensions of all components of the fuel assembly, such as fuel pellets and Zircaloy cladding. Also includes the detailed geometry, including cracking, of the fuel pellets. |
| Mechanical stresses | Mechanical stresses as a function of time and space in the fuel assembly. |
| Radionuclide inventory | Occurrence of radionuclides as a function of time and space in the different parts of the fuel assembly. The distribution of the radionuclides between the pellet matrix and surface is also described here. |
| Material composition | The materials of which the different components in the fuel assembly are composed, excluding radionuclides. |
| Water composition | Composition of water (including any radionuclides and dissolved gases) in the fuel and canister cavities. |
| Gas composition | Composition of gas (including any radionuclides) in the fuel and canister cavities. |

## 1.6 Summary of handling of fuel processes in SR-Site

Table 1-4 summaries the handling of fuel processes in the safety assessment SR-Site, as suggested in this report. In the table, the process is either "mapped" to a model by which it will be quantified or associated with a brief verbal description of how it will be handled.

**Table 1-4. Process table for the fuel describing how fuel processes will be handled in different time frames and in the special case of failed canisters. Green fields denote processes that are neglected or irrelevant for the time period of concern. Red fields denote processes that are quantified by modelling in the safety assessment. Orange fields denote processes that are neglected subject to a specified condition.**

| Process | Intact canister | Failed canister |
|---|---|---|
| F1<br>Radioactive decay | Thermal model | COMP23 |
| F2<br>Radiation attenuation/heat generation | Thermal model | Neglected when releases occur after period of elevated temperatures. |
| F3<br>Induced fission (criticality) | Neglected since there will be insufficient amounts of moderator inside the canister prior to failure. | Neglected since the probability is negligibly small if credit is taken for the burn-up of the fuel. |
| F4<br>Heat transport | Thermal model | Neglected when releases occur after period of elevated temperatures. |
| F5<br>Water and gas transport in canister cavity, boiling/ condensation | Not relevant | Description in Section 2.3.1, integrated with other relevant processes yielding simplified, pessimistic assumptions on retardation in failed canister depending on failure mode. |
| F6<br>Mechanical cladding failure | Not relevant | Pessimistic assumption |
| F7<br>Structural evolution of fuel matrix | Not relevant | Negligible for the fuel types and burn-up relevant for SR-Site. |
| F8<br>Advection and diffusion | Not relevant | Description in Section 2.3.1, integrated with other relevant processes yielding simplified, pessimistic assumptions on retardation in failed canister depending on failure mode. |
| F9<br>Residual gas radiolysis/acid formation | Neglected since negligible amounts of corrodants are produced. | Not relevant |
| F10<br>Water radiolysis | Neglected | Neglected except for fuel dissolution, see that process. |
| F11<br>Metal corrosion | Not relevant | Modelled in COMP23 |
| F12<br>Fuel dissolution | Not relevant | Modelled as constant, pessimistic dissolution rate in COMP23. |
| F13<br>Dissolution of gap inventory | Not relevant | Pessimistic, instantaneous |
| F14<br>Speciation of radionuclides, colloid formation | Not relevant | COMP23 |
| F15<br>Helium production | Neglected since the amount of helium produced will not increase the pressure inside the canister enough to affect its mechanical stability. | Not relevant |
| F16<br>Chemical alteration of the fuel matrix | Not relevant | Neglected since it is not deemed to increase the dissolution rate of the fuel. |
| F17<br>Radionuclide transport | Not relevant | COMP23 |

## 1.7 Initial state of the canister in SR-Site

The following is an overview description of the initial state of the fuel, i.e. its state at the time of deposition. Additional information is given in /SKB 2010c/.

### 1.7.1 Description of cast iron insert and copper canister

The disposal canister for the spent nuclear fuel consists of an outer 5 cm thick copper shell with an insert made from nodular cast iron. The copper shell will act as the corrosion barrier in the repository, while the insert will provide the necessary stability to the whole package when exposed to the different mechanical loads that it may encounter during the one million year time period considered in the safety assessment. The reference design and outer dimensions for the disposal canister are shown in Figure 1-5. As shown in the figure, the insert contains individual channels for each fuel element. For BWR fuel, there are 12 channels in each insert, while for PWR fuel there will be only 4 channels. Figure 1-6 shows the cross section of the BWR and PWR inserts respectively.

The copper in the canister shell is oxygen free and will fulfil the specifications in /EN 1976:1988/ for the grades Cu-OFE (UNS10100) with the following additional requirements: 30–100 ppm phosphorous, < 0.6 ppm hydrogen, < 12 ppm sulphur. In addition, oxygen contents of up to some tens of ppm are allowed.

The material for nodular cast iron will fulfil the requirements (/EN 1563:1997/ grade EN-GJS-400-15U) regarding mechanical properties. The materials composition is as specified in the old Swedish standard SS140717 since EN 1563 does not have a material specification. As additional requirements, the following have been specified: < 0.05% Cu, < 4.5% C, < 6% Si and > 90% Fe.

A summary of the weight for both the BWR and PWR versions of the canister is given in Table 1-5. The given values are those specified in the reference design.


***Figure 1-5.*** *The reference design with a corrosion resistant outer copper shell and a load-bearing insert of nodular cast iron.*

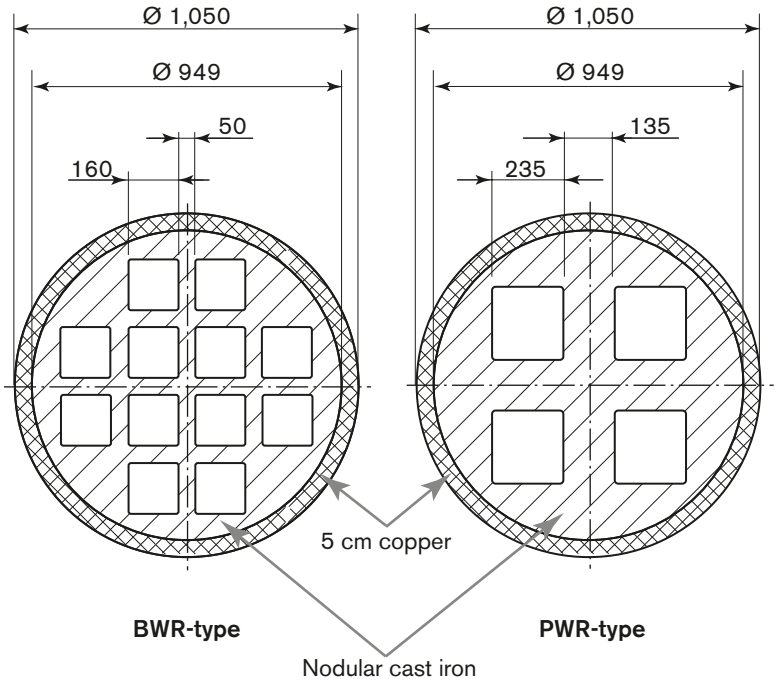


***Figure 1-6.*** *Dimensions (in mm) of the cross section of the BWR and PWR inserts.*

**Table 1-5. Weight of canisters.**

| | Weight (kg) | |
|---|---|---|
| | **BWR-canister** | **PWR-canister** |
| Insert with lid | 13,700 | 16,400 |
| Copper shell | 7,500 | 7,500 |
| Canister without fuel | 21,200 | 23,900 |
| Canister with fuel | 24,600 – 24,700 | 26,500 – 26,800 |

## 1.8 Canister performance and safety

A safety function is defined qualitatively as a role through which a repository component contributes to safety. In order to evaluate the canister's performance in the safety assessment, a number of so called function indicators and criteria that should be fulfilled over time, have been formulated. A safety function indicator is a measurable or calculable property of a repository component that indicates to what extent a safety function is fulfilled. The safety function indicator criterion is a quantitative limit such that if the corresponding function indicator fulfils the criterion, its safety function is fulfilled. For a more elaborate discussion, see the SR-Site main report /SKB 2011/. A summary of the canister safety function indicators and safety function indicator criteria relating to the containment potential of the canister is presented in Table 1-6.

**Table 1-6. Summary of canister safety function indicators and the criteria they should fulfil.**

| Function | Criterion | Rationale |
|---|---|---|
| Provide corrosion barrier | Copper thickness > 0 | As long as the copper thickness is larger than zero, containment is complete and no releases occur. |
| Withstand isostatic load | Load < 45 MPa (requirement on buffer and rock) | The evaluation of the design and manufacturing procedures for the ensemble of deposited reference canisters led to the conclusion that the canisters will fulfil the design premise of withstanding an isostatic load of 45 MPa /SKB 2010c/. |
| Withstand shear load | No specific safety function indicator criterion for the canister relating to shear movements is formulated. Rather the set of conditions included in the design premises are used as criteria for further analyses.<br><br>Shear loads below those specified in design premise (requirement on buffer and rock). | The evaluation of the design and manufacturing procedures for the ensemble of deposited reference canisters led to the conclusion that the canister will fulfil the following design premise: *"The copper corrosion barrier should remain intact after a 5 cm shear movement at a velocity of 1 m/s for buffer material properties of a 2,050 kg/m³ Ca-bentonite, for all locations and angles of the shearing fracture in the deposition hole, and for temperatures down to 0°C. The insert should maintain its pressure-bearing properties to isostatic loads."* /SKB 2010c/. |

## 1.9 Definition of canister variables

The canister is described by the variables in Table 1-7, which, together, characterise the cast iron insert and the copper canister in a suitable manner for the safety assessment.

The fuel and the cavity in the canister are characterised with respect to radiation by the intensity of gamma and neutron radiation and thermally by the temperature. Mechanically, the canister is characterised by stresses in the materials, and chemically by the material composition of the cast iron insert and copper canister.

**Table 1-7. Variables for the cast iron insert and copper canister.**

| Variable | Definition |
|---|---|
| Radiation intensity | Intensity of gamma and neutron radiation as a function of time and space in the cast iron insert and copper canister. |
| Temperature | Temperature as a function of time and space in the cast iron insert and copper canister. |
| Canister geometry | Geometric dimensions of all components of the cast iron insert and copper canister. |
| Material composition | The detailed chemical composition of the materials used for the cast iron insert and copper canister. This also includes cast iron and copper corrosion products. |
| Mechanical stresses | Mechanical stresses as a function of time and space in the cast iron insert and copper canister. |

## 1.10 Summary of handling of canister processes in SR-Site

Table 1-8 summaries the handling of canister processes in the safety assessment SR-Site, as suggested in this report. In the table, the process is either "mapped" to a model by which it will be quantified or associated with a brief verbal description of how it will be handled.

**Table 1-8. Process table for the canister describing how canister processes will be handled in different time frames and in the special case of failed canisters. Green fields denote processes that are neglected or irrelevant for the time period of concern. Red fields denote processes that are quantified by modelling in the safety assessment. Orange fields denote processes that are neglected subject to a specified condition.**

| Process | Intact canister | Failed canister |
|---|---|---|
| C1<br>Radiation attenuation/heat generation | Radiation attenuation: Initial radiation levels given in Canister production report /SKB 2010c/, referring to calculations in the Spent Fuel report /SKB 2010b/.<br>Heat generation: Included in integrated modelling of thermal evolution; thermal model. | Neglected when releases occur after period of elevated temperatures. |
| C2<br>Heat transport | Included in integrated modelling of thermal evolution; thermal model. | Neglected when releases occur after period of elevated temperatures. |
| C3<br>Deformation of cast iron insert | Isostatic and shear loads modelled in design analysis of canister /Raiko et al. 2010/. (Uneven loads from uneven swelling of the buffer and lack of straightness of the deposition hole included).<br>Considered as cause for failure when isostatic or shear loads on canister exceed design premises loads. | Description in Section 2.3.1, integrated with other relevant processes yielding simplified, pessimistic assumptions on retardation of radionuclide transport in failed canister depending on failure mode. |
| C4<br>Deformation of copper canister from external pressure | Isostatic and shear loads modelled in design analysis of canister /Raiko et al. 2010/. (Uneven loads from uneven swelling of the bufferand lack of straightness of the deposition hole as well as creep in copper included).<br>Considered as cause for failure when isostatic or shear loads on canister exceed design premises loads. | Neglected |
| C5<br>Thermal expansion (both cast iron insert and copper canister) | Neglected since the thermal expansion will cause negligible strains in the materials. | Neglected |
| C6<br>Copper deformation from internal corrosion products | Not relevant | Description in Section 2.3.1, integrated with other relevant processes yielding simplified, pessimistic assumptions on retardation in failed canister depending on failure mode. |
| C7<br>Radiation effects | Neglected based on the specified limit on Cu content for the insert. (Cu impurities promote radiation damage). No radiation effect on the copper shell. | Neglected |
| C8<br>Corrosion of cast iron insert | Not relevant | Description in Section 2.3.1, integrated with other relevant processes yielding simplified, pessimistic assumptions on retardation in failed canister depending on failure mode. |
| C9<br>Galvanic corrosion | Not relevant | Neglected, as influence of galvanic corrosion under oxygen-free, reducing conditions lies within the margins of error for the corrosion rate of the iron insert. |
| C10<br>Stress corrosion cracking of cast iron insert | Neglected since stress corrosion cracking is considered unlikely and even if it occurred it would have no consequences for stability of the insert. | Neglected |

| Process | Intact canister | Failed canister |
|---|---|---|
| C11<br>Corrosion of copper canister | Generally, corrosion is modelled based on mass balance and transport capacity considerations whereas reaction rates are disregarded.<br>Sulphide in buffer and backfill modelled.<br>Microbially generated sulphide in buffer pessimistically bounded by supply of nutrients for microbes.<br>Initial oxygen in buffer: Pessimistically assumed that all oxygen corrodes copper neglecting oxygen consumption by buffer pyrite and rock.<br>Initial oxygen in tunnel backfill: Consider consumption by rock and microbes.<br>Potentially intruding oxygen: Integrated handling of rock, backfill and buffer conditions.<br>Pitting (oxygen corrosion): Described as uneven general corrosion.<br>Corrosion due to radiation: Negligible corrosion depths.<br>Chloride assisted corrosion: Neglected if pH > 4 and $[Cl^-]$ < 2 M.<br>Corrosion effects on cold worked material neglected due to small consequences, if any.<br>Corrosion by water modelled as “what-if” case. | Not relevant for failed canister. |
| C12<br>Stress corrosion cracking, copper canister | Neglected due to the combined effect of very low (if any) concentrations of SCC promoting agents and the insufficient availability of oxidants. | Neglected |
| C13<br>Earth currents – stray current corrosion | Neglected due to no increase in corrosion from external electrical field. | Neglected |
| C14<br>Deposition of salts on canister surface | Neglected due to small consequences (and only relevant during bentonite saturation phase). | Neglected |
| C15<br>Radionuclide transport | Not relevant | COMP23 |

## 1.11 Handling of FEPs mapped to the fuel and canister process system

As a point of departure for the safety assessment SR-Can, a processing of features, events and processes, FEPs, of relevance for the long-term safety of a KBS-3 repository was carried out. For SR-Site, a complementary processing was made, focusing on new NEA project FEPs included in a later version of the international NEA FEP database. This work is further described in the SR-Site FEP report /SKB 2010a/. As mentioned in Section 1.1.2, the complementary FEP processing led to the addition of the process chemical alteration of the fuel to the list of fuel and canister processes, as compared with those treated in the previous SR-Can assessment.

The complementary FEP processing has also provided lists of project FEPs in the international NEA FEP database version 2.1 that are related to the different fuel and canister processes. These lists are essentially the same as those developed for SR-Can based on version 1.2 of the NEA FEP database, except that the updated lists also contain all new project FEPs in the later version (2.1) of the NEA FEP database. As in SR-Can, these FEP lists have been used by the experts developing the process descriptions, in order to ensure that all relevant aspects of a process are addressed in the process descriptions and appropriately handled in the SR-Site assessment. The handling of each FEP has been documented by the experts involved in developing the process descriptions in tables created for this purpose. These tables are provided in the SR-Site FEP report /SKB 2010a/ and the handling is also documented in the SKB FEP database.

The results of these checks showed that FEPs were already covered by the process descriptions and included in existing plans for how to handle the process in the SR-Site assessment.

# 2 Fuel processes

## 2.1 Radiation related processes

### 2.1.1 Radioactive decay

#### *Overview/general description*

The process of radioactive decay transforms the radionuclide content of the fuel and of those parts of the canister cavity to which radionuclides have spread. The radioactive disintegrations generate α-, β-, γ- and neutron radiation as well as new nuclides. These may also be radioactive and further decay until a stable nuclide is created.

This process is of fundamental importance, especially since it describes how the radiotoxicity and composition of the fuel evolves over time. The decay products may have chemical properties different from the parent nuclides that can affect their release mechanisms and migration properties. The energy liberated is converted for the most part into heat (Section 2.1.2), and the process thereby also constitutes the basis for the description of the repository's thermal evolution.

#### *Dependencies between process and fuel variables*

Table 2-1 shows how the process influences, and is influenced by, all fuel variables.

**Table 2-1. Direct dependencies between the process "Radioactive decay" and the defined fuel variables and a short note on the handling in SR-Site.**

| Variable | Variable influence on process | | Process influence on variable | |
|---|---|---|---|---|
| | Influence present? (Yes/No) Description | Handling of influence (How/If not – why) | Influence present? (Yes/No) Description | Handling of influence (How/If not – why) |
| Radiation intensity | No. | – | Yes.<br>The radiation intensity is a result of radioactive decay. | The radiation intensity as a function of time is calculated from the radioactive decay of the inventory of radionuclides (see Spent Fuel Report /SKB 2010b/). |
| Temperature | No. | – | Yes.<br>Most of the decay energy is transformed into heat. | The heat generation (and the temperature in the fuel) is calculated as a function of time from the radioactive decay of the inventory of radionuclides (see above). |
| Hydrovariables (pressure and flows) | No. | – | No.<br>But indirectly through radiolysis. | – |
| Fuel geometry | No. | – | No. | – |
| Mechanical stresses | No. | – | No. | – |
| Radionuclide inventory | Yes.<br>This is the source of the process. | Obvious. | Yes.<br>The process both consumes and produces radionuclides. | The radionuclide inventory is calculated as a function of time (see above). |
| Material composition | No. | – | No. | – |
| Water composition | No. | – | Yes.<br>Negligible compared to other processes influencing the water composition. | Neglected. |
| Gas composition | No. | – | Yes.<br>Negligible compared to other processes influencing the gas composition. | Neglected. |

### *Boundary conditions*

There are no boundary conditions of relevance for this process. (The initial condition is the radionuclide inventory in the fuel at the time of deposition of the fuel in the repository.)

### *Model studies/experimental studies*

Radioactive decay has been thoroughly studied experimentally over a long period of time. The theoretical understanding of the process is good and fully sufficient for the needs of the safety assessment.

### *Natural analogues/observations in nature*

Radioactive substances occur naturally, and it is by studies of these that the knowledge of radioactivity grew during the first few decades of the 20$^{th}$ century.

### *Time perspective*

The time it takes for half of all radioactive atoms of a certain nuclide to decay is called the half-life of the radionuclide. The half-lives of various radionuclides vary from fractions of a second to millions of years.

### *Handling in the safety assessment SR-Site*

The process is included in integrated model calculations of the thermal evolution of the repository and of radionuclide transport (See Sections 2.2.1 and 2.6, respectively, for details regarding modelling).

*Boundary conditions:* As stated above, there are no boundary conditions of relevance for this process.

*Handling of variables influencing this process:* According to the influence table above, only the radionuclide inventory is of relevance. This variable is trivially included in the models of radioactive decay.

### *Handling of uncertainties in SR-Site*

**Uncertainties in mechanistic understanding**

The mechanistic understanding of the process is sufficient for the needs of the safety assessment.

**Model simplification uncertainties**

The radioactive decay as a function of time can be calculated with great accuracy when the nuclide content is known (See Sections 2.2.1 and 2.6 for details regarding modelling).

**Input data and data uncertainties**

The half-lives of the relevant radionuclides are generally known with good accuracy. The most important exception to this rule is $^{79}$Se, where the more recent reported half-life has a range from $1.1 \cdot 10^6$ years /Jiang et al. 1997/ to $1.24 \cdot 10^5$ years /He et al. 2000/. The most recently published data are $2.80 \cdot 10^5$ years /He et al. 2002/ and $3.77 \cdot 10^5$ /Bienvenue et al. 2007/.

In 1995 an international collaboration was formed, the Decay Data Evaluation Project, which includes members of the BNM-CEA/LNHB (France), PTB (Germany), INEEL (USA), KRI (Russia), LBNL (USA), NPL (United Kingdom), CIEMAT (Spain), with the objective of providing carefully produced recommended data (/http://www.nucleide.org/DDEP.htm/). In their evaluation, the adopted value is the weighted mean of these two latest values giving $3.56(40) \cdot 10^5$ years.

For other radionuclides, the evaluations published by the Decay Data Evaluation Project will be used when available. Uncertainties concerning the inventory at deposition and half-lives are discussed further in the SR-Site data report /SKB 2010l/.

#### *Adequacy of references supporting the handling in SR-Site*

All data used are published in peer-reviewed journals or result from careful reviews on published data.

### 2.1.2 Radiation attenuation/heat generation

#### *Overview/general description*

The radiation from radioactive decay interacts with the materials in the fuel and the canister cavity. Energy is thereby transferred to the materials and the radiation is attenuated. Most of the transferred energy is converted into thermal energy, i.e. heat is generated. The thermal energy, or heat, that is generated in the fuel after it has been taken out of service is called residual or decay heat and is dependent on the fuel's radionuclide content. This in turn depends on the fuel's burnup and the length of the intermediate storage time before deposition in the repository. At first, the fuel's heat output is dominated by beta and gamma decay, but alpha disintegrations are also of importance in the long term (Spent Fuel Report /SKB 2010b/). The isotopes which dominate during the first few centuries are Cs-137 (Ba-137m) and Sr-90 (Y-90), both with half-lives of around 30 years, resulting in an approximate halving of the heat output in 30 years.

The process is of fundamental importance since it describes how heat is generated by the radiation. Furthermore, attenuation determines how much of the generated radiation reaches the canister.

#### *Dependencies between process and fuel variables*

Table 2-2 shows how the process influences, and is influenced by, all fuel variables.

#### *Boundary conditions*

There are no relevant boundary conditions for this process other than the physical boundaries set by the geometries of the components involved and the loss of radiation over the boundary to the canister.

#### *Model studies/experimental studies*

The fuel's heat output is directly dependent on the radioactive decay process, as discussed in Section 2.1.1.

#### *Natural analogues/observations in nature*

Not applicable.

#### *Time perspective*

Heat generation in the fuel is only of importance for a few hundred years. After 1,000 years, heat generation is only about 5% of that at the time of deposition.

#### *Handling in the safety assessment SR-Site*

The process is modelled for the main scenario in SR-Site. The need for additional modelling is evaluated in the analysis of additional scenarios.

The total power output of the fuel as a function of time has been calculated on the basis of its radionuclide content, decay energies and half-lives (Spent Fuel Report /SKB 2010b/). For modelling of the thermal evolution of the repository, this time dependent power output is approximated by a sum of exponential terms. All the heat generated is assumed to be deposited in the fuel rods.

*Model:* The thermal model is described in /Hedin 2004/ and /Hökmark et al. 2010/.

*Boundary conditions:* Not relevant for this particular part of the thermal model.

**Table 2-2. Direct dependencies between the process "Radiation attenuation/heat generation" and the defined fuel variables and a short note on the handling in SR-Site.**

| Variable | Variable influence on process | | Process influence on variable | |
|---|---|---|---|---|
| | Influence present? (Yes/No) Description | Handling of influence (How/If not – why) | Influence present? (Yes/No) Description | Handling of influence (How/If not – why) |
| Radiation intensity | Yes. The decay energy deposited in the fuel generates heat. | The heat generation is calculated from the radioactive decay of radionuclides (see Spent Fuel Report /SKB 2010b/). | Yes. Attenuation lowers the radiation intensity. | Implicit in the model (see /SKBdoc 1198314/). |
| Temperature | No. | – | Yes. Obvious. Heat generation increases the temperature. | Implicit in the model (see Spent Fuel Report /SKB 2010b/). |
| Hydrovariables (pressure and flows) | Yes. In a failed canister, the presence of water will influence the radiation attenuation. | Neglected. At the time of water intrusion, the γ-radiation will have decayed. The fuel and the cladding will attenuate α- and β-radiation. | No. But indirectly through temperature. | – |
| Fuel geometry | Yes. Most of the decay energy is deposited in the fuel and the geometry of the fuel has a small effect. | Neglected. | No. | – |
| Mechanical stresses | No. | – | Yes. Increased temperature may create increased stresses in the fuel. | Neglected. This is of no importance for the stability of the fuel. |
| Radionuclide inventory | Yes. The radionuclides are the source of heat. | Implicit in the model (see Spent Fuel Report /SKB 2010b/). | No. The decay itself influences the radionuclide inventory. The generated heat does not. | – |
| Material composition | Yes. Different materials have different attenuation properties. | Neglected. All fuel elements have essentially the same material composition. | No. | – |
| Water composition | No. | – | No. | – |
| Gas composition | No. | – | No. | – |

*Handling of variables influencing this process:* For the thermal modelling, all the radiation energy created in the radioactive decays is assumed to be deposited as heat in the fuel rods, yielding a simplified handling of all influences on the process listed in the influence table above. This handling is pessimistic with respect to the principal calculation end-point of the thermal model, namely the peak canister surface temperature, since no radiation energy is taken to escape the canister as gamma radiation.

### *Handling of uncertainties in SR-Site*

#### Uncertainties in mechanistic understanding

The mechanistic understanding of the process is sufficient for the needs of the safety assessment.

#### Model simplification uncertainties

Heat output as a function of time can be calculated with great accuracy when the radionuclide content is known. In the approximate handling through a sum of exponential terms, a sufficient number of terms are included for the approximation error to have negligible influence on the calculation

end-point, the peak canister surface temperature. Also, the simplification of assuming that all heat generated is deposited in the fuel rods is pessimistic since, in reality, some energy will be deposited outside the canister and thereby has a smaller influence on the peak canister surface temperature.

**Input data and data uncertainties**

The uncertainties regarding heat output stem from uncertainties regarding the nuclide content of the fuel. These uncertainties are discussed in the SR-Site data report /SKB 2010l/.

#### *Adequacy of references supporting the handling in SR-Site*

The supporting SKB report /Hökmark et al. 2010/ has undergone a documented factual- and quality review.

### 2.1.3 Induced fission (criticality)

#### *Overview/general description*

**Criticality inside a canister**

Neutrons from radioactive disintegrations can cause nuclear fission in certain isotopes in the fuel. As long as the copper canister is intact, the great majority of neutrons generated by these disintegrations will pass out of the fuel without causing fission and the process can be neglected.

In the case of $^{235}U$ and $^{239}Pu$ in particular, the efficiency of the fission process increases if the neutrons are moderated (slowed down) to lower energies by collisions with light atomic nuclei. This could, to some extent, occur if water were to penetrate a failed canister. The water will then act as a moderator due to its content of light hydrogen nuclei. New neutrons are released by the fissions, and if more neutrons are formed than are consumed the process can become self-sustaining. The system is then said to be critical and large quantities of energy can then be liberated. It is this process that has been utilised under controlled form in the nuclear reactor for energy production.

In the repository, the spent fuel normal criteria for safety against criticality must apply. This means that the effective neutron multiplication factor, $k_{eff}$, including uncertainties, must not exceed 0.95. /SKBdoc 1193244 / has calculated the effective neutron multiplication factor $k_{eff}$ for a number of cases. These cases include criticality in the Encapsulation plant, in the storage room, during transport, and after disposal. For criticality after disposal the consequence parameters such as the position of the assemblies in the canister, the manufacturing tolerances, the size of the fuel compartments in the insert, temperature, and variation with enrichment were included. The calculations were performed for fresh fuel with an initial enrichment of 5% $^{235}U$.

The worst situation in the encapsulation plant occurs if the canister is filled with water during encapsulation. The case when both the canister and the surrounding room are filled with water is worse than if the surrounding room is dry. In the worst case, the effective neutron multiplication factor is:

PWR: $k_{eff} \pm \sigma = 1.0872 \pm 0.0002$

BWR: $k_{eff} \pm \sigma = 0.9942 \pm 0.0002$

For a loaded welded canister filled with argon, $k_{eff}$ is less than 0.4 in the storage room.

During transport the canister is protected by a transport cask. Under normal transport conditions the effective neutron multiplication factor is less than 0.4. The worst situation from a reactivity standpoint will occur if the transport cask and canister are damaged, the cask submerged in water, and both the cask and canister filled with water.

In this case the $k_{eff} \pm \sigma = 1.0952 \pm 0.0002$ for PWR and $k_{eff} \pm \sigma = 1.0012 \pm 0.0002$ for BWR.

A disposal canister deposited in the repository surrounded by 35 cm of bentonite and filled with water gives $k_{eff} \pm \sigma = 1.0888 \pm 0.0002$ for PWR and $k_{eff} \pm \sigma = 0.9959 \pm 0.0002$ for BWR. The interaction between disposal canisters is insignificant.

The main conclusion of this analysis was that unirradiated BWR-fuel with 5% $^{235}U$ enrichment can be stored in a BWR disposal canister if two central positions are left empty ($k_{eff} \pm \sigma = 0.8941 \pm 0.0002$). However, unirradiated PWR-fuel cannot be stored in a disposal canister without reaching criticality if the canister is filled with water ($k_{eff} \pm \sigma = 1.0026 \pm 0.0004$).

It can, therefore, be concluded that the reactivity criteria cannot be met with the conservative assumption that the fuel is fresh. A more realistic assumption would be to take credit for the burnup of the fuel, which will decrease the reactivity. /SKBdoc 1193244/ also calculated the neutron multiplication factor for irradiated fuel with various initial enrichments including the isotopic concentrations for two sets of isotopes:

Set 1: $^{234}U$, $^{235}U$, $^{238}U$, $^{238}Pu$, $^{239}Pu$, $^{240}Pu$, $^{241}Pu$, $^{242}Pu$, $^{241}Am$ $^{237}Np$.

Set 2: Set 1 + $^{95}Mo$, $^{99}Tc$, $^{101}Ru$, $^{103}Rh$, $^{109}Ag$, $^{133}Cs$, $^{143}Nd$, $^{145}Nd$, $^{147}Sm$, $^{149}Sm$, $^{150}Sm$, $^{151}Sm$, $^{151}Eu$, $^{152}Sm$, $^{153}Eu$, $^{155}Gd$.

In calculating the reactivity using these sets, the uncertainties from the following sources were taken into account (for more detail, see /SKBdoc 1193244/):

Canister
Specific power
Integral burnable poison
Burnable poison rods
Declared burnup
Axial temperature distribution
Axial burnup distribution (end effect)
Control rods
Horizontal burnup distribution
Demolition of fuel assemblies
Calculational uncertainty
Manufacturing tolerances
Isotopic prediction
Long-term reactivity change
Change in geometry due to burnup
Defects in the canister

As can be seen in Table 2-3, credit for burnup has to be taken to demonstrate that the canister remains subcritical in the repository for all reasonably conceivable scenarios.

All calculations were performed using Scale 5.1 /ORNL 2005/. Depletion calculations were performed using the Scale SAS2 control sequence and the criticality calculations were performed using Starbucs and CSAS25. The calculations were performed using the Scale 44-group ENDF/B-V library /ORNL 2005/.

**Table 2-3. Burnup requirements to avoid criticality for different enrichments.**

| | **Set 1: Actinides** | | | | |
|---|---|---|---|---|---|
| Enrichment | **5.0** | **4.6** | **4.0** | **3.6** | **3.0** |
| PWR Burnup requirement (MWd/kgU) | 53.9 | 46.6 | 37.4 | 31.3 | 20.6 |
| BWR Burnup requirement (MWd/kgU) | 32.0 | 21.0 | 8.4 | 4.2 | |
| | **Set 2: Actinides plus fission products** | | | | |
| Enrichment | **5.0** | **4.6** | **4.0** | **3.6** | **3.0** |
| PWR Burnup requirement (MWd/kgU) | 38.7 | 34.6 | 28.3 | 22.1 | 14.3 |
| BWR Burnup requirement (MWd/kgU) | 27.8 | 17.3 | 7.0 | 2.7 | |

**Criticality outside a canister**

The possibility of criticality outside the canister has been addressed on several occasions. This scenario was first analysed by /Behrenz and Hannerz 1978/. They concluded that criticality in the tunnel above the deposition holes is a very remote possibility since no process can be envisaged whereby the necessary local concentration could be achieved.

In 1994, /Bowman and Venneri 1994/ published a report claiming that autocritical and explosive conditions could be reached during disposal of all categories of waste containing fissile actinides. /Van Konynenburg 1995/ reviewed that report and found that the authors did not present plausible explanations of a process or processes that could convert actual disposed waste into a configuration close enough to their hypothetical configuration to make the calculations relevant. These reports were later published in a special issue of /Science and Global Security 1996/.

/Naudet 1991/ developed a model for assessing the conditions to achieve a critical state under the conditions in the Oklo reactor zones. /Oversby 1996, 1998/ adapted the reasoning in /Naudet 1991/ to an analysis of the risks for criticality in a high level repository and concluded that if the fuel assemblies were damaged and uranium and plutonium leached out, there are no probable courses of events that could lead to criticality.

The possibility of nuclear criticality in the vicinity of the proposed repository at Yucca Mountain has recently been explored by /Nicot 2008/. /Nicot 2008/ concluded that external nuclear criticality is not a concern at the proposed Yucca Mountain repository for any of the deposited waste. Some of the waste intended for Yucca Mountain contains higher levels of fissile material than what is intended for disposal in a Swedish repository.

#### *Dependencies between process and fuel variables*

Table 2-4 shows how the process influences, and is influenced by, all fuel variables.

#### *Boundary conditions*

There are no relevant boundary conditions for the criticality process other than the physical boundaries set by the geometries of the components involved. (Other important factors for this process include the fuel burnup, i.e. the fuel's content of fissile nuclides, and canister failure followed by the ingress of liquid water.)

#### *Model studies/experimental studies*

Nuclear fission has been thoroughly studied experimentally over a long period of time, and the theoretical understanding of the process is good and fully sufficient for the needs of the safety assessment. The issue of criticality in the canister has been studied in /SKBdoc 1193244/.

#### *Natural analogues/observations in nature*

Criticality has been studied at the natural reactor in Oklo, see /Oversby 1996, 1998/.

#### *Time perspective*

The fraction of fissionable material in the spent fuel changes insignificantly with time, and criticality in a failed, water-filled canister can be dismissed using the same analysis as discussed above.

#### *Handling in the safety assessment SR-Site*

The probability of criticality inside or outside the canister is considered to be negligibly small, based on the results reported in /SKBdoc 1193244/ and in /Oversby 1996, 1998, Van Konynenburg 1995, Nicot 2008/.

**Table 2-4. Direct dependencies between the process "Induced fission (criticality)" and the defined fuel variables and a short note on the handling in SR-Site.**

| Variable | Variable influence on process | | Process influence on variable | |
|---|---|---|---|---|
| | Influence present? (Yes/No) Description | Handling of influence (How/If not – why) | Influence present? (Yes/No) Description | Handling of influence (How/If not – why) |
| Radiation intensity | Yes. Neutron radiation is necessary for criticality to occur. | Neglected. The probability of criticality is considered to be negligibly small (see text). | Yes. Fissions will increase the radiation intensity. | Neglected. The probability of criticality is considered to be negligibly small (see text). |
| Temperature | No. | – | Yes. The fission energy will heat the fuel. | Neglected. The probability of criticality is considered to be negligibly small (see text). |
| Hydrovariables (pressure and flows) | Yes. The presence of liquid water is required. | Neglected. The probability of criticality is considered to be negligibly small (see text). | Yes. The heat generation may cause evaporation of water. | Neglected. The probability of criticality is considered to be negligibly small (see text). |
| Fuel geometry | Yes. Certain fuel geometries are more susceptible to criticality than others. | Neglected. The probability of criticality is considered to be negligibly small (see text). | No. | – |
| Mechanical stresses | No. | – | Yes. Stresses due to increased temperature. | Neglected. The probability of criticality is considered to be negligibly small (see text). |
| Radionuclide inventory | Yes. The amount of fissile material as well as other nuclides in the fuel controls the risk for criticality. | Neglected. The probability of criticality is considered to be negligibly small (see text). | Yes. Fissions lead to production of radionuclides. | Neglected. The probability of criticality is considered to be negligibly small (see text). |
| Material composition | Yes. The amount of fissile material as well as other nuclides in the fuel controls the risk for criticality. | Neglected. The probability of criticality is considered to be negligibly small (see text). | Yes. Fissions lead to production of radionuclides. | Neglected. The probability of criticality is considered to be negligibly small (see text). |
| Water composition | No. | – | No, but indirectly through increased radiolysis. | Neglected. The probability of criticality is considered to be negligibly small (see text). |
| Gas composition | No. | – | Yes. Evaporation of water and gaseous radiolysis products. | Neglected. The probability of criticality is considered to be negligibly small (see text). |

*Boundary conditions:* As stated above, there are no relevant boundary conditions for this process other than the physical boundaries set by the geometries of the components involved. These are used in the reported studies of criticality.

*Handling of variables influencing this process:* All variables influencing criticality according to the influence table above are included in the reported studies of this process.

### *Handling of uncertainties in SR-Site*

#### Uncertainties in mechanistic understanding

The process has been thoroughly studied within reactor physics. The mechanistic understanding is sufficient for the needs of the safety assessment.

**Model simplification uncertainties**

The reactivity of the fuel in the canister can be calculated with sufficient accuracy. Model uncertainties have been included in the assessment.

**Input data and data uncertainties**

Data uncertainties such as variation in burnup axially and horizontally, radionuclide content and manufacturing tolerances for the canister have been included in the assessment.

#### *Adequacy of references supporting the handling in SR-Site*

**Criticality inside a canister**

/SKBdoc 1193244/ presents calculations of criticality in a disposal canister for an SKB-3 repository which are, therefore, directly applicable for the SR-Site safety assessment. The supporting SKB report has undergone a documented factual- and quality review.

**Criticality outside a canister**

The references /Van Konynenburg 1995, Nicot 2008/ are peer reviewed journal articles. /Oversby 1998/ is a peer reviewed conference paper and is a condensed version of the SKB report by /Oversby 1996/. /Oversby 1998/ discusses scenarios directly relevant for a Swedish repository. /Nicot 2008/ discusses, in general terms, what sequence of events would be necessary to produce a concentration of fissile material capable of reaching criticality as well as the specific situation at Yucca Mountain. The first part of this report is also relevant to the Swedish situation.

## 2.2 Thermal processes

### 2.2.1 Heat transport

#### *Overview/general description*

Heat is transported through the fuel and canister cavity by conduction and radiation to the canister insert and beyond to the near and far field. The process is dependent on the geometric configuration of the fuel and the thermal properties of the materials, which are given by their compositions. The heat transfer to the canister insert sets the boundary conditions for the process. The result is a temperature change in the fuel/cavity.

The process constitutes a part of the thermal evolution of the repository.

Heat transfer between the fuel and the canister insert will occur through conduction and radiation. Which one of those that will dominate will depend on the composition of the residual gas in the cavity and the radiation properties[1] of the metal surfaces on the fuel assemblies and the canister insert. The temperature in the fuel and the cavity will be affected by the entire chain of heat transfers between the different components in the repository. In the longer perspective, the temperature evolution in the fuel and cavity will be controlled by the thermal power output of the fuel. In the shorter term, changes in the heat transfer properties of different repository components caused by redistribution of water (moisture) will have a greater influence on the temperature of the fuel. The peak temperature in the fuel will be reached within a few tens of years after deposition.

#### *Dependencies between process and fuel variables*

Table 2-5 shows how the process influences, and is influenced by, all fuel variables.

[1] Expressed as emissivity, i.e. capacity to emit electromagnetic radiation.

**Table 2-5. Direct dependencies between the process "Heat transport" and the defined fuel variables and a short note on the handling in SR-Site.**

| Variable | Variable influence on process | | Process influence on variable | |
|---|---|---|---|---|
| | Influence present? (Yes/No) Description | Handling of influence (How/If not – why) | Influence present? (Yes/No) Description | Handling of influence (How/If not – why) |
| Radiation intensity | No, but indirectly through the temperature. | – | No. | – |
| Temperature | Yes. The temperature and the temperature gradient control heat flow. | The thermal evolution of the fuel and the canister is included in the integrated near-field evolution model /Hedin 2004/. | Yes. Heat transport will increase the temperature at distances away from the heat source. | The thermal evolution of the fuel and the canister is included in the integrated near-field evolution model /Hedin 2004/. |
| Hydrovariables (pressure and flows) | Yes. The gas pressure and the possible presence of water in the canister influence the heat transport in the canister cavity. | Included in the integrated near-field evolution model /Hedin 2004/. | No, but indirectly through increased temperature which will increase the gas pressure. | – |
| Fuel geometry | Yes. | Included in the integrated near-field evolution model /Hedin 2004/. | No. | – |
| Mechanical stresses | No. | – | No, but indirectly through increased temperature that may lead to heat induced stresses. | – |
| Radionuclide inventory | No. The decay influences the temperature. | – | No. | – |
| Material composition | Yes. Different materials have different thermal properties. | The thermal properties of the canister materials are included in the integrated near-field evolution model /Hedin 2004/. | No. | – |
| Water composition | No. | – | No. | – |
| Gas composition | Yes. The heat conduction depends on the type of gas in the cavity. | The thermal properties of gas inside the canister are included in the integrated near-field evolution model /Hedin 2004/. | No. | – |

### *Boundary conditions*

The heat transfer to the canister insert sets the boundary condition for the process.

### *Model studies/experimental studies*

Hedin has developed a model for the thermal evolution of the fuel and the canister as a part of the integrated near-field evolution model for a KBS-3 repository /Hedin 2004/.

### *Natural analogues/observations in nature*

Not applicable.

### *Time perspective*

The peak temperature of the fuel is reached within a few tens of years after deposition. It then takes several thousand years for the fuel to cool to near-ambient temperatures.

### *Handling in the safety assessment SR-Site*

The process is modelled for the main scenario in SR-Site. The need for additional modelling is evaluated in the analysis of additional scenarios.

The process is included in the integrated modelling of the thermal evolution, encompassing the fuel, the canister, the buffer and the host rock. The most important calculation end-point in the modelling is the peak canister surface temperature, which is insensitive to the handling of heat transport in the canister interior. To calculate the peak canister surface temperature, it is sufficient to know the power output as a function of time from the fuel. All other controlling factors are external to the canister.

*Model:* The thermal model described in /Hedin 2004/ and /Hökmark et al. 2010/.

*Boundary conditions:* Heat transfer to the canister insert through both radiation and conduction is explicitly included in the model.

*Handling of variables influencing this process:* All variables influencing this process according to the influence table above are included in the model. The thermal conductivity in metal parts is assumed to be infinite, whereas heat transfer by radiation and conduction across gaps in the canister interior is handled for the explicit geometries of the fuel and canister.

Intruding water modifies the heat conduction properties in the interior of the canister only marginally. The description of heat conduction for the case of a defective canister is therefore assumed to lie within the frame of the uncertainties for the equivalent description for an intact canister. In addition, all conceivable causes of a canister failure are highly unlikely to occur during the fuel induced thermal transient in the repository.

### *Handling of uncertainties in SR-Site*

#### Uncertainties in mechanistic understanding

The mechanistic understanding of the process is sufficient for the needs of the safety assessment, especially since the calculation end-point of concern is insensitive to this process.

#### Model simplification uncertainties

The geometry of the model is simplified to a 2D-format, and heat conduction is neglected in some parts of the canister interior. These simplifications are either irrelevant or pessimistic.

#### Input data and data uncertainties

Uncertainties surrounding the heat transfer between the cladding tubes and the cast iron insert lead to uncertainties in the assessment of the temperature of the fuel. Compared to the uncertainty over heat transfer between the canister surface and the bentonite before full water saturation has been achieved, these uncertainties surrounding the heat transfer from the fuel to the canister insert are small.

As mentioned above, these data do not influence the calculation of the peak canister temperature.

Input data and data uncertainties are discussed in the SR-Site data report /SKB 2010l/.

### *Adequacy of references supporting the handling in SR-Site*

The thermal conductivity of the metals and gases in the canister used in /Hedin 2004/ are basic and well known.

## 2.3 Hydraulic processes

### 2.3.1 Water and gas transport in the canister: boiling/condensation

***Overview/general description***

If the copper canister is penetrated, water can enter the canister cavity as liquid or water vapour. Transport of water, water vapour and other gases in the canister is then determined by the detailed geometry of the canister cavities, the presence of water/vapour in the cavities, and temperature and pressure. Boiling/condensation comprises an integral part of water/gas transport. Pressures and flows of water and gas across the container/buffer interface set the boundary conditions for this process.

The process is strongly coupled to several other processes; for example, corrosion of the canister insert, where water is consumed and hydrogen is formed. It is also of fundamental importance for some other processes that are dependent on the presence of water in the canister, such as fuel dissolution and radionuclide transport.

If the canister is penetrated, water will enter. The process is controlled by the pressure difference between the buffer and the canister cavity (typically 5–7 MPa) and the hydraulic conductivity in the bentonite. Water ingress can be expected to proceed very slowly. In the presence of water in the canister, gas will be generated both by radiolysis (see Section 2.5.3) and by corrosion of the cast iron insert (Section 3.5.1). The build-up of gas pressure in the canister will lead to a gradual decrease in the inflow of water and, when the pressure is sufficiently high, possibly also to gas transport out of the canister and through the bentonite. The process has been investigated by /Wikramaratna et al. 1993/ and /Bond et al. 1997/.

Qualitatively, the course of events can be described as follows: water enters through a penetrating defect in the copper canister and causes anaerobic corrosion of the iron insert surfaces. This leads to hydrogen gas formation, which gradually increases the pressure inside the cavity in the canister and thereby reduces the ingress of water. The corrosion leads to consumption of water and production of hydrogen gas. If the surface area available for corrosion is constant, the rate of water consumption will also be constant and the water level in the canister will reach a peak and then decrease (see also Section 3.5.1). Depending on the size of the hole in the canister and the corrosion rate, /Bond et al. 1997/ see three possibilities.

1) If the hole is so small that water is consumed by corrosion at the same rate as it enters, no water will collect inside the canister. The hydrogen gas pressure builds up gradually and approaches the external water pressure asymptotically. The corrosion rate will be governed by the inward diffusion of water vapour, which also declines asymptotically towards zero as the hydrogen pressure builds up.

The hole sizes for which this scenario applies depend on the corrosion rate. At a corrosion rate of 0.1 μm/year, the area of the hole must be less than about 8 $mm^2$ for the water pressure and bentonite conductivity assumed in the study. At a corrosion rate of 1 μm/year, (see also Section 3.5.1) the corresponding hole size is about 800 $mm^2$. When the inward transport of water due to the pressure difference between the inside and outside of the canister is lower than the inward transport of water by diffusion, canister corrosion will be diffusion-controlled (see below).

2) If the hole in the canister is larger than in case 1), but still sufficiently small, water will collect inside the canister. The water will be completely consumed before the pressure in the canister reaches the external pressure. Then the corrosion rate will be limited by the water supply rate, which will decrease with increasing hydrogen gas pressure leading to a decrease in corrosion rate (as in case 1). The hydrogen gas pressure gradually builds up and approaches the external pressure asymptotically, while the corrosion rate declines asymptotically towards zero.

In the same way as in case 1), the hole size defining this scenario is dependent on the corrosion rate. The combination of a corrosion rate of 0.1 μm/year and a hole size of 20 $mm^2$ belongs to this category, for example. When the inward transport of water due to the pressure difference between the inside and outside of the canister is lower than the inward transport by diffusion, canister corrosion will be diffusion-controlled (see below).

3) If the hole is sufficiently large in relation to the corrosion rate, the hydrogen gas pressure will reach the external pressure while there is still water in the canister. If the water level is then lower than the hole in the copper canister, hydrogen is expelled, but the internal pressure is still high and prevents new water from entering the canister. If the water level in the canister lies above the hole in the copper canister, water will first be pressured out until the water is on a level with the hole. Then hydrogen will be expelled as long as the corrosion continues, i.e. until all water in the canister has been consumed.

As in case 1, the hole size for which this scenario applies is dependent on the corrosion rate and can be illustrated by the cases 0.01 μm/year and hole size 5 $mm^2$, and 1 μm/year and hole size 0.18 $m^2$, both of which belong to case 3 (see also Section 3.5.1). When the inward transport of water due to the pressure difference between the inside and outside of the canister is lower than the inward transport by diffusion, canister corrosion will be diffusion-controlled (see below).

Even after all liquid water has been consumed, iron corrosion will continue, since water vapour can diffuse into the canister. This case has also been modelled by /Bond et al. 1997/ for different corrosion rates, hole sizes in the canister, and areas inside the canister available for corrosion.

The continued corrosion will lead to a continuous increase in the hydrogen pressure. The hydrogen pressure and the transport properties of the surrounding barriers will control the hydrogen release from the canister.

### *Dependencies between process and fuel variables*

Table 2-6 shows how the process influences, and is influenced by, all fuel variables.

**Table 2-6. Direct dependencies between the process "Water and gas transport in the canister: boiling/condensation" and the defined fuel variables and a short note on the handling in SR-Site.**

| Variable | Variable influence on process | | Process influence on variable | |
|---|---|---|---|---|
| | Influence present? (Yes/No) Description | Handling of influence (How/If not – why) | Influence present? (Yes/No) Description | Handling of influence (How/If not – why) |
| Radiation intensity | No. | – | No. | – |
| Temperature | Yes. Influences the distribution between water and vapour. | Neglected for an intact canister. For a failed canister the temperature is assumed to be constant at 11°C. | No. | – |
| Hydrovariables (pressure and flows) | Yes. Obvious. | Neglected for an intact canister. For a failed canister the development inside the canister is based on the modelling by /Bond et al. 1997/. | Yes. Obvious. | Neglected for an intact canister. For a failed canister the development inside the canister is based on the modelling by /Bond et al. 1997/. |
| Fuel geometry | No. | – | No. | – |
| Mechanical stresses | No. | – | Yes. Pressure build-up inside the canister. | Neglected for an intact canister. For a failed canister, see 3.5.1. |
| Radionuclide inventory | No. | – | No. | – |
| Material composition | No. | – | No. | – |
| Water composition | Yes. Water composition influences the corrosion rate. | Neglected for an intact canister. For a failed canister see 3.5.1. | Yes. Release of soluble corrosion products. | See 3.5.1. |
| Gas composition | Yes. Presence of water vapour. | Neglected for an intact canister. For a failed canister see 3.5.1. | Yes. Hydrogen build-up. | See 3.5.1. |

The transport of water and water vapour into the canister will lead to corrosion of the insert. The consequences of corrosion, such as the formation of soluble and solid corrosion products, and gaseous hydrogen will influence the water and gas transport inside the canister and, inversely, the products will influence the water and gas transport in the canister cavity.

#### *Boundary conditions*

Pressures and flows of water and gas at the canister/buffer interface set the boundary conditions for the process. The geometry of the damage in the copper shell forms an important part of these conditions.

#### *Model studies/experimental studies*

The process has been modelled for cracks in the canister by /Wikramaratna et al. 1993/, and in more detail by /Bond et al. 1997/.

No experimental studies of the process of water ingress and water consumption by hydrogen-generating corrosion have been carried out.

#### *Natural analogues/observations in nature*

Not applicable.

#### *Time perspective*

After canister penetration, the time frame is a matter of hundreds to tens of thousands of years /Bond et al. 1997/.

#### *Handling in the safety assessment SR-Site*

For an intact canister, the water and gas transport in the cavity will be negligible from the point of view of long-term safety.

In the case of a canister failure, the process is treated in the SR-Site main report as a part of an integral description of the evolution of the canister interior after damage. The descriptions will be based on the modelling reported in /Bond et al. 1997/ and other sources. Other processes included in the integrated description are advection and diffusion, Section 2.5.1, corrosion of the cast iron insert, Section 3.5.1 and deformation of the canister from internal corrosion products, Section 3.4.4. Several alternative evolutions will be considered to account for conceptual uncertainties arising when integrating a number of processes. Gas release through the buffer must also be included in the description. This is discussed further in the buffer, backfill and closure process report /SKB 2010k/.

The overall important effects of the coupled hydraulic and corrosion processes in the canister interior are *i*) a delay between the occurrence of the penetrating defect in the canister and the onset of radionuclide transport out of the canister and *ii*) the evolution of the hole size as a function of time, which involves also mechanical processes. The purpose of the integral description is to arrive at pessimistic estimates of these two input parameters used in radionuclide transport calculations.

*Model:* The treatment of a developing penetrating defect in the copper shell is further discussed in the Data report, /SKB 2010l, Section 4.2/ based on the modelling in /Bond et al. 1009/.

*Boundary conditions:* The boundary conditions mentioned above are explicitly included in the study by /Bond et al. 1997/.

*Handling of variables influencing this process:* All variables influencing this process according to the influence table above are included in the study by /Bond et al. 1997/. The temperature, however, is assumed to be constant and equal to 11°C, and anaerobic conditions are assumed to prevail in the canister interior.

#### *Handling of uncertainties in SR-Site*

**Uncertainties in mechanistic understanding**

The mechanistic understanding is sufficient for a pessimistic treatment of this process in the safety assessment.

**Model simplification uncertainties**

The integrated internal evolution of a failed canister, of which this process forms a part, can be estimated with sufficient accuracy for the needs of the safety assessment, through pessimistic assumptions.

**Input data and data uncertainties**

For the generation of corrosion gases, the corrosion rates are well-determined empirically and can be modelled with a constant corrosion rate if the water supply is not limiting /Smart et al. 2002a, b/. If the corrosion rate is greater than the supply of water, the corrosion process will be controlled by the transport of water into the canister /Bond et al. 1997/.

Input data and data uncertainties regarding corrosion rates are discussed in Section 3.5.1.

#### *Adequacy of references supporting the handling in SR-Site*

/Bond et al. 1997/ has not been reviewed and approved according to SKB's quality assurance system. In the calculations in SR-Site, however, the information in /Bond et al. 1997/ is used only qualitatively in order to estimate pessimistically the delay time for the start of release as well as the time distribution for when the original small defect has developed into a large defect.

## 2.4 Mechanical processes

### 2.4.1 Mechanical cladding failure

#### *Overview/general description*

Temperature changes in the fuel and mechanical impacts associated with handling and transport will affect the fuel cladding.

Temperature increases lead to increased gas pressure inside the cladding tubes and can cause failure. Uptake of hydrogen during reactor operation may have led to hydride formation with embrittlement, which can lead to failure of the cladding tubes. The increased internal pressure may also lead to delayed failure through creep. In most cases, the damage will be local and result in a leak in the cladding tube.

The process is of importance for the release of radionuclides from the fuel. This can only happen if the cladding tubes are damaged.

#### *Dependencies between process and fuel variables*

Table 2-7 shows how the process influences, and is influenced by, all fuel variables.

#### *Boundary conditions*

There are no relevant boundary conditions for this process other than the physical boundaries set by the geometries of the components involved.

**Table 2-7. Direct dependencies between the process "Mechanical cladding failure" and the defined fuel variables and a short note on the handling in SR-Site.**

| Variable | Variable influence on process | | Process influence on variable | |
|---|---|---|---|---|
| | Influence present? (Yes/No) Description | Handling of influence (How/If not – why) | Influence present? (Yes/No) Description | Handling of influence (How/If not – why) |
| Radiation intensity | No. | – | No. | – |
| Temperature | No, but indirectly through increase of gas pressure. | – | No. | – |
| Hydrovariables (pressure and flows) | Yes, increased gas pressure causes increased creep rate. | Neglected. After failure of the copper canister all cladding tubes are assumed to be damaged. | No. | – |
| Fuel geometry | No. | – | No. | – |
| Mechanical stresses | No. | – | Yes. Increased mechanical stresses in the cladding due to temperature increase. | Neglected. After failure of the copper canister all cladding tubes are assumed to be damaged. |
| Radionuclide inventory | No, but indirectly through heat generation and temperature. | – | No. | – |
| Material composition | Yes. Influence through the alloy used for cladding. | Neglected. After failure of the copper canister all cladding tubes are assumed to be damaged. | – | – |
| Water composition | No. | – | No. | – |
| Gas composition | No. | – | No. | – |

### *Model studies/experimental studies*

Experimental studies and modelling have been carried out for dry storage purposes /BEFAST III 1997/. Hydride formation and delayed failure have been studied for a long time /Northwood and Kosasih 1983, Grigoriev 1996/. /Rothman 1984/ conducted a review of the state of knowledge based on requirements for direct disposal of spent fuel. The conclusion was that failure due to hydride formation, though unlikely, cannot be entirely ruled out.

### *Natural analogues/observations in nature*

Not applicable.

### *Time perspective*

A small fraction of the fuel rods must be assumed to be damaged at the time of disposal. Even after disposal, zirconium hydride can lead to cracks in the cladding.

### *Handling in the safety assessment SR-Site*

The process is of no importance for long-term safety as long as the copper canister is intact. To permit a discussion of retrieval, it can be pessimistically assumed that all cladding tubes may be damaged, but that they still provide physical protection for the fuel, and that the fuel assemblies retain their original geometry.

After failure of the canister, all cladding tubes will pessimistically be assumed to be damaged in the modelling of radionuclide transport.

*Boundary conditions:* As stated above, there are no specific boundary conditions relevant to this process.

*Handling of the variables influencing the process:* With the pessimistic handling of this process, the variables influencing the process are also treated pessimistically.

#### *Handling of uncertainties in SR-Site*

**Uncertainties in mechanistic understanding**

The understanding of the process is not sufficient to permit reliable quantification. In cases where the process is of importance, i.e. when the copper canister is damaged, it will be handled pessimistically, as described above

**Model simplification uncertainties**

Not applicable since the process is not modelled.

**Input data and data uncertainties**

Not applicable since the process is not modelled.

#### *Adequacy of references supporting the handling in SR-Site*

Irrelevant since no credit is taken for the cladding as a barrier against radionuclide release.

### 2.4.2 Structural evolution of the fuel matrix

#### *Overview/general description*

The time at which the fuel will contact water is estimated to be in the range of thousands to millions of years after deposition. The effects of radioactive decay, mainly alpha decay and build-up of helium in the fuel (see further Section 2.5.8), could possibly change the physical and chemical behaviour of the fuel over these long time periods.

Radiation enhanced diffusion, also referred to as "athermal" diffusion, is too slow to be directly observed experimentally. Various models have, therefore, been proposed to estimate this alpha self-irradiation enhanced diffusion /Ferry et al. 2005/. A first upper estimate is based on an extrapolation of the measured athermal diffusion coefficient of uranium atoms during reactor operation. The deduced diffusion coefficient ($D_\alpha$ $m^2/s$) is, thus, proportional to the alpha activity per volume ($A_\alpha$ $Bq/m^3$):

$$D_\alpha \approx 2 \cdot 10^{-41} A_\alpha$$

For $UO_2$ fuel, this equation gives a diffusion coefficient that decreases from $10^{-25}$ $m^2/s$ to $10^{-27}$ $m^2/s$ during the first 10,000 years out of reactor. /Ferry et al. 2005/ also quantify the atom mobility in the spent fuel through more physical modelling. Taking into account the effects of the alpha particle, the electronic excitation and the recoil atoms, a three orders of magnitude lower diffusion coefficient is obtained:

$$D_\alpha \approx 8 \cdot 10^{-45} A_\alpha$$

/Ferry et al. 2008/ describe an experimental study where heavy ion bombardment of iodine implanted $UO_2$ was used to simulate the effect of alpha irradiation on iodine mobility in $UO_2$ fuel. To simulate the ballistic effect, the samples were irradiated with 800 keV ions at fluences of $2 \cdot 10^{16}$ and $5 \cdot 10^{16}$ per $cm^2$. The irradiation damage was similar to the ballistic damage accumulated in MOX fuel with a burnup of 60 MWd/kgHM after 10,000 years. The iodine profiles were then measured with SIMS (Secondary Ion Mass Spectrometry). No measurable displacement of iodine could be detected (less than 50 nm), which is consistent with a diffusion coefficient of about $10^{-28}$ $m^2/s$. Irradiating $UO_2$ pellets with bromine and silver ions simulated the effect of the electronic stopping power of alpha particles on iodine atom mobility. The Br ions had an energy varying between 170 and 220 MeV at a fluence of $10^{15}$ per $cm^2$ and the Ag ions had an energy of 70 MeV at a fluence of $5 \cdot 10^{15}$ per $cm^2$. No mobility of iodine atoms was detected. /Ferry et al. 2008/ concluded that the athermal diffusion process would make a negligible contribution to the Instant Release Fraction (IRF).

/Ferry et al. 2008/ confirm this conclusion and stated that "based on theoretical models supported by experiments simulating α-decay effects on atom mobility in spent fuel, the release of fission products to grain-boundaries should not be significant even on the long-term".

/Van Brutzel and Crocombette 2007/ also modelled athermal diffusion. They studied two mechanisms for accelerated diffusion: the mobility mechanism related to the ballistic collisions during the displacement cascades, and the mobility mechanism related to the thermal diffusion accelerated via the additional point defects created during the irradiation. The values of athermal diffusion coefficients coming from the ballistic collisions and the additional point defects created during the cascades were estimated from these simulations to be less than $10^{-26}$ $m^2/s$ in all cases, including for 1 year old fuel. /Van Brutzel and Crocombette 2007/ did not draw any conclusions on the effect of these processes on the long-term evolution of the IRF. Their data, however, support the conclusions in /Ferry et al. 2005, 2008/.

/Martin et al. 2009/ studied the radiation-induced diffusion in uranium dioxide with molecular dynamics modelling. Their results also show that the contribution from radiation-induced diffusion is too low to be important even for the long-term perspective.

The athermal diffusion mechanism will lead to no significant contribution to release if the diffusion coefficient is less than $1 \cdot 10^{-26}$ $m^2/s$. For a diffusion coefficient of $10^{-26}$ $m^2/s$, the average movement of an atom, given by $x = (Dt)^{0.5}$, would be 5 nm in 100 years or 0.5 μm in $10^6$ years. Therefore, for spent nuclear fuel of the types and burnups that are considered in SR-Site, athermal diffusion is not expected to lead to any increase of the instant release fraction even after a million years.

### *Dependencies between process and fuel variables*

Table 2-8 shows how the process influences, and is influenced by, all fuel variables.

**Table 2-8. Direct dependencies between the process "Structural evolution of the fuel matrix" and the defined fuel variables and a short note on the handling in SR-Site.**

| Variable | Variable influence on process | | Process influence on variable | |
|---|---|---|---|---|
| | Influence present? (Yes/No) Description | Handling of influence (How/If not – why) | Influence present? (Yes/No) Description | Handling of influence (How/If not – why) |
| Radiation intensity | Yes. The alpha decay will cause radiation damage. | The process is neglected for the fuel types and burnup that are relevant for a Swedish repository. | No. | – |
| Temperature | No. The temperature range will be too low to cause any annealing of any radiation damage. | – | No. | – |
| Hydrovariables (pressure and flows) | No. | – | No. | – |
| Fuel geometry | No. | – | No. | – |
| Mechanical stresses | No. | – | No. | – |
| Radionuclide inventory | No, but indirectly through the content of alpha emitters. | – | Yes. If the process was significant, the distribution of radionuclides in the fuel would be altered. | The process is neglected for the fuel types and burnup that are relevant for a Swedish repository. |
| Material composition | No. | – | No. | – |
| Water composition | No. | – | No. | – |
| Gas composition | No. | – | No. | – |

The only variable of importance for this process is the total content of alpha emitters.

### *Boundary conditions*

This is a diffusion process in the fuel rods, meaning that the fuel rod surface is the relevant boundary.

### *Model studies/experimental studies*

The process has been modelled by /Ferry et al. 2005, Van Brutzel and Crocombette 2007, Martin et al. 2009/, see above, and previously by /Lovera et al. 2003/ and /Olander 2004/ (not discussed further here). The results of an experimental study is presented in /Ferry et al. 2005/.

### *Natural analogues/observations in nature*

Attempts have been made by /Lovera et al. 2003/ to apply their models for alpha self-irradiation enhanced diffusion to data from Oklo. Due to alpha decay of the uranium isotopes, lead is built up in the uraninite. The present relative composition of PbO in Oklo ranges between 5.4 and 7.7%. Theoretically, there should be 24.6%, i.e. substantial quantities of the radiogenic lead have left the uraninite. If this loss was through diffusion, the diffusion coefficient would have been in the range of $7.5 \cdot 10^{-27}$ $m^2/s$ to $12.2 \cdot 10^{-27}$ $m^2/s$, i.e. within the range of diffusion coefficients proposed for alpha self-irradiation enhanced diffusion.

/Lovera et al. 2003/ ignored, however, two important facts in their analysis. The Oklo uraninites that contain 5 to 8% Pb have been subjected to episodic loss of Pb on two occasions after their crystallisation at the end of reactor operation. An intrusion of a swarm of dykes at 860 ± 39 Ma caused the expulsion of Pb from the uraninites. This Pb crystallised as mm-sized galena (PbS) crystals, which have an isotopic composition consistent with the Pb having grown in uraninite from 1,950 Ma to 850 Ma. The isotopic composition of Pb in the uraninites surrounding these galena crystals shows an initiation of growth of radiogenic Pb starting at 850 Ma and indicates that Pb was also lost from the uraninites at a later time. Detailed analysis of the isotopic composition data yields results consistent with loss of Pb at the time of the pan-African event, a regional thermal event, at about 500 Ma. Thus, the present Pb content of the uraninites is due to loss of radiogenic Pb during two high temperature events with relatively short duration, followed by ingrowth of new radiogenic Pb from about 500 Ma ago. The isotopic composition of Pb in the mm-sized galenas is consistent with negligible loss of Pb from the uraninites between 1,950 Ma and 850 Ma. The diffusion coefficient of Pb at low temperature from the uraninites during that time period must have been vanishingly small. A complete discussion of the geochronology and petrography of the Oklo 5 to 6% Pb uraninites is provided in /Evins et al. 2005/.

### *Time perspective*

It is a matter of millions of years before the effect will contribute to radionuclide release from the fuel, if at all.

### *Handling in the safety assessment SR-Site*

Based on the findings of /Ferry et al. 2005, 2008, Van Brutzel and Crocombette 2007, Martin et al. 2009/, the process is neglected for the fuel types and burnup that are relevant for a Swedish repository.

### *Handling of uncertainties in SR-Site*

#### Uncertainties in mechanistic understanding

Bounding estimates allow neglect of this process despite an incomplete mechanistic understanding (see above).

#### Model simplification uncertainties

Bounding estimates allow neglect of this process despite model simplifications, see above.

**Input data and data uncertainties**

Bounding estimates allow neglect of this process despite data uncertainties, see above.

#### *Adequacy of references supporting the handling in SR-Site*

/Ferry et al. 2005/ is the final report from the French PRECCI project. The review process is unknown. All other references used to support the handling of this issue in SR-Site are peer reviewed journal papers or peer reviewed conference proceedings papers.

## 2.5 Chemical processes

### 2.5.1 Advection and diffusion

#### *Overview/general description*

Solutes can be transported to and from the interior of the canister by advection and diffusion. These processes are not discussed explicitly, but dealt with integrated with other processes (often with pessimistic simplifications). (See also Section 2.6 for the handling of radionuclide transport).

#### *Dependencies between process and fuel variables*

Table 2-9 shows how the process influences, and is influenced by, all fuel variables.

The advection and diffusion in the canister cavity are influenced by the temperature, and require the presence of water or gas.

**Table 2-9. Direct dependencies between the process "Advection and diffusion" and the defined fuel variables and a short note on the handling in SR-Site.**

| Variable | Variable influence on process | | Process influence on variable | |
|---|---|---|---|---|
| | Influence present? (Yes/No) Description | Handling of influence (How/If not – why) | Influence present? (Yes/No) Description | Handling of influence (How/If not – why) |
| Radiation intensity | No. | – | No. | – |
| Temperature | Yes. | For an intact canister, the process is neglected. In the case of a canister failure, see Section 2.3.1, Section 2.6 and Chapter 13 in the SR-Site main report /SKB 2011/. | No. | – |
| Hydrovariables (pressure and flows) | Yes. | See above. | No. | – |
| Fuel geometry | Yes. | See above. | No | – |
| Mechanical stresses | No. | – | No. | – |
| Radionuclide inventory | No. | – | Yes. The process redistributes radionuclides in the canister interior. | See above. |
| Material composition | No. | – | No. | – |
| Water composition | Yes. Differences in concentration cause diffusion. | See above. | Yes. The process redistributes water solutes in the canister interior. | See above. |
| Gas composition | No. | – | No. | – |

#### *Boundary conditions*

Pressures and flows of water and gas as well as concentrations of radionuclides at the transition to the buffer set the boundary conditions for the process.

#### *Model studies/experimental studies*

There are no direct modelling or experimental studies for the case of a KBS 3 canister interior.

#### *Natural analogues/observations in nature*

Not applicable.

#### *Time perspective*

The process requires water intrusion. Even for an initially defect canister, water intrusion into the canister insert is highly unlikely to occur before at least 1,000 years have elapsed after waste deposition in the repository /Bond et al. 1997/, and, in the general case, before millions of years.

#### *Handling in the safety assessment SR-Site*

For an intact canister, the process is neglected.

In the case of a canister failure, the process is treated in the SR-Site main report as a part of an integral description of the evolution of the canister interior after damage (see Section 2.3.1). In the treatment of transport of dissolved species, the canister interior is essentially regarded as a well-stirred tank.

For the case of radionuclide transport, see Section 2.6.

#### *Handling of uncertainties in SR-Site*

**Uncertainties in mechanistic understanding**

Advection and diffusion are well-understood mechanisms for solute transport.

**Model simplification uncertainties**

See Sections 2.3.1 and 2.6.

**Input data and data uncertainties**

See Sections 2.3.1 and 2.6.

#### *Adequacy of references supporting the handling in SR-Site*

See Sections 2.3.1 and 2.6.

### 2.5.2 Residual gas radiolysis/acid formation

#### *Overview/general description*

Air and water in an intact canister can be decomposed by means of radiolysis. The products can then be converted to corrosive gases such as nitric and nitrous acids. These gases can be of importance for stress corrosion on the canister insert (see Section 3.5.3).

#### *Dependencies between process and fuel variables*

Table 2-10 shows how the process influences, and is influenced by, all fuel variables.

**Table 2-10. Direct dependencies between the process "Residual gas radiolysis/acid formation" and the defined fuel variables and a short note on the handling in SR-Site.**

| Variable | Variable influence on process | | Process influence on variable | |
|---|---|---|---|---|
| | Influence present? (Yes/No) Description | Handling of influence (How/If not – why) | Influence present? (Yes/No) Description | Handling of influence (How/If not – why) |
| Radiation intensity | Yes. The intensity determines the extent of radiolysis. | The amount of radiolysis product (nitric acid) is estimated based on the availability of nitrogen in the canister. | No. | – |
| Temperature | No. | – | No. | – |
| Hydrovariables (pressure and flows) | Yes. The amount of radiolysis products depends on the availability of water and residual gases in the canister. | The amount of radiolysis product (nitric acid) is estimated based on the availability of nitrogen in the canister. | Yes, but any effect is negligible. | Neglected. |
| Fuel geometry | No. Indirectly through the radiation intensity. | – | No. | – |
| Mechanical stresses | No. | – | No. | – |
| Radionuclide inventory | No. Indirectly through the radiation intensity. | – | No. | – |
| Material composition | No. | – | No. | – |
| Water composition | Yes. Dissolved solids and gases will influence the radiolysis products formed. | The water trapped inside the canister will be either reactor water or water from the storage pools at Clab. It can, therefore, be assumed to be clean water with very low ionic strength. | Yes. Radiolysis products will be formed in the water. | The amount of radiolysis product (nitric acid) is estimated based on the availability of nitrogen in the canister. |
| Gas composition | Yes. Gases will influence the radiolysis products formed. | The gas inside the canister is assumed to be at least 90% Ar and air. | Yes. Gaseous radiolysis products will be formed. | The amount of radiolysis product (nitric acid) is estimated based on the availability of nitrogen in the canister. |

### *Boundary conditions*

There are no relevant boundary conditions for this process other than the physical boundary set by the geometries of the components involved.

### *Model studies/experimental studies*

The production of nitric acid has been calculated by /Marsh 1990/, /Henshaw et al. 1990/ and /Henshaw 1994/ for two different dose rates and for different quantities of air and water in the canister. Not unexpectedly, the quantity of nitric acid formed is dependent on the presence of sufficient quantities of water and air. The rate at which nitric acid is formed is dependent on the dose rate. The calculations show that with 50 g of water, i.e. the volume of water corresponding to the void volume inside a fuel pin, just under 160 g of nitric acid can be formed /Henshaw et al. 1990/. The availability of water will limit the amount of nitric acid that can form.

/Jones 1959/ studied the radiation-induced reactions in the nitrogen/oxygen/water homogeneous system and found that the formation of nitric acid was linear with the absorbed dose. The formation proceeded to a total concentration that was stoichiometrically equivalent to the amount of hydrogen initially present in the water. In the current plans for the encapsulation plant, the design goal is that no more than 600 g of water should be transferred to the canister with the fuel elements. In this case, the availability of water will no longer limit the amount of nitric acid produced. Instead, the

availability of nitrogen will be the limiting factor. The void volume in a canister with fuel will be approximately 1 $m^3$, see further the SR-Site data report /SKB 2010l, Section 4.1/. This corresponds to about 800/22.4 mol (NTP) of $N_2$ and for complete conversion of $N_2$ to $HNO_3$, 2·800/22.4=71.4 mol $HNO_3$ or 4,500 g. During the encapsulation, the air in the canister will be replaced by argon gas and at the most 10% residual air will remain in the canister. At that level of residual air, no more than 450 g of nitric acid can be formed.

#### *Natural analogues/observations in nature*

Not applicable.

#### *Time perspective*

The transformation of residual air and water to nitric acid takes place over the course of years to tens of years /Henshaw et al. 1990, Henshaw 1994/.

#### *Handling in the safety assessment SR-Site*

In an intact canister, residual oxygen, water and radiolytically formed nitric acid will be consumed by corrosion reactions with the canister insert. At the expected corrosion rates, it will take about 100 years to consume the oxidants inside the canister. As a consequence, all the oxidants will be consumed before a potential canister failure and will not have to be considered for a failed canister. (For discussions of canister lifetimes, see e.g. /King et al. 2001/.) The total depth of insert penetration by general corrosion is of the order of ten μm, which is negligible. The process is therefore neglected in the safety assessment. The consequences of stress corrosion cracking (SCC) are discussed in Section 3.5.3.

#### *Handling of uncertainties in SR-Site*

**Uncertainties in mechanistic understanding**

The mechanistic understanding is sufficiently good for the purpose of safety assessment.

**Model simplification uncertainties**

Mass balance considerations put an upper bound on the amount of nitric acid that could be produced.

**Input data and data uncertainties**

The maximum allowed amount of water in a canister is 600 g. The uncertainty concerns the quantity of water that is actually inadvertently introduced into the canister. This quantity is expected to be much less than the allowed 600 g.

#### *Adequacy of references supporting the handling in SR-Site*

Irrelevant, since the assessment of the possible total amount of nitric acid formed is based on the amount nitrogen in the residual gas in the canister void volume.

### 2.5.3 Water radiolysis

#### *Overview/general description*

Water that enters a damaged canister and reaches the cavities between the fuel assemblies and the canister insert is affected by the ionising radiation emitted by the spent fuel. This causes the excitation, or ionisation of water molecules followed by breaking of their chemical bonds (*radiolysis*) producing primarily free electrons, OH-radicals and hydrogen atoms. Radicals are atoms or atomic groups resulting from the breaking of a chemical bond and containing a free or unpaired electron, which makes them highly reactive and able to participate in radiolytic chain reactions. Through such reactions with the solution components, a large variety of radicals are formed, as well as the

stable molecular species $O_2$, $H_2O_2$, and $H_2$. Only gamma radiation, which has low Linear Energy Transfer (LET), and hence a relatively long range, is discussed here since it affects the water in the canister cavities. Radiolysis at the fuel/clad gap is dealt with in Section 2.5.5, when fuel dissolution is discussed.

The production of reducing species by radiolysis results in a build-up of hydrogen gas in the void in the canister, while the simultaneous corrosion of the cast iron insert also produces hydrogen, as well as Fe(II) ions in solution. After some time, the hydrogen gas amounts produced by gamma radiolysis will reach a constant value and the result of continued gamma radiolysis will be reformation of water /Christensen and Bjergbakke 1982, 1984/.

The quantity of hydrogen gas produced by gamma radiolysis is dependent on the gamma dose rate. The contribution made by radiolysis to hydrogen gas formation is negligible compared with the contribution made by corrosion of the cast iron insert (see Section 3.5.1).

### *Dependencies between process and fuel variables*

Table 2-11 shows how the process influences, and is influenced by, all fuel variables.

The radiation intensity affects the production of radical and molecular radiolysis products. At the time of water intrusion, the gamma field of the spent fuel is expected to have decreased to negligible levels.

**Table 2-11. Direct dependencies between the process "Water radiolysis" and the defined fuel variables and a short note on the handling in SR-Site.**

| Variable | Variable influence on process | | Process influence on variable | |
|---|---|---|---|---|
| | Influence present? (Yes/No) Description | Handling of influence (How/If not – why) | Influence present? (Yes/No) Description | Handling of influence (How/If not – why) |
| Radiation intensity | Yes.<br>The radiolysis is proportional to the dose rate. | Neglected.<br>In a failed canister the contribution to hydrogen gas production is considerably smaller than the contribution from iron corrosion. For radiolysis effects on fuel dissolution see 2.5.5. | No. | – |
| Temperature | Yes. | Neglected.<br>See text and row above. | No. | – |
| Hydrovariables (pressure and flows) | Yes.<br>Presence of water in the canister is required. | Neglected.<br>See text and first row above. | Yes.<br>Radiolytic gas production. | Neglected.<br>See text and first row above. |
| Fuel geometry | No.<br>Indirectly through radiation intensity. | – | No. | – |
| Mechanical stresses | No. | – | No. | – |
| Radionuclide inventory | No.<br>Indirectly through radiation intensity. | – | No. | – |
| Material composition | No. | – | No.<br>Radiolysis may form corrosive species. | – |
| Water composition | Water solutes participate in radiolytic reactions. | Neglected.<br>See text and first row above. | Yes.<br>Radiolytic production of water solutes. | Neglected.<br>See text and first row above. |
| Gas composition | Yes.<br>Gases participate in radiolytic reactions. | Neglected.<br>See above. | Yes.<br>Radiolytic gas production. | Neglected.<br>See text and first row above. |

The temperature affects the kinetics of radiolytic reactions and can be accounted for in radiolytic modelling. At the time of water intrusion into the canister, the temperature is expected to have decreased to near ambient values and the influence is expected to be negligible.

The presence of water in the canister is a requirement for the radiolysis process to take place, while the production of radiolytic gases affects the pressure in the canister. As discussed above, the effect on pressure is expected to be negligible in comparison to the production of hydrogen by the corrosion of iron.

The fuel geometry affects the resultant gamma field inside the canister while the overall surface area of the fuel is of importance for the beta and alpha fields.

The influence of the radionuclide inventory is accounted for by the radiation intensity.

The composition of the water influences the yields and reactions of the different radiolytic species produced by radiolysis. The different radiolytic reactions in homogeneous solutions are modelled by kinetic radiolytic modelling with reliable results. The presence of excess dissolved hydrogen in the groundwater solution inside the canister affects the gamma radiolysis of water through reactions of molecular hydrogen with radicals such as by the reaction $OH\cdot + H_2 = H_2O + H\cdot$, which converts the oxidising radical OH· to water and the reducing radical H· (atomic hydrogen).

### *Boundary conditions*

There are no relevant boundary conditions for this process other than the physical boundaries set by the geometries of the components involved.

### *Model studies/experimental studies*

Radiolysis of water has been thoroughly studied by both experiments and modelling. Low LET (Linear Energy Transfer) radiation, such as gamma radiation, does not produce any detectable amounts of the stable species $H_2$ and $H_2O_2$ in pure de-aerated water /Allen 1961/, because they react via OH· and H· radicals in a chemical chain reaction to reform $H_2O$. In aerated water, virtually all the hydrated electrons and H· radicals formed are oxidised by $O_2$, and the main products of low LET water radiolysis in a system open to air are a steady state concentration of $H_2O_2$ with constant releases of $H_2$ and $O_2$ /Spinks and Woods 1990/.

Recent experimental and radiolytic modelling studies on gamma radiolysis of water containing relatively small amounts of dissolved hydrogen /Pastina et al. 1999, Pastina and LaVerne 2001/ show that the production of oxidants involves a threshold; i.e. above a certain concentration of dissolved hydrogen no measurable oxidant production occurs. In studies of spent fuel corrosion in the presence of metallic iron /Loida et al. 1996, Grambow et al. 2000/ in 5 M NaCl solutions, no traces of radiolytic oxygen could be detected in the gas phase and reduced corrosion products of iron, such as magnetite and green rust, were analysed on the iron at the end of long term tests. The presence of such corrosion products on iron surfaces indicates extremely low concentrations of radiolytic oxidants in the solution. The absence of any radiolytic gas production in 5 M NaCl solutions containing 0.85 mM dissolved hydrogen was observed in another study /Kelm and Bohnert 2004/. The production of radiolytic gases in 5 M NaCl solutions was shown to restart in the presence of bromide ions /Kelm and Bohnert 2005/ and in the presence of $UO_2$ /Metz et al. 2007/. However, in the presence of spent fuel surfaces the uranium concentrations decreased again, indicating strong interfacial reactions with the fuel surface /Loida et al. 2007, Cui et al. 2008/.

### *Natural analogues/observations in nature*

Not applicable.

### *Time perspective*

The process contributes to hydrogen gas formation during the first centuries after deposition. After that, gamma radiation declines to negligible levels.

#### *Handling in the safety assessment SR-Site*

In a damaged canister, the contributions made by radiolysis to hydrogen gas production and other effects are neglected, since these effects are considerably smaller than the corresponding effects of corrosion by water of the cast iron insert. The process can be neglected regardless of time for water intrusion, since the presence of Fe(II) and hydrogen from iron corrosion will result in negligible effects from radiolysis. In addition, gamma radiolysis is only relevant for a few hundred years after deposition in the repository.

Radiolysis effects on fuel dissolution are dealt with in Section 2.5.5.

#### *Handling of uncertainties in SR-Site*

**Uncertainties in mechanistic understanding**

The mechanistic understanding of the process is sufficient for the needs of the safety assessment.

**Model simplification uncertainties**

Not relevant since the process is not modelled.

**Input data and data uncertainties**

Not relevant since the process is not modelled.

#### *Adequacy of references supporting the handling in SR-Site.*

/Christensen and Bjergbakke 1982, 1984/ are Studsvik reports compiled within Studsvik's Quality Assurance system according to ISO 9001 and were reviewed and approved by two different individuals. All other references are peer-reviewed journal or conference papers.

### 2.5.4 Metal corrosion

#### *Overview/general description*

The cladding tubes for the fuel are made of Zircaloy. Other structural elements in the fuel are made of stainless steel, Inconel, Incoloy or Zircaloy. The PWR control rods will also be encapsulated with the PWR fuel elements. These control rods are made of an alloy containing 80% silver, 15% indium and 5% cadmium and have a Zircaloy cladding. Some of the radioactivity in the fuel is present in the cladding tubes and other metal parts as neutron activation products of alloying elements and impurities present in the as-fabricated materials.

If water enters the canister, the metal parts will corrode. The corrosion rate and the release of activation products from the Zircaloy will be controlled by the dissolution rate of the surface film of zirconium dioxide, which is tightly bound to the metal surface. The dissolution of the oxide film will be controlled by the solubility of $ZrO_2$ in the water in the immediate vicinity of the fuel and the removal of dissolved zirconium species. The solubility of $ZrO_2$ in water is very low, on the order of $10^{-9}$ M / Brown et al. 2005, Bruno et al. 1997/.

Considering the low corrosion rate of Zircaloy and in view of the low solubility of $ZrO_2$ in water, the rate of the release of activation products from the cladding tubes will be very low.

#### *Dependencies between process and fuel variables*

Table 2-12 shows how the process influences, and is influenced by, all fuel variables.

Any water in the canister cavity can lead to corrosion of cladding tubes and other metal parts in the fuel. The process is controlled mainly by the material composition, the chemical environment in the canister cavity, and the temperature.

**Table 2-12. Direct dependencies between the process "Metal corrosion" and the defined fuel variables and a short note on the handling in SR-Site.**

| Variable | Variable influence on process | | Process influence on variable | |
|---|---|---|---|---|
| | Influence present? (Yes/No) Description | Handling of influence (How/If not – why) | Influence present? (Yes/No) Description | Handling of influence (How/If not – why) |
| Radiation intensity | No. Indirectly through radiolysis that may form corrosive species and water composition. | – | No. | – |
| Temperature | Yes. Corrosion rates tend to increase with temperature. | Neglected. This effect is limited under anoxic conditions. | No. | – |
| Hydrovariables (pressure and flows) | Yes. Presence of water is required. | Water is assumed to be present after canister failure. | No. | – |
| Fuel geometry | No. | – | No. | – |
| Mechanical stresses | Yes. May cause stress corrosion cracking of the fuel metal parts. | No credit is given to cladding integrity. | No. | – |
| Radionuclide inventory | No. Indirectly through the radiation intensity. | – | No. | – |
| Material composition | Yes. Different alloys may have different corrosion rates. The effect will most likely be negligible. | Corrosion rate estimates based on stainless steel. | No. | – |
| Water composition | Yes. Metals have different corrosion rates in different waters. The effect will most likely be negligible. | Neglected. Limited influence under anoxic conditions. | Yes. The influence is small due to the low Zr solubility. | See text. |
| Gas composition | No. | – | No. | – |

The process affects the isolating function of cladding tubes and metal parts that enclose the fuel and is, therefore, of importance for the release of radionuclides from the fuel. The corrosion of metal parts also leads to release of the activation products that have formed in the metal parts.

### *Boundary conditions*

There are no relevant boundary conditions for this process other than the physical boundary set by the geometries of the components involved.

### *Model studies/experimental studies*

No studies of the corrosion rate of Zircaloy have been conducted by SKB, but a thorough literature review was performed in 1984 by the Lawrence Livermore National Laboratory for a tuff repository /Rothman 1984/. From Rothman's data, the corrosion rate can be estimated to be approximately 2 nm/year, i.e. penetration of the cladding tubes is estimated to require 400,000 years at a tube thickness of 0.8 mm.

Although no detailed studies of corrosion of Zircaloy in the repository environment have been conducted, similar studies have been conducted for titanium /Mattsson and Olefjord 1984, 1990, Mattsson et al. 1990/. The corrosion properties of titanium are very similar to those of zirconium, since it is protected against general corrosion by a similarly adherent and insoluble surface film of oxide. The results of the investigations showed that the oxide film remained tightly bound to the underlying metal and that the corrosion rate was extremely low, approximately 2 nm/year. This is very similar to the corrosion rate of Zircaloy based on Rothman's data.

Within the range of possible water compositions inside the canister, there is no reason, within the accuracy of the estimated corrosion rates, to expect a dependence of corrosion rate on water composition and amount of water available as long as water or water vapour are present. Due to passivation of the Zircaloy, any radiolytically produced nitric acid is expected to preferentially corrode the cast iron insert.

The principal uncertainty is whether the corrosion rates observed in short-duration experiments are valid for geological time spans. The corrosion rate of Zircaloy (titanium) is measured over a short period compared with the expected life of the cladding tubes. The greatest uncertainty stems from the extrapolation of these short-term data. /Mattsson and Olefjord 1990/ derived a logarithmic growth law for the oxide layer on titanium based on measurements over a three-year period. After a rapid growth of an initial passivating film of about 7 nm, further growth takes place extremely slowly. An extrapolation to $10^6$ years gives an oxide layer thickness of 12 nm.

Data from /Mattsson and Olefjord 1990/ also show, that for longer periods of 5 and 6 years, the growth rate deviates from the logarithmic law. After 6 years the film was 0.7 nm thicker than calculated, while the five-year samples showed a considerable distribution (from 4.9 to 15.5 nm) suggesting extrapolation according to a logarithmic law may not always be appropriate. For shorter exposures, the oxide film was amorphous, but after longer exposure periods it was partially crystallised. It is, therefore, possible that the higher growth rate is attributable to more rapid ion transport through grain boundaries. During the first year the film grows about 8 nm leading to passivation of the freshly exposed surface. Consequently, a rate of 8 nm/year can be regarded as an upper limit for the corrosion rate and corresponds to a life of 100,000 years for the Zircaloy cladding. In a review of corrosion rates of titanium in "fresh" groundwaters (Yucca Mountain J-13 groundwater) or "salt waters" (about 1,000 times more concentrated in most species than J-13 water) the corrosion rates were found to have little dependence on exposure temperature (60°C and 90°C) or the composition of the test medium /Hua et al. 2005/. General corrosion rates, determined from weight loss measurements on planar and creviced specimens from 5 year tests yielded median values of 5 nm/year and 10 nm/year, respectively.

The other engineering materials in the fuel are stainless steels or nickel-base alloys. SKB has not conducted any investigations of the corrosion resistance of these materials under repository conditions and, in general, there are few studies under anaerobic conditions.

Corrosion rates of stainless steel in aerated "fresh" waters at 25–100°C in the interval 0.01–0.25 µm/year are reported in /BSC 2004/. For aerated interstitial clay waters at 25–75°C /Casteels et al. 1986/ report rates in the interval 0.1–0.96 µm/year. Results from the IAEA project on spent fuel performance assessment and research(SPAR) show corrosion rates of stainless steel during interim storage of spent fuel in the presence of radiolysis on the order of 0.3 µm/year /IAEA 2003/. Saline groundwaters may lead to relatively high corrosion rates. A literature review of the corrosion resistance of similar candidate materials for encapsulation of nuclear fuel for the American Nuclear Waste Management Program in aerated "saltwaters" (see above) /BSC 2004/ reports corrosion rates from 2 to 11.4 µm/year. Even higher rates for brief exposures in air saturated seawater are reported by /Gdowski and Bullen 1988/. As with the maximum rate obtained for brief exposures of titanium discussed above, these rates represent conservative upper limits, and the long term rates will be considerably lower.

However, there is no evidence that stainless steel will de-passivate in saline anaerobic groundwaters. A corrosion rate of 0.8 µm/year for stainless steel in anoxic seawater at 24–40°C is reported by /White et al. 1966/. In a state of the art report of the EU-project Cobecoma, in-situ anoxic corrosion experiments in Boom clay revealed that the average uniform corrosion rates of a series of stainless steels at 16 to 140°C were in the range 0.003–0.15 µm/year. Electrochemical experiments and immersion tests performed to investigate the influence of various factors on the pitting susceptibility of stainless steel and Ni alloys showed that these materials were resistant to pitting under all tested experimental conditions ($T_{max}$=140°C, $[Cl^-]_{max}$= 50 g/L, $[S_2O_3]_{max}$= 200 mg/L) /Kursten et al. 2004/. No appreciable general corrosion rates (< 0.1 µm/year) nor sensitivity to localised corrosion were observed for stainless steel tested in granitic-bentonite water at 90°C over one year of exposure /Kursten et al. 2004/.

Under anoxic conditions /Wada et al. 1999/ measured very low corrosion rates (< 0.01 μm/year) of 304 SS stainless steel, the material of the hull-end pieces of the fuel elements, in seawater based groundwater of pH 10. /Smart et al. 2004/ report anaerobic corrosion rates of stainless steel in alkaline environments in the range of 0.01 to 0.1 μm/year. The corrosion rates under anoxic conditions in neutral to alkaline environments were found to be relatively insensitive to pH within the range 6.4 to 13 /Blackwood et al. 2002/.

From these few studies under anoxic conditions, the corrosion rates of stainless steel and nickel based alloys are estimated to be 0.15 μm/year and within the range 0.01–1 μm/year, where the highest rates occur in saline groundwaters. With this estimate for corrosion rates, the lifetimes of the thinnest nickel alloy parts in fuel elements (0.3 mm, /SKBdoc 1198314/) range from a hundred years to ten thousand years, while the lifetimes of thicker stainless steel parts will obviously be longer.

The main constituent in the alloy used in the control rods is silver (80%). Silver is a noble metal and if the alloy is exposed to anoxic groundwaters, no silver corrosion is expected, unless the water contains dissolved sulphides (see e.g. /McNeil and Little 1992/). In that case, the silver corrosion rate will be controlled by the rate of supply of sulphide.

### *Natural analogues/observations in nature*

Not applicable, except for silver and silver alloys. There are, to our knowledge, no systematic studies performed on silver artifacts as analogues.

### *Time perspective*

After water has come into contact with the cladding tubes, corrosion accompanied by release of activation products is expected to proceed at a constant rate for hundreds of thousands of years. The equivalent time frame for stainless steel components or nickel-based alloys is thousands of years.

### *Handling in the safety assessment SR-Site*

Available data suggest a life of the cladding tubes of at least 100,000 years. Although Zircaloy is highly resistant to uniform corrosion, cladding is not assumed to constitute a barrier to radionuclide release from the fuel, due to its potential susceptibility to local corrosion in groundwaters and to hydrogen induced cracking. Following the arguments presented in /Johnson and McGiness 2002/, the amount of $^{14}C$ present in the oxide layer (20%) is assumed to be released immediately upon water contact. The release of the remaining activation products from Zircaloy is assumed to occur at the rate of its uniform corrosion under anoxic conditions. This rate is pessimistically assumed equal to the release rates of activation products from stainless steel. Another reason for this is that the inventory of activation products for all metal parts together is reported in the Spent fuel report /SKB 2010b/. The available experimental data suggest that the release of activation products from all metal parts may be modelled in SR-Site with a constant fractional release rate in the range of $10^{-2}$ to $10^{-4}$ per year. A triangular distribution with a peak at $10^{-3}$ per year seems to give sufficient margin for assessing defendable release rates of the activation products.In SR-Site, however, the cladding tubes are assumed not to have any barrier function against release of radionuclides from the fuel.

The whole radionuclide inventory contained in CRUD (Chalk River Unidentified Deposits) is assumed to be released instantaneously upon water contact. The same is assumed in SR-Site for the radionuclide inventory in the control rods. This is a pessimistic assumption, at least concerning the release of radioactive silver isotopes. They will very probably be released at the rate of corrosion of metallic silver, which is expected to be controlled by the availability of dissolved sulphide in the groundwater /McNeil and Little 1992/.

### *Handling of uncertainties in SR-Site*

**Uncertainties in mechanistic understanding**

The mechanistic understanding of the process of Zircaloy and stainless steel corrosion is sufficient for the needs of the safety assessment.

**Model simplification uncertainties**

The activation products are assumed to be released at a constant rate as the metal corrodes passively. The higher corrosion rates for stainless steel are used as the basis for estimating the release rate of activation products from all metallic parts, including the much more corrosion resistant Zircaloy parts. Release rates are assessed on the basis of lifetime estimations for the thinnest metal parts.

**Input data and data uncertainties**

The release rates of activation products are based on the corrosion rates of metallic parts under repository conditions. There are sufficient data of good quality to support much lower corrosion rates than the ones assumed here for Zircaloy metal parts, which constitute the largest proportion by weight of all metal parts in a fuel element /Håkansson 2007/. The data used for estimation of the corrosion of stainless steel under anoxic conditions are based on the results of /Kursten et al. 2004, White et al. 1966, Wada et al. 1999, Smart et al. 2004/. The uncertainties in the measured corrosion rates depend primarily on the method used to measure corrosion rates, especially for very low rates, as discussed in /Smart et al. 2004/. The uncertainties are further discussed in the SR-Site data report /SKB 2010l/.

***Adequacy of references supporting the handling in SR-Site***

There are several review works, such as /Rothman 1984/, /Johnson and McGinnes 2002 and references therein/, which report much lower corrosion rates for Zircaloy than the ones used here. The papers by /Mattsson and Olefjord 1990/, /Mattsson et al. 1990/, /Hua et al. 2005/ on the corrosion rates of titanium are peer reviewed journal papers. The report by /Kursten et al. 2004/ reviews the research in corrosion of canister materials in European countries and is based on several published works. The papers by /White et al. 1966/, /McNeil and Little 1992/ and /Wada et al. 1999/ are peer reviewed journal or conference papers.

### 2.5.5 Fuel dissolution

***Overview/general description***

If water enters the canister cavity, the fuel may be dissolved/transformed, resulting in the release of uranium and other radionuclides contained in the fuel matrix. The process, which requires that the protective cladding tubes have been breached (Section 2.4.1), is controlled primarily by the chemical environment in the fuel-clad gap, particularly the presence of oxidants, and by the fuel composition, where matrix structure and the presence of radionuclides in the fuel matrix are decisive.

The process is of fundamental importance, since it describes the release of radionuclides from the fuel matrix and its contribution to the source term.

**Non-matrix-bound activity**

Radionuclides that have been segregated to the fuel-clad gap will rapidly go into solution. The quantity of activity released is determined by the solubility and availability of segregated radionuclides. Many of the segregated radionuclides in the gap and within grain boundaries in the fuel have high solubility and mobility and are assumed to be released immediately upon water contact. The release from the gap is independent of the dissolution or transformation of the uranium dioxide matrix of the spent fuel and is discussed in more detail in Section 2.5.6.

**Matrix-bound activity**

The majority of fission products and higher actinides in the fuel exist in solid solution in the uranium dioxide matrix. The release of these radionuclides requires that the uranium dioxide matrix of the spent fuel be dissolved or otherwise altered, for example by oxidation. This can happen only if water has entered the canister and the cladding tubes are breached. The redox conditions under which dissolution of spent fuel occurs are by far the most important factor influencing the dissolution process.

*Redox conditions in connection with water ingress:* When water comes into contact with the fuel, the uranium dioxide will begin to dissolve. This will occur by chemical dissolution of the $UO_2$(s) matrix or by corrosion of the fuel, depending on the redox conditions in the immediate vicinity of the fuel. At the time of liquid water ingress, the corrosion of cast iron by water vapour is expected to have produced substantial amounts of hydrogen, part of which will dissolve in the intruding water and be present together with Fe(II) ions.

Any oxygen remaining in the repository near field after closure, at the time of groundwater ingress, will have been consumed by bacteria, reducing minerals in the rock and bentonite, and minimal corrosion of the Cu container (Section 3.5.4). Furthermore, the oxidation of iron by any intruding oxygen will likely proceed much faster than oxidation of $UO_2$ inside a damaged canister. An estimate of the time required to consume the oxygen in a copper canister shows that any residual oxygen will be consumed by oxidation of copper within a year or so /Kolár and King 1996/. The consumption rate in an iron canister should be comparable, since the corrosion rates of iron and copper are comparable /Wersin et al. 1993/. There are, therefore, no appreciable uncertainties surrounding the assumption that the water that will come into contact with the fuel will be oxygen-free. Any contribution to the oxidative dissolution of fuel should, therefore, be caused only by the radiolytic oxidants produced by water radiolysis.

Even for an initially defect canister, the first entry of water into the canister insert is not expected to occur until more than a thousand years after deposition /Bond et al. 1997/. By that time the predominant form of radiation will be alpha decay. Alpha particles have high LET (Linear Transfer Energy) and a very short range. They can cause radiolysis of a thin layer of water (~35µm) near the fuel surface and produce mainly the molecular radiolysis products $H_2O_2$ and $H_2$. During recent years, several studies have shown a threshold for the alpha activity below which no measurable effect of alpha radiolysis on fuel dissolution can be observed, even in carbonated de-aerated water /Rondinella et al. 2004, Muzeau et al. 2009/. /Poinssot et al. 2007/ give a range of 18 to 33 MBq/g $UO_2$ for this threshold. This gives a time range of 3,500 to 55,000 years, where 3,500 years corresponds to an alpha activity threshold of 33 MBq/g (representative of a fuel with a burnup of 33 MWd/kgU UOX fuel) and 55,000 years corresponds to a threshold of 18 MBq/g (representative of a fuel burnup of 60 MWd/kgHM MOX). From this perspective, the dissolution rates proposed to be used in SR-Site, especially after a few tens of thousands of years, are conservative and it would be legitimate instead to assume chemical equilibrium of the $UO_2$(s) for such old fuels /Poinssot et al. 2007/.

In other experiments performed in the presence of reducing species produced by anaerobically corroding iron, the effect of water radiolysis by alpha radiation on the dissolution of spent fuel has been studied by using solid $UO_2$ doped with $^{233}U$. These samples contained alpha activity that approximated the levels expected 3,000 and 10,000 years after disposal of spent fuel. The tests were performed in the presence of anaerobically corroding iron. The results showed no evidence for enhanced dissolution of samples containing $^{233}U$ over those that contained only normal levels of $^{235}U$ and $^{238}U$ /Ollila et al. 2003, Ollila and Oversby 2006/. The experiments were thoroughly analysed for the location of precipitated uranium. Negligible amounts were found on the corroding iron /Ollila and Oversby 2005/. The release of U from the samples, especially during the first year or so of testing, appeared to be dominated either by high energy surface sites formed by crushing of the samples or by high-energy interior sites at grain boundaries or associated with crystal imperfections. Similarly, low solution concentrations of U from $^{233}U$ doped samples in autoclave tests under a hydrogen overpressure (corresponding to 3,000 years after disposal) have been reported by /Carbol et al. 2005, 2009a/.

Higher burnup may also affect the dissolution rate. It increases the content of fission products and higher actinides resulting in a higher radiation field. It also increases the surface area of the fuel, especially at the fuel rim. Recent studies indicate, however, that both these factors are counteracted effectively by the doping effect caused by increase in fission product and actinide content /Ekeroth et al. 2009, Hanson and Stout 2004/, as discussed further in the section Model studies/experimental studies. This means that the matrix dissolution model used in SR-Site should be valid for all types of fuel, including HBU (High Burn-Up) fuels.

Since no enhanced dissolution due to alpha radiolysis was observed, there is no evidence of a mechanism to produce a redox front of oxidised radionuclides inside the canister. This is discussed further in the section Model studies/experimental studies.

### *Dependencies between process and fuel variables*

Table 2-13 shows how the process influences, and is influenced by, all fuel variables. Further details are given below.

The process is influenced by radiation intensity, which determines the dose rate to water and the production of radiolytic oxidants. As discussed above, the dominating radiation at the time of water intrusion will be alpha radiation and its levels in spent fuel after 1,000 or more years are not expected to cause measurable oxidative dissolution of the uranium dioxide matrix in the presence of anaerobically corroding iron and its corrosion products /Werme et al. 2004/.

The temperature affects both the kinetics of all chemical reactions, including radiolytic and dissolution/precipitation processes, and the chemical equilibria in a damaged canister. At the time of water contact the temperature in the canister is expected to have decreased to near ambient when its influence will be limited.

The presence of water in a damaged canister is required for the process to take place. Any potential beneficiary effect of secondary phase deposits on the rate of dissolution of spent fuel, e.g. by limiting the amount of water contacting the fuel surface, is pessimistically neglected.

**Table 2-13. Direct dependencies between the process "Fuel dissolution" and the defined fuel variables and a short note on the handling in SR-Site.**

| Variable | Variable influence on process | | Process influence on variable | |
|---|---|---|---|---|
| | Influence present? (Yes/No) Description | Handling of influence (How/If not – why) | Influence present? (Yes/No) Description | Handling of influence (How/If not – why) |
| Radiation intensity | Yes. Affects radiolysis. | Neglected. The effect of radiolysis is assumed to be suppressed by the presence of $H_2$ and $Fe^{2+}$. | Yes. | Neglected. Small changes in inventory due to dissolution. |
| Temperature | Yes. Influences kinetics and equilibria. | Neglected. Water ingress is assumed to take place at the earliest 1,000 years after disposal. At that time the temperature of the fuel will have a very limited effect. | No. | – |
| Hydrovariables (pressure and flows) | Yes. Presence of water required for the process to take place. | Water is assumed to be present after failure. | Yes. Secondary phases may restrict water access to the surface. | Pessimistically neglected. |
| Fuel geometry | No, but indirectly through radiation field and radiolysis. | – | Yes. Changes in fuel surface area due to dissolution/ precipitation processes. | Pessimistically neglected. |
| Mechanical stresses | No. | – | No. | – |
| Radionuclide inventory | No. Indirectly through radiation intensity. | – | Yes. | Neglected. Small changes due to release of radionuclides. |
| Material composition | No. (Iron corrosion affects redox conditions indirectly through water composition.) | – | Yes. Potential deposition of radionuclides on material surfaces. | Neglected. |
| Water composition | Yes. Affects radiolytic oxidant production and kinetics of dissolution. | Neglected. The effect of radiolysis is assumed to be suppressed by the presence of $H_2$ and $Fe^{2+}$. | Yes. Soluble radionuclides from fuel dissolution. | Source term for radionuclide release. |
| Gas composition | Yes. Gases such as $H_2$ participate in radiolytic reactions. | The effects of radiolysis is assumed to be suppressed by the presence of $H_2$ and $Fe^{2+}$. | Yes. Release of radioactive gases. | $^{14}C$ and Rn are assumed to be released with $H_2$ when it escapes through the bentonite. |

The surface area of the fuel contacting water influences the dissolution rate, while the fuel geometry in the canister determines the resultant radiation field. Any influence of secondary precipitated phases on the fuel surface is pessimistically neglected, while any increase in fuel surface area due to dissolution of material from grain boundaries is considered negligible for the fuel dissolution rates assessed.

Different scenarios for water intrusion into an initially defective canister are analysed by /Bond et al. 1997/. Based on their analysis, the minimum time before water comes into contact with the fuel can be estimated to be 1,000 years. The radionuclide inventory of the fuel at the time of water intrusion is, therefore, dominated by alpha emitting nuclides, since most of the short-lived beta/gamma emitters will have decayed before water intrusion occurs. The fuel inventory of radionuclides determines the radiation field at the fuel surface and the dose rate to water as a function of time. The decrease of the inventory of a certain radionuclide in the fuel, caused by its dissolution in water, is usually very small. The influence of the doping by fission products and actinides on the stability of the $UO_2$(s) fuel matrix towards corrosion (oxidative dissolution) is discussed in the section Model studies/ experimental studies.

The behaviour of the different materials in the canister, especially the anaerobic corrosion of the cast iron insert, influence fuel dissolution indirectly by changing the water composition and determining the redox conditions inside the canister, see Section 3.5.1. The composition of the different materials is not affected by fuel dissolution other than by the potential deposition of radionuclide precipitates on their surface.

The water composition influences both the radiolytic reactions and the kinetics of matrix dissolution. The most important factors are the redox potential and the concentration of carbonates, but other complexants, such as sulphate, chloride etc, affect the radiolytic reaction chains and, hence, the dissolution process.

The gas produced by the anoxic corrosion of iron influences the fuel dissolution process through changes in water composition. The process of fuel matrix dissolution causes the release of radioactive gases from fission gas bubbles as the dissolution progresses.

### *Boundary conditions*

There are no relevant boundary conditions for this process other than the physical boundary set by the geometries of the components involved. Related transport processes over the canister boundary are handled in Section 2.6.

### *Model studies/experimental studies*

Experimental studies of fuel dissolution under various redox conditions have been conducted for more than 25 years. The majority of data in dilute groundwater conditions have been obtained under oxidising conditions (see for example /Forsyth and Werme 1992, Forsyth 1997/). The increase of the fuel burnup to over 50 MWd/kgU leads to the formation of the high burnup structure (HBS) in the outer region of the fuel pellet (rim), which consists of small grains of submicron size and a high concentration of pores, 1 to 2 micrometres in size. One of the primary driving forces behind HBS formation is the significantly higher burnup experienced by the pellet periphery due to $^{239}$Pu build-up by neutron capture in $^{238}$U, followed by its fission. Both the smaller grain size and the higher radiation dose at the rim are expected to contribute to higher dissolution rates. /Forsyth 1997/ investigated the influence of burnup using fuel material from segments of a stringer rod in which burnup varied between 21 and 49 MWd/kg U along the fuel column. The cumulative fractional release under oxidising conditions increased slightly, almost linearly, with burnup values up to 40–44 MWd/kgU, but then decreased for burnups up to 49 MWd/kg U. Recently this study was extended with data for four higher burnup (55–75 MWd/kg U) fuel samples using the same experimental procedure. The results for the whole series indicate that the releases do not increase proportionally with burnup. The highest cumulative fractional releases are observed for fuels with an intermediate burnup, a slight decrease being observed for fuels with the highest burnup /Ekeroth et al. 2009/. A similar trend is observed in two other systematic studies of fuels with burnup in the range 29–60 MWd/kg U /Jégou et al. 2004/ and 15–70 MWd/kg U /Hanson 2008/.

In experiments carried out within the EU-Project NF-PRO, /Clarens et al. 2008/ compared the releases from the outer (~1 mm) part of a high burnup fuel (average burnup 65 MWd/kg U) with releases from the central part of the pellet. The samples were in the form of powder and obtained by core drilling the fuel pellet. The releases of almost all radionuclides were slightly lower from the outer part, which contained the rim and had higher local burnup. Similar trends in flow-through dissolution tests have been reported /Hanson et al. 2004, Hanson and Stout 2004/ and the observations are discussed in terms of the influence of non-uranium cations. The content of 2+, 3+ and 4+ non-uranium cations in spent fuel increases with burnup, leading to a decrease in dissolution rate by both a surface area effect (if the dopant is less soluble or dissolves more slowly than $UO_2$) and by a semi-conductor effect, which alters the ability for electron transfer, i.e. by limiting the stability of U in the +5 or +6 state. In a study of Gd-doped $UO_2$, a substantial decrease in the dissolution rates was observed with increasing dopant concentration /Casella et al. 2008/. In a combined electrochemical and spectroscopic study of SIMFUELs with varying composition /He et al. 2007/, a measurable, but marginal, effect of doping level on the surface modification of the $UO_2$ fluorite lattice to $UO_{2+x}$ was observed, in contrast to the more marked influence of doping on the anodic destruction of the $UO_2$ structure by conversion to the soluble U(VI) ions. The authors assign this influence to the formation of dopant-vacancy clusters that stabilise the fluorite lattice against the formation of destabilising tetragonal distortions and reduce the availability of oxygen vacancies, which facilitate oxidative dissolution. Recent thermochemical measurements of $UO_{2+x}$ solid solutions with two and three valent oxides /Mazeina et al. 2008/, indicate that they are more resistant to oxidation and oxidative leaching than $UO_2$ because of the additional stability resulting from the energetic contribution of the dopants.

The fractional fuel dissolution rates proposed in /Werme et al. 2004/ were based on the review of all, at that time, available experimental studies carried out under reducing conditions. Several experimental and modelling studies in the presence of 0.05–43 mM dissolved hydrogen or actively corroding iron, both with relatively fresh spent fuel and alpha-doped $UO_2$, have been published recently and these are discussed briefly below.

Long term (1–3 years) fuel leaching experiments performed in sealed vessels, initially under argon atmosphere /Cera et al. 2006/, indicate that the rate of fuel dissolution approaches zero for radiolytically produced $H_2$ concentrations in the range $10^{-5}$–$10^{-4}$ M. The data were successfully modelled by including the effect of metallic particles on fuel surface reduction /Eriksen and Jonsson 2007, Eriksen et al. 2008/.

For fuel itself, the real distribution of activation products and the presence of non redox-sensitive fission products make it possible to judge the fuel dissolution rate via their releases. A systematic reduction by more than two orders of magnitude of the released fraction of strontium or caesium during successive time intervals was observed in experiments lasting over one-year in the presence of a hydrogen atmosphere /Carbol et al. 2005/. For longer leaching periods, the number of intervals over which no release of strontium or caesium could be measured increased. The concentrations of nearly all redox-sensitive nuclides are initially established by the dissolution of a pre-oxidised fuel surface layer but decrease with time to values equivalent to the solubility of their reduced oxides. In all cases the concentrations of higher actinides, such as neptunium and plutonium, are two or more orders of magnitude lower than the uranium concentrations. The ratio between dissolved actinide and uranium concentrations is fairly close to that in the fuel, even though the solubilities of their tetravalent oxides are similar /Cui et al. 2008/. This suggests that co-precipitation of neptunium and plutonium with uranium may have occurred. Similar behaviour has been noticed during a long term leaching experiment on the outer part of a high burnup fuel pellet containing the rim zone /Fors et al. 2008/.

The first results from leaching of MOX fuel under a $H_2$ atmosphere /Carbol et al. 2009b/ exhibit similarities to experiments conducted with uranium dioxide fuel and the data indicate lower releases from fuel regions containing Pu-agglomerates.

Alpha-doped uranium dioxide better simulates the radiation field of several-thousand-year-old fuel. The experimental studies with $UO_2$, doped with the alpha-emitters $^{233}U$ or $^{238}Pu$, have been carried out in the presence of low concentrations of dissolved hydrogen, sulphide ions or actively corroding iron. Experiments with alpha-doped $UO_2$(s) indicate clearly that the presence of a small amount of sulphide and strict anoxic conditions are sufficient to cancel any oxidising effect due to α-radiolysis from a few thousand year old fuel /Ollila 2006/. In most tests with $^{233}U$-doped $UO_2$ (0, 5 and 10%)

under inert ($N_2$) and reducing (Fe(s)) conditions, very low total uranium concentrations were measured, especially in the presence of an iron strip. Estimation of the matrix dissolution rate confirms previously measured low values /Ollila 2006/. The first data from corrosion of alpha doped pellets under anoxic and reducing conditions in 0.5 and 1 M NaCl solutions as well as (Na,Ca)Cl solutions of ionic strength 0.625 M are available and they show no influence of the increased salinity in the corrosion rates /Ollila 2008/.

The initial tests with 10% $^{233}$U-doped $UO_2$ under various hydrogen concentrations showed decreasing U concentrations, an absence of oxidants in the autoclave, and no detectable oxidation of the $UO_2$(s) surface by XPS (X-ray Photoelectron Spectroscopy) analysis /Carbol et al. 2009a, Rondinella et al. 2004/. In spite of this, the measurable but slight increase of U concentrations observed with 10% $^{233}$U-doped pellets, even in the absence of hydrogen (under Ar), makes it difficult to claim a clear hydrogen effect. A $UO_2$ pellet with a much higher doping level (385 MBq/g corresponding to 50 years old fuel) was tested more recently /Muzeau et al. 2009/, and a very clear effect of α-radiolysis was observed under an Ar atmosphere, with U concentrations increasing quickly with time in carbonate solutions. The same system, tested under a 1 bar $H_2$ atmosphere, showed a slight decrease, not increase, in U concentration. These authors showed also that a good quality of alpha doped pellets is required, since in some cases materials with a low density compared to the theoretical $UO_2$ density give very high U releases /Muzeau 2007/. Further, they also gave an explanation why even with good quality pellets, the U releases at the start of the test were proportional to the doping level; i.e. the amount of U released in solution from the pellet with 10% $^{233}$U was higher than that from the pellet with 1% $^{233}UO_2$, while release from depleted $UO_2$ was lowest /Rondinella et al. 2004/. By using XPS measurements, /Jégou et al. 2005, Muzeau et al. 2009/ showed that these materials are sensitive to surface oxidation during storage, especially in the presence of a few layers of water undergoing radiolysis.Thus, the short term U releases reflect this storage effect, not the unoxidized $UO_2$ behaviour sought in the measurements.

Several recent studies have proposed mechanisms for the suppression of fuel oxidation/dissolution based on the catalytic effect of metallic ε-particles (composed of the fission products Mo, Pd, Tc, Rh and Ru) on $H_2$ activation at the fuel surface. The corrosion potential of SIMFUEL pellets decreased both with the number of ε-particles /Broczkowski et al. 2006/ and the dissolved hydrogen concentration /Broczkowski et al. 2005/ to values well below the $UO_2$(s) oxidation threshold, indicating complete inhibition of fuel corrosion. Scanning electrochemical microscopy was used to verify that these effects can be attributed to the reversible decomposition of $H_2$ on metallic ε-particles /Broczkowski et al. 2007/.

A steady-state model for fuel dissolution has been developed using experimentally-determined kinetic parameters /Jonsson et al. 2007, Roth and Jonsson 2008 and references therein/. Studies of the catalytic effect of pure Pd particles on the reaction between $H_2$ and $H_2O_2$ show that the reaction is very fast, practically diffusion controlled and independent of the $H_2$ pressure in the range 1–40 bar /Nilsson and Jonsson 2008/. Based on the reported decrease of the corrosion potential /Broczkowski et al. 2005/ and studies with Pd-doped $UO_2$ /Trummer et al. 2008, 2009/ the relevant parameters for the solid phase reduction of oxidised $U(VI)_{surf}$ mediated by hydrogen via ε-particles were estimated. The results of spent fuel dissolution modelling, including the effect of Fe(II) ions on the decrease in steady state $H_2O_2$ concentrations at the fuel surface and the fuel surface reduction process on ε-particles, have been published recently /Jonsson et al. 2007/. Calculation of maximum fuel dissolution rates using this model shows that an $H_2$ pressure of 0.1 bar is sufficient to effectively inhibit the dissolution of spent fuel aged 100 years or more. In the presence of 1 µM Fe(II), even 0.01 bar $H_2$ will be sufficient to stop fuel dissolution, while for Fe(II) concentrations of 40 µM (as expected inside a failed canister in Sweden), even radiolytically produced hydrogen is sufficient to completely inhibit fuel corrosion /Jonsson et al. 2007/.

Experimental data on both spent fuel and alpha-doped $UO_2$(s) dissolution in the presence of $H_2$ and actively corroding iron indicate that either the presence of a redox front or that of a “chemical pump” process, during which the oxidised uranium released from the fuel surface is reduced and deposited on the surface of iron, are highly improbable.

- More than 99% of the U(VI) released at the start of the leaching experiment was deposited on the surface of the fuel itself /Albinsson et al. 2003/ and very low uranium levels were recovered in the vessel rinse.

- The transfer of a solution containing relatively low U levels (40–200 ppb) after contact with metallic Fe under 10 bar $H_2$ pressure to a similar vessel containing spent fuel equilibrated for a long time under the same conditions /Ollila et al. 2003/ caused a quick decrease of the uranium concentrations to much lower levels (a few ppb). This suggests that spent fuel surfaces under such conditions have stronger reducing properties for U(VI) carbonate species than Fe surfaces.

Similar observations were made during the simultaneous corrosion of spent fuel and iron /Grambow et al. 1996, 2000/. The uranium levels measured in solution were near the $UO_2$(s) solubility, while the post characterisation of the Fe showed no $UO_2$(s), even though magnetite and green rust were formed as corrosion products. Under oxygen free conditions it was shown that magnetite reduces U(VI) /Scott et al. 2005/, while green rust on iron surfaces was shown to precipitate $UO_2$(s) /Cui and Spahiu 2002/. Despite this, during the co-dissolution of fuel and iron, both oxidants and U(VI) were scavenged on the fuel surface and very little, if at all, on the iron surface. The same holds for leaching of $^{233}$U-doped $UO_2$(s). In the presence of iron, extremely low U concentrations were measured in solution and negligible amounts of uranium were detected on iron surfaces /Ollila and Oversby 2005/.

### *Natural analogues/observations in nature*

The oxidation state of uranium in the uranium oxide lattice is an important factor in the process of spent fuel dissolution. In spent nuclear fuel, the uranium is present as $UO_{2.0}$, while in natural uraninite U(VI) is present to varying degrees. In Oklo, the U(VI)/U(IV) ratio varies from 0.10 to 0.19 /Janeczek et al. 1996/ and in Cigar Lake it is even higher /Cramer and Smellie 1994/. This is partly a result of autooxidation, stemming from the decay of U (IV) to stable isotopes of Pb, when Pb will take two electrons from a nearby U in order to reach the preferred oxidation state of Pb (II) /Finch and Murakami 1999/. In the long term, mainly in the period beyond one million years, the same process will be important for the structure of the spent nuclear fuel. On a much shorter time scale, another similar effect may be achieved by the variety of impurities (fission products) found in the spent fuel matrix. The preferred oxidation state of many of these impurities are such that they will partly oxidize a uranium neighbour /He et al. 2007/, discussed above in the section on Model studies/experimental studies. This effect, important for the dissolution behaviour of spent nuclear fuel, has also been observed in natural uraninite /Janeczek et al. 1996/ where impurities, which can be considered chemical analogues to fission products, are common.

A limitation in the studies of natural uraninite in the framework of a safety analysis, is that the conditions under which dissolution and alteration occurred can, in general, not be accurately specified. Therefore, even though natural uraninite is a good analogue for spent fuel in many respects, data on the dissolution and alteration of uraninite that may be used to quantify the dissolution process are rare. Qualitatively, however, it may be noted that laboratory experiments performed to determine dissolution rates of minerals often yield results that indicate a much faster dissolution rate than results from similar studies performed on minerals in a natural setting /White and Brantley 2003/.

### *Time perspective*

After water has come into contact with the fuel, fuel transformation will proceed for hundreds of thousands of years.

### *Handling in the safety assessment SR-Site*

The fuel alteration/dissolution rate in the case of a damaged canister will be modelled using the recommendations in /Werme et al. 2004/ based on available experimental data from studies performed using alpha-doped $UO_2$ and spent fuel under anaerobic and reducing conditions. These studies were performed in the presence of a hydrogen atmosphere or in the presence of actively corroding iron. Several experimental and modelling studies carried out after this review support the recommended rates and would even justify lower ones or the use of a solubility limited model.

In the review by /Werme et al. 2004/, they conclude that the weight of the evidence from experimental studies suggests that the model for fuel dissolution in SR-Site should be a constant fractional dissolution rate in the range of $10^{-6}$ to $10^{-8}$ per year. A triangular distribution with a peak at $10^{-7}$ per year would best represent the available data. Support for this choice was given by /King and Shoesmith

2004/, who used an electrochemical model to predict the lifetime of spent fuel. They found that the maximum fractional dissolution rate in the presence of $H_2$ should be $10^{-7}$ to $10^{-8}$ per year.

Using this recommendation, the expected lifetime of the fuel is 10 million years with a distribution between 1 and 100 million years.

The recommendation of /Werme et al. 2004/ represents by far the most likely scenario, i.e. reducing conditions in the repository and the presence of hydrogen gas and/or corroding iron and iron corrosion products. Under these circumstances other parameters, such as water chemistry, will be less important.

If dilute groundwater reaches the repository, the buffer may be partially or completely eroded, leaving a cavity filled with a slurry of colloidal clay particles in the deposition hole. Should the canister be breached under such circumstances, the clay particles are not expected to affect the fuel corrosion rate. Dissolved U(IV) would, however, be expected to sorb strongly to the clay particles. This sorption increases the amount of U(IV) released in solution from the re-precipitated $UO_2$(s) or the fuel matrix. In this case, no limit to the U(IV) release rate from $UO_2$(s) to satisfy U(IV) solubility limits in the canister void is posed. In the case when all re-precipitated $UO_2$(s) is dissolved due to sorption to clay particles, the remaining U(IV) needed to saturate clay particles is released from the fuel matrix, resulting in an increase of the fuel dissolution rate. In this case, the values for $UO_2$(s) solubility and $K_d$ for U(IV) on clay particles are taken from the data report, while the concentration of clay particles and water flow depend on the scenario analysed.

In the unlikely case of oxygen-containing water coming into contact with spent fuel, the fuel may dissolve with a higher rate. The fractional dissolution rates would become higher than $10^{-8}$ per year for oxygen concentrations higher than $10^{-5}$ mol/m$^3$. For air-saturated waters, fractional dissolution rates in the range $10^{-4}$ to $10^{-5}$ per year, determined experimentally under air-saturated conditions, become appropriate /Forsyth and Werme 1992, Forsyth 1997/. In the presence of oxidants, the corrosion of the uranium dioxide causes an increase in concentration of U(VI) in solution followed by the precipitation of solid U(VI) phases on or near the fuel. The composition of these secondary phases will depend on the groundwater composition. In groundwater or bentonite porewater, uranyl oxides/hydroxides (schoepite) will probably form first, while more stable uranyl silicates (for example, uranophane or soddyite) will form after longer times.

### *Uncertainties*

#### Uncertainties in mechanistic understanding

While there is a sound and increasing experimental database on the effect of the products of anoxic corrosion of iron on spent fuel dissolution, there are considerable uncertainties concerning the exact mechanism involved, especially in the absence of ε-particles. This is also reflected in the wide spread in dissolution rates that /Werme et al. 2004/ propose.

#### Model simplification uncertainties

A constant fractional dissolution rate of the fuel is assumed in the calculations. The release of uranium and all other nuclides is assumed proportional to their inventory in the fuel matrix. Enhancement of radionuclide release from the outer regions of the fuel matrix (the rim zone) or for the higher burnups relevant for forthcoming discharged fuels are not considered based on the influence of the higher doping level observed in experimental studies.

#### Input data and data uncertainties

Input data and input data uncertainties, i.e. the range of fuel dissolution rates recommended by /Werme et al. 2004/ are discussed in the SR-Site data report /SKB 2010l/.

### *Adequacy of references supporting the handling in SR-Site*

The reports /Werme et al. 2004/, /Ollila et al. 2005/ and /King and Shoesmith 2004/ are peer reviewed SKB reports, but not according to the SR-Site quality assurance procedure. Most of the other references are peer reviewed journal or conference papers.

### 2.5.6 Dissolution of the gap inventory

#### *Overview/general description*

In the event of canister damage, water can enter the canister. If the fuel cladding is breached, the water can come into contact with the fuel. Most of the radionuclides in the fuel are evenly distributed in the $UO_2$ matrix and are released only when the uranium dioxide fuel matrix dissolves (see Section 2.5.5). A small fraction of the inventory of a few radionuclides has segregated to the fuel-clad gap and possibly also to grain boundaries in the fuel; see Section 1.4.4.

Most segregated radionuclides are also highly soluble and can quickly go into solution upon contact with water, and the release is, therefore, considered as instantaneous in the safety assessment. The quantity of radionuclides released is determined mainly by the availability and solubility of segregated material. In SR-Can, the release of segregated nuclides in fuel was based on a compilation by /Werme et al. 2004/. Recently, calculations of the fission gas release of BWR and PWR equilibrium cores for various burnup and linear power ratings have been carried out /Oldberg 2009, Nordström 2009/. These calculations were used as a basis to make a better estimation of the segregated nuclide fraction for the whole fuel inventory (SR-Site data report, /SKB 2010l /).

#### *Dependencies between process and fuel variables*

Table 2-14 shows how the process influences, and is influenced by, all fuel variables.

The temperature influences the kinetics of dissolution of the segregated radionuclides. At the time of water intrusion, the temperature is expected to have decreased to near ambient values.

The presence of water in a damaged canister is required for the process to take place.

**Table 2-14. Direct dependencies between the process "Dissolution of the gap inventory" and the defined fuel variables and a short note on the handling in SR-Site.**

| Variable | Variable influence on process | | Process influence on variable | |
|---|---|---|---|---|
| | Influence present? (Yes/No) Description | Handling of influence (How/If not – why) | Influence present? (Yes/No) Description | Handling of influence (How/If not – why) |
| Radiation intensity | No. | – | No. | – |
| Temperature | Yes. | Neglected. Instant release of the segregated inventory is assumed. | No. | – |
| Hydrovariables (pressure and flows) | Yes. Presence of water necessary for the process. | Water is assumed to be present after failure. | No. | – |
| Fuel geometry | Yes. | Neglected. Instant release of the segregated inventory is assumed. | No. | – |
| Mechanical stresses | No. | – | No. | – |
| Radionuclide inventory | Yes. Segregated inventory determines release. | Instant release of the segregated inventory is assumed. | Yes. Dissolution decreases radionuclide inventory. | Instant release of the segregated inventory is assumed. |
| Material composition | Yes. | Instant release of the segregated inventory is assumed. | No. | – |
| Water composition | Yes. Limited influence of water composition due to fast release. | Instant release of the segregated inventory is assumed. | Yes. Small changes in composition due to limited amounts of segregated nuclides. | Source term for radionuclide release. |
| Gas composition | No. | – | Yes. Gaseous products potentially formed. | Source term for radiouclide release. |

The fuel surface area in contact with water influences the release of the segregated nuclides. This influence is accounted for in the estimation of the size of the instant release fraction.

The radionuclide inventory in the gap and grain boundaries determines the contribution of the segregated nuclides to the source term, while the dissolution of these radionuclides affects the radionuclide inventory of the fuel.

In principle, the composition of materials, such as fuel cladding, affects the dissolution of that part of the instant release fraction, which has diffused into the zirconium oxide layer during reactor operation.

Upon water contact, some segregated radionuclides, such as $^{14}C$ may produce gaseous products such as methane or carbon dioxide.

### *Boundary conditions*

There are no relevant boundary conditions for this process other than the physical boundary set by the geometries of the components involved.

### *Model studies/experimental studies*

The immediate release of caesium and iodine from the fuel on contact with water is experimentally verified (see e.g. /Johnson and Tait 1997/). /Johnson and McGinnes 2002/ have made a more recent assessment of the instant release fraction from light water reactor fuel. An experimental study of the dissolution of segregated metallic ε-particles extracted from spent fuel under various redox conditions /Cui et al. 2004/ indicates very limited releases for the redox conditions expected in a damaged canister.

An update of the instant release fraction including fuels with higher burnup and linear power ratings based on calculations of fission gas release for BWR and PWR equilibrium cores /Oldberg 2009, Nordström 2009/ has been carried out for each of the canister types to be used in SR-Site (SR-Site data report /SKB 2010l/).

It has been experimentally shown that fractions of the content of the fission gases, Cs and I can leave the fuel matrix during reactor operation. It is also known that Tc, Ru, Rh, Pd and Mo form metallic inclusions in the fuel. There are no major systematic studies of segregants in light water reactor fuel, with the exception of the release of the fission gases. Uncertainties surrounding the extent, and in some cases the very existence of segregations of certain radionuclides, are great. Uncertainties are discussed in greater detail in SR-Site data report /SKB 2010l/.

### *Natural analogues/observations in nature*

Not applicable.

### *Time perspective*

The release of segregated radionuclides occurs relatively rapidly (on the order of days) and is pessimistically assumed to occur instantaneously upon water contact.

### *Handling in the safety assessment SR-Site*

The process is only relevant if containment by the copper shell has been breached.

Immediate release of the instant release fraction of radionuclides upon water contact in a damaged canister will be assumed for all scenarios in SR-Site. Input data will be based on distributions for the instant release fractions assessed in SR-Site data report /SKB 2010l/.

*Boundary conditions:* As stated above, there are no relevant boundary conditions for this process other than the physical boundaries set by the geometries of the components involved. These become irrelevant with the pessimistic handling of the process.

*Handling of variables influencing this process:* the influences of temperature, fuel geometry, material composition and water composition are pessimistically neglected in the handling of this process. The influence of radionuclide inventory is trivially handled by assessing the fraction of segregated nuclides and assuming it is immediately released upon water contact. The requirement that water is present in the canister interior is handled by assessing a time after which a continuous water pathway has been established between the fuel and the canister interior.

#### *Handling of uncertainties in SR-Site*

**Uncertainties in mechanistic understanding**

The mechanistic understanding of the process is sufficient for the needs of the safety assessment.

Any mechanistic/conceptual uncertainties are handled pessimistically since immediate release upon water contact is assumed.

**Model simplification uncertainties**

The uncertainties concerning the dissolution process are covered by the pessimistic assumption that the instant release fraction of the radionuclide inventory is released immediately upon water contact.

**Input data and data uncertainties**

Input data and input data uncertainties for this process are discussed in the SR-Site data report /SKB 2010l/.

#### *Adequacy of references supporting the handling in SR-Site.*

Not relevant since the process is handled pessimistically. The estimation of the fraction released as IRF is justified in SR-Site data report /SKB 2010l/, which will undergo a documented factual and quality review.

### 2.5.7 Speciation of radionuclides, colloid formation

#### *Overview/general description*

Radionuclides that have segregated from the fuel or are exposed to water in the fuel matrix and other metal parts can dissolve in the canister cavity and thereby become available for transport or precipitation when their solubility limit as an insoluble phase is reached. The distribution of a given nuclide between dissolved and solid phases is determined by the solubilities of the solid phases formed. These are in turn dependent primarily on the chemical environment in the canister cavity and the temperature. The low solubility of many key radionuclides is an important constraint, limiting their concentration inside a breached canister and, hence, their rate of transport out of the canister. Radionuclide solubility refers to the total aqueous concentration of all the chemical species and isotopes of a radioactive element that are in equilibrium with each other and with a pure crystalline or amorphous solid phase containing the given element. If true equilibrium with a characterised solid has been established, chemical thermodynamics allows the estimation of the maximum concentration of all soluble species for a given radionuclide in a specified groundwater composition. The solubility-limited concentrations and chemical speciation of important radionuclides to be used in SR-Site have been reported in /Duro et al. 2006b, Grivé et al. 2010/

Radionuclides can be released in the form of colloidal or pseudo-colloidal particles from the spent fuel. Alternatively, colloidal particles may form during the nucleation of new solid phases inside the canister. This is of no importance for radionuclide dispersal from the canister, as long as the bentonite buffer, which acts as an efficient filter for colloids, remains in place.

In the case of an advective flow scenario and major bentonite loss, the relatively high flow lowers further the concentrations of minor radionuclides such as, e.g., thorium, making it difficult to reach saturation with respect to the corresponding solid phases. On the other hand, several major radionuclides, especially the actinides, may reach solubility limits of their amorphous oxides after a certain period of time and form colloidal oxide particles. Pu(IV) especially is known to have a high

tendency to form colloids, and the formation of Pu colloids has been considered while modelling experimental data in the SKB fuel programme /Bruno et al. 1998/. The measured concentrations of U, Pu and Np in fuel tests simulating conditions inside a damaged canister /Carbol et al. 2009b, Fors et al. 2008, Cui et al. 2008/ are very low and the trend observed in their variation with time indicates the formation of an actinide co-precipitate rather than separate oxide phases. The Pu concentrations were almost two orders of magnitude lower than the U concentrations and Np concentrations almost one order of magnitude lower than the Pu concentrations, which is close to the relative proportions of U, Pu and Np in the spent fuel. The measured Pu concentrations under such conditions, expected to be lowered further in the advective flow case by the relatively high flow, do not suggest an over-saturation with respect to the estimated solubility of $Pu(OH)_4(am)$ /Bruno et al. 1998/ or the solubility product in the SKB database for Pu /Duro et al. 2006a/.

### *Dependencies between process and fuel variables*

Table 2-15 shows how the process influences, and is influenced by, all fuel variables.

The temperature influences both the kinetics of dissolution/precipitation processes as well as the solubility and complexation equilibria. For many solids, even the crystallinity of the solid formed depends on temperature; e.g. $UO_2(s)$ precipitated from near neutral solutions at low temperatures is amorphous and the crystallinity increases with temperature /Rai et al. 2003/. At the time of a possible water intrusion into the canister, the temperature is expected to have decreased to near ambient values and its influence on solubility and complexation equilibria is expected to be small.

The presence of water in a damaged canister is necessary for the process to take place and the rate of water renewal affects the precipitation/dissolution process. In view of the large residence times of the groundwater in the canister and the relatively fast kinetics of inorganic ligand complexation and dissolution/precipitation reactions, the assumption of chemical equilibrium is not expected to introduce

**Table 2-15. Direct dependencies between the process "Speciation of radionuclides, colloid formation" and the defined fuel variables and a short note on the handling in SR-Site.**

| Variable | Variable influence on process | | Process influence on variable | |
|---|---|---|---|---|
| | Influence present? (Yes/No) Description | Handling of influence (How/If not – why) | Influence present? (Yes/No) Description | Handling of influence (How/If not – why) |
| Radiation intensity | No. | – | No. | – |
| Temperature | Yes. | Neglected. Water ingress is assumed to take place at the earliest 1,000 years after disposal. At that time the temperature of the fuel will have a very limited effect. | No. | – |
| Hydrovariables (pressure and flows) | Yes. Presence of water necessary for the process. | Water is assumed to be present after failure. | Yes. | Effect of precipitates pessimistically neglected. |
| Fuel geometry | No. | – | Yes. | Influence of solids pessimistically neglected. |
| Mechanical stresses | No. | – | No. | – |
| Radionuclide inventory | No. | – | No. | – |
| Material composition | No. Indirectly through water composition. | – | Yes. Deposition of precipitated solids on materials. | Modelled using solubility limits. |
| Water composition | Yes. | Included in the modelling. | Yes. Dissolved radionuclides in water. | Source term for radionuclide release. |
| Gas composition | No. Indirectly through water composition. | – | Yes. Dissolution of gaseous radionuclides. | Source term for radionuclide release. |

uncertainties in the calculation of solubility-limited concentrations. Further, by assuming solubility equilibrium, maximum expected concentrations of a given radionuclide are obtained. Moreover, both the relatively slow crystallisation of amorphous phases to more crystalline ones (Ostwald ripening) and the slow formation of solid phases as silicates, are pessimistically neglected. The amounts of solids precipitated are not expected to be so large as to affect water flow or its presence in the fuel gap and any such influence on fuel dissolution is pessimistically neglected.

The radionuclide inventory does not in principle affect the precipitation or complexation processes, but determines the maximum availability for any given radionuclide at a given time.

Due to corrosion of the cast iron insert, reducing conditions are expected to exist inside the canister (see Section 3.5.1). Any oxidised forms of radionuclides released from the fuel will very probably be precipitated in their reduced forms by interaction with iron corrosion products present on the surface of the cast iron insert. This will give rise to a redox front inside the canister.

The composition of the groundwater inside the canister determines both the composition of radionuclide precipitates and their maximum soluble concentration. For redox-sensitive radionuclides, redox conditions in the groundwater are extremely important, and their variation can cause several orders of magnitude difference in the radionuclide concentration in some cases. Groundwater parameters, such as pH and the concentration of strong complexing ligands, (e.g. carbonate), influence most of the equilibria**,** especially those of actinide and lanthanide elements. High salinity groundwaters affect the equilibria through their high ionic strength. Moreover, the dissolution/precipitation of radionuclides changes the composition of the groundwater inside the canister.

The presence of dissolved gases affects the redox conditions inside the canister, but is not expected to influence solubility or complexation equilibria. The influence of pressure of the magnitude expected inside the canister on chemical equilibria is negligible /Marion et al. 2005/. On the other hand, certain radionuclides may enter the gas phase during the dissolution of either the rapid release fraction (Section 2.5.6) or the fuel matrix (Section 2.5.5) and establish a Henry's Law equilibrium.

#### *Boundary conditions*

There are no relevant boundary conditions for this process other than the physical boundary set by the geometries of the components involved.

The presence of liquid water in a breached canister and sufficient progress of fuel dissolution to establish oversaturation with respect to a given element are necessary requirements for the process to take place. The chemical properties of the solution and the temperature influence the solubility of the potential solid phases.

#### *Model studies/experimental studies*

The quantitative estimation of radionuclide solubilities requires reliable thermodynamic equilibrium constants, obtained through experimental studies of appropriate chemical systems. The need for chemical equilibrium data in the field of nuclear waste management has contributed to a large number of basic thermodynamic studies on many radionuclides during the last 30 years. Most of this information has been reviewed by international expert teams within the framework of the NEA-TDB project /Grenthe et al. 1992, Silva et al. 1995, Rard et al. 1999, Lemire et al. 2001, Guillaumont et al. 2003, Olin et al. 2005, Gamsjäger et al. 2005, Brown et al. 2005/. More recently, a state-of-the-art report on the chemical thermodynamics of solid solutions relevant to radioactive waste management has been published within the same project /Bruno et al. 2007/.

In solubility calculations for a safety assessment, potential solubility-limiting phases are postulated for each radioelement. The most likely solid phases expected to form under the conditions that prevail are chosen. For example, amorphous phases are chosen instead of crystalline ones, while stable sulphides and silicates, whose formation is uncertain, are often disregarded entirely in the modelling.

The calculations determine the solubility of the radioelement phase in the groundwater in equilibrium with all the soluble species it forms for the given range of conditions, i.e. the speciation of all radionuclides in the aqueous phase is determined simultaneously. Speciation is important for

both solubility and the transport properties of the radionuclide in buffer and rock. The following methodology was used in deriving the solubility limits to be used in SR-Site /Duro et al. 2006b/.

Solubility limits are defined for three different water compositions resulting from geochemical processes and climate changes. Special care has been taken to select a reliable and fully consistent thermodynamic database /Duro et al. 2006a/. Chemical thermodynamic modelling has been used to assess solubility limits by varying the groundwater parameters, including redox potential and pH, for a range of pure solid phases which could potentially form under the expected conditions.

The output of the thermodynamic modelling is compared to literature data on the formation of identified minerals and measured concentrations in natural and laboratory systems. The extensive available spent fuel leaching data obtained under oxidising or initially argon-purged atmospheres for important elements in the safety assessment have been discussed. A review of the solubility limits used in eight international safety assessment exercises has also been carried out /Duro et al. 2006b, Grivé et al. 2010/. In safety assessments, usually no credit is taken for the expected co-precipitation of elements with similar chemical properties, since the solubilities of the component elements in ideal solid solutions are lower than those of the corresponding pure components. One exception is radium-calcium-barium sulphate co-precipitation /Berner and Curti 2002/, for which there is abundant literature /Doerner and Hoskins 1925, Berner and Curti 2002/. Based on the results of /Berner and Curti 2002/, /Berner 2002/ proposed a solubility for Ra based on co-precipitation with Ba in the Opalinus Clay safety assessment /Nagra 2002/. A second exception is the use of Ra-Ca-carbonate co-precipitation used in the Japanese H 12 analysis (quoted in /Duro et al. 2006b/). There may still be, however, some uncertainties in using solid solution solubilities for safety assessment purposes at SKB. The NEA state-of-the-art report /Bruno et al. 2007/ discusses the possibilities for solid solution formation under repository conditions and suggests that at the relatively low temperatures expected in a repository when ion diffusion in the solid phase is negligible, the transition from adsorbed layer or surface precipitate to solid solution is expected to occur only in solids with high re-crystallisation rates.

For this reason, the case of radium-barium-sulphate co-precipitation, for which there are literature reports of high rates for barite re-crystallisation /Hahn 1936, Goldschmidt 1940/, has been investigated in some more detail. As a first stage, a report summarising the thermodynamic and kinetic evidence in the literature for this specific case as well as its application on a KBS-3 repository has been compiled /Grandia et al. 2008/. If Ra and Ba are released simultaneously from spent fuel, all existing evidence indicates that Ra will be readily incorporated into the precipitating $BaSO_4$ to form a Ra-Ba-sulphate solid solution. It is concluded that the behaviour of the system can be described by the established aqueous-solid solution formalism, assuming that the system behaves ideally. However, Ba and Ra have different sources; Ba is a fission product or a daughter of fission products, while Ra is a uranium decay product. If they are not released simultaneously, Ba from fuel dissolution can be expected to have precipitated as barite in sulphate rich solutions when the Ra released from secondary sources such as $UO_2$ precipitated in the canister, reaches its peak after about 300,000 years. In order to obtain further evidence for the co-precipitation kinetics in this case, an experimental study of the barite re-crystallisation and its co-precipitation with Ra has been carried out /Bosbach et al. 2010/. The experimental investigation of the uptake of $^{226}Ra$ and $^{133}Ba$ by two different barite powders (0.31 and 3.2 $m^2/g$) in aqueous solutions shows that there is a significant uptake of Ra into the bulk of barite crystals. The kinetics of Ra-uptake in barite shows that the uptake rate drops significantly within 400 days, even though a zero exchange rate cannot be unambiguously demonstrated. These measurements will continue. In view of the long contact times expected under repository conditions, together with the small mass transfer processes involved, it is quite likely that equilibrium will be reached relatively fast.

#### *Natural analogues/observations in nature*

Elemental concentrations in natural systems, such as rocks, minerals or sea water, as well as elemental concentration measurements in relevant natural analogue sites, are discussed for most of the elements in /Duro et al. 2006b/. The comparison of the results of thermodynamic modelling with data from natural and laboratory systems is used to check the consistency of the models with available experimental data.

### *Time perspective*

If the canister is breached and water comes into contact with fuel, the process continues throughout the life of the repository.

### *Handling in the safety assessment SR-Site*

The process is only relevant if the copper shell has been breached.

The process will be handled by applying concentration limits in the canister cavity water in the integrated radionuclide transport calculations.

*Model:* The near-field radionuclide transport model COMP23 /Cliffe and Kelly 2005/.

Concentration limits used in the calculations will be based on the results reported in /Duro et al. 2006b, Grivé et al. 2010/.

The solubilities and the speciation recommended in /Duro et al. 2006b/ pertain to reducing conditions in the canister cavity, but for redox-sensitive radionuclides, calculations for a range of redox conditions have also been carried out.

*Boundary conditions:* The process is confined to the canister and no precipitation of radionuclides in the form of solid phases is considered to take place in the buffer or in the far field.

*Handling of variables influencing this process:* The concentration limits applied are valid for a temperature of 15°C, which is a reasonable temperature for the canister interior after a few hundred years of deposition /Duro et al. 2006b/. The influence of water composition is handled by calculating concentration limits for i) a site-specific reference groundwater, ii) saline groundwater, iii) a post-glaciation ice-melting groundwater and iv) a bentonite groundwater composition resulting from the interaction of the reference groundwater with bentonite.

### *Handling of uncertainties in SR-Site*

#### Uncertainties in mechanistic understanding

The calculation of the solubility limits for each element of interest is based on equilibrium chemical thermodynamics and the fundamental understanding of the processes is sufficient for the needs of the safety assessment. Pessimistic assumptions are made whenever there are conceptual uncertainties. For example, all the uranium resulting from spent fuel dissolution is assumed to contribute to the ingrowth of radium, including uranium in precipitated $UO_2$, thus, neglecting any Ra formation inside grains. The uranium concentration giving rise to radium in-growth has not been limited by its low solubility under the reducing conditions expected to exist in the canister.

#### Model simplification uncertainties

The model does not account for any changes in water chemistry during the calculation.

#### Input data and data uncertainties

Input data and input data uncertainties for this process, i.e. the concentration limits to be used, are discussed in the SR-Site data report /SKB 2010l/, based on the data reported in /Duro et al. 2006b, Grivé et al. 2010/.

### *Adequacy of references supporting the handling in SR-Site*

/Duro et al. 2006b/ and /Grandia et al. 2008/ are peer reviewed SKB reports, but not according to the SR-Site quality assurance procedure. /Bosbach et al. 2010/ and /Grivé et al. 2010/ are SKB reports that have undergone a documented factual and quality review, and the other references are peer reviewed journal articles or review books.

### 2.5.8 Helium production

#### *Overview/general description*

Helium builds up in spent fuel due to the alpha decay of actinides. Some of that helium may reach the gap between the fuel pellet and the Zircaloy cladding. This leads to a pressure build-up inside the tube, which can in turn lead to mechanical tube rupture (see Section 2.4.1). If, or when, the cladding ruptures, a negligible pressure increase arises in the canister cavity.

Most of the helium, however, will be trapped within the fuel matrix. This self-irradiation and internal pressure build-up has the potential to detrimentally affect the mechanical stability of the $UO_2$ fuel matrix, open the grain boundaries and, thereby, possible increase the Instant Release Fraction (IRF).

#### *Dependencies between process and fuel variables*

Table 2-16 shows how the process influences, and is influenced by, all fuel variables.

#### *Boundary conditions*

There are no relevant boundary conditions for this process other than the physical boundary set by the geometries of the components involved.

**Table 2-16. Direct dependencies between the process "Helium production" and the defined fuel variables and a short note on the handling in SR-Site.**

| Variable | Variable influence on process | | Process influence on variable | |
|---|---|---|---|---|
| | Influence present? (Yes/No) Description | Handling of influence (How/If not – why) | Influence present? (Yes/No) Description | Handling of influence (How/If not – why) |
| Radiation intensity | Yes. The alpha decay rate determines the rate of helium build-up. | Neglected. It is pessimistically assumed that all fuel rods are breached as soon as water contacts the fuel. The helium build-up in the canister void is negligibly small. | No. | – |
| Temperature | No. | – | No. | – |
| Hydrovariables (pressure and flows) | No. | – | No. | – |
| Fuel geometry | No. | – | No. | – |
| Mechanical stresses | No. | – | Yes. Mechanical stresses in the cladding and possibly in the fuel. | Neglected. It is pessimistically assumed that all fuel rods are breached as soon as water contacts the fuel. The helium build-up has no detrimental effect on the mechanical stability of the fuel. |
| Radionuclide inventory | Yes. Influenced by the content of alpha emitters. | Neglected. See above. | No. | – |
| Material composition | No. | – | No. | – |
| Water composition | No. | – | No. | – |
| Gas composition | No. | – | Yes. May result in He release. | Neglected. Marginal amount in comparison to the $H_2$. |

### *Model studies/experimental studies*

At 1,000 years after discharge from the reactor, fuel with a burnup of 60 MWd/kgU would contain about $9 \cdot 10^{18}$ He atoms/g. At an age of $10^5$ years, the concentration of He will have increased to about $3.2 \cdot 10^{19}$ atoms/g. After a million years, the concentration would be about two times higher than that.

A number of experimental studies of the possible consequences of helium build-up have been performed using He ion implantation /Desgranges et al. 2003, Roudil et al. 2004, Guilbert et al. 2003/. The implanted amounts were in the range $2 \cdot 10^{18}$ atoms/g to $2 \cdot 10^{20}$ atoms/g. Only in one case at $3.6 \cdot 10^{19}$ atoms/g /Guilbert et al. 2003/ was mechanical damage observed after heating to 500 and 600°C. After annealing, the samples showed flaking at the surface with the largest effect seen in the 600°C sample. This was caused by gas bubbles coalescing and growing, initiating a crack in the $UO_2$, followed by flaking off of the material above the implantation location. Since there was a dramatic difference in the behaviour of the samples heated to 500 and 600°C, it is by no means clear whether gas bubbles could coalesce at the much lower temperatures that will pertain in the repository. The concentration of He used in these tests was also far greater than the amount which will be present in spent fuel disposed of in the Swedish repository, even at very long times after disposal.

/Ferry et al. 2008/ analysed the effect of helium build-up in the central and intermediate zones as well as in the rim structure of the fuel pellet. They conclude that, for the zones of the fuel that have not undergone restructuring, He release through diffusion to the grain boundaries should be relatively low. Therefore, for the central and intermediate zones of the fuel pellet only grain micro-cracking due to over-pressure or formation of gas bubbles with helium should cause significant helium release from the uranium dioxide grains. By assuming a realistic number density and size distribution of intra-granular fission gas bubbles at the end of the irradiation and that all helium atoms formed are trapped in these bubbles, the concentration of helium required to reach a critical bubble pressure is $4 \cdot 10^{20}$ atoms/cm$^3$ (about $3.8 \cdot 10^{19}$ atoms/g for 94% theoretical density) in 10 nm bubbles. For larger bubbles, the critical pressure is about $10^{21}$ atoms/cm$^3$ (~ $9.6 \cdot 10^{19}$ atoms/g). Using the data presented by /Ferry et al. 2008/, one can conclude that the helium produced by alpha-decay is not sufficient to produce micro-cracking of grains in $UO_2$ fuel for several hundred thousand years.

The rim region of the fuel has undergone fission at a rate up to three times higher than the mean fission rate of the pellet. This is caused by a build-up of fissile plutonium and other actinides due to capture of epithermal neutrons. The higher fission rate causes a restructuring of the fuel matrix yielding sub-micrometre grains and a higher porosity (exceeding 10%). These large pores form sharp angles at the grain boundary, where crack-tips can be initiation points for crack growth and fracture of the ceramic. /Ferry et al. 2008/ analysed the effect of helium in this region by considering the helium pressure necessary to exceed the fracture toughness of the material. Their conclusion was that even in the rim region, conditions for crack propagation in the grain boundaries would not occur. The rim inventory should, therefore, not contribute to the Instant Release Fraction.

It can be concluded that, for the burnup range relevant for Swedish conditions, the mechanical stability of the spent fuel to be disposed of in Sweden will not be detrimentally affected by the accumulation of He in the fuel after disposal.

The amounts of He formed after 100,000 years (see above) correspond to 1.7 to 2.2 dm$^3$ (STP) He for each fuel pin. This is equivalent to a pressure rise of 3.4 to 4.4 MPa if released to the void volume (50 cm$^3$) in the fuel pin. In addition, the fuel pins may also have been pre-pressurised to a few MPa. If all the accumulated helium was released to the void inside the canister, the pressure rise would be 0.50 to 0.65 MPa (or about twice the level due to pre-pressurisation) after 100,000 years, and about 1 to 1.3 MPa after 1,000,000 years. This is considerably lower than the pressure external to the canister and will have negligible consequences for its stability.

### *Natural analogues/observations in nature*

/Roudil et al. 2008/ have studied a sample of natural uranium dioxide (pitchblende) from Pen Ar Ran in France. The sample was 320 Ma old and had not been subjected to any single events that could have caused helium loss. The sample had retained less than 5% of the total amount of radiogenic helium formed. The retained amount corresponds roughly to the expected solubility of helium in

uranium dioxide. The authors deduced a diffusion coefficient that is nine orders of magnitude higher than that expected in well-crystallised $UO_2$ nuclear fuel. The reason for this is not presently clear.

### *Time perspective*

The helium build-up proceeds continuously as long as there is uranium left in the fuel.

### *Handling in the safety assessment SR-Site*

It is pessimistically assumed that all fuel rods are breached as soon as water contacts the fuel, i.e. the ability of the cladding to prevent or retard radionuclide transport is pessimistically neglected.

The helium build-up in the canister void is neglected. The helium build-up has no detrimental effect on the mechanical stability of $UO_2$ fuel. For MOX fuel, the helium production is higher and may exceed the critical values discussed in /Ferry et al. 2008/. The much higher measured fission gas releases from MOX fuel /Johnson and McGinnes 2002, Johnson et al. 2005/, however, indicates that the grain boundary inventory most probably has already been swept out to the fuel-cladding gap prior to removal from reactor.

If the helium is released to the void in the canister, the resulting pressure increase will not have any consequences for the mechanical stability of the canister.

*Boundary conditions:* As stated above, there are no relevant boundary conditions for this process other than the physical boundaries set by the geometries of the components involved.

*Handling of variables influencing this process:* The influence of the radionuclide inventory is explicitly included in all estimates justifying the neglect of this process.

### *Handling of uncertainties in SR-Site*

**Uncertainties in mechanistic understanding**

Uncertainties related to i) the fraction of the created alpha particles that actually contribute to helium pressure build-up, and ii) the impact of this pressure build-up on cladding integrity are treated pessimistically.

The main uncertainty related to the mechanical alterations of the fuel matrix is the uncertainty associated with future burnup levels.

**Model simplification uncertainties**

The simplifications with respect to cladding barrier function and pressure build-up in the canister interior are pessimistic.

**Input data and data uncertainties**

/Ferry et al. 2008/ state that the main uncertainty of their model is the value of the critical bubble pressure, which is based on a fracture stress derived from three-point bending tests on polycrystalline $UO_2$, and that a larger value is to be expected in mono-crystalline $UO_2$. For the rim section, a conservative expression has been used for the calculation. It would be necessary to validate this model by more microscopic approaches. The degree of confidence in this model is, however, relatively poor due to the lack of other data to confirm the calculations.

### *Adequacy of references supporting the handling in SR-Site*

/Ferry et al. 2008/ is a peer reviewed conference paper and addresses directly the issue of helium build-up in $UO_2$ fuel.

### 2.5.9 Chemical alteration of the fuel matrix

#### *Overview/general description*

In 1992, /Janeczek and Ewing 1992/ discussed the possibility of spent $UO_2$ fuel alteration under reducing conditions through the formation of coffinite, $USiO_4 \cdot nH_2O$. The reaction can be written in simplified form as

$$UO_2 + H_4SiO_4 \Leftrightarrow USiO_4 + 2H_2O$$

Via this process, fission products and actinides in the $UO_2$ matrix could potentially be mobilised and released at a rate higher than the dissolution rate of the uranium.

#### *Dependencies between process and fuel variables*

Table 2-17 shows how the process influences, and is influenced by, all fuel variables.

#### *Boundary conditions*

There are no relevant boundary conditions for this process other than the physical boundary set by the geometries of the components involved.

#### *Model studies/experimental studies*

The thermodynamic data for coffinite are very limited and mainly based on estimations. Coffinite naturally occurs as fine-grained crystals often intergrown with associated minerals and organic material. Synthetic coffinite prepared by /Fuchs and Hoekstra 1959/ contained excess silica and some uraninite. /Robit-Pointeau et al. 2006/ attempted unsuccessfully to synthesise coffinite, and /Hemingway 1982/ also reports and references unsuccessful attempts to produce coffinite. It seems unlikely, therefore, that there will be material available for proper characterisation, and data must be estimated largely from geological information. /Brookins 1975/ predicted that uraninite would be

**Table 2-17. Direct dependencies between the process "Chemical alteration of the fuel matrix" and the defined fuel variables and a short note on the handling in SR-Site.**

| Variable | Variable influence on process | | Process influence on variable | |
|---|---|---|---|---|
| | Influence present? (Yes/No) Description | Handling of influence (How/If not – why) | Influence present? (Yes/No) Description | Handling of influence (How/If not – why) |
| Radiation intensity | No. | – | No. | – |
| Temperature | Yes. The process, if it occurs will take place in the long term and at the ambient constant temperature. | The process is neglected. Release of matrix-bound radionuclides will occur during the $UO_2$ dissolution. | No. | – |
| Hydrovariables (pressure and flows) | Yes. The process requires supply of silicates. | The process is neglected. Release of matrix-bound radionuclides will occur during the $UO_2$ dissolution. | No. | – |
| Fuel geometry | No. | – | No. | – |
| Mechanical stresses | No. | – | No. | – |
| Radionuclide inventory | No. | – | No. | – |
| Material composition | No. | – | No. | – |
| Water composition | Yes. The process requires sufficiently high silicate content in the water. | The process is neglected. Release of matrix-bound radionuclides will occur during the $UO_2$ dissolution. | No. | – |
| Gas composition | No. | – | No. | – |

unstable towards coffinite if the activity of $H_4SiO_4$ exceeded $10^{-6.9}$ (8 ppb $SiO_2$). This value is much lower than what is normally found in groundwater. Typical values for Scandinavia are 10–15 ppm. Since silica in groundwater always exceeds the value given by /Brookins 1975/, /Langmuir 1978/ considered this value unreasonably low since it would make coffinite more stable than uraninite in natural waters. He proposed a value of $10^{-3}$ (60 ppm), since this is the value found in the groundwaters at Grants mineral belt in New Mexico, where both uraninite and coffinite occur in uranium ore deposits. Based on this assumption, /Langmuir 1978/ estimated a $\Delta G$ of formation of −452 kcal/mol (−1,891 kJ/mol), but this value was later corrected by /Langmuir and Chatham 1980/ to −449.9 kcal/mol (−1,882 kJ/mol). The value given by the OECD/NEA (recalculated to −1,883.6 kJ/mol, considering auxiliary available data) is also based on estimation /Langmuir and Chatham 1980/.

This observation that uraninite is more abundant than coffinite also appears to be contradictory to the assumption that coffinite could be a long-term alteration product of the uranium dioxide in spent fuel. The difficulties in producing synthetic coffinite indicate that it most likely forms only under rather specific conditions. /Hemingway 1982/ proposes a model for the deposition of coffinite, which involves reduction of U(VI) from solution on surfaces with amorphous silica coatings. He also concludes that coffinite is metastable with respect to uraninite and quartz at all geologically important temperatures. Based on calorimetric measurements /Mazeina et al. 2005/ found thorite ($ThSiO_4$ polymorph) and huttonite ($ThSiO_4$ polymorph) to be less stable than quartz and thorianite ($ThO_2$) under normal conditions but stabilised at higher temperatures relative to its binary oxides owing to the entropy contribution.

The primary goal of the Palmottu Natural Analogue Project /Kaija et al. 2000/ was to test and model a number of analogous features to those being considered relevant to the performance assessment (PA) of spent nuclear fuel under repository conditions in crystalline bedrock. The Palmottu mineralisation site is a U-Th deposit in mica gneisses and granites typical of the rocks in the Fennoscandian Shield. The main U-bearing ore minerals at this site are uraninite [$UO_{2+x}$, $(0.01 < x < 0.25)$] and monazite (a thorium (and uranium) bearing rare earth phosphate). Coffinite is a widespread alteration product of uraninite, which formed soon after the precipitation of its precursor mineral. The majority of the uranium has remained in the ancient U(IV) phases, uraninite and coffinite, throughout its geological history (1,700–1,800 Ma), demonstrating that reducing conditions have prevailed in the bedrock for most of its existence. The alteration of the uraninite at Palmottu proceeded under reducing conditions, observed by the formation of uranous silicate phases instead of uranyl compounds. Evidently the silica-rich residual hydrothermal solutions of the uraniferous pegmatites were responsible for the alteration. There is no evidence for recent low-temperature conversion of uraninite to coffinite.

At both Oklo and Cigar Lake, coffinite is present as a uraninite alteration product (see e.g. /Janeczek and Ewing 1992/). The alteration, however, took place through hydrothermal dissolution followed by re-precipitation under reducing conditions. There are no indications of a solid state transformation of uraninite to coffinite.

### *Natural analogues/observations in nature*

Almost all information about coffinite comes from observations in nature, see above.

### *Time perspective*

The process cannot start until the copper canister has failed. Then, it is a matter of millions of years before the process will contribute to the release from the fuel, if at all.

### *Handling in the safety assessment SR-Site*

Since the alteration of the uranium dioxide fuel to coffinite, if it occurs, will most likely happen through a dissolution and re-precipitation process, any release of matrix-bound radionuclides will occur during the $UO_2$ dissolution. Even if some of these radionuclides may be incorporated in the precipitating coffinite, it is pessimistic to assume that all matrix-bound radionuclides will be released to the near-field. The formation of coffinite will not, therefore, increase the release rate from the fuel and can be disregarded in SR-Site.

### *Handling of uncertainties in SR-Site*

**Uncertainties in mechanistic understanding**

Not applicable.

**Model simplification uncertainties**

Not applicable.

**Input data and data uncertainties**

Not applicable

### *Adequacy of references supporting the handling in SR-Site*

The review process for the reports by /Hemingway 1982/ and /Kaija et al. 2000/ is unknown. All other cited papers are peer reviewed journal or conference papers. The information they contain concerns the stability and formation of coffinite under conditions that closely resemble repository conditions.

## 2.6 Radionuclide transport

### *Overview/general description*

If water enters a breached canister, corrosion of the cast iron insert and the fuel's metal parts begins, see Sections 3.5.1 and 2.5.4. With time, water may come into contact with the fuel, thereby causing radionuclides to be released as water-soluble species or colloids (Section 2.5.7). Radionuclides are also present in the metal parts of the fuel and released when they corrode.

Released radionuclides can be transported in the interior of the canister and exit through a breach in the copper shell. Radionuclides dissolved in water inside the canister can be transported either advectively with the water, or by diffusion in the water. Transport in water is the predominant mode of mobilisation of radionuclides, although some nuclides occur in gaseous form in the canister and may also be transported in the gas phase; e.g. $^{14}C$, $^{222}Rn$ and $^{85}Kr$.

The geometry of transport pathways in a breached canister is determined by the original geometry of the canister and the fuel modified by any changes caused by corrosion. For water to contact the fuel and release and transport radionuclides there must be penetrating breaches in both the cast iron insert and the Zircaloy cladding. Even if such breaches have occurred, the remaining structures can be expected to constitute a considerable transport barrier, both to the inflow of water (Section 2.3.1) and to the outward transport of soluble nuclides. The structure of the four-metre-long cladding tubes and other metal parts of the fuel, the cast iron insert and the copper canister prevent effective transport. Corrosion deposits from the cast iron insert in particular can be expected to obstruct transport (see Section 3.5.1).The surfaces of all of these structures may act as sorption sites for certain radionuclides.

### *Dependencies between process and fuel variables*

Table 2-18 shows how the process influences, and is influenced by, all fuel variables.

### *Boundary conditions*

The inner boundary is determined by radionuclide inventories in the fuel, and the release rate from the fuel and the concentrations of radionuclides in the water phase inside the canister.

The outer boundary is determined by size and shape of the defect in the copper canister.

**Table 2-18. Direct dependencies between the process "Radionuclide transport" and the defined fuel variables and a short note on the handling in SR-Site.**

| Variable | Variable influence on process | | Process influence on variable | |
|---|---|---|---|---|
| | Influence present? (Yes/No) Description | Handling of influence (How/If not – why) | Influence present? (Yes/No) Description | Handling of influence (How/If not – why) |
| Radiation intensity | No. | – | No. | – |
| Temperature | Yes. Diffusion is temperature dependent. | Neglected. Water ingress is assumed to take place at the earliest 1,000 years after disposal. At that time the temperature will have a very limited effect. | No. | – |
| Hydrovariables (pressure and flows) | Yes. | Water is assumed to be present after failure. | No. | – |
| Fuel geometry | No. | – | No. | – |
| Mechanical stresses | No. | – | No. | – |
| Radionuclide inventory | Yes. Obvious. | Included in modelling. | No. Obvious. | – |
| Material composition | No. | – | No. | – |
| Water composition | Yes. Affects solubility. | Included in modelling. | Yes. Dissolved radionuclides in water. | Source term for radionuclide release. |
| Gas composition | No. | – | Yes. | Release of gaseous radionuclides. |

### *Model studies/experimental studies*

No direct studies of radionuclide transport are known for the conditions that are expected in a breached canister. The general knowledge of processes such as advection, diffusion and sorption is good, however, and the processes have been thoroughly studied.

### *Natural analogues/observations in nature*

Not applicable.

### *Time perspective*

After the copper shell has been breached, radionuclide transport in the interior of the canister is a relevant process in all of the safety assessment's time perspectives.

### *Handling in the safety assessment SR-Site*

The process is only relevant if the copper shell has been breached.

Radionuclide transport in the interior of the canister is simplified for modelling purposes in the following way: After a given delay time has passed since the breach of the canister's copper shell, the entire cavity initially available in the canister, about 1 $m^3$, is assumed to be filled with water. The length of this delay time is determined based on the size of the breach in the copper shell and the subsequent water flux and the rate of cast iron corrosion, see further the SR-Site data report /SKB2010l/.

After the delay time, all the water in the canister is assumed to be available for the fuel dissolution process, i.e. to be in direct contact with all the fuel without being impaired by Zircaloy cladding or other structures. The water is assumed to be thoroughly mixed, i.e. there are no concentration gradients throughout the interior of the canister. The fuel dissolution process then determines the rate of

release of matrix-bound radionuclides. Segregated nuclides and radionuclides in the structural parts of the fuel (e.g. cladding) are assumed to be available for dissolution in water immediately after the end of the delay time. Sorption of radionuclides on the internal parts of the canister is pessimistically neglected.

Transport of radionuclides through the breach in the copper shell is modelled as diffusion with an assumed geometry of the breach.

The modelling is carried out using the transport model COMP23 /Cliffe and Kelly 2005/, integrated with the modelling of fuel dissolution, precipitation/dissolution of solubility-limited radionuclides and radioactive decay. Transport through the buffer/backfill and out to the surrounding geosphere is also handled in this model.

The micropores in the buffer are expected to prevent all colloidal transport out of the canister. Colloid transport in the interior of the canister is therefore not dealt with, since the buffer completely envelops the canister.

Radionuclide transport in the gas phase is handled by approximate calculations.

### *Handling of uncertainties in SR-Site*

#### Uncertainties in mechanistic understanding

The uncertainties surrounding water/gas flux in the interior of the canister (Section 2.3.1), corrosion of the cast iron insert (Section 3.5.1) and corrosion of the metal parts of the fuel (Section 2.5.4) are particularly large. An assessment of the geometric conditions and, therefore, the geometry of the transport pathways is, hence, also uncertain. The sorption properties of the materials in a damaged canister are also difficult to assess.

#### Model simplification uncertainties

Radionuclide transport in the interior of the canister is, therefore, simplified pessimistically in the safety assessment (see Handling in Safety Assessment).

#### Input data and data uncertainties

Input data and input data uncertainties for this process are discussed in the SR-Site data report /SKB 2010l/, based on the data reported in /Duro et al. 2006b, Grivé et al. 2010/.

### *Adequacy of references supporting the handling in SR-Site*

/Duro et al. 2006b/ is reviewed and approved following SKB's Quality Assurance system.

# 3 Cast iron insert and copper canister

## 3.1 Radiation-related processes

### 3.1.1 Radiation attenuation/heat generation

#### *Overview/general description*

The gamma- and neutron radiation (from the radioactive disintegrations in the fuel) that extend into the canister interacts with the cast iron insert and the copper shell. Energy is thereby transferred to the materials and the radiation is attenuated. Most of the transferred energy is converted into thermal energy to generate heat.

In the cases of alpha and beta disintegrations, most of the radiation energy remains in the fuel since the fuel itself largely attenuates the radiation. In the case of gamma radiation, some of the surplus energy will escape the fuel and generate heat by attenuation in the canister materials. This fraction is estimated to comprise less than 35% of the total heat output, see information given by /Håkansson 2000/.

The radiation attenuation in the canister will also have the potential to affect the mechanical properties of the canister materials. This is dealt with in Section 3.4.6.

#### *Dependencies between process and canister variables*

Table 3-1 shows how the process influences**,** and is influenced by, all canister variables.

The heat generation in the canister materials is caused by the radiation and, consequently, influenced by the radiation intensity and also by the canister geometry (metal thickness) and material. The attenuation/heat generation may also give rise to changes in the materials properties, see Section 3.4.6.

**Table 3-1. Direct dependencies between the process "Radiation attenuation/heat generation" and the defined canister variables and a short note on the handling in SR-Site.**

| Variable | Variable influence on process | | Process influence on variable | |
|---|---|---|---|---|
| | Influence present? (Yes/No) Description | Handling of influence (How/If not – why) | Influence present? (Yes/No) Description | Handling of influence (How/If not – why) |
| Radiation intensity | Yes. The radiation intensity causes the heat generation. | In the modelling of heat generation and dissipation, it is assumed that all heat generation takes place in the fuel itself. | No. | – |
| Temperature | No. | – | Yes. Radiation attenuation results in heat generation. | In the modelling of the temperature distribution in the canister, it is assumed that all heat generation takes place in the fuel itself. |
| Canister geometry | Yes. The degree of radiation will depend on the canister geometry, in particular the thickness of the various components. | The canister geometry and the relevant materials are explicitly included in the calculations leading to the neglect of this process. | No. | – |
| Material composition | Yes. Different materials attenuate radiation to different degrees. | See above. | No. | – |
| Mechanical stresses | No. | – | No, but indirectly via the temperature. | See Section 3.4.4. |

### *Boundary conditions*

Part of the gamma- and neutron radiation from the radioactive disintegrations escapes the fuel into the canister and the canister materials will attenuate the energy. Most of the energy attenuation occurs in the inner parts of the canister. The remaining energy will cross the canister/buffer boundary and be dissipated outside the canister.

### *Model studies/experimental studies*

Calculations of the canister's radiation attenuation (i.e. dose rate calculations) have been performed by /SKBdoc 1077122/.

### *Natural analogues/observations in nature*

Not applicable.

### *Time perspective*

Immediately after deposition, the gamma-radiation is dominated by the decay of $^{137}Cs$. This isotope has a half-life of approximately 30 years. In other words the radiation intensity is approximately halved every 30 years.

### *Handling in the safety assessment SR-Site*

In the modelling of heat generation and dissipation, it is assumed that all heat generation takes place in the fuel itself. With this approach, the temperature in the fuel will be overestimated initially, but this will be of little importance for the temperature distribution in the near field shortly after deposition and beyond.

The process is not explicitly modelled, but the dissipated energy is accounted for. Section 3.4.6 discusses radiation effects on canister materials.

*Boundary conditions:* The relevant boundary conditions are explicitly included in the calculations leading to the neglect of this process /SKBdoc 1077122/.

*Handling of variables influencing this process:* The influencing variables, i.e. the radiation intensity, the canister geometry and the relevant materials are explicitly included in the calculations leading to the neglect of this process /SKBdoc 1077122/.

### *Handling of uncertainties in SR-Site*

**Uncertainties in mechanistic understanding**

The mechanistic understanding of this process is sufficient for the needs of the safety assessment.

**Model simplification uncertainties**

Not relevant, since the process is not explicitly modelled in the safety assessment. (The model study used to justify the neglect of the process does not entail simplifications of any importance.)

**Input data and data uncertainties**

Not relevant since the process is not explicitly modelled in the safety assessment. (The available data are sufficiently accurate for the model study used to justify the neglect of the process.)

### *Adequacy of references supporting the handling in SR-Site*

The supporting /SKBdoc 10077122/ has undergone a documented factual- and quality review.

## 3.2 Thermal processes

### 3.2.1 Heat transport

#### *Overview/general description*

Heat is transported in the metal in the cast iron insert and copper canister by conduction. As friction stir welding is used, there will be an important contribution to the heat transfer from iron to copper from conduction, since there will be air in the gap between cast iron and copper. There will also be a contribution due to heat conduction through the bottom contact between the insert and the copper canister.

The process is controlled by, and influences, the temperature distribution in the materials. The heat flow towards adjacent subsystems (fuel and buffer) comprises the boundary conditions. The process is a part of the repository's thermal evolution.

#### *Dependencies between process and canister variables*

Table 3-2 shows how the process influences, and is influenced by, all canister variables.

The radioactive decay (to which the radiation intensity is related) constitutes the heat source. The radiation intensity in the canister itself has negligible influence on the process. The transport of heat from the fuel is influenced by the canister geometry (metal thickness) and material. The temperature has a negligible influence on the heat transport through conduction, but a larger influence on the transport of heat through radiation.

The process is controlled by, and influences, the temperature distribution in the materials.

Due to the high thermal conductivity of iron and copper, very small temperature differentials arise within the metal components.

#### *Boundary conditions*

The boundary conditions are the heat flow from the fuel into the canister and from the canister out into the buffer.

**Table 3-2. Direct dependencies between the process "Heat transport" and the defined canister variables and a short note on the handling in SR-Site.**

| Variable | Variable influence on process | | Process influence on variable | |
|---|---|---|---|---|
| | Influence present? (Yes/No) Description | Handling of influence (How/If not – why) | Influence present? (Yes/No) Description | Handling of influence (How/If not – why) |
| Radiation intensity | No. The radioactive decay (to which the radiation intensity is related) constitutes the heat source. | – | No. | – |
| Temperature | Yes. Obvious. | The process is included in the modelling of the canister material temperatures. | Yes. Heats the canister materials. | The process is included in the modelling of the canister material temperatures. |
| Canister geometry | Yes. Obvious. | The gap between the copper shell and cast iron insert is included in the temperature modelling. | No. | – |
| Material composition | Yes. Obvious. | The heat transport in the gap between the copper shell and the cast iron insert is modelled. | No. | – |
| Mechanical stresses | No. | – | No, but indirectly via the temperature. | See Section 3.4.4. |

### *Model studies/experimental studies*

In SR-Can temperature calculations were carried out for the thermal evolution after disposal with model and benchmarking described in /Hedin 2004/. The calculations were carried out for a heat load of 1,700 W, which is estimated to be the highest heat load in a canister. The canister was assumed to be filled with air. The surface temperature of the outer copper shell was below 100°C.

### *Natural analogues/observations in nature*

Not applicable.

### *Time perspective*

Heat generation is halved every 30 years during the initial post-closure period. The highest temperatures and the greatest heat flows occur within tens of years after deposition and repository closure.

### *Handling in the safety assessment SR-Site*

A simplified handling of the temperature modelling in the canister materials is adopted in SR-Site. The process is modelled with results from the modelling of the buffer and the host rock as boundary conditions. The most important calculation end-point in that modelling /Hökmark et al. 2010/ is the peak buffer inner surface temperature, which is insensitive to the handling of heat transport in the canister interior, which also means that the canister surface peak temperature is insensitive to the temperature distribution in the canister. The peak temperature in the iron insert is of concern for the analyses of canister material properties, and can be described from the maximum copper temperature.

Boundary conditions: The canister outer surface temperature is controlled by the time dependent heat generation rate and by the thermal properties of the canister/buffer interface, the buffer, and the host rock. Heat transfer due to both conduction and radiation at the boundary between the canister and buffer is included in the analysis of the canister surface temperature.

Handling of variables influencing this process: All variables influencing this process according to the influence table (Table 3-2) are included in the modelling of the temperature of the cast iron insert.

The thermal conductivity in metal parts is assumed to be infinite, and heat transfer by radiation and conduction across the gap between copper and iron canister is considered. Heat conduction through the bottom contact between the insert and copper canister is pessimistically neglected, since data are uncertain for this contribution.

The maximum temperature in the iron insert could be estimated by the heat transfer across the gap between the iron insert and the copper shell. The flow of heat is the sum of the radiation and conduction in the gap. The heat flow in the solid metals results in negligible temperature gradients due to the high thermal conductivity of the metals. The heat flow per unit area, is described by /Carslaw and Jaeger 1959/:

$$\frac{P}{\pi DL} = \frac{\lambda_{gas}(T_{Fe} - T_{Cu})}{\Delta r} + \varepsilon_{tot}\sigma(T_{Fe}^4 - T_{Cu}^4)$$

where $P$ is the power output from the canister, $D$ is the average canister diameter for the gap, $L$ is the length of fuel elements generating the heat, $\lambda_{gas}$ is the thermal conductivity of the gas in the gap, $\Delta r$ is the thickness of the gap, $\varepsilon_{tot}$ is the combined emissivity of the two materials in the gap, $\sigma$ is the Stefan-Boltzmann constant and $T_{Fe}$ and $T_{Cu}$ are the temperatures in the cast iron and copper respectively.

The temperature in the cast iron insert, $T_{Fe}$ can be solved analytically or numerically from this expression. Using the following input data: $P$=1,700 W, $D$=0.9505 m, $L$=3.68 m (active length of the fuel elements), $\lambda_{gas}$=0.0178 W/m,K (argon), $\varepsilon_{Fe}$=0.6 and pessimistically $\Delta r$ =0.00175 m, $\varepsilon_{Cu}$=0.020 and $T_{Cu}$=102°C, gives a maximum $T_{Fe}$ of 117°C.

#### *Handling of uncertainties in SR-Site*

**Uncertainties in mechanistic understanding**

The fundamental understanding of this process is deemed sufficient for the needs of the safety assessment.

**Model simplification uncertainties**

Model simplifications essentially involve a simplified geometry. The effects of such simplifications have been evaluated by benchmarking against complex models, which demonstrates that they have no significant influence on the calculation result; see further /Hedin 2004/.

**Input data and data uncertainties**

The copper surface temperature is used as input for the calculation of the temperature of the cast iron insert. The uncertainties of the temperature distribution in the buffer/rock system is discussed in /Hökmark et al. 2010/. The simplified calculations are based on pessimistic data for copper surface temperature, copper emissivity (polished copper) and size of the copper-iron gap (the Canister production report states the reference design as 0.0015 m /SKB 2010c/).

#### *Adequacy of references supporting the handling in SR-Site*

The supporting reference /Hökmark et al. 2010/ is an SKB report that has undergone a documented factual- and quality review. The simplified calculation is built on basic knowledge documented in books.

## 3.3 Hydraulic processes

Water and gas flux in the interior of the canister is described in Section 2.3.1 and will not be further dealt with here.

## 3.4 Mechanical processes

### 3.4.1 Introduction

Mechanical interactions with the buffer occur at the boundary between the canister and buffer. They arise from the buffer through the clay matrix, which generates both compressive and shear stresses. The porewater and gas in the buffer generate only compressive stresses. Shear stresses may appear in the event of rock movements. Changes in these three factors take place during the water saturation process and can also occur in response to external forces. The weight of the canister influences the buffer, while the influence of the weight of the buffer on the canister is negligible.

The mechanical interaction between buffer and canister involves the following:

- Swelling pressure and water pressure are exerted on the canister.
- Shear stresses transfer from the rock movements via the buffer to the canister, especially during an earthquake.
- Trapped gas in the buffer exerts pressure on the canister.
- Canister corrosion products exert pressure on the canister.

#### *Swelling and water pressures are exerted on the canister*

Swelling pressure develops as the buffer undergoes wetting. Water pressure on the canister does not arise until the bentonite is saturated. The total pressure will not exceed the sum of the swelling pressure and the water pressure. During glaciations, the pressure will increase further. This additional pressure will at most correspond to the weight of the ice-sheet formed at the repository location.

If the wetting is even, the swelling pressure increases evenly on the canister's periphery, except on the end surfaces where wetting of the buffer takes the longest time because of its thickness. If the wetting is uneven, the build-up of swelling pressure on the canister will be uneven. In the event of unfortunate combinations of wetting areas, the canister may be subjected to uneven stresses. Uneven stresses can also be caused by bent ("banana" shaped) deposition holes or rock fall-out from the walls of the deposition holes.

If the buffer is water-saturated before the maximum temperature has been reached, the water will expand, a process that will be hindered by the confined volume. Thus, the pressure could theoretically be very large. However, such a pore pressure increase is compensated by water drainage out through the rock. Scoping calculations show that no big pressure ever has time to build up /Pusch and Börgesson 1992/.

#### *Transfer of shear stresses from the rock via the buffer to the canister*

Rock movements in the form of shear along a fracture plane intersecting the depositon hole affect the canister via the buffer. The buffer thereby acts to cushion the sharp and hard rock wedge. Since the movement does not change the total volume of the buffer, the effect is essentially a shear deformation, whereby the shear strength of the buffer regulates the impact.

#### *Trapped gas in the buffer exerts pressure on the canister*

Gas generated or confined at the canister surface exerts a pressure on the canister. This gas pressure is, however, limited to the bentonite's opening pressure (see the SR-Site Buffer Process report, /SKB 2010k/). The gas is released through the bentonite either through temporary channels that form, or by dissolving in the water and diffusing out.

#### *Canister corrosion products exert pressure on the canister*

External corrosion of the copper canister, which can be both local and general, increases the canister volume, since the corrosion products have a lower density than copper. This increase causes consolidation of the buffer and an increase in the pressure between buffer and canister. Copper corrosion is, however, so slow (see Section 3.5.4) that even corrosion over hundreds of thousands of years will not lead to more than a marginal increase in pressure, well within the error margins for the estimated buffer pressure on the canister throughout the one million year time period of the safety assessment.

In the event of a defect in the copper shell, a similar effect may occur in the cast iron. Preliminary modelling /Bond et al. 1997/ on the event of a small breaching hole, showed that the influence was not significant.

### 3.4.2 Deformation of cast iron insert

#### *Overview/general description*

When the canister is loaded mechanically, for example when the buffer swells, stresses will be built up in the canister material, which deforms elastically at first but plastically if the stresses are large. The size of the deformation for a given load is dependent on the strength of the cast iron insert, which is determined by its material properties and geometry.

The cast iron insert is the most important mechanical barrier in the repository. If it collapses, a number of safety functions are jeopardised. The process is**,** therefore, of central importance to the function of the repository.

Under normal conditions in a geologic repository, the cast iron insert is expected to be subjected to an external load composed of a maximum swelling pressure from the bentonite of up to 15 MPa and a water pressure of 4 MPa. The pressure can be regarded as isostatic, i.e. evenly distributed over the entire surface. A canister can be subjected to an increased load during an ice age. An ice sheet, several kilometres thick floating on the groundwater gives a maximum increase in pressure proportional to its maximum thickness. The expected pressure increase is about 28 MPa. It must be noted that the total stress on the canister is the bentonite swelling pressure added to a part of the

hydraulic pressure, rather than just the sum /Harrington and Birchall 2007/. The reducing factor for the pore water pressure is estimated to be in the range 0.86–92 /Harrington and Birchall 2007/. The total load from these three causes can, thus, be estimated to be 45 MPa.

As the bentonite becomes water saturated, uneven pressure distributions can arise. They may be associated with uneven water ingress or with oval or slightly curved deposition holes. In some cases an uneven stress could possibly persist for a long time. Such loads will, in addition to compressive stresses, also give rise to flexural stresses (tensile and compressive stresses).

Deviations from the normal load can also arise due to rock displacements across the deposition hole. This could result in flexural and tensile and compressive stresses in the canister insert.

The load situations described above have been discussed and analysed extensively by /Raiko et al. 2010/. These scenarios will, therefore, not be discussed in any detail in this report. The main results and conclusion in /Raiko et al. 2010/ are presented below in Section Model studies/experimental studies.

A mechanical load also results from internal pressure build-up due to gas formation caused by alpha decay. The large void in the canister will make the effects of gas build-up negligible for all reasonable time periods (see Section 2.5.8).

If the copper canister is breached and water contacts the canister insert, it will corrode (see Section 3.5.1). The corrosion rate is low, but leads to a progressive reduction in the mechanical strength of the insert. This will eventually lead to failure. When and how this failure occurs depends on the extent of the breach, the geometry of the corrosion attack, and the load situation for the canister in question.

### *Dependencies between process and canister variables*

Table 3-3 shows how the process influences, and is influenced by, all canister variables.

**Table 3-3. Direct dependencies between the process "Deformation of cast iron insert" and the defined canister variables and a short note on the handling in SR-Site.**

| Variable | Variable influence on process | | Process influence on variable | |
|---|---|---|---|---|
| | Influence present? (Yes/No) Description | Handling of influence (How/If not – why) | Influence present? (Yes/No) Description | Handling of influence (How/If not – why) |
| Radiation intensity | No.<br>Discussed in 3.4.6. | – | No. | – |
| Temperature | Yes.<br>The mechanical properties are temperature dependent. | Neglected.<br>The maximum mechanical load will occur after the period of increased temperature in the repository. | No. | – |
| Canister geometry | Yes.<br>The geometry and the properties of the material will determine the strength of the canister insert. | The canister's mechanical stability is modelled using the actual canister dimensions. | Yes.<br>A deformation will obviously alter the canister geometry. | Inherent in the model. |
| Material composition | Yes.<br>The geometry and the choice of material will determine the strength of the canister insert. | The canister's mechanical stability is modelled using the actual properties of the canister material. | No. | – |
| Mechanical stresses | Yes.<br>Stresses are the direct cause of the deformation. | Inherent in the model. | Yes.<br>A deformation will alter the mechanical stresses. | Inherent in the model. |

### *Boundary conditions*

The swelling pressure from the bentonite will control the development of even and uneven pressure situations.

Rock displacements across the deposition hole can cause an additional load on the canister.

### *Model studies/experimental studies*

The mechanical external loads on the canister insert in the repository are discussed and analysed in /Raiko et al. 2010/. Their analyses include:

- asymmetric loads due to uneven water saturation of the buffer,
- asymmetric loads after buffer saturation,
- isostatic pressure load,
- glacial pressure load.

Their main conclusions are the following.

During water saturation, the worst case that may occur is for a curved deposition hole. Simplified calculations of the stresses in the canister insert yield a maximum bending stress $\sigma_b$ = 105 MPa. This bending stress in the cast iron insert for this case as well as for all other calculated cases is lower than the yield strength. Thus, the insert will withstand them elastically, without plastic deformation or risk of damage.

The worst case for asymmetric loads after buffer saturation is a curved deposition hole and a local rock fall out of 3.75% of the cross section area. Simplified calculations give a maximum bending stress that is a little higher than the highest bending stress during the water saturation phase, but lower than the yield strength. The insert will withstand them elastically, without plastic deformation or risk of damage. These asymmetric load cases are acting after bentonite saturation for a very long time. The probability of occurrence for these extreme load cases is very low, which means that they should not be combined with other low probability cases, like shear loads.

As was mentioned above, the design pressure of the canister is 45 MPa external pressure and the highest pressure will occur during a glacial period when the temperature of the insert will be between 0 and 20°C. The load case will affect all the canisters in the repository. Consequently, the reliability of the canister's mechanical integrity needs to be high for this load case, since the possible risk concerns all the canisters in the repository. The external collapse loads for nominal insert cylinders are 99 and 128 MPa for BWR- and PWR-inserts, respectively, and even higher for the steel lids in both designs. Since the maximum anticipated isostatic pressure load is 45 MPa, the canister design can be considered very robust and the risk of global collapse vanishingly small.

The analyses mentioned above do not include creep of the cast iron. Due to the logarithmic behaviour of the creep in cast iron at the temperatures in the repository /Martinsson et al. 2010/ the effect of not considering creep is considered negligable.

For the shear load case, the stresses and strains in the canister are high, depending on the shear amplitude, shear angle and the intersection point. The governing case for the insert is perpendicular to the canister main axis at 3/4 of its length. The analyses show that there is a lot of capacity left in the insert structure after a 5 cm shear movement.

The damage tolerance analysis for the different load cases leads to a number of requirements on inspection of the insert where the most rigorous requirements are derived from the shear load case. The inspection requirements from the 45 MPa isostatic case are, however, more modest.

### *Natural analogues/observations in nature*

Not applicable.

### *Time perspective*

The load from the groundwater pressure and the bentonite swelling pressure is expected to build up over a period from a few years to some thousands of years after deposition. The maximum glacial load can be expected after tens of thousands of years.

### *Handling in the safety assessment SR-Site*

Isostatic load and uneven loads: The isostatic load on the canister over the one million year assessment period is assessed in SR-Site. This load will be compared to the isostatic collapse load that can be estimated from the experimental and model studies cited above. The comparison will be used to assess whether canister integrity may be jeopardised due to isostatic over pressure.

Effects of rock shear: The likelihood of violating the criteria for rock shear movements that the canister can sustain will be assessed based on estimated rock and buffer conditions. If violation occurs, the canister integrity will be assumed to be lost.

Creep effects in the cast iron insert: For the temperature range in question, creep is expected to be negligible for all the load cases considered /Martinsson et al. 2010/.

All these load situations will also imply loads on the copper shell. The effects on the copper shell are discussed in Section 3.4.3.

### *Handling of uncertainties in SR-Site*

The uncertainties in the analyses of the mechanical behaviour of the cast iron insert are discussed in detail in /Raiko et al. 2010/. Therefore, only brief summaries of their conclusions are given below.

#### Uncertainties in mechanistic understanding

*Isostatic load:* The cylindrical part of the safety factor against the design pressure is at least 2. This has also been confirmed in pressure tests /Nilsson et al. 2005/. The understanding of the process is, therefore, sufficient for the needs of the safety assessment.

*Uneven swelling loads:* By using worst-case scenarios, the need for a detailed mechanistic understanding is not necessary. The fundamental understanding is, therefore, sufficient for the needs of the safety assessment.

*Effects of rock shear:* The analysis methods are well established, although there are some uncertainties. The contact between the channel tubes for the fuel elements are considered as welded to the cast iron. This is not the case in reality and this will affect the results.

#### Model simplification uncertainties

Isostatic load and uneven loads: The 2D analyses have been validated by comparison to full 3D analyses. At the interesting stress levels, 2D is marginally pessimistic. Also, the used simplified tension model was validated against a generalised tension model and no effects of the model simplifications could be traced. There are, therefore, no model simplification uncertainties of any importance for the safety assessment.

Uneven swelling loads: The bentonite density distribution, deposition hole deviation and temporary swelling distribution are combined in the most unfavourable way. The uncertainty in the assumptions can, therefore, be set to zero since the worst scenario philosophy is applied.

Effects of rock shear: When analysing the damage tolerance the displacements after shearing were used as input for the damage tolerance calculations. The uncertainty in this data transfer was analysed and the differences considered so small that they did not significantly influence the results.

#### Input data and data uncertainties

Isostatic load: the calculations were based on statistically well-documented data. The uncertainties were judged to be small in comparison to the design load of 45 MPa.

Uneven swelling loads: The pessimistic approach in the analysis will give pessimistic results with a low probability of occurrence and these uneven loads pose no threat to the canister integrity. The data and the data uncertainties are, therefore, sufficient for safety assessment purposes.

Effects of rock shear: Uncertainties in the damage tolerance will result in uncertainties in the acceptable defect sizes. The sources of the uncertainties are variations in bentonite density, effects of strain rate, scatter in strain-stress data, scatter in fracture toughness data and the assumption that the channel tubes are integrated parts of the insert. As a result of this, pessimistic defect sizes are recommended to be used in the safety assessment.

#### *Adequacy of references supporting the handling in SR-Site*

The supporting references are SKB reports that have undergone a documented factual- and quality review.

### 3.4.3 Deformation of copper canister from external pressure

#### *Overview/general description*

The copper canister is primarily a corrosion barrier. The mechanical strength of the copper canister is of subordinate importance, but the canister must withstand the loads associated with handling, transport and deposition. The copper must also possess sufficient ductility to allow straining, either plastically or by creep when the external load against the insert deforms the canister. Furthermore, the copper canister must sustain loads caused by deformations of the cast iron insert in response to external loads.

When the load from the groundwater pressure and the swelling of the bentonite develops, the copper will deform until it makes contact with the cast iron insert.

A rock shear movement will also result in deformation of the copper canister.

#### *Dependencies between process and canister variables*

Table 3-4 shows how the process influences, and is influenced by, all canister variables.

#### *Boundary conditions*

The swelling pressure from the bentonite will control the development of even and uneven pressure situations.

Rock displacements across the deposition hole can cause an additional load on the canister.

#### *Model studies/experimental studies*

The behaviour of the copper canister under the anticipated load situations in the repository are discussed and analysed in /Raiko et al. 2010, Hernelind 2010/. The analyses include creep analysis after saturation, effects of uneven swelling pressure, glacial load, effects of slits and notches, rock shear movements, and cold work.

For the isostatic load after saturation, the copper shell will make full contact with the insert after about 10 years at 75°C. The maximum strain, which is less that 12%, will occur at the radii in the lid and bottom. In the cylindrical part, the strain is less than 0.3%.

The results obtained from glacial load creep analysis are, in summary, that the maximum strain (16%) in the copper shell that includes the plastic strain and the creep strain components occurs after 100,000 years at the geometrically singular point at the root of the weld. At the global level the strains are much lower. The singular point peak creep strain value cannot cause any global damage.

Uneven swelling can give rise to high stresses and local creep. /Raiko et al. 2010/ show, however, that this will not lead to cracking.

**Table 3-4. Direct dependencies between the process "Deformation of copper canister from external pressure" and the defined canister variables and a short note on the handling in SR-Site.**

| Variable | Variable influence on process | | Process influence on variable | |
|---|---|---|---|---|
| | Influence present? (Yes/No) Description | Handling of influence (How/If not – why) | Influence present? (Yes/No) Description | Handling of influence (How/If not – why) |
| Radiation intensity | No. Discussed in Section 3.4.6. | – | No. | – |
| Temperature | Yes. The mechanical properties are temperature dependent. | Neglected. The maximum mechanical load will occur after the period of increased temperature in the repository. | No. | – |
| Canister geometry | Yes. The geometry and the choice of material will determine the strength of the copper shell. | The canister's mechanical stability is modelled using the actual canister dimensions. | Yes. The copper will be deformed at normal load. | Inherent in the model. |
| Material composition | Yes. The geometry and the choice of material will determine the strength of the copper shell. | The canister's mechanical stability is modelled using the actual canister materials properties. | No. | – |
| Mechanical stresses | Yes. Stresses are the direct cause of the deformation. High stresses in the material may also lower its strength. | Inherent in the model. | Yes. A deformation will alter the mechanical stresses. | Inherent in the model. |

For the rock shear load case, the peak values for plastic strain occur at a few "hot spots" and the visible global values are considerably lower. The highest peak value in the copper shell, 29%, occurs when the rock shear is perpendicular to the axis of the canister at midpoint, for 10 cm shear. The corresponding global value is less that 10%. Most of the copper strain is caused by the immediate plasticity during the rapid rock shear load and the creep after the shear will only relax the stresses in the bentonite-copper-iron assembly.

### *Natural analogues/observations in nature*

Not applicable.

### *Time perspective*

The load from the groundwater pressure and the bentonite swelling pressure is expected to build up over a period from a few years up to some thousands of years. The maximum glacial load can be expected after tens of thousands of years.

### *Handling in the safety assessment SR-Site*

*Isostatic load and uneven loads:* The isostatic load on the canister over the one million year assessment period is assessed in SR-Site. This load will cause the copper to deform until the cast iron insert supports it. This will result in a maximum strain of the copper of about a few percent and, therefore, will not cause failure of the copper canister /Raiko et al. 2010/. Failure of the waste package will be controlled by the strength of the cast iron insert.

*Effects of rock shear:* The likelihood of violating the criteria for rock shear movements that the canister can sustain is assessed based on estimated rock and buffer conditions. If violation occurs, the canister integrity will be assumed to be lost. Creep is not a concern, since the copper deformation

is controlled by the surrounding material, which implies small creep rates as soon as the final deformation has been established.

#### *Handling of uncertainties in SR-Site*

The uncertainties in the analyses of the mechanical behaviour of the cast iron insert are discussed in detail in /Raiko et al. 2010/. Therefore, only brief summaries of their conclusions are given below.

**Uncertainties in mechanistic understanding**

The tensile and creep behaviour of copper are sufficiently well understood for developing models that reproduce data from laboratory tests /Jin and Sandström 2009a, Raiko et al. 2010/.

**Model simplification uncertainties**

The same creep model is used for all load cases. The uncertainty in the model is estimated to be a factor of five in creep rate. The performed analysis show low sensitivity for this uncertainty.

**Input data and data uncertainties**

The creep rate has a strong temperature dependence and the time to closing the gap between the copper shell and the insert will depend strongly on the canister temperature at water saturation. This will, however, not affect the strains when the copper is making full contact with the insert.

For the glacial load case, the temperature was conservatively assumed to be 27°C, leading to a higher creep rate than a more realistic temperature. The length of the glaciation was set to 100,000 years, much longer than the expected duration of a glacial period.

#### *Adequacy of references supporting the handling in SR-Site*

The supporting references are SKB reports that have undergone a documented factual- and quality review.

### 3.4.4 Thermal expansion

#### *Overview/general description*

The canisters reach their maximum temperature in the repository after about 10 years. If the radial gap between the cast iron insert and the copper is closed at this temperature due to creep or plastic deformation (see Section 3.4.3), cooling down to ambient temperature will cause a tensile strain in the copper shell due to the fact that the copper will shrink more than the cast iron when the temperature is decreasing. The resulting tensile strain can be estimated using the following formula;

$$\Delta\varepsilon = -\Delta T \Delta\alpha$$

where;

$\Delta\varepsilon$ is the increase in tensile strain,

$\Delta T$ is the temperature change of the system (10–100 = 90°C),

$\Delta\alpha$ is the difference in thermal expansion coefficients for the copper shell and the cast iron insert ($17 \cdot 10^{-6} - 11 \cdot 10^{-6} = 6 \cdot 10^{-6}$ °C$^{-1}$).

This gives;

$\Delta\varepsilon = 0.00054$ (0.054%)

which is of no importance compared to the creep ductility of the copper (> 15%).

#### *Dependencies between process and canister variables*

Table 3-5 shows how the process influences, and are influenced by, all canister variables.

**Table 3-5. Direct dependencies between the process "Thermal expansion" and the defined canister variables and a short note on the handling in SR-Site.**

| Variable | Variable influence on process | | Process influence on variable | |
|---|---|---|---|---|
| | Influence present? (Yes/No) Description | Handling of influence (How/If not – why) | Influence present? (Yes/No) Description | Handling of influence (How/If not – why) |
| Radiation intensity | No. | – | No. | – |
| Temperature | Yes. It is caused by temperature | Neglected based on simple calculations. | No. | – |
| Canister geometry | Yes. The dimensions and the gap size control the final results. | Neglected based on simple calculations. | No. | – |
| Material composition | Yes. Determines the thermal expansion properties. | Neglected based on simple calculations. | No. | – |
| Mechanical stresses | No. | – | Yes. May increase the stress level. | Neglected based on simple calculations. |

### *Boundary conditions*

The heat flow from the fuel and the pressure from the groundwater and the swelling of the bentonite will form the boundaries for this process.

### *Model studies/experimental studies*

See Overview/general description.

### *Natural analogues/observations in nature*

Not applicable.

### *Time perspective*

Heating to the maximum temperature takes place very quickly after deposition. Cooling to the ambient temperature takes hundreds to thousands of years.

### *Handling in the safety assessment SR-Site*

The process is neglected based on the calculation results presented above.

### *Handling of uncertainties in SR-Site*

#### Uncertainties in mechanistic understanding

The mechanistic understanding of this process is sufficient for the needs of the safety assessment.

#### Model simplification uncertainties

Not relevant since the process is not modelled in more detail in the safety assessment. The model simplification uncertainties in the calculations used to justify the neglect of the process are insignificant.

#### Input data and data uncertainties

Not relevant since the process is not modelled in more detail in the safety assessment. The data uncertainties in the calculations used to justify the neglect of the process are insignificant.

#### *Adequacy of references supporting the handling in SR-Site*

Not relevant since the process is not explicitly modelled in the safety assessment, based on fundamental knowledge.

### 3.4.5 Deformation from internal corrosion products

#### *Overview/general description*

If the copper canister is breached, water or water vapour will enter into the gap between the canister insert and the copper shell and give rise to anaerobic corrosion of the insert (see Section 3.5.1). If the water is also able to penetrate the insert, anaerobic corrosion of the inside of the channels for the fuel assemblies will occur.

In both cases, this leads to a build-up of corrosion products, which in turn causes mechanical stresses in the canister.

The process is of interest if the initial breaching occurs relatively early and is of limited extent. Under these conditions, the process will delay the occurrence of a large opening in the canister and hence the loss of all resistance to radionuclide transport offered by the canister. (For a canister failure causing a large breaching any transport resistance for radionuclides is neglected.) If the breaching is caused by a rock shear movement, the transport resistance is assumed to be delayed by the time for water to enter and give a continuous water pathway. Breaching caused by copper corrosion over an extended area following the loss of the buffer will take of the order of hundreds of thousands of years and the time required to penetrate the insert through corrosion is small in comparison and will be pessimistically disregarded in the safety assessment.

The sequence of events leading to the development of these stresses is expected to proceed as described below for a case with a small initial defect where the buffer is present.

Water runs into the gap between the canister insert and the copper shell and into the canister insert, leading to anaerobic corrosion. This leads to hydrogen gas generation, which increases the pressure inside the canister, whereupon the inflow of water decreases. This gas pressure is, however, limited to the opening pressure of the bentonite (see the SR-Site Buffer Process report /SKB 2010k/) and will not be able to cause deformation of the outer copper shell. After some time, the transport of water or water vapour into the canister by diffusion will be greater than the leakage of water into the canister due to the pressure difference. The time required for this varies with the size of the penetration in the copper canister and the corrosion rate, and is reasonably expected to be thousands of years. The inward diffusion of water vapour will prevent corrosion from ceasing entirely. The process leads to a slow build-up of corrosion products. These products occupy a larger volume than the equivalent quantity of cast iron, and with time an internal mechanical pressure is built up against the copper canister. This leads to local deformation and may cause ultimately failure of the copper canister.

#### *Dependencies between process and canister variables*

Table 3-6 shows how the process influences, and is influenced by, all canister variables.

#### *Boundary conditions*

There are no relevant boundary conditions for this process other than the physical boundary set by the geometries of the components involved. The corrosion process is coupled to the inward transport of water for which boundary conditions are discussed in Section 2.3.1.

#### *Model studies/experimental studies*

Different evolutions of an initial canister defect with subsequent corrosion of the canister insert have been modelled by /Bond et al. 1997/.

**Table 3-6. Direct dependencies between the process "Deformation from internal corrosion products" and the defined canister variables and a short note on the handling in SR-Site.**

| Variable | Variable influence on process | | Process influence on variable | |
|---|---|---|---|---|
| | Influence present? (Yes/No) Description | Handling of influence (How/If not – why) | Influence present? (Yes/No) Description | Handling of influence (How/If not – why) |
| Radiation intensity | No. | – | No. | – |
| Temperature | No. | – | No. | – |
| Canister geometry | Yes. The canister geometry determines the size of the gap. | The actual geometries are considered. | Yes. May cause expansion of the copper shell. | Several alternative cases that may lead to an enlargement of the initial failure are discussed. |
| Material composition | Yes. The material composition and the nature of the corrosion products determine the degree of volume expansion, which leads to deformation. | The actual materials are considered. | No. | – |
| Mechanical stresses | No. | – | Yes. Stresses will build up in the canister materials. | Several alternative cases that may lead to an enlargement of the initial failure are discussed. |

Regardless of the size of the canister penetration and the corrosion rate, a sufficiently large hydrogen gas pressure is expected to build up after some time to prevent liquid water from entering the canister. After that, the corrosion will nevertheless be able to continue due to the fact that water vapour can diffuse into the canister.

/Bond et al. 1997/ developed a model for this diffusion-limited corrosion. The purpose was to predict how the solid corrosion products build up in the gap between insert and copper canister. The model takes into account the change in the size of the gap during the corrosion process, possible changes in the corrosion rate, and the escape of corrosion-generated hydrogen gas from the canister.

The gap is expected to eventually fill with magnetite, $Fe_3O_4$, and the calculations were used to analyse the consequences of this for the strength of the canister. Two situations were analysed: one extreme case where the entire outside surface area of the insert corroded and one case where the corrosion was limited to an area around the original defect. The latter case progresses into the former after the copper material around the original defect begins to give way. This is calculated in the model to take around 20,000 years. According to the calculations, it takes at least 100,000 years from the time of the initial penetration before more extensive damage occurs on the copper canister.

Experimental studies of the possible pressure build-up from the corrosion products showed no jacking effects caused by expanding corrosion products /Smart et al. 2003/. Further studies by /Smart et al. 2006/ gave similar results.

### *Natural analogues/observations in nature*

Some archaeological analogues are discussed by /Smart et al. 2003, Smart and Adams 2006/.

### *Time perspective*

The process will start immediately after penetration of the outer copper shell.

### *Handling in the safety assessment SR-Site*

For an intact canister, the process is neglected. For canister failures due to rock shear movements or copper corrosion over an extended area following loss of the buffer, a pessimistic approach is used for the potential delay in the loss of transport resistance caused by the process , see further the SR-Site data report /SKB 2010l, Section 4.2/.

In the hypothetical case of a small, early canister failure, the process is treated in the SR-Site as a part of the evolution of the canister interior after damage (see Section 2.3.1, and further the SR-Site data report /SKB 2010l, Section 4.2/).

Due to the uncertainties in the development of the annulus between the copper and the cast iron, several alternative cases are considered. As a base case, the corrosion in the filled annulus ceases and the insert remains tight. Conceivable alternative cases are:

- Corrosion in the filled annulus continues and the copper shell expands followed by creep relaxation of the bentonite.
- Corrosion in the filled annulus continues and the copper shell expands followed by compression of the bentonite.
- Corrosion in the filled annulus ceases but continues inside the cavity of the insert.

All these evolutions will eventually lead to failure of the cast iron insert and an enlargement of the initially small penetration in the copper shell. This will lead to an increase in the release rate of radionuclides from the canister.

The consequences of all these developments can be pessimistically bounded by estimating conservative values of the time at which the larger failure occurs and of the size of this failure. This is further developed in the SR-Site data report /SKB 2010l, Section 4.2/.

*Boundary conditions:* The inward transport of water is included in the study by /Bond et al. 1997/.

*Handling of variables influencing this process:* The influencing variables in the table are included in the modelling by /Bond et al. 1997/ and in the cases considered in the integrated treatment of the process.

### *Handling of uncertainties in SR-Site*

**Uncertainties in mechanistic understanding**

There are uncertainties surrounding the behaviour of the canister insert under the loading caused by growing corrosion products and over the available surface area as corrosion progresses. The experimental studies /Smart et al. 2003, 2006/ seem to indicate that the corrosion products do not exert enough pressure to displace the copper shell. Further studies are ongoing at the Äspö Hard Rock Laboratory (the MiniCan project /Smart and Rance 2008/).

As discussed above, despite these uncertainties, it is possible to put an upper bound on the consequences of this process in the safety assessment.

**Model simplification uncertainties**

Modelling requires assumptions regarding the properties of the corrosion products. These, and other aspects of the model, are not verified experimentally.

Rather than attempting a justification of model simplifications, the consequences of this process are given a pessimistic upper bound in the safety assessment, as discussed above.

**Input data and data uncertainties**

The corrosion rates of freely exposed metal are relatively well known. There are, however, large uncertainties concerning the form and distribution of the corrosion over the insert surface area when the metal is exposed to a limited amount of water or water vapour. There is also uncertainty over the density and porosity of corrosion products and, therefore, the degree of expansion.

Rather than seeking defensible treatment of data uncertainties, the consequences of this process are given a pessimistic upper bound in the safety assessment, as discussed above.

#### *Adequacy of references supporting the handling in SR-Site*

/Bond et al. 1997/ has not been reviewed and approved according to SKB's quality assurance system. In the calculations in SR-Site, however, the information in /Bond et al. 1997/ is used only qualitatively in order to estimate the time distribution for when the original small defect has developed into a large defect.

### 3.4.6 Radiation effects

#### *Overview/general description*

Neutron and gamma radiation from the fuel can give rise to minor material changes in the cast iron insert and the copper canister.

The effects of irradiation of the canister materials over a long period of time have been discussed by /Guinan 2001/. By comparing with experiments in the literature, /Guinan 2001/ concluded that the magnitude of any physical property changes (e.g. yield stress, creep rates, enhanced solute segregation, dimensional changes, or brittleness) resulting from exposure to neutron and gamma radiation over the one million year time period of the safety assessment will be negligible for both the copper and the cast iron. /Guinan 2001/ assumed, however, pure iron in the cast iron insert. This is not the case for the industrially produced inserts.

Precipitation of copper particles is a well-known problem in reactor vessels (see e.g. /Odette and Lucas 1998, Chaouadi and Gérard 2005/). Depending on the Cu content in the material, precipitation may occur as a result of radiation, potentially leading to embrittlement of the material. Such an accelerated ageing process occurs gradually over the lifetime of the reactor; i.e. over a time period of several decades. Recently, /Brissoneau et al. 2004/ suggested that similar ageing processes may be of relevance also in materials to be used for long-term storage of nuclear waste. The dose-rate due to the radioactive decay in the fuel is much lower compared to that in a reactor. The temperature, however, is also lower (about 100°C compared to 300°C in a reactor), and Cu supersaturation more readily achieved. Also the balance between defect production and defect annihilation in the material will be different. Calculations by /Brissoneau et al. 2004/ showed that the copper content will have to be lower than 0.05% to avoid precipitation embrittlement. These calculations, however, have not yet been supported by results from irradiation experiments.

The atoms in the canister materials might also capture the neutrons. These nuclear reactions can lead to formation of activation products in the canister insert

#### *Dependencies between process and canister variables*

Table 3-7 shows how the process influences, and is influenced by, all canister variables.

#### *Boundary conditions*

There are no relevant boundary conditions for this process other than the physical boundary set by the geometries of the components involved. (Neutron and gamma- radiation from the fuel is required for this process to occur.)

#### *Model studies/experimental studies*

See Overview/general description.

#### *Natural analogues/observations in nature*

Not applicable.

**Table 3-7. Direct dependencies between the process "Radiation effects" and the defined canister variables and a short note on the handling in SR-Site.**

| Variable | Variable influence on process | | Process influence on variable | |
|---|---|---|---|---|
| | Influence present? (Yes/No) Description | Handling of influence (How/If not – why) | Influence present? (Yes/No) Description | Handling of influence (How/If not – why) |
| Radiation intensity | Yes. It causes the process. | Neglected. Based on modelling results. | No. | – |
| Temperature | Yes. At repository temperatures any effect can be neglected. | Neglected. Based on modelling results. | Yes. The heating caused by the process is negligible | Neglected. Based on modelling results. |
| Canister geometry | No. | – | No. | – |
| Material composition | No. | – | Yes. Radiation embrittlement will occur to some extent in all materials. | Neglected. Based on modelling results. |
| Mechanical stresses | No. | – | No. | – |

### *Time perspective*

The neutrons come from spontaneous fission and from (α, n) reactions in the fuel. Both processes diminish greatly with time, and 1,000 years after deposition the radiation dose has declined by a factor of thirty (Spent Fuel Report /SKB 2010b/).

### *Handling in the safety assessment SR-Site*

The specifications for the material for the cast iron insert require that the copper content be kept below 0.05%. The process is, therefore, neglected for the cast iron based on the results presented in /Brissoneau et al. 2004/. It is also neglected for the copper shell based on the results presented in /Guinan 2001/.

### *Handling of uncertainties in SR-Site*

#### Uncertainties in mechanistic understanding

The mechanistic understanding of this process is deemed sufficient for the needs of the safety assessment.

#### Model simplification uncertainties

Not relevant since the process is not further modelled in the safety assessment.

#### Input data and data uncertainties

Not relevant since the process is not further modelled in the safety assessment.

### *Adequacy of references supporting the handling in SR-Site*

/Brissoneau et al. 2004/ is published in a peer-reviewed journal. Their calculations are made for a container for long-term storage of spent nuclear fuel and, therefore, relevant for SR-Site even though the studied material is low-carbon steel rather than cast iron. The calculations by /Guinan 2001/ are made directly for the KBS-3 canisters. The report is not peer- or factual reviewed, but it is scientifically consistent with other references that are peer reviewed articles or papers.

## 3.5 Chemical processes

### 3.5.1 Corrosion of cast iron insert

#### *Overview/general description*

Water in the canister cavity and in the annulus between copper and cast iron will corrode the cast iron insert. As a consequence of this process, the cast iron insert's integrity and mechanical strength may be jeopardised. Another consequence of corrosion is the formation of gaseous hydrogen and solid corrosion products, of which the latter can exert pressure against the copper canister.

The process is central to the canister's hydraulic, mechanical and chemical evolution if the copper shell should be breached.

Corrosion can be caused by water inside an intact canister. This possibility cannot be ruled out since some water may be present in the canister enclosed in fuel pins. Once oxygen inside the canister has been consumed by corrosion, this water will cause anaerobic corrosion on the insides of the insert.

Corrosion can also be caused by water that has entered a defective canister. Groundwater at repository depth is expected to be oxygen-free. The cast iron insert will, therefore, corrode anaerobically to generate hydrogen gas and form a solid corrosion product, most likely magnetite, and also some dissolved Fe(II). The magnetite is expected to consist of a thin adherent epitaxial layer and an outer, looser layer with poor adhesion. The resistance of the inner layer to ion transport will determine the corrosion rate. Since this layer appears to achieve a constant thickness while the outer non-protective layer continues to thicken as corrosion continues, the corrosion rate is expected to remain constant over a long period, see below. Alternatively, if the water supply is low, the corrosion rate will be determined by the availability of water.

#### *Dependencies between process and canister variables*

Table 3-8 shows how the process influences, and is influenced by, all canister variables.

**Table 3-8. Direct dependencies between the process "Corrosion of cast iron insert" and the defined canister variables and a short note on the handling in SR-Site.**

| Variable | Variable influence on process | | Process influence on variable | |
|---|---|---|---|---|
| | Influence present? (Yes/No) Description | Handling of influence (How/If not – why) | Influence present? (Yes/No) Description | Handling of influence (How/If not – why) |
| Radiation intensity | Yes. Gamma-radiation may influence the corrosion that takes place during the first several hundred years. | See Section 3.5.3. | No. | – |
| Temperature | Yes. Corrosion reactions are generally temperature dependent. | Neglected. The temperature dependence of the corrosion is marginal in the temperature range considered. | No. | – |
| Canister geometry | Yes. | See Section 2.3.1. | Yes. The corrosion products have a larger volume than the metal. | Neglected. After failure the influence of the corrosion products on the canister geometry and on transport resistance for radionuclides is neglected. |
| Material composition | Yes. Different materials have different corrosion properties. | Actual insert material is considered in the evaluation. | Yes. Corrosion products are formed. | Actual corrosion products are considered in the evaluation. |
| Mechanical stresses | Yes. Possible environmentally assisted cracking. | See Section 3.5.3. | Yes. The corrosion products may exert a pressure on the canister components. | Neglected. After failure the influence of the corrosion products on the stress levels in the insert is neglected. |

The corrosion rate of iron under anoxic conditions is dependent on the water composition and the temperature. The corrosion products and the corrosion process affect the chemical conditions in the cavity in the canister mainly by generating high concentrations of dissolved hydrogen gas and small concentrations of dissolved Fe(II). The corrosion rate has been shown to be independent of both the hydrogen gas pressure and the concentration of $Fe^{2+}$ in the system /Smart et al. 2002a, b/. This suggests that transport processes in the magnetite layer on the iron surface most likely determine the corrosion rate (see below).

### *Boundary conditions*

The boundary conditions for this process are the physical boundary set by the geometries of the components involved and the composition of water in the canister void. The corrosion process is also coupled to the inward transport of water for which boundary conditions are discussed in Section 2.3.1.

### *Model studies/experimental studies*

**Corrosion caused by water inside an intact canister:** The fuel elements will be dried before being transferred to the canister, but some water may nevertheless be transferred. A very pessimistic assumption would be that one fuel pin per fuel element with maximum water fill is transferred to each canister.

The scope of the corrosion this could cause can be modelled using a simple mass balance approach:

The total quantity of water that can be accommodated in the void in a fuel pin is 50 g. It is expected that no more than 12 fuel pins containing that amount of water will be transferred to the canister. The total maximum amount of water will, therefore, be 600 g. If this water reacts solely with the iron in the canister and is assumed to form $Fe_3O_4$, a maximum of about 1,400 g of iron could corrode. This will result in a relatively uniform corrosion depth of less than 10 μm for the cast insert. In the design premises /SKB 2009c/ it is specified that the atmosphere in the canister should be replaced by > 90% to argon. The handling is further described in the Spent fuel report /SKB 2010b, Section 4.8/.

**Corrosion caused by water that has entered a defective canister:** Anaerobic corrosion of cast iron has been studied experimentally by /Smart et al. 2002a, b/ who found that the corrosion rate is well below 1 μm/year after a few thousand hours even in the water that gave the highest corrosion rate in the tests, see Table 3-9. In /Smart et al. 2002a, b/ a series of different corrosion experiments are reported. Part of the study was to investigate the influence of corrosion products and water chemistry on the corrosion rates. Some of the experimental results are, therefore, not directly applicable to the situation in the repository. The mean corrosion rates were low and generally less than 1 μm/year. In high ionic strength water at pH 7 to 8, the corrosion rate for cast iron was measured as 0.1 μm/year whereas at pH 10.5, the rate was as low as 0.01 μm per year. It is difficult to judge what can be considered as a pessimistic upper bound for the corrosion rate. The measured rates span nearly two orders of magnitude, although most data indicate a rate of less than 0.1 μm/year.

The galvanic coupling between the cast iron and the copper will have a very limited influence on the corrosion rate. Experimental results indicate that the corrosion rate in de-aerated groundwater of iron coupled to copper is close to that of uncoupled iron /Smart et al. 2005/, see Section 3.5.2.

**Table 3-9. Composition (ppm) of synthetic Äspö groundwater mimicking water from borehole KAS-03.**

| $Na^+$ | $K^+$ | $Ca^{2+}$ | $Mg^{2+}$ | $Cl^-$ | $HCO_3^-$ | $SO_4^{2-}$ | pH |
|---|---|---|---|---|---|---|---|
| 3,000 | 7 | 4,400 | 50 | 12,000 | 11 | 710 | 7–8 |

In the reaction between cast iron and water, magnetite and hydrogen are produced. Initially, the corrosion rate is quite high but falls off rapidly to very low rates as the surface film of magnetite develops. The rate of hydrogen production at the highest measured long-term corrosion rate is about 0.5 $dm^3/(m^2 \cdot y)$ /Smart et al. 2002b/. The total internal surface area in the canister insert is approximately 33 $m^2$, which means the annual production of hydrogen would be 16 $dm^3$ at normal pressure or 0.33 $dm^3$ at the pressure at repository level (500 m depth).

The corrosion rate has proved to be independent of both the hydrogen gas pressure /Smart et al. 2002a/ and the concentration of $Fe^{2+}$ /Smart et al. 2002a, b/ in the system. The long-term corrosion rate is also independent of whether or not the water is present as a liquid or as vapour /Smart et al. 2002b/. This suggests that the corrosion rate is most likely determined by the ion transport properties of the magnetite layer on the iron surface:

The magnetite consists of two layers: a thin, strongly adherent layer and an outer, looser layer with poor adhesion /Smart et al. 2002b/. Smart et al. explain the formation of these two layers by saying that the adherent layer is formed directly on the metal surface by the reaction:

$$3Fe + 4H_2O \rightarrow Fe_3O_4 + 4H_2$$

while the looser layer is probably formed by the precipitation of dissolved iron:

$$Fe + 2H_2O \rightarrow Fe^{2+} + H_2 + 2OH^-$$

$$Fe^{2+} + 2\ OH^- \rightarrow Fe(OH)_2$$

$$3Fe^{2+} + 4H_2O \rightarrow Fe_3O_4 + 8\ H^+ + 3H_2 + 2e^-$$

The adherent layer forms very quickly and then does not increase further in thickness. Continuing corrosion leads to the thickening of the looser non-protective layer. Corrosion is controlled by ion transport across the adherent layer and should continue at a constant rate over long periods of time.

The corroding iron insert will influence the water chemistry in the void in the canister by generating high concentrations of dissolved hydrogen gas and small concentrations of dissolved Fe(II). EQ3/6 is a computer programme that calculates the speciation of dissolved elements in water based on thermodynamic principles /Wolery 1992a, b/. Calculations with EQ3/6 show that the solubility of dissolved iron in the void in the canister is, as expected, dependent on the redox conditions, but can rarely be higher than $10^{-7}$ mole/$dm^3$ The hydrogen will be dissolved to a concentration equivalent to a maximum hydrogen gas pressure of maximum 18 MPa. The iron concentrations are too low to be of any significant importance for the water chemistry. The hydrogen will have no influence on the corrosion of the iron insert (as mentioned above).

#### *Natural analogues/observations in nature*

There are some studies of archaeological artefacts reported in the literature. Recent studies by /Neff et al. 2003, 2005/ review some newer studies as well as data from their own investigations. /Neff et al. 2005/ carefully studied the corrosion products on artefacts from the 2nd century AD to the 16th century AD. In a further publication, /Neff et al. 2006/ analysed archaeological artefacts to determine the average corrosion rate of low carbon steel after long burial periods. The corrosion products found indicate that some corrosion took place with oxygen present. Nevertheless, the conclusion from the study is that the estimated average corrosion rates do not exceed 4 μm/year.

/Neff et al. 2003/ found that the measured or estimated corrosion rates vary over a relatively large range and the corrosion products, when identified, indicate that oxygen had been present in the system. The reported rates range from 0.01 μm/year to extreme values of 1,000 μm/year. At one site where the conditions had been oxygen free and the carbonate content in the water had been high ($10^{-2}$ M), siderite is identified as the main corrosion product /Matthiesen et al. 2003, 2007/. This site at Nydam Mose in Denmark was waterlogged and the buried objects are military equipment sacrificed in the period 200–500 AD. The estimated corrosion rates range from an upper limit of 5 μm/year down to 0.03 μm/year or less. The average corrosion rate for 151 analysed lances is about 0.2 μm/year.

### *Time perspective*

At a corrosion rate of 1 μm/year, metallic iron will be present for tens of thousands of years after failure of the copper canister. The length of time iron is present is inversely proportional to the constant corrosion rate.

### *Handling in the safety assessment SR-Site*

Even with a pessimistic assumption of 600 g of water per canister, the effects of the corrosion of the canister insert prior to failure of the copper canister can be neglected.

In the case of a canister breach, the process is treated as part of an integral description of the evolution of the canister interior after damage (see further Section 2.3.1).The treatment aims at bounding the consequences of the effects of the set of integrated processes. This is further developed in the SR-Site data report /SKB 2010l, Section 4.2/.

*Boundary conditions:* The boundary conditions mentioned above are included in the integrated treatment, see Section 2.3.1.

*Handling of variables influencing this process:* Of the influencing variables in the table, the canister geometry and the material properties are included in the integrated treatment, see Section 2.3.1. The temperature, though, is assumed to be constant and equal to about 15°C and anaerobic conditions are assumed to prevail in the canister interior. Radiation effects are neglected based on the discussion in Section 2.5.3.

### *Handling of uncertainties in SR-Site*

**Uncertainties in mechanistic understanding**

There are no major uncertainties in the understanding of the corrosion of iron under oxygen free, reducing conditions.

**Model simplification uncertainties**

In a breached canister, the process is modelled with a constant corrosion rate unless the supply of water is limiting. Several developments, in which this process is integrated with a number of others, are considered in order to bracket the possible scenarios.

Rather than seeking justification of model simplifications, the consequences of this process are given a pessimistic upper bound in the safety assessment, as discussed above.

**Input data and data uncertainties**

Intact canister: There are uncertainties regarding the quantity of water that could conceivably be left in the canister, even after replacement of the air by argon. The uncertainties are, however, of no importance, since the extent of corrosion pessimistically achievable would be negligible.

Damaged canister: The uncertainties regarding the corrosion rate are discussed above, see Model studies/Experimental studies and most data indicate a rate of less than 0.1 μm per year. The experimental investigations show that if the protective corrosion product layer of magnetite is damaged, it will reform very quickly and the measured corrosion rates can be assumed to apply even for long periods of time.

### *Adequacy of references supporting the handling in SR-Site*

The cast iron and mild steel corrosion rate data reported in /Smart et al. 2002a, b/ are obtained under conditions simulating those in a KBS-3 repository. Both reports are published in peer-reviewed journals.

### 3.5.2 Galvanic corrosion

#### *Overview/general description*

If the copper shell is breached and groundwater comes into contact with the cast iron insert, electrochemical reactions on the copper surface will influence the corrosion of the insert. The consequences of galvanic corrosion have been investigated by /Smart et al. 2005/.

If the groundwater contained oxygen, the rate of cast iron corrosion was very high, up to 100 μm per year /Smart et al. 2005/. At the time of water intrusion into the canister, however, the water is expected to be oxygen-free and reducing. In oxygen-free water, the measured corrosion rates of cast iron galvanically coupled to copper were in the same range as those measured for cast iron in the absence of galvanic coupling to copper /Smart et al. 2005/.

#### *Dependencies between process and canister variables*

Table 3-10 shows how the process influences, and is influenced by, all canister variables.

#### *Boundary conditions*

The boundary conditions for this process are the physical boundaries set by the geometries of the components involved and the composition of the water in the canister void. The corrosion process is coupled to the inward transport of water for which boundary conditions are discussed in Section 2.3.1.

#### *Model studies/experimental studies*

See Overview/general description.

**Table 3-10. Direct dependencies between the process "Galvanic corrosion" and the defined canister variables and a short note on the handling in SR-Site.**

| Variable | Variable influence on process | | Process influence on variable | |
|---|---|---|---|---|
| | Influence present? (Yes/No) Description | Handling of influence (How/If not – why) | Influence present? (Yes/No) Description | Handling of influence (How/If not – why) |
| Radiation intensity | No. | – | No. | – |
| Temperature | Yes. Corrosion reactions are generally temperature dependent. | Neglected. The influence of galvanic corrosion under oxygen-free, reducing conditions lies within the margins of error for the corrosion rate of the iron insert. | No. | – |
| Canister geometry | No. There will always be a galvanic contact regardless of geometry. | – | No. | – |
| Material composition | Yes. Galvanic corrosion requires two metals. | Neglected. The influence of galvanic corrosion under oxygen-free, reducing conditions lies within the margins of error for the corrosion rate of the iron insert. | No. | – |
| Mechanical stresses | No. | – | Yes. Growth of corrosion products will cause stresses in the canister materials. | Neglected. The influence of galvanic corrosion under oxygen-free, reducing conditions lies within the margins of error for the corrosion rate of the iron insert. |

#### *Natural analogues/observations in nature*

Not applicable.

#### *Time perspective*

The process takes place after canister penetration.

#### *Handling in the safety assessment SR-Site*

The influence of galvanic corrosion under oxygen-free, reducing conditions lies within the margins of error for the corrosion rate of the iron insert and is, therefore, not dealt with specifically.

#### *Handling of uncertainties in SR-Site*

**Uncertainties in mechanistic understanding**

There are no major uncertainties in the understanding of galvanic corrosion.

**Model simplification uncertainties**

In oxygen-free water, the effects will be small and the uncertainties surrounding the exact contribution made by galvanic corrosion are judged to be negligible compared with the uncertainties in assessments of the corrosion rate. A cautious hypothesis for the corrosion rate for anaerobic corrosion of the canister insert will cover any contributions from galvanic corrosion.

**Input data and data uncertainties**

The uncertainties are negligible compared to those handled in Section 3.5.1.

#### *Adequacy of references supporting the handling in SR-Site*

The data presented by /Smart et al. 2005/ were obtained under conditions that simulated repository conditions and are, therefore, relevant and adequate. The supporting reference is not peer- or factual reviewed, but it is scientifically consistent with other references that are peer reviewed articles or papers.

### 3.5.3 Stress corrosion cracking of cast iron insert

#### *Overview/general description*

The stress corrosion cracking (SCC) of metals requires a combination of static tensile stresses, a specific chemical environment and, a susceptibility of the material. Unfavourable combinations of these conditions can lead to the initiation and propagation of cracks. The propagation rate can vary over a wide range, from $10^{-9}$ mm/s to $10^{-1}$ mm/s.

In a canister with an intact copper shell, nitric acid from the radiolysis of residual quantities of air could conceivably cause SCC in areas of tensile stress in the cast iron insert.

Shortly after deposition and closure, the temperature of the insert nearest the fuel is expected to be over 150°C. At this temperature there will be no water in liquid form in the canister, and the relative humidity is too low for a water film to form on the metal surface, even if there was water in the canister trapped in the fuel rods. For a water film to form, a relative humidity of approximately 40% is required. Under these conditions, nitric acid is not stable but decomposes to $NO_2$, the dominant radiolysis product in dry air /Reed and Van Konynenburg 1991a, b/. For SCC conditions to develop, the water and oxygen content of the canister must survive until the temperature falls sufficiently to allow water/nitric acid condensation on the canister; i.e. their consumption by prior corrosion must be extremely low.

For SCC to occur, a corrosive environment must exist while tensile stresses are present in the material. In the deep repository, the canister insert is under external pressure and tensile stresses occur on the cast insert only locally and in small areas, according to calculations /Dillström et al. 2010/. In addition, there is a requirement in the design premises /SKB 2009c/ to replace the air in the insert with > 90% argon, which will lower the risk caused by nitrate. It is, therefore, highly improbable that SCC could lead to penetrating cracks in the canister, and above all that this would jeopardise the integrity of the canister.

Stress corrosion cracking (SCC) of metals can occur under a combination of static tensile stresses, a specific chemical environment and metallurgical susceptibility. Unfavourable combinations of these conditions can lead to the formation and propagation of cracks. The temperature dependence of the extent of this process for carbon steel in nitrate follows a typical Arrhenius behaviour /Beavers et al. 1985/.

### *Dependencies between process and canister variables*

Table 3-11 shows how the process influences, and is influenced by, all canister variables.

### *Boundary conditions*

Nitric acid from radiolysis of residual quantities of moist air in the void inside the canister (the fuel boundary) could conceivably cause SCC in areas with tensile stresses in the cast iron insert.

### *Model studies/experimental studies*

See Overview/general description.

### *Natural analogues/observations in nature*

Not applicable.

### *Time perspective*

It is estimated that an equilibrium concentration of nitric acid will have been reached a few decades after closure of the canister.

**Table 3-11. Direct dependencies between the process "Stress corrosion cracking of cast iron insert" and the defined canister variables and a short note on the handling in SR-Site.**

| Variable | Variable influence on process | | Process influence on variable | |
|---|---|---|---|---|
| | Influence present? (Yes/No) Description | Handling of influence (How/If not – why) | Influence present? (Yes/No) Description | Handling of influence (How/If not – why) |
| Radiation intensity | Yes. The agents that may cause SCC are produced through radiolysis. | Neglected. Process neglected since tensile stresses only occur locally in small areas. | No. | – |
| Temperature | Yes. Negligible influence on this process. | Neglected. | No. | – |
| Canister geometry | No. | – | No. | – |
| Material composition | Yes. Different materials have different sensitivities to SCC. | Actual insert material is considered. | No. | – |
| Mechanical stresses | Yes. Tensile stresses required. Compressive stresses prevent SCC. | Neglected. Process neglected since tensile stresses only occur locally in small areas. | Yes. SCC relaxes tensile mechanical stresses. | Pessimistically neglected. |

#### *Handling in the safety assessment SR-Site*

Stress corrosion cracking, if it occurs, is deemed to be of no importance for the integrity of the canister.

#### *Handling of uncertainties in SR-Site*

**Uncertainties in mechanistic understanding**

There are uncertainties in the understanding of stress corrosion cracking, but they will be of no importance for the safety assessment, since the extent of the process will be limited.

**Model simplification uncertainties**

Stress corrosion cracking of the insert will not be modelled.

**Input data and data uncertainties**

The probability of SCC jeopardising the canister integrity is deemed to be small, since only local areas in the insert have tensile stresses. The uncertainty of the quantity of water that may have been left in the canister is bounded by the design premises of exchanging the atmosphere from air to > 90% argon.

#### *Adequacy of references supporting the handling in SR-Site*

The supporting references are peer reviewed articles or conference papers that is available in the open literature.

### 3.5.4 Corrosion of copper canister

#### *Overview/general description*

A range of studies over several decades (see e.g. /King et al. 2001, 2010/ for a review) have identified the following substances as capable of corroding the copper canister material under repository conditions:

- oxygen,
  - atmospheric corrosion in the encapsulation plant and repository,
  - corrosion in unsaturated bentonite by oxygen introduced during the repository operating period,
  - corrosion by oxygen trapped in the air-filled pore spaces in the buffer or available in the groundwater transported through the buffer during and after the bentonite becomes saturated,
  - corrosion caused by oxygen in penetrating glacial meltwater,
- nitric acid formed by gamma-radiolysis of nitrogen compounds in moist air in the gap between canister and buffer,
- oxidants formed by radiolysis of water, after water saturation,
- sulphide transported in from the buffer or from the groundwater via the buffer.

The corrosion processes are marginally affected by the changes in temperature expected in the deep repository. The consequences of corrosion are corrosion products and a change in the thickness of the copper shell. After very long time spans the consequence is a breach of the shell, allowing groundwater into the container.

The copper shell is the canister's corrosion barrier. Its design purpose is to provide protection against penetration of the canister by corrosion in the repository for a long time after water saturation. It is also supposed to provide protection against penetration of the canister by atmospheric corrosion before deposition as well as after deposition, before water saturation.

After the fuel has been encapsulated, the copper canisters will be transported to the geologic repository and deposited. However, some storage time may be inevitable. During that period, the canisters will be exposed to indoor air either at the encapsulation plant or at the repository site and to the atmosphere inside the vessel that will be used for transporting the canister to the repository site.

During transport and handling of the canister it will be inevitable that marks will be incurred from bumping into other objects or from scraping of the surfaces. This will result in locally cold worked areas. It has been known for a hundred years that indentations and scars on a steel surface will stimulate rusting /Cushman and Gardner 1910/. It is, therefore, not unreasonable to assume that there will be similar effects on copper. The effects of cold work on corrosion and corrosive wear has been studied by /Yin and Li 2005, Li and Li 2005, Tao and Li 2008/. They found that the corrosion potential and the electron work function decreased while the corrosion rate increased with an increase in plastic strain. /Yin and Li 2005/ measured a decrease in corrosion potential in 0.1 M $HNO_3$ of about 12 mV for an 80% reduction in thickness, while in 3.5% NaCl, the corresponding decrease was 7 mV with the largest decrease at 50% reduction in thickness. /Gubner et al. 2006/, using a Kelvin probe measured surface potentials which were 90 – 200 mV lower in the electron beam weld than in the parent material in a canister lid weld. In a later study, however, no galvanic enhancement of corrosion in the weld could be observed /Gubner and Andersson 2007/. It is, therefore, unlikely that a galvanic cell will be established between small cold worked areas and the larger non-deformed areas on the canister surface.

After emplacement in the deposition holes, it will no longer be possible to actively control the composition of the atmosphere to which the canister is exposed. The buffer and backfill are not saturated with water during the installation and water must be provided by the host rock. This wetting process, leading to the final water-saturated conditions around the spent fuel canisters, the form of its progress, and its duration will influence the form and the extent of the corrosion during this phase in the canister service life. The rate at which the buffer resaturates can vary greatly between different deposition holes. Depending on accessibility of water, the time to fully saturate the buffer can range from 10 to over several thousands of years /Åkesson et al. 2010/.

After water saturation, oxygen may still be present in the canister's surroundings. This oxygen will be consumed by reactions with the copper canister and by reactions with minerals in the bentonite buffer or the host rock. Microbes in the deposition tunnel backfill may also play an important role in oxygen consumption. /Wersin et al. 1994/ estimated the time this takes to be between 10 and 300 years. More recent numerical calculations /Grandia et al. 2006/, coupling chemical processes consuming oxygen with the hydrodynamic saturation of the backfill, have been used to estimate the timescale for reaching anoxic conditions in the tunnels of the repository. The study shows that several inorganic oxygen consumption processes may take place with the accessory minerals present in the bentonite in the buffer and in the backfill. As in the study by /Wersin et al. 1994/, the calculated oxygen consumption times are highly dependent on the postulated value for the surface area of the reacting minerals. Nevertheless, the study concludes that anoxic conditions are reached after a period of the order of one month after the backfill becomes water saturated. Experiments by /Lazo et al. 2003/ also indicate a very rapid oxygen consumption. The uptake (disappearance) of dissolved oxygen was studied in bentonite suspensions in 0.1 M NaCl media at (25±2)°C. In MX-80 and Montigel bentonites, the concentration ranged from 18 to 73 g/L. The experiments were performed in a magnetically stirred closed glass vessel, in an $N_2$-glove box. Redox potentials where measured with Pt-wires, and dissolved $O_2$ was measured both with a membrane electrode and with an oxygen optode. The experiments with MX-80 show that dissolved $O_2$ disappears in approximately 5 days under these conditions. Redox potentials decreased from about +500 to about +125 mV versus a Standard Hydrogen Electrode (SHE). The data for the Montigel bentonite showed similar time scales for $O_2$ uptake but lower redox potentials at the end of the experiments, about –175 mV SHE. The consumption of the oxygen in "bubbles" of entrapped air during the saturation phase will most probably be considerable slower. The rate limiting process is most likely the dissolution of oxygen at the interface between the air bubble and the saturated, virtually oxygen-free bentonite.

The calculations do not include the possible effects of microbial respiration, although the density of the backfill is low enough to allow some microbial activity. The effect of microbes would be to shorten the time to reach anoxic conditions in the saturated backfill.

When the oxygen is consumed, the reducing conditions that prevailed before the repository was excavated are expected to be restored. During the period when oxygen is present, one might argue that localised corrosion is also possible, which can lead to localised deeper corrosion attacks than the average due to general corrosion. As will be argued below, however, pitting corrosion under repository conditions will be very unlikely.

When the water is reducing, copper would be immune to corrosion, see e.g. /King et al. 2001, 2010/. However, under deep repository conditions, dissolved sulphide or very high chloride concentrations are conceivable. High chloride concentration in combination with very low pH could cause copper corrosion in oxygen-free water. /Beverskog and Puigdomenech 1998/ calculated Pourbaix diagrams for 0.2 and 1.5 molal chloride concentrations and later for 5 molal chloride concentration in /Beverskog and Pettersson 2002/. At 5 molal chloride, copper corrodes below pH 5 at 25°C to the extent that $[Cu(aq)]_{TOT} > 10^{-6}$ molal. The corresponding pH value for 1.5 molal chloride is approximately 3.2. A simplified calculation may be done with data (ΔG and activity coefficients) from /Puigdomenech and Taxén 2000/ which gives a $CuCl_3^{2-}$ concentration close to $10^{-6}$ M for the combination of pH=4 and $[Cl^-]$=2 M. It is therefore suggested this combination is used as the safety function indicator critera in SR-Site.

Dissolved sulphides are, therefore, the only corrosive substances that can react with the copper canister after the oxygen in the repository has been consumed. At the proposed repository depth, the groundwaters have very low sulphide concentrations, mostly much lower than $5 \cdot 10^{-5}$ M, and the solubility of the sulphide minerals present in the bentonite is, at most, of the same order of magnitude. This means that the corrosion of the copper canister due to sulphides will be controlled by the availability and supply of sulphides from the groundwater and the buffer.

A review of copper corrosion under expected repository conditions has been performed by /King et al. 2001, 2010/. In these reviews the corrosion processes and mechanisms discussed below are elaborated in more detail.

/King et al. 2001, 2010/ state that modelling calculations have shown that during deglaciation, oxygenated glacial meltwater can be transported down to the repository level. No evidence of such an occurrence is found in the bedrock, which makes this scenario unlikely and it was, therefore, not addressed in /King et al. 2001, 2010/. Recent calculations /Sidborn et al. 2010/ have shown, however, that this scenario cannot be completely ruled out. Thus, its consequences for the corrosion of the copper canister will be discussed further below.

**Atmospheric corrosion in the encapsulation plant and repository**

The formation of a water film on a metal surface is of fundamental importance to atmospheric corrosion. The thickness of this water film varies from a few monolayers at low relative humidity to thousands of monolayers at 100% relative humidity /Leygraf 2002/. When the relative humidity exceeds the "critical relative humidity" the corrosion rate increases markedly with increasing humidity. This critical relative humidity depends on the surface conditions of the metal but is generally in the range 50–70%. Below this critical level, the corrosion rate is, for all practical, purposes negligible.

When the thickness of the water film exceeds about three monolayers, its properties become similar to those of bulk water /Phipps and Rice 1979/. This occurs approximately at the critical relative humidity. As this film thickens, water-soluble pollutants will dissolve in the moisture film in equilibrium with the gaseous phase. The $SO_2$ present in the air will dissolve forming $HSO_3^-$ and can be oxidised to sulphate by oxidants in the air (e.g. stoichiometrically by ozone, and catalytically by $NO_2$ /Leygraf and Graedel 2000/). The $NO_2$ present in the air is assumed to be absorbed in the moisture film as $HNO_3$. The actual indoor humidity will depend on the ventilation of the facility, but will be below the critical humidity at least during the winter months.

The indoor air is expected to have a temperature of about 20°C. The expected maximum surface temperature for a canister with a heat generation of 1.7 kW is somewhat less than 50°C when the canister is exposed to freely circulating air. When inside a radiation shield, the temperature may approach 100°C.

The elevated surface temperature (50°C) of the copper canister will ensure a relative humidity considerably lower than the critical humidity close to the canister surface. The corrosion rate can, therefore, be assumed to be very low. /Rice et al. 1981/ have reported corrosion rates for copper exposed at ambient temperature in different atmospheres. The exposure times were 1 to 1.5 years. For city atmospheres, they reported corrosion rates of 6 to 27 nm/year. These rates are in agreement with those for the corrosion of copper in dry air as described by /Evans and Miley 1937/. They found that a layer of predominantly copper oxide was formed on the surface and that this layer inhibited further corrosion when it had reached a thickness of 9–10 nm. These data refer to room temperature. There are, as far as we know, limited data available for the relevant canister temperature. /Roy and Sircar 1981/ report logarithmic oxidation kinetics in dry air at temperatures between 75°C and 150°C, while /Pinnel et al. 1979/ report parabolic kinetics. Both studies were performed in dry air and, although the rate laws they propose give quite different kinetics for the growth of the oxide layer at 100°C, they predict a total oxide thickness after a few years exposure in the range 30 to 70 nm.

/Taxén 2004/ describes an atmospheric corrosion study at the Äspö Hard Rock Laboratory (HRL). Copper coupons were exposed to the natural atmosphere of the HRL with and without compacted bentonite present. Tests were performed at ambient temperature and, in the case of the test with bentonite, at 75°C. Corrosion rates were estimated based on mass loss or from electrochemical stripping of the corrosion products under galvanostatic conditions. Corrosion rates were < 0.1 μm/year. This is significantly lower than typical surface atmospheric corrosion rates in Sweden, which are about 0.5 μm/year in urban atmosphere and can be up to and even over 2 μm/year in coastal areas /Taxén 2004/. This suggests that the HRL atmosphere is less corrosive than normal surface atmospheres. It is assumed that the Äspö HRL atmosphere would be typical of the atmosphere in the repository. The only corrosion product detected was $Cu_2(OH)_3Cl$ (paratacamite), although the presence of $Cu_2O$ is also likely and may not have been detected due to sampling artifacts /Taxén 2004/.

Storing the copper canisters for extended periods of time before disposal for these conditions will have a negligible effect on their service life after disposal. The total corrosion attack even after two years storage will be less that 1 μm. The most likely corrosion product will be copper oxide.

**Copper corrosion by initially entrapped oxygen**

In the presence of oxygen, copper will be oxidised to $Cu_2O$ or CuO in pure water, depending on the redox potential. In groundwater a duplex layer is formed, with an inner layer of cuprous oxide ($Cu_2O$) and an outer layer of a precipitated basic Cu(II) salt such as atacamite/paratacamite ($Cu_2(OH)_3Cl$), brochantite ($Cu_4(OH)_6SO_4$), or malachite ($Cu_2(OH)_2CO_3$). The nature of the Cu(II) solid is dependent on the predominant anion in the groundwater /McNeil and Little 1992/. These compounds can also form under atmospheric corrosion conditions.

The total extent of corrosion under aerobic conditions will be limited by the available amount of oxygen trapped in the repository after closure. In the present design, the disposal tunnel cross section, width x height, is 4.2·5.8 $m^2$. Each disposal tunnel is 300 m in total length and will contain a maximum of 50 canister positions separated by 6 m. The tunnels will be backfilled with a combination of bentonite blocks (60% of the tunnel volume) and bentonite pellets (20% of the tunnel volume). The blocks have 40% porosity, filled to 65% by water (corresponding to a 17% water to solid mass ratio), i.e. 35% of the porosity is air filled. The pellets also have 40% porosity but only 40% water content. The remaining 20% of the tunnel volume is air. The deposition holes, which are 8.5 m deep and have a diameter of 1.75 m will be backfilled (almost 100% of the volume) with bentonite blocks /SKB 2010k/. Using these data and, conservatively, using the molar volume at 0°C (22.4 $dm^3$), the amount of oxygen per canister in the repository can be calculated to be about 475 moles. Of this amount, 455 moles come from the tunnel backfill and 21 moles from the buffer in the deposition hole. Not all of this oxygen will be available to corrode the canister. Some of it will be pushed out from the tunnel into the rock during the wetting process. However, if all of it corroded the canister, this amount would cause a maximum depth of corrosion of 768 μm if it were evenly distributed over the canister surface. It would, however, seem more likely that the oxygen from the tunnel would corrode the lid and the top part of the canister. Assuming that the corrosion attack is limited to the lid and topmost 10% of the canister, the depth of corrosion would be 5.5 mm.

Evenly distributed corrosion over the canister surface may be a reasonable conservative assumption for the oxygen from the buffer, although it is probably more realistic to assume that half of the oxygen will diffuse towards the oxygen free rock. The resulting corrosion depths for these two scenarios will be approximately 34 µm and 17 µm, respectively, neglecting all other oxygen sinks in the buffer.

Most of the residual oxygen is present in the tunnel backfill and is expected to be consumed not only by the copper corrosion reaction but also through reactions with oxidisable minerals and through microbial activities (see Overview/general description above). /Grandia et al. 2006/ concluded that anoxic conditions are reached after a period of the order of one month after the backfill becomes water saturated. This makes it unlikely that any substantial amount of oxygen from the porewater in the backfill or from trapped air bubbles would reach the canister. If one assumes the same diffusivity, $1 \cdot 10^{-10}$ m$^2$/s, for oxygen as for tritiated water (HTO /Ochs and Talerico 2004/) in bentonite, the diffusion length (L) over one month will about 16 mm (assuming $L = \sqrt{Dt}$), i.e. a negligible fraction of the oxygen in the backfill will reach the copper canister. Only that fraction which is within a few centimetres of the canister surface will reach the canister. If one uses the estimate by /Wersin et al. 1994/ of a maximum 300 years before all oxygen is consumed, the diffusion length will be about 1 metre, i.e. one may assume that the oxygen within a few metres of the canister top will cause copper corrosion. The oxygen in a 3 m high, 1.75 m diameter cylinder on top of the canister would corrode about 260 µm of the lid and topmost 10% of the canister surface.

There are two reported experimental determinations of the oxygen consumption rate in bentonite. /Lazo et al. 2003/ performed their experiments in bentonite/water slurries of different densities. Two kinds of bentonite were studied, MX-80 and Montigel. The dissolved oxygen disappeared in about five days in these experiments. It was observed, however, that pyrite oxidation is perhaps not the main process for $O_2$ consumption, as MX-80 contains 0.3% $FeS_2$ while Montigel bentonite has a negligible amount. Another possible mechanism for $O_2$ consumption could be oxidation of Fe(II) from siderite or in the alumino-silicate framework of the bentonite. The microbial activity was suppressed by the use of a microbial inhibitor ($NaN_3$). The microbial $O_2$-consumption may not have been completely eliminated, but the results suggest that microbial $O_2$ consumption was very limited in the bentonite suspensions /Lazo et al. 2003/. Preliminary determinations of oxygen depletion in bentonite by /Carlsson and Muurinen 2007, Muurinen and Carlson 2010/ also indicate rapid oxygen consumption.

For the unrealistic assumption that there will be no consumption of oxygen in the backfill, the oxygen must diffuse towards the rock, which will be oxygen free. Provided there is a sufficient consumption of oxygen in the rock, the amount of oxygen that can reach the canister will be only a fraction compared to that which will diffuse towards the top of the deposition hole. The size of this last fraction will correspond to the area of the deposition hole in the tunnel floor in relation to the total area around the tunnel section. With the tunnel dimensions of width = 4.2 m, height = 5.8 m and length = 6 m (tunnel length assigned to one canister), the total wall area will be $2 \cdot (4.2+5.8) \cdot 6$ m = 120 m$^2$ and the deposition hole area $(1.75/2)^2 \cdot \pi \approx 2.4$ m$^2$. This corresponds to only 2% of the oxygen in the backfill. If one further assumes that this oxygen will corrode only the lid and topmost 10% of the canister, the corrosion depth will be 106 µm.

The total extent of corrosion will, thus, be determined by the amount of oxygen available in the buffer and backfill and the accessibility of this oxygen to the copper. An inhomogeneous increase in water content in the bentonite will also most probably result in an uneven swelling of the buffer. As a consequence of this, the gap may close in some areas while it remains open in others. Non-uniform wetting of the surface could establish conditions for localised corrosion of the canister. Although localised corrosion may initiate, it is unlikely to propagate to significant depths. A major limiting factor is the amount of $O_2$ trapped in the buffer material and in the backfill. Eventually the entire surface will be wetted and the differential $O_2$ concentration cell that acted initially as the driving force for localised corrosion will disappear.

**Localised corrosion**

The total extent of the corrosion by $O_2$ trapped in the buffer material and in the backfill will result in average corrosion depths as discussed above. A remaining question is, whether or not there are reasons to expect locally deeper corrosion attacks.

Pitting of Cu water pipes has been studied extensively since the 1960's, see e.g. /Mattsson 1988, Edwards et al. 1994, Lytle and Nadagouda 2010/. At least three types of pitting have been recognised /Mattson 1988/. Type I pitting, the most common of all, was reported first by /Campbell 1950/ and a general theory for pit formation was proposed by /Lucey 1967/. Type I pitting is associated with cold, hard and moderately hard waters free of naturally occurring inhibitors, but containing $HCO_3^-$, $SO_4^{2-}$, $Cl^-$ and $O_2$, and occurs on Cu pipes with a residual surface carbon film remaining from the manufacturing process /Mattsson 1980/. Type II pitting is associated with hot potable waters (> 60°C) with a pH < 7.4, a $HCO_3^-$ to $SO_4^{2-}$ concentration ratio < 1, and a high $O_2$ concentration. This type tends to produce pits with a larger depth to width ratio than the approximately hemispherical pits characteristic of Type I pitting. Type III is, like type I, restricted to cold water installations, but does not seem to bear any relation to the presence of a continuous carbon film. The main cause is likely to be found in the water composition. It is observed in cold water with low $HCO_3^-$ and $Cl^-$ content and high $O_2$ concentration. In some observations the pH has been low /Mattsson 1988/, while others report high pH /Edwards et al. 1993/.

Although pitting studies in potable waters may not be directly relevant to the pitting of Cu canisters in saline porewaters, the proposed mechanisms provide some insight into the possibility of localised corrosion in a repository. It is useful to consider three phases in the life of a pit: birth, propagation, and death. A conclusion that can be drawn is that the mechanistic Cu pitting studies indicate that an oxidant (either $O_2$ or Cu(II)) is a pre-requisite for pit propagation (see e.g. /King et al. 2001, 2010/). Pitting of Cu water pipes is only sustained because of the high $O_2$ concentration in fresh water and because it is continually replenished by the movement of water in the pipe. This would not be the case for pits on Cu canisters, both because of the limited amount of $O_2$ available and because of the restricted mass-transport conditions, which will limit the supply of $O_2$ to the corrosion sites. Therefore, pits on Cu canisters will be far more likely to die than those on Cu water pipes.

The main anions in the bentonite porewater will be chloride, bicarbonate and sulphate. There are a number of studies of the pitting of Cu in concentrated $Cl^-$ and $Cl^-/HCO_3^-$ solutions (for more detail, see /King et al. 2001, 2010/). These studies have mainly been concerned with initiation events and the determination of breakdown potentials. In these mixtures, the bicarbonate ions promote passivity, while chloride ions promote film breakdown, making copper more susceptible to pitting corrosion. /King et al. 2001/ estimate the breakdown potential to be in the range of approximately − 0.1 $V_{SCE}$ (0.14 $V_{SHE}$) to + 0.3 $V_{SCE}$ (0.54 $V_{SHE}$) for bentonite porewaters containing between 0.001 M and 0.1 M $Cl^-$ and with up to 0.02 M $HCO_3^-$ (SCE=saturated calomel electrode, SHE=standard hydrogen electrode). Pourbaix gives a simple criterion for pitting corrosion in bicarbonate free chloride solution (0.01 M) based on the conditions for forming CuCl /SKI 2006/. If the potential inside the pit is higher than 270 $mV_{SHE}$, pits will grow, and they will stifle if the potential is below this value. This potential translates to 350 to 420 $mV_{SHE}$ when measured with a reference electrode outside the pit. This is considerably higher than the potentials (−130 to −80 $mV_{SHE}$) measured by /Saario et al. 2004/ in compacted bentonite after about one month. This suggests that pitting is impossible under these conditions.

A number of corrosion studies have been performed under conditions that simulate the canister near-field environment. Copper coupons have been exposed to compacted buffer material wetted by (initially) aerated saline porewaters, and exposed for extended periods of time (up to 6 years) usually at elevated temperature /Aaltonen and Varis 1993, Karnland et al. 2000, King et al. 1992, 1997, Litke et al. 1992, Rosborg and Werme 2008/. These experiments simulate the likely environmental conditions soon after emplacement of the canisters and saturation of the buffer material. It is during this period in the evolution of repository conditions that localised corrosion is most likely, since the environment will be oxidising (required for Types I and II pitting of Cu water pipes and for the corrosion potential, $E_{CORR,}$ to be more positive than the breakdown potential, $E_b$). Furthermore, the porewater concentration of $HCO_3^-$ may be significant because of the dissolution of carbonate minerals and the concentration of $Cl^-$ may be sufficient to cause film breakdown, but not so high as to cause general dissolution of the surface. Thus, short-term laboratory and field tests can be used to study the period of most aggressive localised corrosion. Despite the relative aggressiveness of the conditions in these tests, no evidence for pitting is observed. Thus, both /Aaltonen and Varis 1993/ and /Karnland et al. 2000/ report no localised corrosion of Cu exposed to compacted clay over periods of up to 2 years. /Litke et al. 1992/ reported non-uniform corrosion in the form of under-deposit corrosion. In this case, the whole surface had been corroded resulting in an uneven general corrosion with variations

in corrosion depth of 30 μm for an average corrosion depth of slightly over 40 μm. These data indicate that no pitting is to be expected, but that there may be unevenness around the average corrosion depth of roughly the same magnitude as the total corrosion depth. /Rosborg and Werme 2008/ report an average corrosion rate of less than 0.5 μm per year after 6 years exposure at elevated temperatures. The general corrosion was unevenly distributed on the copper surface without, however, any signs of active pits, i.e. similar to the type of attack reported by /Litke et al. 1992/.

The extent of surface roughening by under-deposit corrosion has been studied in Canada /Brennenstuhl et al. 2002/. The electrochemical noise between coupled identical electrodes, one immersed in bulk solution and the other exposed to a freely swollen 1:1 bentonite:sand mixture, was measured as a function of various factors. Of the various factors studied, temperature, $O_2$ concentration and pH had the greatest effect on the extent of localised corrosion. The study is not conclusive, but results suggested that the degree of localised corrosion in a repository should decrease with time as the canister temperature and the $O_2$ concentration decrease. A mean roughness of 12.4 μm was predicted, with a maximum peak-to-trough surface roughness of 88 μm.

Another approach to predicting the extent of localised corrosion on Cu canisters is to make projections based on observed pit depths. Because pitting has not been observed on Cu exposed to simulated repository conditions, the required pit depth data have been taken from literature studies of the long-term burial of Cu alloys /Romanoff 1989/ and from an analysis of pit depths on three lightning conductor plates /Hallberg et al. 1984/ and on archaeological artefacts /Bresle et al. 1983/. Whilst the environmental conditions and Cu alloys are different from those to be used in a repository, these studies have the great advantage of having been "conducted" over long periods of time. Thus, the long-term soil corrosivity measurements of /Romanoff 1989/ were conducted for times up to 14 years. The lightning conductor plates studied by /Hallberg et al. 1984/ had been buried for 50 to 80 years. The Bronze Age artefacts studied by /Bresle et al. 1983/ had been exposed for an estimated period of 3,000 years. These pit depths can be used to estimate the pitting factor (PF), which is the ratio between the greatest corrosion depth achieved and the depth of the general corrosion process, and for which PF = 1 for general corrosion. From these studies, /Romanoff 1989/ reported the highest pitting factor of 25, but observed that it decreased with time. The results of /Bresle et al. 1983/ indicated a probable pitting factor of 2 to 5. /Hallberg et al. 1984/ found a pitting factor of 5 for two of the lightning conductors and no pitting for the third. These data indicate that, for extended exposure times, a pessimistic estimate of the pitting factor would be 5. The use of a pitting factor, however, will overestimate the pit depth at larger general corrosion depths, since general corrosion destroys the separation of anodes and cathodes required to drive deep pitting.

An alternative use of the same pit depth data has been developed in the Canadian programme /King and Kolár 2000, King and LeNeveu 1992/. The data were analysed using extreme-value statistics, in which the deepest pits on a collection of samples (or within a given area of the surface of one or more samples) of the same exposure time are fitted to an extreme-value distribution of the form,

$$F(x) = exp[–exp(–ax + b)]$$

where $F(x)$ is the cumulative probability that the depth of the deepest pit is less than or equal to a depth $x$, $a$ is the scale (or shape) parameter, and $b/a$ is the location parameter of the distribution. The fitting procedure produces values for $a$ and $b$ for a given set of data for a given exposure period. Fitting several sets of data with different exposure periods gives the time dependence of the scale and location parameters. From these fits and calculations the time dependence of the cumulative probability ($F(x)$) can be calculated. Then the probability of a pit of a certain depth can be calculated for the full population of canisters emplaced in the repository. Applying these data to Swedish canisters, one can calculate that there is a probability of $10^{-6}$ of a pit exceeding about 7.5 mm after $10^6$ years. This approach predicts, however, very deep pits after shorter exposure times. With the same probability ($10^{-6}$) it predicts a 5 mm deep pit after 10 years. This is consistent with the very high pitting factors observed on some specimens by /Romanoff 1989/.

Unlike the critical potential approach to pitting, neither the pitting factor nor the extreme-value analysis approach allows for pit death. Propagation is assumed to continue indefinitely regardless of the evolution in the repository environment, albeit at a diminishing rate in the extreme-value approach. Based on the experimental data available the most realistic understanding of the pitting during the period when oxygen is present is that it will have the appearance of uneven general

corrosion as discussed above. The used experimental data /Romanoff 1989, Bresle et al. 1983/ were obtained under conditions more closely simulating actual disposal conditions, whereas some of the data discussed in the statistical evaluations were obtained after exposure in poorly characterised environments /Bresle et al. 1983/. However, they clearly illustrate the tendency of pit growth rates to decrease with exposure time.

Inevitably, some manufacturing and handling flaws, such as scratches and indentations will remain in the canister when it is deposited. Conceivably, these flaws could act as initiation point for localised corrosion. This possibility has been investigated by /King 2004/. /King 2004/ concludes that it is unlikely that the presence of pre-existing flaws on the canister surface will impact the service life of the canister as a result of localised corrosion. These flaws will not act as preferential sites for pit initiation, which instead occurs at grain boundaries due to the localised breakdown of protective surface films /King 2004/. Environmental factors and the presence of a defected film are more important for pit initiation than the presence of a pit-shaped discontinuity.

After consumption of the oxygen initially present, reducing conditions are expected but the possibility of oxygen intrusion for altered geochemical conditions exists and can be handled by mass balance calculations if the amount of intrusive oxygen can be estimated.

**Corrosion caused by nitric acid during the buffer saturation phase**

Gamma irradiation of moist air in the canister-buffer gap leads to the formation of nitric acid. /Reed and Van Konynenburg 1988/ reviewed the effect of ionising radiation on moist air systems. Of the papers reviewed, the study by /Jones 1959/ of the nitrogen/oxygen/water homogeneous systems appear to be directly applicable to repository conditions. /Jones 1959/ found that the formation of nitric acid was linear with the absorbed dose. The formation proceeded to a total concentration that was stoichiometrically equivalent to the hydrogen of the water initially present. The *G*-value (in molecules per 100 eV) for the nitric acid production increased with oxygen concentration to a maximum of 2.25 at 15.4% oxygen and was 2.00 for 20.1% and 1.2 for air. In a repository, there will be a continuous supply of water and a continuous production of nitric acid can be expected.

If the formation of nitric acid is linear with the absorbed dose, the rate of its formation will be given by:

$$d[HNO_3]/dt = (G \cdot V \cdot \rho \cdot D_0/A_v) \cdot e^{-ln2 \cdot t/T}$$

and the total amount of produced $HNO_3$ as a function of time:

$$HNO_3 = ( G \cdot V \cdot \rho \cdot D_0/A_v) \cdot (T/ln2) \cdot (1 - \cdot e^{-ln2 \cdot t/T})$$

where $G$ is the G value (in number of molecules/eV), $V$ the irradiated air volume ($dm^3$), $\rho$ the density of the air ($g/dm^3$), $D_o$ the initial dose rate (eV/g·y), $A_v$ Avogadro's number, $t$ the irradiation time (years) and $T$ the half-life (years) of the radiation source.

Using the following input data:

$G$ = 0.02 molecules per eV

$V$ = 161 $dm^3$ (canister length= 48.35 dm, canister diameter = 10.5 dm, air gap between canister and bentonite buffer = 0.1 dm)

$\rho$ = 1.184 $g/dm^3$

$D_0 = 5.5 \cdot 10^{19}$ eV/(g·y) (corresponding to 1 Gy/h)

$T$ = 30 years (gamma radiation from $^{137}Cs$ decay is the dominant contributor to the radiation field)

$t$ = 1,000 years

then a total production of 0.015 moles of nitric acid is obtained, which, if consumed uniformly, corresponds to a corrosion depth of less than 7 nm.

**Corrosion by water radiolysis products after water saturation**

After water saturation, radiolysis of water near the canister will occur. This will lead to the formation of oxidants and hydrogen. If these radiolysis products are not removed, a steady state will soon be reached whereby the further production of hydrogen and oxidants ceases. If the radiolysis products are removed, however, for example by the diffusion of hydrogen away from the canister or by reaction of the oxidants with copper or other oxidisable species in the system, radiolysis can continue. Calculations of radiolysis outside a canister have been made by /Christensen and Pettersson 1997/. An estimate of the maximum possible amount of oxidised copper can be made if one assumes that the oxidation of copper will be as efficient as the oxidation of dissolved Fe(II) in Christensen and Pettersson's calculations. Considering the oxidation of Fe(II) to Fe (III) (as in the calculations of Christensen and Pettersson), after about 317 years ($10^{10}$ s, after which the gamma dose rate has substantially decreased) the amount of precipitated Fe(III) would be 1 mol per irradiated $dm^3$ water. Assuming that the oxidants present in a 5 mm water layer surrounding the canister reach and react with the copper surface, the total volume of irradiated bentonite porewater for a bentonite porosity of 0.4 and canister dimensions of $h_{can}$ = 4.85 m, $r_{can}$ = 0.525 m will be, neglecting the details of the lid and bottom designs:

$V_{irradiated} = (4.85 \cdot 2 \cdot 0.525 + 2 \cdot 0.525^2] \cdot \pi \cdot 0.005 \cdot 0.4\ m^3 = 0.035\ m^3 = 35\ dm^3$

In Christensen and Pettersson's calculations this would yield a total amount of precipitated Fe(III) of 35 moles which would translate into 35 moles of corroded copper. For a canister surface area of $[48.5 \cdot 10.5 \cdot \pi + 2 \cdot (10.5/2)^2 \cdot \pi]\ dm^2$ and a copper density of 8,920 $g/dm^3$, this gives a corrosion depth of approximately 14 µm. At a dose rate of 13 Gy/h, /Simpson 1984/ finds lower corrosion rates than without irradiation. This observation is corroborated by /King and Litke 1987/. They used dose rates in the range 14 to 27 Gy/h for irradiation of copper in a saline solution (about 1 M chloride) at 150°C.The experiments were performed in aerated and de-aerated solutions and the corrosion rates were about a factor of four lower in the presence of radiation. /King and Litke 1987/ attributed this to the more protective nature of the surface film formed in irradiated solutions.

Available information shows that there is no evidence for enhanced corrosion rates caused by gamma radiation. On the contrary, at least for dose rates in the range of 10–100 Gy/h, the experimental data seem to indicate a lower corrosion rate in the presence of radiation /King et al. 2010/.

**Corrosion in the absence of oxygen**

In the absence of oxygen, copper is thermodynamically immune to corrosion in pure water. However, cuprous sulphide ($Cu_2S$) is thermodynamically stable at potentials below the $H_2/H_2O$ equilibrium line /Pourbaix and Pourbaix 1992/. Because of this thermodynamic stability and because of the presence of sulphide ions in deep Swedish groundwaters, copper canisters may be subject to corrosion in the presence of sulphide under the long-term reducing conditions expected to develop in the repository. The corrosion products would be $Cu_2S$, or other copper sulphides, and hydrogen.

Various workers have studied the electrochemical and corrosion behaviour of Cu alloys in sulphide environments. The majority of these studies are associated with corrosion of Cu alloys in polluted seawater (see e.g. /Al-Hajji and Reda 1993/ and references therein). However, care should be taken in applying the results of these studies to the corrosion of Cu canisters, because most of them involved Cu-Ni alloys (commonly used in marine heat exchangers) and because the particularly aggressive forms of corrosion observed in these applications are associated with *alternating* oxidising and reducing conditions. High chloride concentrations in combination with low pH can also cause corrosion on copper (see Overview/general description above).

After the oxygen has been consumed and reducing conditions reinstated, copper corrosion under deep repository conditions will be controlled by the availability of dissolved sulphides. This sulphide may be present in the bentonite buffer and backfill and also in the deep groundwaters. At the proposed repository depth, the groundwaters have very low sulphide concentrations, mostly much lower than $5 \cdot 10^{-5}$ M /Tullborg et al. 2010/, and the solubility of the sulphide minerals present in the bentonite is, at most, of the same order of magnitude /Duro et al. 2006b/. At these low concentrations, the transport of sulphide from, or through, the buffer to the copper surface is very slow and this transport resistance will completely control the rate of the corrosion process.

Various authors have attempted to determine whether copper corrodes in the absence of $O_2$ and sulphide. /Betova et al. 2003/ applied a combination of experimental techniques to investigate the extent of corrosion in simulated groundwaters with different salinity. The results were found to be in accordance with thermodynamic predictions. /Betova et al. 2004/ and /Bojinov et al. 2004/ report attempts to measure corrosion of copper using an on-line electrical resistance probe in 1.52 M NaCl and 1 M NaCl solutions, respectively. The solutions initially contained only trace levels of $O_2$ (< 5 ppb) and eventually became anoxic. Tests were carried out at room temperature and at 80°C. Corrosion was observed initially as the residual $O_2$ was consumed, but then virtually stopped as the solution became anoxic, with an estimated $O_2$ concentration of < 0.001 ppb. At this time, the potential of the copper electrode reached the thermodynamic immunity region. /Saario et al. 2004/ also concluded that the corrosion of copper stopped in compacted bentonite when the $O_2$ was locally exhausted at the surface and anoxic conditions had been established. There is no evidence, therefore, that copper corrodes in oxygen-free concentrated $Cl^-$ solutions at neutral pH, consistent with thermodynamic predictions.

Contradictory to these results, /Szakálos et al. 2007/ claimed to have detected hydrogen formed by the corrosion of copper in deionised water at temperatures between 8°C and 85°C. Hydrogen gas was detected using an ion pump or as a pressure increase using a pressure gauge. The results show measurable hydrogen generation rates at all temperatures and under all conditions studied. The authors interpreted their observation of corrosion at redox potentials at which metallic copper is thermodynamically stable in terms of the formation of a previously unreported species $H_xCuO_y$. Powder XRD and secondary ion mass spectrometry (SIMS) were used to identify the $H_xCuO_y$ species that, if as suggested, is thermodynamically stable at E/pH values below the stability line of $H_2O$. It was claimed that the effect was reproducible, although few details of the repeat test were given. One interesting observation was that the corrosion rate, as measured by the current from the ion pump (used to measure the rate of $H_2$ production), apparently increased with time. Extensive reviews of the literature concerning corrosion of ferrous and non-ferrous metals over the past thirty years have not encountered documented evidence for a general corrosion process the rate of which increases with time. The conclusions drawn by /Szakálos et al. 2007/ have also been questioned by /Johansson 2008/ leading to a rebuttal by /Szakálos et al. 2008/.

**Copper corrosion after water saturation; bacterial corrosion**

Normally, bacterial reduction of sulphate to sulphide does not pose any threat to the integrity of the canister, since this does not lead to elevated levels of dissolved sulphide in the groundwater. The worst case would be if the bacteria formed a biofilm on the canister surface or were present in the buffer near the canister. Corrosion would then be controlled by the transport of sulphate to the canister, and could be considerably accelerated, since the flux of sulphate is expected to be much bigger than that of sulphide, due to sulphate concentrations in the groundwater and in the bentonite of up to tens of mM.

In the SR-Can safety assessment, the clay density limit for microbial sulphide production was set at 1,800 kg/m$^3$. Microbial activity was assumed not to occur at densities above this limit. The limit was based on experiments where the numbers of surviving microbes after initial additions to the clay rapidly decreased with increasing densities above 1,800 kg/m$^3$ /Motamedi et al. 1996, Pedersen et al. 2000a, b/. The underlying mechanisms for the observed stifling of the bacterial growth were, however, not fully understood. Recent experiments at a depth of 450m at the Äspö hard rock laboratory, set up under in-situ conditions with respect to groundwater pressure and SRB levels, showed that copper corrosion from sulphate reducing bacteria (SRB) occurred even at a density of 2,000 kg/m$^3$ /Masurat et al. 2010/. Lactate was added to the bentonite as a source of energy and organic carbon. The mean copper sulphide production rate was 34 ± 20 fmol $Cu_xS$ mm$^{-2}$ day$^{-1}$ for copper plates that had one edge exposed to groundwater and 15 ± 5 fmol $Cu_xS$ mm$^{-2}$ day$^{-1}$ for copper plates completely embedded in the bentonite. However, there was a short period in the total experimental time frame of 80 days where the bentonite compaction was below the required values making it possible that some of the sulphate-reducing activity occurred before full compaction.

New experiments were designed with the bentonite set to full compaction before the start of the corrosion tests. This design ensures that the analysed copper corrosion could only be due to sulphide diffusing from the outside of the bentonite and from microbial sulphate reduction inside the bentonite

at the tested densities /Pedersen 2010/. In both types of experiments, the experimental conditions were, however, much more favourable for microbial activity than can be expected in the repository as lactate was added to the experiments as a source of energy and organic carbon. The formation of copper sulphide in this type of experiment was also shown to be dominated by diffusive transport /Pedersen 2010/. In the experiments by /Masurat et al. 2010/ it can thus not be excluded that some of the formed copper sulphide stemmed from sulphide diffusing in from the circulating groundwater, and not only from sulphide produced by microbial activity in the bentonite. The experimental results from /Masurat el al. 2010/ are thus overestimates the sulphide production in the bentonite in for several reasons.

**Copper corrosion after water saturation: sulphate corrosion**

A simple reaction between copper and sulphate is thermodynamically impossible /Swedish Corrosion Institute 1983, Grauer 1990/. However, if an additional electron donor such as Fe(II) is available, copper can react with sulphate to give copper sulphide. It is, however, a part of the general knowledge of chemistry, and unanimously accepted in the geochemical literature that purely chemical reduction of sulphate does not occur at temperatures below 100°C. /Grauer 1990, Goldstein and Aizenshtat 1994/ have reviewed abiotic (thermochemical) sulphate reduction. /Grauer 1990/ concludes that at temperatures relevant for repository conditions, corrosion of copper by sulphate in the absence of sulphate reducing bacteria can be ruled out with a probability verging on certainty. /Goldstein and Aizenshtat 1994/ find that reduction of sulphate through oxidation of certain organic molecules only occurs at geochemically meaningful rates at temperatures above 175°C. /Cross et al. 2004/ determined the reaction kinetics for aqueous sulphate reacting with aqueous acetate and elemental sulphur. The half-life of the sulphate was extrapolated to be 1,650 years at 150°C and 372,000 years at 100°C. Therefore, inorganic sulphate corrosion of copper can be deemed impossible under repository conditions.

**Copper corrosion by glacial meltwater**

Glacial meltwater is essentially meteoric water and has, consequently, practically no dissolved solids. /Auqué et al. 2006/ give as an example of interacted glacial meltwater, groundwater data from Grimsel /Hoehn et al. 1998/. This specific water has a total amount of dissolved solids of 0.08 g/L and it has been depleted of oxygen. The maximum theoretical oxygen concentration that a meltwater may have is 1.34 mM /Sidborn et al. 2010/, but when evaluating the maximum consequences for canister corrosion in SR-Site /SKB 2011/, the oxygen content of glacial meltwaters has been set to 1.5 mM. /Sidborn et al. 2010/ show that for a few recharge flow paths in Forsmark, infiltrating glacial meltwater may still retain most of its oxygen content when reaching the repository level when the ice front margin is located on top of the repository.

In order for the meltwater to also reach the canister without oxygen depletion, one has to assume that the buffer has been eroded away. The slow transport through an intact buffer would most certainly result in the more or less complete removal of oxygen from the water contacting the canister. Also, if uptill the time of contact of meltwater with the canister, the repository has been oxygen-free and dissolved sulphide has been present, there would be a copper sulphide film on the canister surface.

There are a number of analogous corrosion scenarios that have been extensively studied and which can be used to evaluate the evolution of the corrosion behaviour of the canisters in the event of the intrusion of $O_2$-containing glacial melt water. One such analogue is the corrosion of copper alloys (typically brass, a Cu-Zn alloy, or Cu-Ni) heat exchangers exposed to polluted seawater. Rapid corrosion results from the alternating exposure to anaerobic (during which a $Cu_2S$ film forms) and aerobic conditions /Syrett 1981/. The $Cu_2S$ film catalyses the $O_2$ reduction reaction leading to rapid corrosion. The film can also be transformed to a $Cu_2O$ film, resulting in volume changes and mechanical stresses in the film and the loss of the previously protective surface layer. The spalling of the corrosion product is exacerbated under high flow conditions (fluid velocities of the order of m/s), resulting in localised attack. For a canister in a repository, provided the amount of intruding water, and hence the amount of $O_2$, is limited, then the catalysis of the $O_2$ reduction reaction by the $Cu_2S$ will simply result in faster consumption of the $O_2$ rather than any increase in the overall amount of corrosion. Even in deposition holes in which the bentonite has been eroded, the rates of mass transport are unlikely to be high enough to cause localised attack as a result of the local spalling of

the corrosion product. Under these conditions, the maximum amount of corrosion can be estimated from the amount of $O_2$ in the intruding water, with a small allowance for some degree of surface roughening. The extent of this roughening could be estimated from /Jacobs and Edwards 2000/ to be some hundred μm, for corrosion depths in the mm scale.

For the case when a $Cu_2O$ film has been formed on the canister surface, corrosion of water pipes for potable water can be used as an analogue. The very low chloride concentration and high oxygen content of the meltwater would favour passivation (and pitting) over general corrosion (active dissolution).

As already discussed in subsection "Localised corrosion" above, pitting corrosion of water pipes has been studied extensively, and the pitting is normally categorized in three types:

Type I: This is cold water pitting that is generally caused by a carbonaceous film on the copper surface as a residue from lubricants used in the production of the copper pipes. This type of pitting will not occur on the canisters, since no such film is present.

Type II: This is hot pitting and, consequently, not expected on copper exposed to glacial melt water.

Type III: This is cold water pitting that is not associated with the presence of a carbon film; it is generally explained as caused by the water composition.

The Type III pitting corrosion appears to occur "epidemically", frequently as a result in a change in the water supply or water quality in a community /Mattsson 1988, Lytle and Nadagouda 2010/ and is rarely observed /Myers and Cohen 1995/. A common denominator is the observation of sulphate in the crusts covering the corrosion pits, indicating that the sulphate content in the water is important for this type of pitting /Mattsson 1988, Lytle and Nadagouda 2010, Edwards et al. 1994/. /Cong et al. 2009/ also observed that sulphate tends to stabilize pits. Glacial melt water is essentially pure water and contains, therefore, none of the anions that are observed or assumed to promote pitting corrosion.

### *Dependencies between process and canister variables*

Table 3-12 shows how the process influences, and is influenced by, all canister variables.

**Table 3-12. Direct dependencies between the process "Corrosion of copper canister" and the defined canister variables and a short note on the handling in SR-Site.**

| Variable | Variable influence on process | | Process influence on variable | |
|---|---|---|---|---|
| | Influence present? (Yes/No) Description | Handling of influence (How/If not – why) | Influence present? (Yes/No) Description | Handling of influence (How/If not – why) |
| Radiation intensity | Yes. | Neglected. Radiation effects on corrosion are negligible. | No. | – |
| Temperature | Yes. Complex dependence on temperature depending on the relative importance of kinetic and transport steps. | Neglected. The corrosion is modelled using transport control and mass balance. | No. | – |
| Canister geometry | No. | – | Yes. | Included in modelling of effect of corrosion. |
| Material composition | Yes. Different materials have different corrosion behaviour. | Actual copper material is considered. | Yes. Corrosion products are formed. | Actual corrosion products formed under the foreseen conditions are considered. |
| Mechanical stresses | Yes. | Dealt with in Section 3.5.5. | Yes. | Neglected. The growth of corrosion products is too slow to create additional pressure on the canister. |

The temperature in the repository will be elevated during the oxidising phase, with a maximum of up to 100°C on the copper surface. The corrosion reactions are temperature dependent, generally with increasing rates at higher temperatures. This is, however, of subordinate importance, since the diffusion of reactants is rate controlling and diffusivity is much less affected by the temperature. The influence of temperature on the chemical equilibria for the corrosion reactions is completely negligible for the temperature range encountered in the repository.

### *Boundary conditions*

The boundary condition for the copper corrosion process will be the rate of supply of corrosive agents from the near field to the canister – buffer boundary.

### *Model studies/experimental studies*

See Overview/general description.

### *Natural analogues/observations in nature*

Corrosion of copper under oxidising conditions can be studied on archaeological artefacts, and such studies have been conducted to assess the risk of pitting /Bresle et al. 1983, Hallberg et al. 1984/. This was discussed above. A natural analogue study assessing general corrosion over longer periods of time is reported in /Hallberg et al. 1988/. /Hallberg et al. 1988/ examined a bronze cannon from the Swedish warship Kronan, which had lain buried at a depth of 26 m with its muzzle downward in the mud on the bottom of the Baltic Sea since 1676. Microprobe analysis of a bronze core taken from the muzzle showed concentrations of 96.3% Cu and 3.3% Sn and combined Zn and Fe < 0.5%. The dominant corrosion product was cuprite, $Cu_2O$. The estimated corrosion rate was $1.5 \cdot 10^{-5}$ mm/year with no evident pitting.

/Milodowski et al. 2003/ present an analysis of the corrosion of native copper plates that have survived in a water-saturated clay environment for more than 176 million years. Although the native copper is affected by corrosion, the study shows that a significant proportion (30–80% of the original thickness) of the copper sheets is preserved in the saturated compacted clay environment of the Littleham Mudstone. Apart from the recent weathering effects due to exposure at outcrops, petrographical studies demonstrate that most of the observed corrosion and alteration of the native copper is geologically old (i.e. predating the main sediment compaction) and also occurred before the end of the Lower Jurassic Period. This demonstrates that the native copper can remain stable in a saturated and compacted clay environment for geological timescales well in excess of the timescales considered for safety assessment of a deep geologic repository for spent nuclear fuel.

### *Time perspective*

Sulphide corrosion will proceed as long as metallic copper is available and sulphide is present in the buffer, the deposition tunnel backfill or the groundwater. Oxygen corrosion will occur initially and possibly intermittently during deglaciations. Microbially induced corrosion must also be considered if microbial activity in the buffer cannot be completely excluded.

### *Handling in the safety assessment SR-Site*

The process is modelled for the main scenario in SR-Site. The modelling, which essentially consists of steady state mass balance and transport rate expressions is described in the Corrosion calculation report /SKB 2010n/. The transport models are based on simple diffusion expressions, as well as on integrated flow and corrosion calculations using the concept of equivalent flow, that have been developed and applied to canister corrosion over several decades. The contributions to the overall corrosion are considered in the following way.

- Corrosion prior to disposal and after disposal before sealing and backfilling will amount to less than 1 μm. This will be of negligible importance for the service life of the canister.

- The initially entrapped oxygen will lead to uneven general corrosion. All of the oxygen in the buffer in the deposition hole will corrode the canister since other sinks for oxygen are neglected. For the oxygen entrapped in the backfill there are several possible sinks. Modelling has shown that only a small fraction of the total amount of oxygen will contribute to the canister corrosion. A reasonable estimate would be a corrosion depth of less than 500 μm, including an unevenness around the average corrosion depth on the order of ±50 μm, the latter based on the observations made by /Litke et al. 1992, Brennenstuhl et al. 2002/.
- Under oxygen-free conditions, the copper will be corroded by sulphide initially present in the buffer and sulphide supplied over time by transport in the groundwater. These contributions are modelled as transport-limited and any kinetic limitations due to interfacial reactions are disregarded.
- Microbial activity in the buffer will be limited by the availability of organic material in the buffer and backfill, as well as limited by swelling pressure of the bentonite. The extent of corrosion is evaluated using mass balance and mass transport models (simple diffusion models), see further /SKB 2010n/.
- The likelihood of, and the quantitative effect of, oxygen penetration during deglaciation are assessed in dedicated model studies (see further the SR-Site main report /SKB 2011, Section 12.6/). The corrosion model used to quantify corrosion by penetrating oxygen in the groundwater, is based on mass balances and similar transport rate expressions to those employed for sulphide in the groundwater. Any localised corrosion would be in the form of uneven general corrosion and the extent of this roughening could be estimated to be some hundred μm, for corrosion depths on the mm scale, as described above.
- Corrosion effects due to cold work are neglected based on the discussion presented above.
- Chloride assisted corrosion is not considered significant as long as pH > 4 and $[Cl^-] < 2$ M.
- The findings by /Szakálos et al. 2007/ on corrosion of copper by water will need further confirmation by other scientists before they can be considered for safety assessments. The consequences for the service life of the canister can, however, be estimated from the published data by /Szakálos et al. 2007/ on the equilibrium hydrogen pressure for the reaction between copper and water stated, as discussed in /SKB 2010n/.
- Nitric acid corrosion is neglected based on the discussion presented above.

*Boundary conditions:* The boundary conditions, i.e. the rate of supply of corrosive agents from the near field to the canister – buffer boundary, are explicitly included in the model.

*Handling of influences/couplings:* Any temperature dependence of reaction rates is pessimistically neglected since all reactions are assumed to be instantaneous. The influence of the material properties is included through mass balance expressions and stoichiometric formulae. The reduction in copper canister thickness is explicitly calculated.

### *Handling of uncertainties in SR-Site*

**Uncertainties in mechanistic understanding**

There are no mechanistic uncertainties of any importance for the safety assessment. The extent of corrosion due to the residual oxygen in the repository is determined using an approach with mass balance (and mass transport) and the corrosion rate under reducing conditions is determined by calculating the mass transport flux of corrosive agents to the canister surface. The mechanistic understanding of mass transport is sufficient for the needs of the safety assessment.

**Model simplification uncertainties**

The model simplifications are pessimistic; e.g. interfacial reaction kinetics is ignored and steady-state rather than transient transport rate expressions are employed.

**Input data and data uncertainties**

Input data and data uncertainties for the modelling of canister corrosion are discussed in the Corrosion calculations report /SKB 2010n/ and the Data report /SKB 2010l/. Important input data include the amount of initially entrapped oxygen in the repository, diffusivities in the buffer, the solubility of sulphide in the buffer material, the initial amount of sulphide present in the buffer, the sulphide concentration in the groundwater over time, and the possible amounts of oxygen that could penetrate to repository depth during a deglaciation.

### *Adequacy of references supporting the handling in SR-Site*

**Overview/general description**

/Yin and Li 2005, Li and Li 2005, Tao and Li 2008/ are peer reviewed journal papers directly addressing the effects of cold work on copper corrosion.

**Atmospheric corrosion in the encapsulation plant and repository**

The cited papers are peer reviewed journal or conference papers. The conditions for the exposure of copper to indoor or repository atmospheres are sufficiently close to the expected conditions to be adequate for the data to be used in SR-Site.

**Copper corrosion by initially entrapped oxygen**

Of the cited references only the conference paper by /Lazo et al. 2003/ has been peer reviewed. There is a wide spread in the estimated oxygen consumption times in the two modelling reports by /Grandia et al. 2006/ and /Wersin et al. 1994/, respectively. The results of /Grandia et al. 2006/ agree quite well with the experimental data of /Lazo et al. 2003/. The calculated oxygen consumption times depend strongly on the assumed values for the surface area of the reactive minerals. /Wersin et al. 1994/ considered only oxygen consumption by pyrite in the buffer. /Grandia et al. 2006/ considered the backfill, minerals other than pyrite, and microbial activity for oxygen consumption, which would lead to a faster oxygen consumption. Both experiments and modelling are, however, concordant: the bentonite has a strong capacity for consuming oxygen and the amount of oxygen that actually corrodes the canister is a small fraction of all the available oxygen. The references must, therefore, be regarded as adequate support for the suggested handling in SR-Site.

**Localised corrosion**

Various experimental and modelling approaches have been developed to study the pitting of Cu. Although the extensive database on the pitting of Cu water pipes provides some useful mechanistic information, the results of corrosion experiments under simulated repository conditions suggest that canisters will not undergo classical pitting, but rather a form of under-deposit corrosion, in which there is no permanent separation of anodic and cathodic sites.

The mechanistic Cu pitting studies indicate that an oxidant (either $O_2$ or Cu(II)) is a pre-requisite for pit propagation. Since the near-field environment in the repository will evolve from initially oxidising to ultimately reducing, pitting will only be possible (if at all) in the early stages of repository life. Given this evolution in localised corrosion behaviour with repository conditions, the most suitable pitting models are those that include the description of possible pit death, which neither the pitting factor nor extreme-value approaches do (albeit some “dead” pits are included inte extreme-value analysis.

Experiments performed under conditions simulating repository conditions have either shown no tendency towards pitting or only uneven general corrosion. This is in line with what the mechanistic Cu pitting studies indicate. These references, therefore, appear to be the most relevant ones for the handling in SR-Site since they all consistently give similar results.

**Corrosion caused by nitric acid during the buffer saturation phase**

/Jones 1959/, which is a peer-reviewed paper, reports a G-value for nitric acid production. These G-values are similar or even higher than G-values reported by others /Reed and Van Konynenburg 1988/. /Jones 1959/ also observed that the formation of nitric acid was linear with the absorbed dose and that the formation proceeded to a total concentration that was stoichiometrically equivalent to the hydrogen of the water initially present. This allows the data of /Jones 1959/ to be directly applied to the repository conditions.

**Corrosion by water radiolysis products after water saturation**

The calculations in /Christensen and Pettersson 1997/ are directly applicable to the repository situation. The report has been produced within Studsvik's Quality Assurance System according to ISO 9001 and requires review and approval by two different individuals.

**Corrosion in the absence of oxygen**

There is overwhelming evidence in the peer-reviewed literature for copper's stability in oxygen-free water. It is also well established in the literature that copper will corrode by hydrogen evolution in sulphide containing waters. Even though there are little data available on copper corrosion rates in sulphide containing water, the rate of transport of sulphide to the canister can be determined sufficiently accurately to allow determination of the canister corrosion rates.

**Copper corrosion after water saturation; bacterial corrosion**

In SR-Can, microbial activity in the buffer was considered impossible based on available data at that time. Recent data indicate that this may not be the case. These data are published in peer-reviewed journals, apart from the cited references, there are very little data available. The corrosion attack from microbial activity in the buffer must, for the time being, be considered as a worst case.

**Copper corrosion after water saturation: sulphate corrosion**

It is a part of the general knowledge of chemistry, and unanimously accepted in the geochemical literature that purely chemical reduction of sulphate does not occur at temperatures below 100°C. Peer reviewed data presented by /Goldstein and Aizenshtat 1994/ and /Cross et al. 2004/ are in agreement with this claim.

**Copper corrosion by glacial meltwater**

All the references supporting the main conclusions are peer reviewed journal articles dealing with situations analogous to the meltwater situations.

### 3.5.5 Stress corrosion cracking of the copper canister

#### *Overview/general description*

/King and Newman 2010/ discuss in detail the current knowledge of stress corrosion cracking (SCC) in copper and copper alloys and evaluate the risk for SCC of the copper canisters in the repository environment. Classically, SCC has been described as the consequence of the action of a suitably corrosive environment on a susceptible material in the presence of a tensile stress. In terms of the factors affecting the corrosiveness of the environment, the most important are the redox potential, the porewater salinity and pH, temperature, and the generation of specific species that are known to support SCC. The chemical species of interest are those that have been shown to support the SCC of copper, namely, nitrite, ammonia, and acetate ions. Those factors that affect the loading on the canister, and hence the level of possible tensile stress, are the hydrostatic head and bentonite swelling pressure and future glaciation events. Calculations by /Jin and Sandström 2009a, b/ have shown that tensile stresses are present at the canister surface and that there are areas with tensile stresses throughout the copper wall thickness.

The four main mechanisms proposed to account for the SCC of Cu in various environments are:

- the film-rupture mechanism,
- the tarnish-rupture mechanism,
- film-induced cleavage model, and
- the surface-mobility model.

The film-rupture mechanism involves crack propagation following the rupture of some form of film at the crack tip. The conditions must be suitable for the formation of a protective film, most likely $Cu_2O$. Provided the pH inside the crack is not too acidic, a $Cu_2O$ film would be present at potentials achieved in the presence of either $O_2$ or Cu(II).

The tarnish rupture mechanism is similar to the film rupture mechanism in that it involves a film (tarnish) and dissolution. The environmental requirements for the tarnish rupture mechanism are similar to those for film rupture. A film or tarnish must clearly be present and has been associated in the literature with the formation of $Cu_2O$.

Mechanisms that require a degree of oxidation or dissolution are only possible whilst oxidant is present in the repository and then only if other environmental and mechanical loading conditions are satisfied. These constraints will limit the period during which the canisters could be susceptible to cracking via film rupture (slip dissolution) or tarnish rupture mechanisms to the aerobic period after deposition of the canisters

In the film-induced cleavage model, a crack initiates in a surface film and is projected into the underlying ductile metal, inducing a cleavage-like crack. Formation of the surface layer in which the crack initiates requires oxidation of the surface. There is, however, some question about whether a $Cu_2S$ film could play the same role as $Cu_2O$ in promoting SCC via a tarnish rupture (or, indeed, film rupture) mechanism. Sulphidation of copper does not always produce a well-adhered or protective film. Therefore, once a small crack is present, the continuing reaction on the walls and external surface increases the diffusion limitation for sulphide reaching the crack tip. In principle, crack propagation in such a situation is impossible if the free-surface reaction is already under sulphide diffusion control, since no sulphide can reach the crack tip.

The surface-mobility model was introduced by /Galvele 1987/. It postulates that a crack tip under stress captures vacancies, not from the bulk of the material but from the surface, i.e. surface self-diffusion of metal atoms away from the crack tip grows the crack. There are obvious similarities between such a process and creep crack growth and since it relies on a kind of creep, it does not require an oxidising environment or any environment at all. The values of the surface diffusion coefficient are, however, relatively low for bare engineering metals and the model relies on contamination of the surface to increase the values. /Galvele 1987/ estimates the surface diffusion coefficient from the melting point of the surface compound that is assumed to be present at the crack tip, using an established correlation.

Two other SCC mechanisms, the adsorption-induced dislocation emission and vacancy injection and embrittlement models, are also discussed by /King and Newman 2010/. Although these models are still in the development stage, the authors consider it unlikely that they could induce cracking during the long-term anaerobic phase.

/Taniguchi and Kawasaki 2008/ reported the SCC of pure copper (with 45 ppm P) in synthetic seawater solutions containing sulphide. The experiments were carried out at a temperature of 80°C with 0, 0.001, 0.005, and 0.01 M $HS^-$, added to solution as $Na_2S$. Tensile specimens were strained to failure by SSRT (slow strain rate tests) at a strain rate of $8 \cdot 10^{-7}$ per second. Loss of ductility was reported at a $HS^-$ concentration of 0.01 M due to intergranular SCC. Only single experiments were reported. From these data, the authors concluded that pure copper is susceptible to SCC in sulphide solutions above a threshold concentration of between 0.005 M and 0.01 M. This concentration is 2–3 orders of magnitude higher than that expected in a Swedish repository.

In their review of stress corrosion cracking of copper canisters, /King and Newman 2010/ conclude that:

- The classic film rupture and tarnish rupture mechanisms require the presence of a $Cu_2O$ film and sufficient crack-tip strain to either rupture the film to allow crack growth by dissolution or to fracture the tarnish to promote crack growth. These mechanisms would only be possible for a limited period during the evolution of the repository environment.
- Sulphide ions are unlikely to support either film rupture or tarnish rupture mechanisms in the repository, not least because there will be no sulphide in the crack as the supply of sulphide to the free surface will be diffusion limited through the compacted bentonite.
- The formulation of the crack growth law is flawed but, in its corrected form, predicted crack growth rates of the order of $10^{-20}$ m/s. Therefore, even if cracking were to occur via this mechanism, the crack velocity would be too small to lead to canister failure, even over repository timescales.

Work in the Canadian nuclear waste disposal programme has focused on experimental studies of the SCC of OFP (oxygen-free, phosphorous doped) Cu in the three environments (ammonia, acetate and nitrite) known to support cracking /Ikeda and Litke 2004, 2007, 2008, Litke and Ikeda 2006, 2008/. The major conclusions from the experimental work are:

1. except under the most aggressive conditions, OFP copper exhibits largely ductile behaviour in ammonia, acetate, and nitrite solutions,
2. only specimens covered by a visible surface oxide exhibited cracking and only at potentials and pH values consistent with a $Cu_2O$ film,
3. the presence of $Cl^-$ ions inhibits the SCC of OFP copper, and
4. in nitrite solutions, the susceptibility to cracking decreases with increasing temperature.

From their review of SCC in copper, /King and Newman 2010/ conclude that the probability of SCC during the early aerobic period is low because of the absence of the necessary conditions for cracking and that there is no well-founded SCC mechanism that would result in cracking during the long-term anaerobic phase in the repository.

Similar to what was discussed in connection with localised corrosion, flaws and marks on the canister surface can, conceivably, also act as initiation points for SCC. This could happen either through their effect on the local environment or via stress concentration or intensification. According to /King 2004/, there is no evidence that surface discontinuities will affect the initiation of SCC by ennoblement of the corrosion potential or the formation of locally aggressive conditions. /King 2004/ also concludes that stress concentration could lead to crack initiation under some circumstances for a pre-existing crack-like flaw, but will be smaller than the minimum threshold stress intensity factor ($K_{ISCC}$) for copper reported in the literature. Therefore, any cracks that do initiate will tend to become dormant. There is thus no evidence that weld discontinuities will adversely affect the SCC behaviour of copper canisters. The predicted service life of the canisters is not affected by the presence of such features.

#### *Dependencies between process and canister variables*

Table 3-13 shows how the process influences, and is influenced by, all canister variables.

#### *Boundary conditions*

Concentrations of nitrites, ammonium or acetate at the canister – buffer interface constitute the boundary conditions for this process.

#### *Model studies/experimental studies*

See Overview/general description.

**Table 3-13. Direct dependencies between the process "Stress corrosion cracking of the copper canister" and the defined canister variables and a short note on the handling in SR-Site.**

| Variable | Variable influence on process | | Process influence on variable | |
|---|---|---|---|---|
| | Influence present? (Yes/No) Description | Handling of influence (How/If not – why) | Influence present? (Yes/No) Description | Handling of influence (How/If not – why) |
| Radiation intensity | No. | – | No. | – |
| Temperature | Yes. Lower temperatures increase the sensitivity to SCC. | Neglected. The process is neglected as a failure mode for the canister, see text. | No. | – |
| Canister geometry | No. | – | No. | – |
| Material composition | Yes. Different materials have different sensitivities to SCC. | Actual copper material is considered. The process is neglected as a failure mode for the canister, see text. | No. | – |
| Mechanical stresses | Yes. Tensile stresses at the canister surface are a prerequisite for SCC. | Neglected. The process is neglected as a failure mode for the canister, see text. | Yes. An SCC crack will relieve the tensile stresses. | Neglected. The process is neglected as a failure mode for the canister, see text. |

### *Natural analogues/observations in nature*

Not applicable.

### *Time perspective*

If SCC occurs, it will occur during an early phase in the repository when oxidising conditions still prevail (< 300 years).

### *Handling in the safety assessment SR-Site*

Based on the discussion above, the process is neglected as a failure mode for the canister.

### *Handling of uncertainties in SR-Site*

#### Uncertainties in mechanistic understanding

There is no evidence that SCC could occur in the repository environment, but the possibility cannot be entirely ruled out based on available knowledge.

#### Model simplification uncertainties

SCC is not modelled.

#### Input data and data uncertainties

Not relevant.

### *Adequacy of references supporting the handling in SR-Site*

Most of the literature on mechanisms for SCC is peer reviewed papers. The report by /King and Newman 2010/ has undergone a documented factual- and quality review.

### 3.5.6 Earth currents – stray current corrosion

#### *Overview/general description*

**Sources of earth currents**

There are several sources for electrical currents in the earth's crust, both natural and anthropogenic. Currents caused by natural sources, earth currents or telluric currents, originate mostly from the interior of the earth, water currents in the ocean, atmospheric discharges, the sun and the space in the universe. Anthropogenic currents are mostly referred to as stray currents and originate mainly from transmission of electric power, rail transport, grounding to the (real) earth of various electric installations and radio communication. An overview of processes occurring in the geosphere is given in the Geosphere process report /SKB 2010i, Section 5.14/.

Another natural source is of an electrochemical nature. Oxidation of sulphide ores coupled to reduction of oxygen can give rise to a "battery-effect". Natural self-potentials are generally small ranging from a fraction of a millivolt to a few tens of millivolts. Anomalous potentials on the order of a few hundred millivolts are often found in association with ore bodies /Parasnis 1997/.

Man-made sources include all types of electrical power installations. High Voltage Direct Current transmissions (HVDC) are locally very strong sources. Monopolar HVDC uses the ground to close the electrical circuit. Thousands of amperes are forced through the earth's crust over hundreds of kilometres. Although the electrodes are usually located in the sea and major parts of the current stay in the seawater, neighbouring land is usually affected.

**Charge carriers**

In water, the current is carried by ions, e.g. $Na^+$ and $Cl^-$ (or other charged particles). Also in the ground, in clay, soil and rock, ions are the dominant charge carriers /Stumm and Morgan 1996/. Only certain minerals have significant electronic conductance. The abundant minerals of granite and other rock types of relevance for the Swedish programme are poor conductors, wherefore ions in the porewater of the rock matrix are the dominant charge carriers /Schön 1996/.

**Alternating and direct currents**

Depending on the source, earth currents are alternating or direct. Most man-made sources are alternating. Although the source may be alternating, it is possible that a direct current component arises. A mineral with rectifying properties could, like a diode in a network of resistors, cause a DC component to arise in the vicinity of the rectifying mineral. Alternating currents do not generally cause corrosion /Koerts and Wetzer 2001/, and corrosion effects have only been observed at very high AC densities. HVDC transmission uses, as the name implies, direct current.

**Corrosion effects on the canister caused by earth currents**

DC earth currents are known to cause corrosion. Primarily, constructions stretching over long distances, such as pipelines, are affected. In this context, a small metallic object such as a five metre high copper canister will be relatively insensitive to direct currents, because the voltage drop across it will be low. As a result of the HVDC cable located about 30 km north of the Forsmark site (the Fenno-Scan cable), man-made earth currents are a potential source of enhanced corrosion. Indications of such corrosion have been seen on stainless steel logging equipment used in the Forsmark site investigation /Nissen et al. 2005/. The Fenno-Scan cable is operated in a monopolar mode, but the construction of the second cable is under way, while the normal operating mode in the near future will be bipolar mode.

The deposited copper canister will be surrounded by partly saturated and/or fully saturated bentonite buffer. Depending on the degree of saturation, the electrical resistance of the bentonite will vary. Generally, the higher the degree of saturation, the lower the electrical resistance becomes. A fully saturated buffer will have an electrical resistivity on the order of 1 ohm.m. When the bentonite blocks are deposited, their water content is around 17% (see the Buffer production report /SKB 2010d). Therefore completely dry bentonite (which could be assumed to be isolating) never surrounds the copper canister. The bentonite buffer is surrounded by saturated rock, constituting

the walls of the deposition hole. At repository depth at the investigated sites, the rock matrix has a typical resistivity on the order of $10^4$ ohm.m /Nielssen and Ringgaard 2007/.

The current to affect the copper canister will be propagated from the rock or backfill, through the buffer, and further on to the canister. Metallic copper has negligible resistance and current transport must be electronic, while current in the bentonite will be ionic. Thus, conduction across the copper-buffer interface can be achieved if both thermodynamically possible and kinetically favoured reactions are available for interfacial charge transfer. The rate of such interfacial reactions is inversely proportional to the polarisation resistance across the copper/buffer interface.

In case the buffer is fully saturated, large potential gradients over the deposition hole cannot be maintained, as the buffer resistance is so low. A case has been postulated where uneven buffer saturation creates a situation where the buffer above and below the canister is fully saturated, but where the blocks surrounding the canister are not. Even so, the blocks are partly saturated at deposition and will to some extent propagate current. Furthermore, the deposition hole is surrounded by saturated rock that will also propagate current. This makes it unlikely that sufficiently large potential gradients can be maintained over the deposition hole to affect the copper corrosion.

The total corrosion that an external electrical field can cause can be estimated from the resistances in the circuit. A value of the transfer resistance, where current transport changes from ions in the bentonite to electrons in the copper, the polarisation resistance, may be the dominating resistance in the circuit. This value is not constant but varies with the voltage and will decrease strongly above a certain voltage.

The external potential field will be superimposed on the corrosion potential of the canister. The maximal effect is attained when the external current that passes in at one end of the canister will pass out from the other end of the canister. The end where current exits the canister will suffer more corrosion, the other end will suffer less corrosion than without external field. The initial corrosion processes are likely to be:

$O_2 + 2H_2O + 4e^- \rightarrow 4\ OH^-$ Cathodic process

$2\ Cu(s) + 2OH^- \rightarrow Cu_2O(s) + H_2O + 2e^-$ Anodic process

Also with a moderately strong (< ~0.5 Volt) electrical field, these two processes must balance in terms of charge. With an electrical field, the cathodic process will be stimulated at one end of the canister and suppressed at the other end. In the same way the anodic process will be stimulated at one end and suppressed at the other. The cathodic reduction of oxygen is of course limited by the supply of oxygen.

The corrosion caused by atmospsheric oxygen and oxygen initially remaining in the buffer (and backfill) will cause the formation of a copper oxide layer on the canister. If this oxide layer is different at the different ends of the canister the polarity of the electrical field will determine what happens. If the corrosion has been more extensive in the upper end, and the upper end of the canister is positive relative to the lower end, the current will gradually relocate this corrosion and the corrosion products from the upper end to the lower end. If the polarity is the opposite there will be a tendency to relocate all corrosion and corrosion products towards the upper end of the canister.

More extensive corrosion than that limited by the supply of oxygen takes place only when an additional cathodic process is possible. The most likely sustainable process is the cleavage of water to form molecular hydrogen:

$2H_2O + 2e^- \rightarrow H_2 + 2\ OH^-$

The exact potential difference required to drive the cleavage of water at one side of the canister and the oxidation of copper to $Cu_2O(s)$ at the other depends on the equivalent partial pressure of hydrogen. As more reaction products are formed, higher potential differences are required. As an example, stability diagrams /Puigdomenech and Taxén 2000/ indicate that at 1.0 atmosphere hydrogen pressure, the potential difference is about 0.5V at 25°C and slightly less at 100°C.

Groundwaters in the Forsmark area frequently have hydrogen contents in the order of $10^{-5}$ M /Hallbeck and Pedersen 2008/, equivalent to a partial pressure in the order of $10^{-2}$ atmospheres.

At a partial pressure of $10^{-2}$ atmospheres of hydrogen, only potential differences larger than the equilibrium between $Cu/Cu_2O$ at one end of the canister and $H_2/H^+$ at the other end can drive a corrosion process. At 25°C we find a limiting potential difference of about 400 mV, while 360 mV for 100°C (estimated from calculations of $\Delta G$ for the combined reactions above). At lower potential differences, the ambient partial pressure of $10^{-2}$ atmospheres hydrogen maintains immunity with respect to the formation of $Cu_2O(s)$

When sulphide, $HS^-$, is present, copper can corrode to $Cu_2S(s)$ with evolution of hydrogen. If $Cu_2S(s)$ is considered to be the copper sulphide formed, the corrosion reactions can be written:

$2H_2O + 2e^- \rightarrow H_2 + 2OH^-$ Cathodic process

$2\ Cu(s) + OH^- + HS^- \rightarrow Cu_2S(s) + H_2O + 2e^-$ Anodic process

The anodic process is here limited by the access of sulphide at the copper surface. Thus, the rate of anodic reaction is relatively insensitive to the potential. The process cannot proceed faster than the supply of sulphide allows. Therefore, the corrosion attack by sulphide is expected to be mostly uniform also in the presence of an external electrical field. The cathodic process on the other hand is sensitive to the electrochemical potential. This process is likely to become preferentially located to one end of the canister.

As described in Section 3.5.4 (subsection Localised corrosion in Overview/general description), pitting corrosion does not occur while the corrosion potential is lower than the breakdown potential of the film. The difference can be regarded as a margin against pitting, and is estimated to be about 200mV as a minimum /King 2002/. In order for an external electrical field to cause pitting corrosion, the potential at one end of the canister should be raised by 200mV. However, the total potential across the canister required to raise the potential at the anodic side by 200 mV is influence also by the current-potential characteristics of the cathodic reactions that take place at the opposite end of the canister.

With reduction of solid corrosion products or reduction of oxygen under activation control as cathodic reactions, the cathodic current can increase strongly with the negative potential. In this case, the shift in potential at the cathodic side may be small compared to a 200 mV shift at the anodic side. During a period when the conditions of an excess supply of oxygen may prevail or when there are reducible corrosion products present, the total voltage across the canister can be approximated with the shift at the anodic side. Thus, a voltage across the canister of 200 mV would, during this period, consume the whole margin against pitting. When there are no reducible corrosion products at the cathodic side of the canister and the oxygen supply is limited by diffusion, there is no strong potential dependence of the cathodic current close to the corrosion potential. The polarisation curve around the corrosion potential is likely to be almost linear over a wide range of potentials or to curve upwards. If the polarisation curve is linear, the total potential across the canister required to consume the margin against pitting is about 400 mV (200mV + 200mV). If the polarisation curve curves upwards, the potential difference across the canister must be higher than 400 mV in order to consume the marginal against pitting.

When the supply rate of oxygen to the cathode is not enough to drive the anodic processes, hydrogen evolution (reduction of water) can take place. An estimate of the potential across the canister required to drive pitting corrosion is found by considering the free corrosion potentials in Section 3.5.4 as being close to or higher than the potential required to oxidize copper metal to cuprous oxide, at least under neutral or alkaline conditions /King 2004/. As described previously in this section, the potential difference between the hydrogen evolution and oxide formation is about 400 mV. An additional 200 mV must be added to reach pitting conditions. Thus, with hydrogen evolution as the cathodic reaction, the potential difference across the canister required to cause pitting corrosion is about 600 mV.

High concentrations of sulphide have been found to decrease the value of the pitting potential for copper /King et al. 2010/. Effects have been found down to sulphide concentrations of 0.001 M, which though is nearly one order of magnitude higher than found in Forsmark /Tullborg et al. 2010/. For 0.01 M $HS^-$, the margin against pitting has been estimated to about 200 mV /King et al. 2010/. For sulphide driven copper corrosion, the cathodic process, hydrogen evolution can give currents that increase strongly with increasing cathodic polarisation. The anodic process is the formation

of solid copper sulphides, which may be either diffusion controlled or show a passive behaviour. In both cases the polarisation curve is likely to be flat at the anodic side while it can show strong non-linearity at the cathodic side. For these high sulphide concentrations, a potential difference of 200 mV across the canister would consume almost the whole the margin against pitting. But, because solid copper sulphides are the only stable corrosion product of copper in this potential range, the growth rate of such a pit would be limited by the diffusion of sulphide to and into the actual pit. There are indications of a threshold effect of sulphide so that the effect of sulphide on the pitting potential disappears below a certain concentration and also that the effect of sulphide decreases with increasing concentrations of other ions in the water /King et al. 2010/.

Nevertheless, in all cases one effect of an imposed voltage across a canister is that the margin against pitting corrosion is decreased, but the margins increase as the system is depleted of oxygen.

Anodic potentials are also a prerequisite for other forms of localized corrosion, stress corrosion cracking. To the extent that a margin against these forms of corrosion can be formulated in terms of potential, this margin will also be decreased by an imposed voltage across a canister. Still, for stress corrosion cracking to occur, high concentrations of detrimental ions are needed (see Section 3.5.5), which could not be foreseen in the repository.

#### *Dependencies between process and canister variables*

Table 3-14 shows how the process influences, and is influenced by, all canister variables.

#### *Boundary conditions*

The earth currents are generated in the far field and transferred to the canister at the canister/ buffer boundary.

#### *Model studies/experimental studies*

**Measurements of self potential and self potential gradients at the Forsmark site**

In the Forsmark site investigation, self potential gradients at depth at the target area have been measured and compared with the power output of the HVDC cable /Nissen et al. 2005/. In the site investigations the term self potential is used for the "natural" potential of the rock, as measured with

**Table 3-14. Direct dependencies between the process "Earth currents – stray current corrosion" and the defined canister variables and a short note on the handling in SR-Site.**

| Variable | Variable influence on process | | Process influence on variable | |
|---|---|---|---|---|
| | Influence present? (Yes/No) Description | Handling of influence (How/If not – why) | Influence present? (Yes/No) Description | Handling of influence (How/If not – why) |
| Radiation intensity | No. | – | No. | – |
| Temperature | Yes. Temperature will influence the stability of copper. | The polarization will redistribute the corrosion within the immunity area considered. | No. | – |
| Canister geometry | Yes. The dimensions of the canister determine its conductance. | The process is neglected due to small effects. | Yes. To the extent that the process occurs, the effect would be a reduction of canister thickness. | The process is neglected due to small effects. |
| Material composition | Yes. Different materials have different electrical conductivities. | The process is neglected due to small effects. | No. | – |
| Mechanical stresses | No. | – | No. | – |

a tool that does not induce an electric field (however, in Forsmark this natural potential is affected by the HVDC power output). The results show that the self potential of the repository rock is clearly affected by the HVDC power output, and that local self potential gradients can be significant. The obtained self potential gradients, as measured over a distance of 1.5 m in packed-off boreholes, were in the range of about 10 to 100 mV/m (cf. Figure 5-3 and Appendix 2 of /Nissen et al. 2005/).

In the site investigations (e.g. /Nielssen and Ringgaard 2007/), the self potential has routinely been measured in open boreholes (as oppose to packed-off boreholes) in the geophysical programme. The open borehole functions as a conductor homogenising the electric field, and as a result, the large self potential gradients measured when packing off the borehole are not seen. The reported results from these measurements are self potentials, and not potential gradients. However, when studying data points at a distance of about 5 metres apart (the scale of the canister), typical self potential gradients on the order of 10 mV/m or less can be extracted (cf. Appendices 1 and 2 of /Nielssen and Ringgaard 2007/). Occasionally gradients up to 50 mV/m are seen.

By comparing self potentials in boreholes hundreds of metres from each other, large-scale potential gradients can be estimated. In this case, the effect from the open borehole functioning as a conductor is less significant. /Nissen et al. 2005/ report measurements of self potentials in boreholes KFM01A and KFM04A. The distance between the boreholes is about 600 m. At repository depth, the measured self potentials in these boreholes differed by about 1 V (cf. Appendix 1 of /Nissen et al. 2005/) resulting in a potential gradient on the order of 1 mV/m. It should be noted that these measurements were not necessarily performed at the same power output from the HVDC cable, which may affect the estimated gradient by a factor of up to half an order of magnitude.

**Estimation of potential gradients over the canister at the Forsmark site**

In the case of copper canister corrosion, the local self potential gradients on the metre scale must be studied. As mentioned above the possible self potentials of natural rock are estimated to be up to a few tens of millivolts, which means very low potential gradients could be sustained over the canister. One of the criteria for choosing the Forsmark site is a general absence of ore bodies /SKB 2010m/. An assessment of the ore potential, which was carried out in support of model version 1.1, came to the conclusion that there is no potential for metallic and industrial mineral deposits within the candidate area at Forsmark. A potential for iron oxide (magnetite) mineralisation was recognised in an area to the south-west of the candidate area, predominantly in the felsic to intermediate metavolcanic rocks

For the present situation in Forsmark the influence of the HCDC cable must be taken into account. Such installations could be envisaged also during later occasions of the assessment time, but would be restricted to temperate periods when habition is possible. Further, it is only HCDC cables operated in monopolar mode that can cause currents through the earth. The cables could be operated in bipolar mode, with a separate cable to lead the current back.

For the Forsmark site one may use a bounding case where uneven buffer saturation causes the buffer above and below the canister to be fully saturated, but where the bentonite rings surrounding the canister are not. If it is assumed that the bentonite rings have a relatively high electrical resistance, the self potential gradient measurements performed when packing off the borehole may serve as a proxy of this case. Here the borehole would represent the deposition hole and the packer would represent the bentonite rings. Based on the self potential gradient data of /Nissen et al. 2005/, the maximum potential difference over the 5 m long canister is in this pessimistic case suggested to be about 0.5 V.

Similarly, the self potential measurements in open boreholes may serve as a proxy of the case where the entire buffer is fully saturated. In this case, the majority of the current running through the deposition hole and the rock block holding the deposition hole will be propagated in the buffer. Therefore, the open borehole would represent the deposition hole. In this case, based on the data in, for example, /Nielssen and Ringgaard 2007/, one can assume a typical potential difference over the canister of about 0.05 V. However, occasionally the potential difference may be up to 0.25 V. This case is deemed as more realistic than the one in the paragraph above.

### *Natural analogues/observations in nature*

See “Model studies/experimental studies”.

### *Time perspective*

Earth currents generated by natural causes may be present throughout the one million year time period of the safety assessment. Man made earth currents in general are expected not to occur during glaciations and other periods of no habitation. The special situation caused by the Fenno-Scan cable is expected to be present during a much shorter period, decades up to, at the most, 100 years.

### *Handling in the safety assessment SR-Site*

The effect of natural earth currents on canister corrosion can be neglegted as it is unlikely that sufficiently large potential gradients can be maintained over the deposition hole to affect the copper corrosion as the electrical resistance of a fully saturated bentonite buffer and the rock surrounding the deposition hole is low.

For occasions when a HVDC cable is operated in monopolar mode, measured self potential gradients at Forsmark can be used to estimate the influence on copper canister corrosion of such installations. The present and possible future cable installations will, however, exist for only short times compared to the total assessment time for SR-Site.

The corrosion of the canister in the presence of an external field would still be limited by the availability of groundwater constituents for either the cathodic reaction (oxygen), the anodic reaction (sulphide), or ions causing stress corrosion cracking (nitrite, ammonium, acetat). Cathodic reactions would also be counteracted by any dissolved hydrogen gas present. The external field would thus not increase the corrosion adopted in the assessment.

The effect of earth currents on canister corrosion can thus be neglected in the long-term perspective, based on the discussion presented above.

### *Handling of uncertainties in SR-Site*

#### Uncertainties in mechanistic understanding

There are no uncertainties in the mechanistic understanding of any importance for the safety assessment.

#### Model simplification uncertainties for the above handling in SR-Site

Not applicable since the process is not modelled.

#### Input data and data uncertainties for the above handling in SR-Site

Not applicable since the process is not modelled.

### *Adequacy of references supporting the handling in SR-Site*

In the SR-Site the thermodynamic calculations of the basic system copper-water in the report is used for an estimation of the margins to corrosion. The report /Puigdomench and Taxén 2000/ is not peer- or factual reviewed, but it is scientifically consistent with other references that are peer reviewed articles or papers. The supporting SKB report /King el al. 2010/ has undergone a documented factual- and quality review.

The other supporting references are either books describing geochemical phenomena, or reports from the Forsmark site investigation.

### 3.5.7 Deposition of salts on the canister surface

#### *Overview/general description*

In the KBS-3 safety assessment, the maximum surface temperature was calculated to be 80°C; i.e. well below the 100°C required to threaten the chemical stability of the bentonite /SKBF/KBS 1983, Pusch 1983/. In the present design, the heat generation in the fuel is 1,700 W, and this will result in an increased canister surface temperature. The actual temperature will, among other things, depend on heat transfer to the surrounding bentonite. At elevated temperatures, the corrosion reactions may proceed at an increased rate, but this will be of negligible importance since the corrosion is modelled under mass transport and mass balance control. A more important consequence of the higher canister surface temperature is the possible redistribution and enrichment of salts in the bentonite and their deposition onto the canister surface. The extent to which this may occur will depend on the salt content in the groundwater as well as in the bentonite. The salts that may be of concern are chlorides and sulphates from the groundwater and sulphates and carbonates from the impurities in the bentonite. Of these, the chlorides are most important since the presence of high chloride concentrations may have an effect on the corrosion properties of copper.

In the Long Term Test of Buffer Materials (LOT) /Karnland et al. 2000/, copper heaters are buried in compacted bentonite. Two of these packages have been retrieved and analysed. These two heaters had surface temperatures of 90°C and 130°C, respectively. Examination of their surfaces showed that in both cases the copper surfaces were covered with a thin layer of calcium sulphate/calcium carbonate. No chloride enrichments were apparent even though the groundwater had a chloride content of over 8,000 mg/L. The second LOT recovery after 6 years exposure at 130°C showed the same surface coverage of anhydrite and calcite. The longer exposure did not, however, seem to cause more precipitation /Karnland et al. 2009/. Similar salt deposits were observed in a heater experiment performed in Stripa /Pusch et al. 1992/.

It is at this time not established whether or not the precipitation of the sulphates and the carbonates were caused by evaporation of water or by the lower solubility of the calcium salts at elevated temperatures. In the latter case, they are likely to redissolve as the temperature decreases again. Alternatively, the deposits can be redissolved when contacted with water undersaturated with respect to calcium carbonate and calcium sulphate. Even if this surface cover remains over longer periods of time, credit cannot be taken for it having protective properties. The deposits are not electrically conductive, so they are not expected to increase the risk of pitting corrosion, see e.g. /Adeloju and Duan 1994/. Also, an increase in the chloride concentration would lower the susceptibility of copper to pitting corrosion, since it would favour general corrosion /King et al. 2001/. A high chloride concentration will, however, not lead to increased general corrosion, since the near field pH is always expected to be slightly alkaline and, consequently, the extent of the corrosion will be determined by the amount of available oxygen.

Thus, exposure to temperatures over 100°C is not expected to have an effect on the corrosion behaviour of the copper canister. The maximum allowed surface temperature of the canister is, therefore, set more by the requirements for chemical stability of the bentonite buffer than by any possible influence on canister corrosion.

#### *Dependences between process and canister variables*

Table 3-15 shows how the process influences, and is influenced by, all canister variables.

#### *Boundary conditions*

The heat is generated in the canister and transferred to the canister buffer boundary.

#### *Model studies/experimental studies*

See above.

**Table 3-15. Direct dependencies between the process "Deposition of salts on the canister surface" and the defined canister variables and a short note on the handling in SR-Site.**

| Variable | Variable influence on process | | Process influence on variable | |
|---|---|---|---|---|
| | Influence present? (Yes/No) Description | Handling of influence (How/If not – why) | Influence present? (Yes/No) Description | Handling of influence (How/If not – why) |
| Radiation intensity | No. | – | No. | – |
| Temperature | Yes. See discussion above. | Neglected. The process has no implications for safety. | No. | – |
| Canister geometry | No. | – | No. | – |
| Material composition | No. | – | Yes. Surface deposits may occur. | Neglected. The process has no implications for safety. |
| Mechanical stresses | No. | – | No. | – |

### *Natural analogues/observations in nature*

Not applicable.

### *Time perspective*

Elevated temperatures will remain for several hundred years. The effects discussed above will, however, only occur during the bentonite saturation phase.

### *Handling in the safety assessment SR-Site*

The process has no implications for safety and is, therefore, ignored.

### *Handling of uncertainties in SR-Site*

**Uncertainties in mechanistic understanding**

There are uncertainties concerning the mechanisms for possible salt deposition. There are no major uncertainties in understanding the consequences of such a deposit on the lifetime of the canister.

**Model simplification uncertainties for the above handling in SR-Site**

Not applicable.

**Input data and data uncertainties for the above handling in SR-Site**

Not applicable.

### *Adequacy of references supporting the handling in SR-Site*

/Adeloju and Duan 1994/ is a peer-reviewed paper. /Karnland et al. 2009/ has undergone a documented factual- and quality review.

## 3.6 Radionuclide transport

See Section 2.6 "Radionuclide transport ".

# 4 References

SKB's (Svensk Kärnbränslehantering AB) publications can be found at www.skb.se/publications. References to SKB's unpublished documents are listed separately at the end of the reference list. Unpublished documents will be submitted upon request to document@skb.se.


**Aaltonen P, Varis P, 1993.** Long term corrosion tests of OFHC-coppers in simulated repository conditions – final report. Report YJT-93-05, Nuclear Waste Commission of Finnish Power Companies.

**Adeloju S B, Duan Y Y, 1994.** Influence of bicarbonate ions on stability of copper oxides and copper pitting corrosion. British Corrosion Journal, 29, pp 315–320.

**Al-Hajji J N, Reda M R, 1993.** The corrosion of copper-nickel alloys in sulfide-polluted seawater: the effect of sulfide concentration. Corrosion Science 34, pp 163–177.

**Albinsson Y, Ödegaard-Jensen A, Oversby V M, Werme L, 2003.** Leaching of spent fuel under anaerobic and reducing conditions. In: Finch R J, Bullen D B (eds). Scientific basis for nuclear waste management XXVI. Warrendale, PA: Materials Research Society. (Materials Research Society Symposium Proceedings 757), pp 407–413.

**Allen A O, 1961.** The radiation chemistry of water and aqueous solutions. Princeton, N.J.: Van Nostrand.

**Auqué L F, Gimeno M J, Gómez J B, Puigdomenech I, Smellie J, Tullborg E-L, 2006.** Groundwater chemistry around a repository for spent nuclear fuel over a glacial cycle. Evaluation for SR-Can. SKB TR-06-31, Svensk Kärnbränslehantering AB.

**Beavers J A, Thompson N G, Parkins R N, 1985.** Stress-corrosion cracking of low strength carbon steels in candidate high level waste repository environments: environmental effects. Nuclear and Chemical Waste Management, 5, pp 279–296.

**BEFAST III, 1997.** Further analysis of extended storage of spent fuel. Final report of a Co-ordinated Research Programme on the Behaviour of Spent Fuel Assemblies during Extended Storage (BEFAST III) 1991–1996. IAEA-TECDOC-944, International Atomic Energy Agency.

**Behrenz P, Hannerz K, 1978.** Criticality in a spent fuel repository in wet crystalline rock. KBS TR 108, Svensk Kärnbränslehantering AB.

**Berner U, 2002.** Project Opalinus Clay. Radionuclide concentration limits in the near field of a repository for spent fuel and vitrified high level waste. Nagra NTB 02-10, National Cooperative for the Disposal of Radioactive Waste, Switzerland.

**Berner U, Curti E, 2002.** Radium solubilities for SF/HLW wastes using solid solution and co-precipitation models. Internal Report TM-44-02-04, Paul Scherrer Institute, Villigen, Switzerland.

**Betova I, Beverskog B, Bojinov M, Kinnunen P, Mäkelä K, Pettersson S-O, Saario T, 2003.** Corrosion of copper in simulated nuclear waste repository conditions. Electrochemical and Solid-State Letters, 6, pp B19–B22.

**Betova I, Heinonen J, Kinnunen P, Lilja C, Ruokola E, Saario T, 2004.** Application of an on-line corrosion probe and a reference electrode for copper corrosion studies in repository conditions. In: Oversby V M, Werme L O (eds). Scientific Basis for Nuclear Waste Management XXVII. Warrendale, PA: Materials Research Society. (Materials Research Society Symposium Proceedings 807), pp 429–434.

**Beverskog B, Puigdomenech I, 1998.** Pourbaix diagrams for the copper-chlorine system at 5–100°C. SKI Report 98:19, Statens kärnkraftinspektion (Swedish Nuclear Power Inspectorate).

**Beverskog B, Puigdomenech I, 2002.** Pourbaix diagrams for the copper in 5 m chloride solution, SKI Report 02:23, Statens kärnkraftinspektion (Swedish Nuclear Power Inspectorate).

**Bienvenu P, Cassette P, Andreoletti G, Bé M-M, Comte J, Lépy M-C, 2007.** A new determination of $^{79}$Se half-life. Applied Radiation and Isotopes, 65, pp 355–364.

**Blackwood D J, Naish C C, Sharland S M, Thompson A M, 2002.** Experimental and modelling study to assess the initiation of crevice corrosion in stainless steel containers for radioactive waste. Report AEAT/ERRA-0300, AEA Technology, Abingdon, UK.

**Bojinov M, Laitinen T, Mäkelä K, Snellman M, Werme L, 2004.** Corrosion of copper in 1 M NaCl under strictly anoxic conditions. In: Oversby V M, Werme L O (eds). Scientific Basis for Nuclear Waste Management XXVII. Warrendale, PA: Materials Research Society. (Materials Research Society Symposium Proceedings 807), pp 429–434.

**Bond A E, Hoch A R, Jones G D, Tomczyk A J, Wiggin R M, Worraker W J, 1997.** Assessment of a spent fuel disposal canister. Assessment studies for a copper canister with cast steel inner component. SKB TR 97-19, Svensk Kärnbränslehantering AB.

**Bosbach D, Böttle M, Volker M, 2010.** Experimental study of $Ra^{2+}$ uptake by barite (BaSO4). Kinetics of solid solution formation via $BaSO_4$ dissolution and $Ra_xBa_{1-x}SO_4$ (re) precipitation. SKB TR-10-43, Svensk Kärnbränslehantering AB.

**Bowman C D, Venneri F, 1994.** Underground supercriticality from plutonium and other fissile material. LA-UR-94-4022A, Los Alamos National Laboratory. (Also published in Science and Global Security, 5, pp 279–320.)

**Brennenstuhl A M, McBride A, Ramamurthy S, Davidson R, 2002.** The effects of microstructural and environmental factors on underdeposit corrosion of oxygen-free phosphorous-doped copper. Report 06819-REP-01200-10079-R00, Ontario Power Generation, Nuclear Waste Management Division.

**Bresle Å, Saers J, Arrhenius B, 1983.** Studies in pitting corrosion on archaeological bronzes. Copper. SKB TR 83-05, Svensk Kärnbränslehantering AB.

**Brissoneau L, Barbu A, Bocquet J-L, 2004.** Radiation effects on the long-term ageing of spent fuel storage containers. Packaging, Transport, Storage and Security of Radioactive Material, 15, pp 121–130.

**Broczkowski M E, Noël J J, Shoesmith D W, 2005.** The inhibiting effects of hydrogen on the corrosion of uranium dioxide under nuclear waste disposal conditions. Journal of Nuclear Materials, 346, pp 16–23.

**Broczkowski M E, Goldik J S, Santos B G, Noël J J, Shoesmith D W, 2006.** Corrosion of nuclear fuel inside a failed copper nuclear waste container. In: Dunn D, Poinssot C, Begg B (eds). Scientific Basis for Nuclear Waste Management XXX. Warrendale, PA: Materials Research Society. (Materials Research Society Symposium Proceedings 985), pp 3–14.

**Broczkowski M E, Noël J J, Shoesmith D W, 2007.** The influence of dissolved hydrogen on the surface composition of doped uranium dioxide under aqueous corrosion conditions. Journal of Electroanalytical Chemistry, 602, pp 8–16.

**Brookins D G, 1975.** Coffinite-uraninite stability relations in the Grants mineral belt. American Association of Petroleum Geologists Bulletin, 59, p 905.

**Brown P, Curti E, Grambow B, Ekberg C, 2005.** Chemical thermodynamics. Vol. 8. Chemical thermodynamics of Zirconium. Amsterdam: Elsevier.

**Bruno J, Cera E, de Pablo J, Duro L, Jordana S, Savage D, 1997.** Determination of radionuclide solubility limits to be used in SR 97. Uncertainties associated to calculated solubilities. SKB TR 97-33, Svensk Kärnbränslehantering AB.

**Bruno J, Cera E, Duro L, Pon J, de Pablo J, Eriksen T, 1998.** Development of a kinetic model for the dissolution of the $UO_2$ spent nuclear fuel. Application of the model to the minor radionuclides. SKB TR-98-22, Svensk Kärnbränslehantering AB.

**Bruno J, Bosbach D, Kulik D, Navrotsky A, 2007.** Chemical thermodynamics. Vol. 10. Chemical thermodynamics of solid solutions of interest in radioactive waste management. Paris: Nuclear Energy Agency, OECD.

**BSC, 2004.** Aqueous corrosion rates for waste package materials. ANL-DSD-MD-000001 Rev 01. Las Vegas: Bechtel SAIC Company.

**Campbell H S, 1950.** Pitting corrosion in copper water pipes caused by films of carbonaceous material produced during manufacture. Journal of the Institute of Metals, 77, pp 345–356.

**Carbol P, Cobos-Sabate J, Glatz J-P, Grambow B, Kienzler B, Loida A, Martinez Esparza Valiente A, Metz V, Quiñones J, Ronchi C, Rondinella V, Spahiu K, Wegen D H, Wiss T, 2005.** The effect of dissolved hydrogen on the dissolution of $^{233}U$ doped $UO_2$(s), high burn-up spent fuel and MOX fuel. SKB TR-05-09, Svensk Kärnbränslehantering AB.

**Carbol P, Fors P, Gouder T, Spahiu K, 2009a.** Hydrogen suppresses $UO_2$ corrosion. Geochimica et Cosmochimica Acta, 73, pp 4366–4375.

**Carbol P, Fors P, Van Winckel S, Spahiu K, 2009b.** Corrosion of irradiated MOX fuel in the presence of dissolved $H_2$. Journal of Nuclear Materials, 392, pp 45–54.

**Carlsson T, Muurinen A, 2007.** Measurements of Eh and pH in compacted MX-80 bentonite. In: Dunn D, Poinssot C, Begg B (eds). Scientific Basis for Nuclear Waste Management XXX. Warrendale, PA: Materials Research Society. (Materials Research Society Symposium Proceedings 985), NN13-09.

**Carslaw H S, Jaeger J C, 1959.** Conduction of heat in solids. 2nd ed. Oxford: Clarendon.

**Casella A, Hanson B, Miller W, 2008.** Factors affecting $UO_2$ dissolution under geological disposal conditions. In: Proceedings of the 12th International High-Level Waste Management Conference. Las Vegas, Nevada, 7–11 September 2008. New York: American Nuclear Society, pp 388–394.

**Casteels F, Dresselaars G, Tas H, 1986.** Corrosion behaviour of container materials for geological disposal of high level waste. Commission of European Communities Report, EUR 10398, pp 3–40.

**Cera E, Bruno J, Duro L, Eriksen T, 2006.** Experimental determination and chemical modelling of radiolytic processes at the spent fuel/water interface. Long contact time experiments. SKB TR-06-07, Svensk Kärnbränslehantering AB.

**Chaouadi R, Gérard R, 2005.** Copper precipitate hardening of irradiated RPV materials and implications on the superposition law and re-irradiation kinetics. Journal of Nuclear Materials, 345, pp 65–74.

**Christensen H, Bjergbakke E, 1982.** Radiolysis of groundwater from HLW stored in copper canisters. SKBF/KBS TR 82-02, Svensk Kärnbränslehantering AB.

**Christensen H, Bjergbakke E, 1984.** Radiolysis of concrete. SKBF/KBS TR 84-02, Svensk Kärnbränslehantering AB.

**Christensen H, Pettersson S-O, 1997.** Beräkning av radiolys utanför intakt kapsel. Report STUDSVIK/M-97/67, Studsvik Material AB (in Swedish).

**Clarens F, Serrano-Purroy D, Martínez-Esparza A, Wegan D, Gonzalez-Robles E, de Pablo J, Casas I, Giménez J, Christiansen B, Glatz J-P, 2008.** RN fractional release of high burn-up fuel: effect of HBS and estimation of accessible grain boundary. In: Lee W E, Roberts J W, Hyatt N C, Grimes R W (eds). Scientific Basis for Nuclear Waste Management XXXI. Warrendale, PA: Materials Research Society. (Materials Research Society Symposium Proceedings 1107), pp 439–446.

**Cliffe K A, Kelly M, 2005.** COMP23 version 1.2.2. User's manual. SKB R-04-64, Svensk Kärnbränslehantering AB.

**Cong H, Michaels H T, Scully J R, 2009.** Passivity and pit stability behavior of copper as a function of selected water chemistry variables. Journal of The Electrochemical Society, 156, pp C16–C27.

**Cramer J, Smellie J (eds), 1994.** Final report of the AECL/SKB Cigar Lake analog study. SKB TR 94-04, Svensk Kärnbränslehantering AB.

**Cross M M, Manning D A C, Bottrell S H, Worden R H, 2004.** Thermochemical sulphate reduction (TSR): experimental determination of reaction kinetics and implications of the observed reaction rates for petroleum reservoirs. Organic Geochemistry, 35, pp 393–404.

**Cui D, Spahiu K, 2002.** The reduction of U(VI) on corroded iron under anoxic conditions. Radiochimica Acta, 90, pp 623–628.

**Cui D, Low J, Sjöstedt C J, Spahiu K, 2004.** On Mo-Ru-Tc-Pd-Rh-Te alloy particles extracted from spent fuel and their leaching behavior under Ar and $H_2$ atmospheres. Radiochimica Acta, 92, pp 551–555.

**Cui D, Ekeroth E, Fors P, Spahiu K, 2008.** Surface mediated processes in the interaction of spent fuel or α-doped $UO_2$ with $H_2$. In: Shuh D K, Chung B W, Albrecht-Schmitt T, Gouder T, Thompson J D (eds). Actinides 2008 – basic science, applications and technology. Warrendale, PA: Materials Research Society. (Materials Research Society Symposium Proceedings 1104), pp 87–99.

**Cushman A S, Gardner H A, 1910.** The corrosion and preservation of iron and steel. New York: McGraw-Hill.

**Desgranges L, Ripert M, Piron J P, Kodja H, Gallier J P, 2003.** Behaviour of fission gases in an irradiated nuclear fuel under α external irradiation. Journal of Nuclear Materials, 321, pp 324–330.

**Dillström P, Alverlind L, Andersson M, 2010.** Framtagning av acceptanskriterier samt skadetålighetsanalyser av segjärnsinsatsen. SKB R-10-11, Svensk Kärnbränslehantering AB.

**Doerner H A, Hoskins W M, 1925.** Co-precipitation of radium and barium sulphates. Journal of the American Chemical Society, 47, pp 662–675.

**Duro L, Grivé M, Cera E, Domenech C, Bruno J, 2006a.** Update of a thermodynamic database for radionuclides to assist solubility limits calculation for performance assessment. SKB TR-06-17, Svensk Kärnbränslehantering AB.

**Duro L, Grivé M, Cera E, Gaona X, Domènech C, Bruno J, 2006b.** Determination and assessment of the concentration limits to be used in SR-Can. SKB TR-06-32, Svensk Kärnbränslehantering AB.

**Edwards M, Ferguson J F, Reiber S H, 1993.** The pitting corrosion of copper. Journal of American Water Works Association, 86, pp 74–90.

**Ekeroth E, Low J, Zwicky H-U, Spahiu K, 2009.** Corrosion studies with high burnup LWR fuel in simulated groundwater. In: Hyatt N C, Pickett D A, Rebak R B (eds). Scientific Basis for Nuclear Waste Management XXXII. Warrendale, PA: Materials Research Society. (Materials Research Society Symposium Proceedings 1124), Q02-07.

**EN 1563:1997.** Founding. Spheroidal graphite cast iron. Brussels: European Committee for Standardization.

**EN 1976:1988.** Copper and copper alloys. Cast unwrought copper products. (UNS10100: Copper Development Association Inc. Application Data Sheet. Standard designations for copper and copper alloys (www.copper.org)).

**Eriksen T, Jonsson M, 2007.** The effect of hydrogen on dissolution of spent fuel in 0.01 mol×$dm^{-3}$ $NaHCO_3$ solution. SKB TR-07-06, Svensk kärnbränslehantering AB.

**Eriksen T E, Jonsson M, Merino J, 2008.** Modelling time resolved and long contact time dissolution studies of spent nuclear fuel in 10 mM carbonate solution: a comparison between two different models and experimental data. Journal of Nuclear Materials, 375, pp 331–339.

**Evans U R, Miley H A, 1937.** Measurements of oxide films on copper and iron. Nature, 139, pp 282–283.

**Evins L Z, Jensen K A, Ewing R C, 2005.** Uraninite recrystallization and Pb loss in the Oklo and Bangombé natural fission reactors, Gabon. Geochimica et Cosmochimica Acta, 69, pp 1589–1606.

**Ferry C, Poinssot C, Broudic V, Cappelaere C, Desgranges L, Garcia P, Jégou C, Lovera P, Marimbeau A, Piron J P, Poulesquen A, Roudil D, Gras J M, Bouffioux P, 2005.** Synthesis on the spent fuel long term evolution. Report CEA-R-6084, Commissariat à l'Énergie Atomique.

**Ferry C, Piron J-P, Poulesquen A, Poinssot C, 2008.** Radionuclides release from spent fuel under disposal conditions: re-evaluation of the Instant Release Fraction. In: Lee W E, Roberts J W, Hyatt N C, Grimes R W (eds). Scientific Basis for Nuclear Waste Management XXXI. Warrendale, PA: Materials Research Society. (Materials Research Society Symposium Proceedings 1107), pp 447–454.

**Finch R, Murakami T, 1999.** Systematics and paragenesis of uranium minerals. Reviews in Mineralogy and Geochemistry, 38, pp 91–179.

**Fors P, Cabol P, Van Winkel S, Spahiu K, 2008.** High burn-up $UO_2$ fuel corrosion under reducing conditions. In: Proceedings of the 12th International High-Level Waste Management Conference. Las Vegas, Nevada, 7–11 September 2008. New York: American Nuclear Society, pp 380–387.

**Forsyth R, 1995.** Spent nuclear fuel. A review of properties of possible relevance to corrosion processes. SKB TR 95-23, Svensk Kärnbränslehantering AB.

**Forsyth R, 1997.** The SKB Spent Fuel Corrosion Programme. An evaluation of results from the experimental programme performed in the Studsvik Hot Cell laboratory. SKB TR 97-25, Svensk Kärnbränslehantering AB.

**Forsyth R S, Werme L O, 1992.** Spent fuel corrosion and dissolution. Journal of Nuclear Materials, 190, pp 3–19.

**Forsyth R S, Mattsson O, Schrire D, 1988.** Fission product concentration profiles (Sr, Xe, Cs and Nd) at the individual grain level in power-ramped LWR fuel. SKB TR 88-24, Svensk Kärnbränslehantering AB.

**Forsyth R S, Eklund U-B, Werme L O, 1994.** A study of fission product migration and selective leaching by means of a power-bump test. In: Barkatt A, Van Konynenburg R (eds). Scientific Basis for Nuclear Waste Management XVII. Pittsburgh, PA: Materials Research Society. (Materials Research Society Symposium Proceedings 333), pp 385–390.

**Fuchs L H, Hoekstra H R, 1959.** The preparation and properties of uranium (IV) silicate. American Mineralogist, 44, pp 1057–1063.

**Galvele J R, 1987.** A stress corrosion cracking mechanism based on surface mobility. Corrosion Science, 27, pp 1–33.

**Gamsjäger H, Bugajski J, Gajda T, Lemire R J, Preis W, 2005.** Chemical thermodynamics. Vol. 6. Chemical thermodynamics of nickel. Amsterdam: Elsevier.

**Gdowski G E, Bullen D B, 1988.** Survey of degradation modes of candidate materials for high-level radioactive-waste disposal containers. Vol 2, Oxidation and corrosion. Report UCID-21362, Lawrence Livermore National Laboratory, University of California.

**Goldschmidt B, 1940.** Etude du fractionnement par crystallisation mixte a l´aide des radioelements. Annales de Chimie, Serie XI, 13, pp 88–174.

**Goldstein T P, Aizenshtat Z, 1994.** Thermochemical sulfate reduction: a review. Journal of Thermal Analysis and Calorimetry, 42, pp 241–290.

**Grambow B, Loida A, Dressler P, Geckeis H, Gago J, Casas I, de Pablo J, Gimenez J, Torrero M E, 1996.** Long-term safety of radioactive waste disposal: chemical reaction of fabricated and high burnup spent $UO_2$ fuel with saline brines. Final report. Wissenschaftliche Berichte FZKA 5702, Forschungszentrum Karlsruhe.

**Grambow B, Loida A, Martínez-Esparza A, Díaz-Arocas P, de Pablo J, Paul J-L, Marx G, Glatz J-P, Lemmens K, Ollila K, Christensen H, 2000.** Source term for performance assessment of spent fuel as a waste form. EUR 19140, European Commission.

**Grandia F, Domènech C, Arcos D, Duro L, 2006.** Assessment of the oxygen consumption in the backfill. Geochemical modelling in a saturated backfill. SKB R-06-106, Svensk Kärnbränslehantering AB.

**Grandia F, Merino J, Bruno J, 2008.** Assessment of the radium-barium co-precipitation and its potential influence on the solubility of Ra in the near-field. SKB TR-08-07, Svensk Kärnbränslehantering AB.

**Grauer R, 1990.** The reducibility of sulphuric acid and sulphate in aqueous solution (translated from German). SKB TR 91-39, Svensk Kärnbränslehantering AB.

**Gray W J, 1999.** Inventories of iodine-129 and cesium-137 in the gaps and grain boundaries of LWR spent fuels. In: Wronkiewicz D J, Lee J H (eds). Scientific Basis for Nuclear Waste Management XXII. Warrendale, PA: Materials Research Society. (Materials Research Society Symposium Proceedings 556), pp 487–494.

**Gray W J, Strachan D M, Wilson C N, 1992.** Gap and grain boundary inventories of Cs, Tc and Sr in spent LWR fuel. In: Sombret C G (ed). Scientific Basis for Nuclear Waste Management XV. Warrendale, PA: Materials Research Society. (Materials Research Society Symposium Proceedings 257), pp 353–360.

**Grenthe I, Fuger J, Konings R J M, Lemire R, Muller A B, Nguen-Trung C, Wanner H, 1992.** Chemical thermodynamics. Vol. 1. Chemical thermodynamics of uranium. Amsterdam: Elsevier.

**Grigoriev V, 1996.** Hydrogen embrittlement of zirconium alloys. Report STUDSVIK/M-96/73, Studsvik Material AB.

**Grivé M, Domènech C, Montoya V, Garcia D, Duro L, 2010.** Determination and assessment of the concentration limits to be used in SR-Can. Supplement to TR-06-32. SKB R-10-50, Svensk Kärnbränslehantering AB.

**Gubner R, Andersson U, 2007.** Corrosion resistance of copper canister weld material. SKB TR-07-07, Svensk Kärnbränslehantering AB.

**Gubner R, Andersson U, Linder M, Nazarov A, Taxén C, 2006.** Grain boundary corrosion of copper canister weld material. SKB TR-06-01, Svensk Kärnbränslehantering AB.

**Guilbert S, Sauvage T, Erramli H, Barthe M-F, Desgardin P Blondiaux G, Corbel C, Piron J P, 2003.** Helium behavior in $UO_2$ polycrystalline disks. Journal of Nuclear Materials, 321, pp 121–128.

**Guillaumont R, Fanghänel T, Fuger J, Grenthe I, Neck V, Palmer D A, Rand M H, 2003.** Chemical thermodynamics. Vol. 5. Update on the chemical thermodynamics of Uranium, Neptunium, Plutonium, Americium and Technetium. Amsterdam: Elsevier.

**Guinan M W, 2001.** Radiation effects in spent nuclear fuel canisters. SKB TR-01-32, Svensk Kärnbränslehantering AB.

**Hahn O, 1936.** Applied radiochemistry. Ithaca, N.Y.: Cornell University Press.

**Hallbeck L, Pedersen K, 2008.** Explorative analysis of microbes, colloids and gases. SDM-Site Forsmark. SKB R-08-85, Svensk Kärnbränslehantering AB.

**Hallberg R O, Engvall A-G, Wadsten T, 1984.** Corrosion of copper lightning conductor plates. British Corrosion Journal, 19, pp 85–88.

**Hallberg R O, Östlund P, Wadsten T, 1988.** Inferences from a corrosion study of a bronze cannon, applied to high level nuclear waste disposal. Applied Geochemistry, 3, pp 273–280.

**Hanson B, 2008.** Examining the conservatisms in dissolution rates of commercial spent nuclear fuel. In: Proceedings of the 12th International High-Level Waste Management Conference. Las Vegas, Nevada, 7–11 September 2008. New York: American Nuclear Society, pp 404–411.

**Hanson B D, Stout R B, 2004.** Reexamining the dissolution of spent fuel: a comparison of different methods for calculating rates. In: Hanchar J M, Stroes-Gascoyne S, Browning L (eds). Scientific Basis for Nuclear Waste Management XXVIII. Warrendale, PA: Materials Research Society. (Materials Research Society Symposium Proceedings 824), pp 89–94.

**Hanson B D, Friese J I, Soderquist C Z, 2004.** Initial results from dissolution testing of spent fuel under acidic conditions. In: Hanchar J M, Stroes-Gascoyne S, Browning L (eds). Scientific Basis for Nuclear Waste Management XXVIII. Warrendale, PA: Materials Research Society. (Materials Research Society Symposium Proceedings 824), pp 113–118.

**Harrington J F, Birchall D J, 2007.** Sensitivity of total stress to changes in externally applied water pressure in KBS-3 buffer bentonite. SKB TR-06-38, Svensk Kärnbränslehantering AB.

**He H, Keech P G, Broczkowski M E, Noël J J, Shoesmith D W, 2007.** Characterization of the influence of fission product doping on the anodic reactivity of uranium dioxide. Canadian Journal of Chemistry, 85, pp 702–713.

**He M, Jiang S, Jiang S, Chen Q, Qin J, Wu S, Dong Y, Zhao Z, 2000.** Measurement of $^{79}Se$ and $^{64}Cu$ with PXAMS. Nuclear Instruments and Methods in Physics Research Section B: Beam Interactions with Materials and Atoms, 172, pp 177–181.

**He M, Jiang S, Jiang S, Diao L, Wu S, Li C, 2002.** Measurements of the half-life of $^{79}Se$ with PX-AMS. Nuclear Instruments and Methods in Physics Research Section B: Beam Interactions with Materials and Atoms, 194, pp 393–398.

**Hedin A, 2004.** Integrated near-field evolution model for a KBS-3 repository. SKB R-04-36, Svensk Kärnbränslehantering AB.

**Hemingway B S, 1982.** Thermodynamic properties of selected uranium compounds and aqueous species at 298.15 K and 1 bar and at higher temperatures; preliminary models for the origin of coffinite deposits. Open File Report 82-619, US Geological Survey.

**Henshaw J, 1994.** Modelling of nitric acid production in the Advanced Cold Process Canister due to irradiation of moist air. SKB TR 94-15, Svensk Kärnbränslehantering AB.

**Henshaw J, Hoch A, Sharland S M, 1990.** Further assessment studies of the Advanced Cold Process Canister. AEA-D&R-0060, AEA Decommissioning & Radwaste.

**Hernelind J, 2010.** Modelling and analysis of canister and buffer for earthquake induced rock shear and glacial load. SKB TR-10-34, Svensk Kärnbränslehantering AB.

**Hocking W H, Duclos A M, Johnson L H, 1994.** Study of fission-product segregation in used CANDU fuel by X-ray photoelectron spectroscopy (XPS) II. Journal of Nuclear Materials, 209, pp 1–26.

**Hoehn E, Eikenberg J, Fierz T, Drost W, Reichlmayr E, 1998.** The Grimsel Migration Experiment: field injection–withdrawal experiments in fractured rock with sorbing tracers. Journal of Contaminant Hydrology, 34, pp 85–106.

**Hua F, Mon K, Pasupathi P, Gordon G, Shoesmith D, 2005.** A review of the corrosion of titanium grade 7 and other titanium alloys in nuclear waste repository environments. Corrosion, 61, pp 987–1003.

**Håkansson R, 2000.** Beräkning av nuklidinnehåll, resteffekt, aktivitet samt doshastighet för utbränt kärnbränsle. SKB R-99-74, Svensk Kärnbränslehantering AB.

**Hökmark H, Lönnqvist M, Fälth B, 2010.** THM-issues in repository rock. Thermal, mechanical, thermo-mechanical and hydro-mechanical evolution of the rock at the Forsmark and Laxemar sites. SKB TR-10-23, Svensk Kärnbränslehantering AB.

**IAEA, 2003.** Spent fuel performance assessment and research, Final report of the co-ordinated research project SPAR. IAEA-TECDOC-1343, International Atomic Energy Agency.

**Ikeda B M, Litke C D, 2004.** Status report for 2003 on stress corrosion cracking of OFP copper in ammonia. Report 06819-REP-01300-10078-R00, Ontario Power Generation, Nuclear Waste Management Division.

**Ikeda B M, Litke C D, 2007.** Stress corrosion cracking of copper in nitrite/chloride mixtures at elevated temperatures. NWMO TR-2007-04, Nuclear Waste Management Organization, Canada.

**Ikeda B M, Litke C D, 2008.** The effect of high chloride concentration on stress corrosion cracking behaviour of copper. NWMO TR-2008-12, Nuclear Waste Management Organization, Canada.

**Jacobs S, Edwards M, 2000.** Sulfide scale catalysis of copper corrosion. Water Research, 34, pp 2798–2808.

**Janeczek J, Ewing R C, 1992.** Coffinitization – a mechanism for the alteration of $UO_2$ under reducing conditions. In: Sombret C G (ed). Scientific Basis for Nuclear Waste Management XV. Warrendale, PA: Materials Research Society. (Materials Research Society Symposium Proceedings 257), pp 497–504.

**Janeczek J, Ewing R C, Oversby V M, Werme L O, 1996.** Uraninite and $UO_2$ in spent nuclear fuel: a comparison. Journal of Nuclear Materials, 238, pp 121–131.

**Jégou C, Peuget S, Broudic V, Roudil D, Deschanels X, Bart J M, 2004.** Identification of the mechanism limiting the alteration of clad spent fuel segments in aerated carbonated groundwater. Journal of Nuclear Materials, 326, pp 144–155.

**Jégou C, Muzeau B, Brudic V, Poulesquen A, Roudil D, Jorion F, Corbel C, 2005.** Effect of alpha radiation on $UO_2$ surface reactivity in aqueous media. Radiochimica Acta, 93, pp 35–42.

**Jiang S, Guo J, Jiang S, Li C, Cui A, He M, Wu S, Li S, 1997.** Determination of the half-life of $^{79}Se$ with the accelerator mass spectrometry technique. Nuclear Instruments and Methods in Physics Research Section B, 123, pp 405-409.

**Jin L-Z, Sandström R, 2009a.** Non-stationary creep simulation with a modified Armstrong-Frederick relation applied to copper canisters. Computational Materials Science, 46, pp 339–346.

**Jin L-Z, Sandström R, 2009b.** Modified Armstrong-Frederick relation for handling back stresses in FEM computations. In: Shibli I A, Holdworth S R (eds). Proceedings of the 2nd international ECCC conference. Creep & fracture in high temperature components: design and life assessment issues. Dübendorf, Switzerland, 21–23 April 2009, pp 836–847.

**Johansson L-G, 2008.** Comment on "Corrosion of copper by water" [Electrochemical and Solid-State Letters, 10, C63, (2007)]. Electrochemical and Solid-State Letters, 11, S1.

**Johnson L H, McGinnes D F, 2002.** Partitioning of radionuclides in Swiss power reactor fuels. Nagra NTB 02-07, National Cooperative for the Disposal of Radioactive Waste, Switzerland.

**Johnson L H, Tait J C, 1997.** Release of segregated nuclides from spent fuel. SKB TR 97-18, Svensk Kärnbränslehantering AB.

**Johnson L H, Poinssot C, Ferry C, Lovera P, 2004.** Estimates of the instant release fraction of $UO_2$ and MOX fuel at t = 0. Nagra NTB 04-08, National Cooperative for the Disposal of Radioactive Waste, Switzerland.

**Johnson L, Ferry C, Poinssot C, Lovera P, 2005.** Spent fuel radionuclide source-term model for assessing spent fuel performance in geological disposal. Part I: Assessment of the instant release fraction. Journal of Nuclear Materials, 346, pp 56–65.

**Jones A R, 1959.** Radiation–induced reactions in the $N_2$-$O_2$-$H_2O$ system. Radiation Research, 10, pp 655–663.

**Jonsson M, Nielsen F, Roth O, Ekeroth E, Nilsson S, Hossain M M, 2007.** Radiation induced spent nuclear fuel dissolution under deep repository conditions. Environmental Science & Technology, 41, pp 7087–7093.

**Kaija J, Blomqvist R, Suksi J, Rasilainen K, 2000.** The Palmottu Natural Analogue Project, Summary Report 1996–1999. The behaviour of natural radionuclides in and around uranium deposits, Nr. 13. Report YST-102, Nuclear Waste Commission of Finnish Power Companies.

**Kamimura K, 1992.** FP gas release behaviour of high burn-up MOX fuels for thermal reactors. In: Fission gas release and fuel rod chemistry related to extended burnup. Proceeding of a Technical Committee Meeting held in Pembroke, Ontario, Canada, 28 April – 1 May 1992. IAEA-TECDOC-697, International Atomic Energy Agency, pp 82–88.

**Karnland O, Sandén T, Johannesson L-E, Eriksen T E, Jansson M, Wold S, Pedersen K, Motamedi M, Rosborg B, 2000.** Long term test of buffer material. Final report on the pilot parcels. SKB TR-00-22, Svensk Kärnbränslehantering AB.

**Karnland O, Olsson S, Dueck A, Birgersson M, Nilsson U, Hernan-Håkansson T, Pedersen K, Nilsson S, Eriksen T E, Rosborg B, 2009.** Long term test of buffer material at the Äspö Hard Rock Laboratory, LOT project. Final report on the A2 test parcel. SKB TR-09-29, Svensk Kärnbränslehantering AB.

**Kelm M, Bohnert E, 2004.** A kinetic model for the radiolysis of chloride brine, its sensitivity against model parameters and a comparison with experiments. FZK Wissenschaftliche Berichte FZKA 6977, Forschungszentrum Karlsruhe.

**Kelm M, Bohnert E, 2005.** Gamma radiolysis of NaCl brine: effect of dissolved radiolysis gases on the radiolytic yield of long-lived products. Journal of Nuclear Materials, 346, pp 1–4.

**King F, 2002.** Corrosion of copper in alkaline chloride environments. SKB TR-02-25, Svensk Kärnbränslehantering AB.

**King F, 2004.** The effect of discontinuities on the corrosion behaviour of copper canisters. SKB TR-04-05, Svensk Kärnbränslehantering AB.

**King F, Kolár M, 2000.** The copper container corrosion model used in AECL's second case study. 06819-REP-01200-10041-R00, Ontario Power Generation, Nuclear Waste Management Division.

**King F, LeNeveu D, 1992.** Prediction of the lifetimes of copper nuclear waste containers. In: Proceedings of the Topical Meeting on Nuclear Waste Packaging, Focus '91. Las Vegas, 30 September – 2 October 1991. La Grange Park: American Nuclear Society, pp 253–261.

**King F, Litke C D, 1987.** The corrosion of copper in synthetic groundwater at 150°C. Part I. The results of short term electrochemical tests. Technical Record TR-428, Atomic Energy of Canada Ltd.

**King F, Newman R, 2010.** Stress corrosion cracking of copper canisters. SKB-TR-10-04, Svensk Kärnbränslehantering AB.

**King F, Shoesmith D W, 2004.** Electrochemical studies of the effect of $H_2$ on $UO_2$ dissolution. SKB TR-04-20, Svensk Kärnbränslehantering AB.

**King F, Litke C D, Ryan S R, 1992.** A mechanistic study of the uniform corrosion of copper in compacted Na-montmorillonite/s and mixtures. Corrosion Science, 33, pp 1979–1995.

**King F, Ryan S R, Litke C D, 1997.** The corrosion of copper in compacted clay. Report AECL-11831, COG-97-412-I, Atomic Energy of Canada Ltd.

**King F, Ahonen L, Taxén C, Vuorinen U, Werme L, 2001.** Copper corrosion under expected conditions in a deep geologic repository. SKB TR-01-23, Svensk Kärnbränslehantering AB.

**King F, Lilja C, Pedersen K, Pikänen P, Vähänen M, 2010.** An update of the state-of-the-art report on the corrosion of copper under expected conditions in a deep geologic repository. SKB TR-10-67, Svensk Kärnbränslehantering AB.

**Koerts H C, Wetzer J M, 2001.** Literature survey on corrosion of underground metallic structures induced by alternating currents. KEMA Report 40030204-TDP 01-16792A, KEMA, The Netherlands.

**Kolár M, King F, 1996.** Modelling the consumption of oxygen by container corrosion and reaction with Fe(II). In: Murphy W M, Knecht D (eds). Scientific Basis for Nuclear Waste Management XIX. Warrendale, PA: Materials Research Society. (Materials Research Society Symposium Proceedings 412), pp 547–554.

**Kursten B, Smailos E, Azkarate I, Werme L, Smart N R, Marx G, Cuñado M A, Santarini G, 2004.** COBECOMA. State-of-the-art document on the corrosion behaviour of container materials. Final report. Brussels: European Commission.

**Langmuir D, 1978.** Uranium solution-mineral equilibria at low temperatures with applications to sedimentary ore deposits. Geochimica et Cosmochimica Acta, 42, pp 547–569.

**Langmuir D, Chatham J R, 1980.** Groundwater prospecting for sandstone-type uranium deposits: a preliminary comparison of the merits of mineral-solution equilibria, and single tracer methods. Journal of Geochemical Exploration, 13, pp 201–219.

**Lazo C, Karnland O, Tullborg E-L, Puigdomenech I, 2003.** Redox properties of MX-80 and Montigel bentonite-water systems. In: Finch R J, Bullen D B (eds). Scientific Basis for Nuclear Waste Management XXVI. Warrendale, PA: Materials Research Society. (Materials Research Society Symposium Proceedings 757), II8.1.

**Lemire R J, Fuger J, Nitsche H, Potter P, Rand M H, Rydberg J, Spahiu K, Sullivan J C, Ullman W J, Vitorge P, Wanner H, 2001.** Chemical thermodynamics. Vol. 4. Chemical thermodynamics of Neptunium and Plutonium. Amsterdam: Elsevier.

**Leygraf C, 2002.** Atmospheric corrosion. In: Marcus P (ed). Corrosion mechanisms in theory and practice. 2nd ed. New York: Marcel Dekker, pp 529–562.

**Leygraf C, Graedel T E, 2000.** Atmospheric corrosion. New York: Wiley.

**Li W, Li D Y, 2005.** Variations of work function and corrosion behaviors of deformed copper surfaces. Applied Surface Science, 240, pp 388–395.

**Litke C D, Ikeda B M, 2006.** The effect of acetate concentration, chloride concentration and applied current on stress corrosion cracking of OFP copper. Report 06819-REP-01300-10005, Ontario Power Generation, Nuclear Waste Management Division.

**Litke C D, Ikeda B M, 2008.** The stress corrosion cracking behaviour of copper in acetate solutions. NWMO TR-2008-21, Nuclear Waste Management Organization, Canada.

**Litke C D, Ryan S R, King F, 1992.** A mechanistic study of the uniform corrosion of copper in compacted clay-sand soil. AECL-10397, COG-91-304, Atomic Energy of Canada Ltd.

**Loida A, Grambow B, Geckeis H, 1996.** Anoxic corrosion of various high burnup spent fuel samples. Journal of Nuclear Materials, 238, pp 11–22.

**Loida A, Metz V, Kienzler B, 2007.** Alteration behaviour of high burnup spent fuel in salt brine under hydrogen overpressure and in presence of bromide. In: Dunn D, Poinssot C, Begg B (eds). Scientific Basis for Nuclear Waste Management XXX. Warrendale, PA: Materials Research Society. (Materials Research Society Symposium Proceedings 985), pp 15–20.

**Lovera P, Ferry C, Poinssot C, Johnson L, 2003.** Synthesis report on the relevant diffusion coefficients of fission products and helium in spent nuclear fuels. Report CEA-R-6039, Commisariat à l'Énergie Atomique.

**Lucey V F, 1967.** Mechanisms of pitting corrosion of copper in supply waters. British Corrosion Journal, 2, pp 175–187.

**Lytle D A, Nadagouda M N, 2010.** A comprehensive investigation of copper pitting corrosion in a drinking water distribution system. Corrosion Science, 52, pp 1927–1938.

**Marion G M, Kargel J S, Catling D C, Jakubowski S D, 2005.** Effect of pressure on aqueous chemical equilibria at subzero temperatures with applications to Europa. Geochimica et Cosmochimica Acta, 69, pp 259–274.

**Marsh G P, 1990.** A preliminary assessment of the advanced cold process canister. Report AEA-InTec-0011, AEA Technology.

**Martin G, Maillard S, Van Brutzel L, Garcia P, Dorado B, Valot C, 2009.** A molecular dynamics study of radiation induced diffusion in uranium dioxide. Journal of Nuclear Materials, 385, pp 351–357.

**Martinsson Å, Andersson-Östling H C M, Seitisleam F, Wu R, Sandström R, 2010.** Creep testing of nodular iron at ambient and elevated temperatures. SKB R-10-64, Svensk Kärnbränslehantering AB.

**Masurat P, Eriksson S, Pedersen K, 2010.** Microbial sulphide production in compacted Wyoming bentonite MX-80 under in situ conditions relevant to a repository for high-level radioactive waste. Applied Clay Science, 47, pp 58–64.

**Matthiesen H, Hilbert L R, Gregory D J, 2003.** Siderite as a corrosion product on archaeological iron from a waterlogged environment. Studies in Conservation, 48, pp 183–194.

**Matthiesen H, Hilbert L R, Gregory D, Sørensen B, 2007.** Corrosion of archaeological iron artefacts compared to modern iron at the waterlogged site Nydam, Denmark. In: Dillmann P, Piccardo P, Matthiesen H, Beranger G (eds). Corrosion of metallic heritage artefacts: investigation, conservation and prediction for long-term behaviour. Cambridge: Woodhead Publishing, pp 272–292.

**Mattsson E, 1980.** Corrosion of copper and brass: practical experience in relation to basic data. British Corrosion Journal, 15, pp 6–13.

**Mattsson E, 1988.** Counteracting of pitting in copper water pipes by bicarbonate dosing. Materials and Corrosion, 39, pp 499–503.

**Mattsson H, Olefjord I, 1984.** General corrosion of Ti in hot water and water saturated bentonite clay. SKB/KBS TR 84-19, Svensk Kärnbränslehantering AB.

**Mattsson H, Olefjord I, 1990.** Analysis of oxide formed on titanium during exposure in bentonite clay. I. The oxide growth. Materials and Corrosion, 41, pp 383–390.

**Mattsson H, Li C, Olefjord I, 1990.** Analysis of oxide formed on Ti during exposure in bentonite clay. II. The structure of the oxide. Materials and Corrosion, 41, pp 578–584.

**Matsson I, Grapengiesser B, Andersson B, 2007.** On-site γ-ray spectroscopic measurements of fission gas release in irradiated nuclear fuel. Applied Radiation and Isotopes, 65, pp 36–45

**Mazeina L, Ushakov S, Navrotsky A, Boatner L A, 2005.** Formation enthalpy of $ThSiO_4$ and enthalpy of the thorite-huttonite phase transition. Geochimica et Cosmochimica Acta, 69, pp 4675–4683.

**Mazeina L, Navrotsky A, Greenblatt M, 2008.** Calorimetric determination of energetics of solid solutions of $UO_{2+x}$ with CaO and $Y_2O_3$. Journal of Nuclear Materials, 373, pp 39-43.

**McNeil M B, Little B J, 1992.** Corrosion mechanisms for copper and silver objects in near-surface enviroments. Journal of the American Institute for Conservation, 31, pp 355–366.

**Metz V, Bohnert E, Kelm M, Schild D, Reinhardt J, Kienzler B, Buchmeiser M R, 2007.** γ-radiolysis of NaCl brine in the presence of $UO_2$(s): effects of hydrogen and bromide. In: Dunn D, Poinssot C, Begg B (eds). Scientific Basis for Nuclear Waste Management XXX. Warrendale, PA: Materials Research Society. (Materials Research Society Symposium Proceedings 985), pp 33–40.

**Milodowski A E, Styles M T, Werme L, Oversby V M, 2003.** The corrosion of more than 176 million year old native copper plates from a deposit in mudstone in South Devon, United Kingdom. Paper 03681. In: Corrosion 2003 (NACE International Conference), San Diego, 16–20 March 2003, pp 1–10.

**Motamedi M, Karnland O, Pedersen K, 1996.** Survival of sulfate reducing bacteria at different water activities in compacted bentonite. FEMS Microbiology Letters, 141, pp 83–87.

**Muurinen A, Carlsson T, 2010.** Experience of pH and Eh measurements in compacted MX-80 bentonite. Applied Clay Science, 47, pp 23–27.

**Muzeau 2007.** Mecanismes de l'alteration sous eau du combustible irradie de type UOX. Ph. D. thesis, University Paris XI.

**Muzeau B, Jégou C, Delaunay F, Broudic V, Brevet A, Catalette H, Simoni E, Corbel C, 2009.** Radiolytic oxidation of $UO_2$ pellets doped with alpha emitters ($^{238/239}$Pu). Journal of Alloys and Compounds, 467, pp 578–589.

**Myers J R, Cohen A, 1995.** Pitting corrosion of copper in cold potable water systems. Materials Performance, 34, pp 60–62.

**Nagra, 2002.** Project Opalinus Clay. Safety report. Demonstration of disposal feasibility for spent fuel, vitrified high-level waste and long-lived intermediate-level waste (Entsorgungsnachweis). Nagra NTB-02-05, National Cooperative for the Disposal of Radioactive Waste, Switzerland.

**Naudet R, 1991.** Oklo: des réacteurs nucléaires fossiles, étude physique. Paris: Commisariat à l'Énergie Atomique.

**Neff D, Dillmann P, Beranger G, 2003.** An analytical study of corrosion products formed on buried ferrous archaeological artefacts. In: Féron D, Macdonald D D (eds). Prediction of long term corrosion behaviour in nuclear waste systems (EFC 36). Leeds: Maney Publishing, pp 295–315.

**Neff D, Dillmann P, Bellot-Gurlet L, Beranger G, 2005.** Corrosion of iron archaeological artefacts in soil: characterisation of the corrosion system. Corrosion Science, 47, pp 515–535.

**Neff D, Dillmann P, Descostes M, Beranger G, 2006.** Corrosion of iron archaeological artefacts in soil: estimation of the average corrosion rates involving analytical techniques and thermodynamic calculations. Corrosion Science, 48, pp 2947–2970.

**Nicot J-P, 2008.** Methodology for bounding calculations of nuclear criticality of fissile material accumulations external to a waste container at Yucca Mountain, Nevada. Applied Geochemistry, 23, pp 2065–2081.

**Nielsen U T, Ringgaard J, 2007.** Forsmark site investigation. Geophysical borehole logging in boreholes KFM02B and KFM08D. SKB P-07-60, Svensk Kärnbränslehantering AB.

**Nilsson S, Jonsson M, 2008.** On the catalytic effect of Pd(s) on the reduction of $UO_2^{2+}$ with $H_2$ in aqueous solution. Journal of Nuclear Materials, 374, pp 290–292.

**Nissen J, Gustafsson J, Sandström R, Wallin L, Taxén C, 2005.** Forsmark site investigation. Some corrosion observations and electrical measurements at drill sites DS4, DS7 and DS8. SKB P-05-265, Svensk Kärnbränslehantering AB.

**Nordström E, 2009.** Fission gas release data for Ringhals PWRs. SKB TR-09-26, Svensk Kärnbränslehantering AB.

**Northwood D O, Kosasih U, 1983.** Hydrides and delayed hydrogen cracking in zirconium and its alloys. International Metals Reviews, 28, pp 92–121.

**Ochs M, Talerico C, 2004.** SR-Can. Data and uncertainty assessment. Migration parameters for the bentonite buffer in the KBS-3 concept. SKB TR-04-18, Svensk Kärnbränslehantering AB.

**Odette G R, Lucas G E, 1998.** Recent progress in understanding reactor pressure vessel steel embrittlement. Radiation Effects and Defects in Solids, 144, pp 189–231.

**Olander D, 2004.** Thermal spike theory of athermal diffusion of fission products due to alpha decay of actinides in spent fuel ($UO_2$). SKB TR-04-17, Svensk Kärnbränslehantering AB.

**Oldberg K, 2009.** Distribution of fission gas release in 10x10 fuel. SKB TR-09-25, Svensk Kärnbränslehantering AB.

**Olin Å, Noläng B, Osadchii E, Öhman L and Rosen E, 2005.** Chemical thermodynamics. Vol. 7. Chemical thermodynamics of selenium. Amsterdam: Elsevier.

**Ollila K, 2006.** Dissolution of unirradiated $UO_2$ and $UO_2$ doped with $^{233}U$ in 0.01 M NaCl under anoxic and reducing conditions. Posiva 2006-08, Posiva Oy, Finland.

**Ollila K, 2008.** Dissolution of unirradiated $UO_2$ and $UO_2$ doped with $^{233}U$ in low and high ionic strength NaCl under anoxic and reducing conditions. Posiva Working Report 2008-50, Posiva Oy, Finland.

**Ollila K, Oversby V M, 2005.** Dissolution of unirradiated $UO_2$ and $UO_2$ doped with $^{233}U$ under reducing conditions. SKB TR-05-07, Svensk Kärnbränslehantering AB.

**Ollila K, Oversby V, 2006.** Testing of uranium dioxide enriched with $^{233}U$ under reducing conditions. In: Van Iseghem P (ed). Scientific Basis for Nuclear Waste Management XXIX. Warrendale, PA: Materials Research Society. (Materials Research Society Symposium Proceedings 932), pp 167–173.

**Ollila K, Albinsson Y, Oversby V, Cowper M, 2003.** Dissolution rates of unirradiated $UO_2$, $UO_2$ doped with $^{233}U$, and spent fuel under normal atmospheric conditions and under reducing conditions using an isotope dilution method. SKB TR-03-13, Svensk Kärnbränslehantering AB.

**ORNL 2005.** SCALE: a modular code system for performing standardized computer analysis. ORNL/TM-2005/39, Oak Ridge National Laboratory.

**Oversby V M, 1996.** Criticality in a high level waste repository. A review of some important factors and an assessment of the lessons that can be learned from the Oklo reactors. SKB TR 96-07, Svensk Kärnbränslehantering AB.

**Oversby V M, 1998.** Criticality in a repository for spent fuel: lessons from Oklo. In: McKinley I G, McCombie C (eds). Scientific Basis for Nuclear Waste Management XXI. Warrendale, PA: Materials Research Society. (Materials Research Society Symposium Proceedings 506), pp 781–788.

**Parasnis D S, 1997.** Principles of applied geophysics. 5th ed. London: Chapman & Hall.

**Pastina B, LaVerne J A, 2001.** Effect of molecular hydrogen on hydrogen peroxide in water radiolysis. Journal of Physical Chemistry A, 105, pp 9316–9322.

**Pastina B, Isabey J, Hickel B, 1999.** The influence of water chemistry on the radiolysis of primary coolant water in pressurized water reactors. Journal of Nuclear Materials, 264, pp 309–318.

**Pedersen K, 2010.** Analysis of copper corrosion in compacted bentonite clay as a function of clay density and growth conditions of sulphate-reducing bacteria. Journal of Applied Microbiology, 108, pp 1094–1104.

**Pedersen K, Motamedi M, Karnland O, Sandén T, 2000a.** Mixing and sulphate-reducing activity of bacteria in swelling, compacted bentonite clay under high-level radioactive waste repository conditions. Journal of Applied Microbiology, 89, pp 1038–1047.

**Pedersen K, Motamedi M, Karnland O, Sandén T, 2000b.** Cultivability of microorganisms introduced into a compacted clay buffer under high-level radioactive waste repository conditions. Engineering Geology, 58, pp 149-161.

**Phipps P B P, Rice D W, 1979.** The role of water in atmospheric corrosion. In: Brubaker G R, Phipps P B P (eds). Corrosion chemistry. Washington, D.C.: American Chemical Society. (ACS Symposium Series 89), pp 235–261.

**Pinnel M R, Tompkins H G, Heath D E, 1979.** Oxidation of copper in controlled clean air and standard laboratory air at 50°C to 150°C. Applications of Surface Science, 2, pp 558–577.

**Pourbaix M, Pourbaix A, 1992.** Potential-pH equilibrium diagrams for the system $SH_2O$ from 25 to 150°C: influence of access of oxygen in sulphide solutions. Geochimica et Cosmochimica Acta, 56, pp 3157–3178.

**Poinssot C, Ferry C, Poulesquen A, 2007.** New perspectives for the spent nuclear fuel radionuclides release model in a deep geological repository. In: Dunn D, Poinssot C, Begg B (eds). Scientific Basis for Nuclear Waste Management XXX. Warrendale, PA: Materials Research Society. (Materials Research Society Symposium Proceedings 985), pp 111–116.

**Puigdomench I, Taxén C, 2000.** Thermodynamic data for copper. Implications for the corrosion of copper under repository conditions. SKB TR-00-13, Svensk Kärnbränslehantering AB.

**Pusch R, 1983.** Stability of deep-sited smectite minerals in crystalline rock – chemical aspects. SKBF/KBS TR 83-16, Svensk Kärnbränslehantering AB.

**Pusch R, Börgesson L, 1992.** PASS – Project on alternative systems study. Performance assessment of bentonite clay barrier in three repository concepts: VDH, KBS-3 and VLH. SKB TR 92-40, Svensk Kärnbränslehantering AB.

**Pusch R, Karnland O, Lajudie A, Lechelle J, Bouchet A, 1992.** Hydrothermal field test with French candidate clay embedded steel heater in the Stripa mine. SKB TR 93-02, Svensk Kärnbränslehantering AB.

**Rai D, Yui M, Moore D A, 2003.** Solubility and solubility product at 22°C of $UO_2$(c) precipitated from aqueous U(IV) solutions. Journal of Solid State Chemistry, 32, pp 1–17.

**Raiko H, Sandström R, Rydén H, Johansson M, 2010.** Design analysis report for the canister. SKB TR-10-28, Svensk Kärnbränslehantering AB.

**Rard J A, Rand M H, Anderegg G, Wanner H, 1999.** Chemical thermodynamics. Vol. 3. Chemical thermodynamics of Technetium. Amsterdam: Elsevier.

**Reed D T, Van Konynenburg R A, 1988.** Effects of ionizing radiation on moist air systems. In: Apted M J, Westerman R E (eds). Scientific basis for nuclear waste management XI. Pittsburgh, PA: Materials Research Society. (Materials Research Society Symposium Proceedings 112), pp 393–404.

**Reed D T, Van Konynenburg R A, 1991a.** Effect of ionizing radiation on the waste package environment. In: High level radioactive waste management: proceedings of the second annual international conference. Las Vegas, Nevada, 28 April – 3May 1991. New York: American Society for Civil Engineers, pp 1396–1403.

**Reed D T, Van Konynenburg R A, 1991b.** Progress in evaluating the corrosion of candidate HLW container metals in irradiated air-steam mixtures. In: Proceedings of the Topical Meeting on Nuclear Waste Packaging, Focus ‘91. Las Vegas, 30 September – 2 October 1991. La Grange Park: American Nuclear Society, pp 185–192.

**Rice D W, Peterson P, Rigby E B, Phipps P B P, Cappel R J, Tremoureux R, 1981.** Atmospheric corrosion of copper and silver. Journal of The Electrochemical Society, 128, pp 275–284.

**Robit-Pointeau V, Poinssot C, Vitorge p, Grambow B, Cui D, Spahiu K, Catalette H, 2006.** Assessment of the relevance of coffinite formation within the near-field environment of spent

nuclear fuel geological disposals. In: Van Iseghem P (ed). Scientific Basis for Nuclear Waste Management XXIX. Warrendale, PA: Materials Research Society. (Materials Research Society Symposium Proceedings 932), pp 89–96.

**Romanoff M, 1989.** Underground corrosion. Houston: NACE International.

**Rondinella V V, Cobos J, Wiss T, 2004.** Leaching behaviour of low-activity alpha-doped $UO_2$. In: Hanchar J M, Stroes-Gascoyne S, Browning L (eds). Scientific Basis for Nuclear Waste Management XXVIII. Warrendale, PA: Materials Research Society. (Materials Research Society Symposium Proceedings 824), pp 167–173.

**Rosborg B, Werme L, 2008.** The Swedish nuclear waste program and the long-term corrosion behaviour of copper. Journal of Nuclear Materials, 379, pp 142–153.

**Roth O, Jonsson M, 2008.** Oxidation of $UO_2$ in aqueous solutions. Central European Journal of Chemistry, 6, pp 1–14.

**Rothman A J, 1984.** Potential corrosion and degradation mechanisms of Zircaloy cladding on spent fuel in a tuff repository. Report UCID-20172, Lawrence Livermore National Laboratory.

**Roudil D, Deschanels X, Trocellier P, Jégou C, Peuget S, Bart J-M, 2004.** Helium thermal diffusion in a uranium dioxide matrix. Journal of Nuclear Materials, 325, pp 148–158.

**Roudil D, Jégou C, Broudic V, Muzeau B, Peuget S, Deschanels X, 2007.** Gap and grain boundary inventories from pressurized water reactor spent fuels. Journal of Nuclear Materials, 362, pp 411–415.

**Roudil D, Bonhoure J, Pik R,Cuney M, Jégou C, Gauthier-Lafaye F 2008.** Diffusion of radiogenic helium in natural uranium oxides. Journal of Nuclear Materials, 378, pp 70–78.

**Roy S K, Sircar S C, 1981.** A critical appraisal of the logaritmic rate law in thin-film formation during oxidation of copper and its alloys. Oxidation of Metals, 15, pp 9–20.

**Saario T, Betova I, Heinonen J, Kinnunen P, Lilja C, 2004.** Effect of the degree of compaction of bentonite on the general corrosion rate of copper. In: Prediction of long term corrosion behaviour in nuclear waste systems. Proceedings of the 2nd International Workshop. Nice, 12–16 September 2004. ANDRA (Agence Nationale pour la Gestion des Déchets RadioActifs).

**Schön J H, 1996.** Physical properties of rock: fundamentals and principles of petrophysics. Oxford: Pergamon.

**Science and Global Security, 1996.** Vol. 5, No. 3, (Special Issue).

**Scott T B, Allen G C, Heard P J, Randel M G, 2005.** Reduction of U(VI) to U(IV) on the surface of magnetite. Geochimica et Cosmochimica Acta, 69, pp 5639–5646.

**Sidborn M, Sandström B, Tullborg E-L, Salas J, Maia F, Delos A, Molinero J, Hallbeck L, Pedersen K, 2010.** SR-Site: Oxygen ingress in the rock at Forsmark during a glacial cycle. SKB TR-10-57, Svensk Kärnbränslehantering AB.

**Silva R J, Bidoglio G, Rand M H, Robouch P B, Wanner H, Puigdomenech I, 1995.** Chemical thermodynamics. Vol. 2. Chemical thermodynamics of Americium. Amsterdam: Elsevier.

**Simpson J P, 1984.** Experiments on container materials for Swiss high-level waste disposal projects Part II. Nagra NTB 84-01, National Cooperative for the Disposal of Radioactive Waste, Switzerland.

**SKB, 1999.** SR 97 – Processes in the repository evolution. Background report to SR 97. SKB TR-99-07, Svensk Kärnbränslehantering AB.

**SKB, 2006a.** Fuel and canister process report for the safety assessment SR-Can. SKB TR-06-22, Svensk Kärnbränslehantering AB.

**SKB, 2006b.** Long-term safety for KBS-3 repositories at Forsmark and Laxemar – A first evaluation. Main report of the SR-Can project. SKB TR-06-09, Svensk Kärnbränslehantering AB.

**SKB, 2008.** Site description of Forsmark at completion of the site investigation phase. SDM-Site Forsmark. SKB TR-08-05, Svensk Kärnbränslehantering AB.

**SKB, 2009a.** Underground design Forsmark. Layout D2. SKB R-08-116, Svensk Kärnbränslehantering AB.

**SKB, 2009b.** Site description of Laxemar at completion of the site investigation phase. SDM-Site Laxemar. SKB TR-09-01, Svensk Kärnbränslehantering AB.

**SKB, 2009c.** Design premises for a KBS-3V repository based on results from the safety assessment SR-Can and some subsequent analyses. SKB TR-09-22, Svensk Kärnbränslehantering AB.

**SKB, 2010a.** FEP report for the safety assessment SR-Site. SKB TR-10-45, Svensk Kärnbränslehantering AB.

**SKB, 2010b.** Spent nuclear fuel for disposal in the KBS-3 repository. SKB TR-10-13, Svensk Kärnbränslehantering AB.

**SKB, 2010c.** Design, production and initial state of the canister for the safety assessment SR-Site. SKB TR-10-14, Svensk Kärnbränslehantering AB.

**SKB, 2010d.** Design, production and initial state of the buffer for the safety assessment SR-Site. SKB TR-10-15, Svensk Kärnbränslehantering AB.

**SKB, 2010e.** Design, production and initial state of the backfill and plug for the safety assessment SR-Site. SKB TR-10-16, Svensk Kärnbränslehantering AB.

**SKB, 2010f.** Design, production and initial state of the closure for the safety assessment SR-Site. SKB TR-10-17, Svensk Kärnbränslehantering AB.

**SKB, 2010g.** Design, construction and initial state of the underground openings for the safety assessment SR-Site. SKB TR-10-18, Svensk Kärnbränslehantering AB.

**SKB, 2010h.** Climate and climate related issues for the safety assessment SR-Site. SKB TR-10-49, Svensk Kärnbränslehantering AB.

**SKB, 2010i.** Geosphere process report for the safety assessment SR-Site. SKB TR-10-48, Svensk Kärnbränslehantering AB.

**SKB, 2010j.** Handling of future human actions in the safety assessment SR-Site. SKB TR-10-53, Svensk Kärnbränslehantering AB.

**SKB, 2010k.** Buffer, backfill and closure process report for the safety assessment SR-Site. SKB TR-10-47, Svensk Kärnbränslehantering AB.

**SKB, 2010l.** Data report for the safety assessment SR-Site. SKB TR-10-52, Svensk Kärnbränslehantering AB.

**SKB, 2010m.** Comparative analysis of safety related site characteristics. SKB TR-10-54, Svensk Kärnbränslehantering AB.

**SKB, 2010n.** Corrosion calculations report for the safety assessment SR-Site. SKB TR-10-66, Svensk Kärnbränslehantering AB.

**SKB, 2011.** Long-term safety for the final repository for spent nuclear fuel at Forsmark. Main report of the SR-Site project. SKB TR-11-01, Svensk Kärnbränslehantering AB.

**SKBF/KBS, 1983.** KBS-3 – Final storage of spent nuclear fuel – KBS-3, III Barriers. SKBF/KBS, Svensk Kärnbränsleförsörjning AB.

**SKI, 2006.** Engineered barrier system – Assessment of the corrosion properties of copper canisters. Report from a workshop at Lidingö, Sweden, April 27-29, 2005. SKI Report 2006:11, Statens kärnkraftinspektion (Swedish Nuclear Power Inspectorate).

**Smart N R, Adams R, 2006.** Natural analogues for expansion due to the anaerobic corrosion of ferrous materials. SKB TR-06-44, Svensk Kärnbränslehantering AB.

**Smart N R, Rance A P, 2008.** Miniature canister corrosion experiment – results of operations to May 2008. SKB TR-09-20, Svensk Kärnbränslehantering AB.

**Smart N R, Blackwood D J, Werme L, 2002a.** Anaerobic corrosion of carbon steel and cast iron in artificial groundwaters: Part 1 – Electrochemical aspects. Corrosion, 58, pp 547–559.

**Smart N R, Blackwood D J, Werme L, 2002b.** Anaerobic corrosion of carbon steel and cast iron in artificial groundwaters: Part 2 – Gas generation. Corrosion, 58, pp 627–637.

**Smart N R, Rance A P, Fennell, P, Werme L, 2003.** Expansion due to anaerobic corrosion of steel and cast iron: experimental and natural analogue studies. In: Féron D, Macdonald D D (eds). Prediction of long term corrosion behaviour in nuclear waste systems (EFC 36). Leeds: Maney Publishing, pp 280–294.

**Smart N R, Blackwood D J, Marsh G P, Naish C C, O'Brien T M, Rance A P, Thomas M I, 2004.** The anaerobic corrosion of carbon and stainless steels in simulated cementitious environments: a summary review of Nirex research. Report AEAT/ERRA-0313, AEA Technology.

**Smart N R, Rance A P, Fennell P A H, 2005.** Galvanic corrosion of copper-cast iron couples. SKB TR-05-06, Svensk Kärnbränslehantering AB.

**Smart N R, Rance A P, Fennell P A H, 2006.** Expansion due to anaerobic corrosion of iron. SKB TR-06-41, Svensk Kärnbränslehantering AB.

**Spinks J W T, Woods R J, 1990.** An introduction to radiation chemistry. 3rd ed. New York: Wiley.

**Stroes-Gascoyne S, 1996.** Measurements of instant-release source terms for $^{137}$Cs, $^{90}$Sr, $^{99}$Tc, $^{129}$I and $^{14}$C in used CANDU fuels. Journal of Nuclear Materials, 238, pp 264–277.

**Stumm W, Morgan J J, 1996.** Aquatic chemistry: chemical equilibria and rates in natural waters. 3rd ed. New York: Wiley.

**Swedish Corrosion Institute, 1983.** Corrosion resistance of a copper canister for spent nuclear fuel. SKBF/KBS TR 83-24, Svensk Kärnbränsleförsörjning AB.

**Syrett B C, 1981.** The mechanism of accelerated corrosion of copper-nickel alloys in sulphide-polluted seawater. Corrosion Science, 21, pp 187–209.

**Szakálos P, Hultquist G, Wikmark G, 2007.** Corrosion of copper by water. Electrochemical and Solid-State Letters, 10, pp C63–C67.

**Szakálos P, Hultquist G, Wikmark G, 2008.** Response to the Comment on "Corrosion of Copper by Water" [Electrochemical and Solid-State Letters, 10, C63 (2007)]. Electrochemical and Solid-State Letters, 11, S2.

**Taniguchi N, Kawasaki M, 2008.** Influence of sulfide concentration on the corrosion behavior of pure copper in synthetic seawater. Journal of Nuclear Materials, 379, pp 154–161.

**Tao S, Li D Y, 2008.** Nanocrystallization effect on the surface electron work function of copper and its corrosion behaviour. Philosophical Magazine Letters, 88, pp 137–144.

**Taxén C, 2004.** Atmospheric corrosion of copper 450 metres underground. Results from three years exposure in the Äspö HRL. In: Oversby V M, Werme L O (eds). Scientific Basis for Nuclear Waste Management XXVII. Warrendale, PA: Materials Research Society. (Materials Research Society Symposium Proceedings 807), pp 423–428.

**Thomas L E, Guenther R J, 1989.** Characterization of low-gas-release LWR fuels by transmission electron microscopy. In: Lutze W, Ewing R C (eds). Scientific Basis for Nuclear Waste Management XII. Pittsburgh, PA: Materials Research Society. (Materials Research Society Symposium Proceedings 127), pp 293–300.

**Thomas L E, Beyer C E, Charlot L A, 1992.** Microstructural analysis of LWR spent fuels at high burnup. Journal of Nuclear Materials, 188, pp 80–89.

**Trummer M, Nilsson S, Jonsson M, 2008.** On the effects of fission product noble metal inclusions on the kinetics of radiation induced dissolution of spent nuclear fuel. Journal of Nuclear Materials, 378, pp 55–59.

**Trummer M, Roth O, Jonsson M, 2009.** $H_2$ inhibition of radiation induced dissolution of spent nuclear fuel. Journal of Nuclear Materials, 383, pp 226-230.

**Tullborg E-L, Smellie J, Nilsson A-C, Gimeno M J, Brüchert V, Molinero J, 2010.** SR-Site – sulphide content in the groundwater at Forsmark. SKB TR-10-39, Svensk Kärnbränslehantering AB.

**Van Brutzel L, Crocombette J-P, 2007.** Atomic scale modelling of the primary damage state of irradiated $UO_2$ matrix. In: Aktaa J, Samaras M, Serrano de Caro M, Victoria M, Wirth B (eds). Structural and Refractory Materials for Fusion and Fission Technologies. Warrendale, PA: Materials Research Society. (Materials Research Society Symposium Proceedings 981E), JJ01-01.

**Van Konynenburg R A, 1995.** Comments on the draft paper "Underground supercriticality from plutonium and other fissile material" written by C. D. Bowman and F. Venneri (LANL). Report UCRL-ID-120990 COM, University of California.

**Wada R, Nishimura T, Fujiwara K, Tanabe M and Mihara M, 1999.** Experimental study on hydrogen gas generation rate from corrosion of Zircaloy and stainless steel under anaerobic alkaline conditions. In: Proceedings of the 7th International Conference on Radioactive Waste Management and Environmental Remediation, ICEM '99. Nagoya, Japan, 26-30 September 1999. New York: American Society of Mechanical Engineers.

**Werme L O, Forsyth R S, 1988.** Spent $UO_2$ fuel corrosion in water: release mechanisms. In: Apted M J, Westerman R E (eds). Scientific basis for nuclear waste management XI. Pittsburgh, PA: Materials Research Society. (Materials Research Society Symposium Proceedings 112), pp 443–452.

**Werme L O, Johnson L H, Oversby V M, King F, Spahiu K, Grambow B, Shoesmith D W, 2004.** Spent fuel performance under repository conditions: a model for use in SR-Can. SKB TR-04-19, Svensk Kärnbränslehantering AB.

**Wersin P, Bruno J, Spahiu K, 1993.** Kinetic modelling of bentonite – canister interaction. Implications for Cu, Fe and Pb corrosion in a repository for spent nuclear fuel. SKB TR 93-16, Svensk Kärnbränslehantering AB.

**Wersin P, Spahiu K, Bruno J, 1994.** Time evolution of dissolved oxygen and redox conditions in a HLW repository. SKB TR 94-02, Svensk Kärnbränslehantering AB.

**White A F, Brantley S L, 2003.** The effect of time on the weathering of silicate minerals: why do weathering rates differ in the laboratory and field? Chemical Geology, 202, pp 479–506.

**White J H, Yaniv A E, Schick H, 1966.** The corrosion of metals in the water of the Dead Sea. Corrosion Science, 6, pp 447–460.

**Wikramaratna R S, Goodfield M, Rodwell W R, Nash P J, Agg P J, 1993.** A preliminary assessment of gas migration from the copper/steel canister. SKB TR 93-31, Svensk Kärnbränslehantering AB.

**Wolery T J, 1992a.** EQ3NR, A computer program for geochemical aqueous speciation-solubility calculations: Theoretical Manual, User's Guide and related documentation (Version 7.0). UCRL-MA-110662 PT III, Lawrence Livermore National Laboratory.

**Wolery T J, 1992b.** EQ3NR, A software package for geochemical modelling of aqueous system Version 7.0). UCRL-MA-110662 PT I-IV, Lawrence Livermore National Laboratory.

**Yin S, Li D Y, 2005.** Effects of prior cold work on corrosion and corrosive wear of copper in $HNO_3$ and NaCl solutions. Materials Science and Engineering A, 394, pp 266–276.

**Åkesson M, Kristensson O, Börgesson L, Dueck A, Hernelind J, 2010.** THM modelling of buffer, backfill and other system components. Critical processes and scenarios. SKB TR-10-11, Svensk Kärnbränslehantering AB.

#### Unpublished documents


| SKBdoc id, version | Title | Issuer, year |
|---|---|---|
| 1077122 ver 2.0 | Strålskärmsberäkningar för kopparkapslar innehållande BWR, MOX och PWR bränsleelement | SKB, 2010 |
| 1193244 ver 4.0 | Criticality safety calculations of disposal canisters | SKB, 2010 |
| 1198314 ver 1.0 | Källstyrkor för bränsleelement under driftskede för clink, slutförvarsanläggning och slutförvar | Alara Engineering, 2010 |